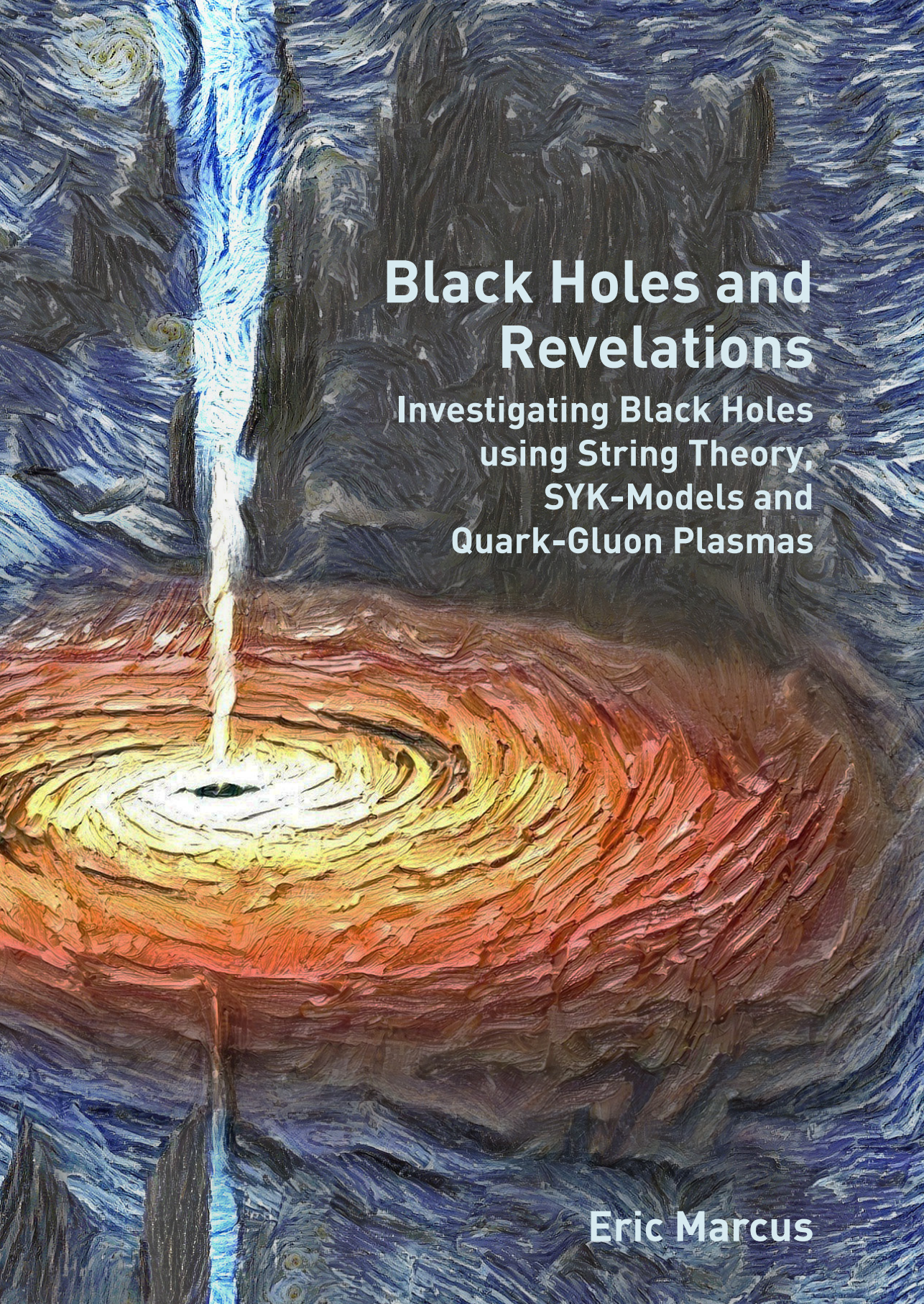
Black Holes and Revelations
Investigating Black Holes using String Theory, SYK-Models and Quark-Gluon Plasmas
Eric Marcus

Black Holes and Revelations

Investigating Black Holes using String Theory,
SYK-Models and Quark-Gluon Plasmas

Eric Marcus

PhD thesis, Utrecht University, September 2021
ISBN: 978-90-393-7394-1
About the cover: it depicts a supermassive black hole slowly 'eating' a nearby star. The image was created by the author using neural network techniques; in this case the style is based on Starry Night by Van Gogh.

Black Holes and Revelations

Investigating Black Holes using String Theory,
SYK-Models and Quark-Gluon Plasmas

Zwarte Gaten en Openbaringen

Zwarte Gaten bestudeerd met Snaartheorie,
SYK-Modellen en Quark-Gluon Plasma's

(met een samenvatting in het Nederlands)

Proefschrift

ter verkrijging van de graad van doctor aan de Universiteit Utrecht op gezag van de rector magnificus, prof. dr. H.R.B.M. Kummeling, ingevolge het besluit van het college voor promoties in het openbaar te verdedigen op woensdag 22 september 2021 des middags te 12:15 uur

door

Eric Jeffrey Marcus

geboren op 13 mei 1994
te Meppel

Promotor: Prof. dr. S.J.G. Vandoren
Copromotor: Dr. U. Gürsoy

To my parents

Publications

Part I of this thesis is centred around black holes in string theory and M-theory. It is based on the following publications:

[1] C. Hull, E. Marcus, K. Stemerdink and S. Vandoren, *Black holes in string theory with duality twists, JHEP* **07** (2020) 086,

[2] C. Couzens, E. Marcus, K. Stemerdink and D. van de Heisteeg, *The Near-Horizon Geometry of Supersymmetric Rotating AdS_4 Black Holes in M-theory,* accepted for publication in JHEP.

Part II of this thesis concerns new class of Sachdev-Ye-Kitaev models. The second part is based upon the publication:

[3] E. Marcus and S. Vandoren, *A new class of SYK-like models with maximal chaos, JHEP* **01** (2019) 166,

Part III of the thesis concerns the study of magnetohydrodynamics during heavy ion collisions, and is based upon the publications:

[4] U. Gürsoy, D. Kharzeev, E. Marcus and K. Rajagopal, *Magnetohydrodynamics and charged flow in heavy ion collisions, Nucl phys. A* **956** (2016) 389,

[5] Proceedings paper: U. Gürsoy, D. Kharzeev, E. Marcus, K. Rajagopal and C. Shen, *Charge-dependent Flow Induced by Magnetic and Electric Fields in Heavy Ion Collisions, Phys. Rev. C* **98** (2018) 055201,

[6] Proceedings paper: U. Gürsoy, D. Kharzeev, E. Marcus, K. Rajagopal and C. Shen, *Charge-dependent flow induced by electromagnetic in heavy ion collisions, Nucl. Phys. A* **1005** (2021) 121837.

Before moving on, we comment on the overlap of the first part of this thesis with the upcoming theses of K. Stemerdink and D. van de Heisteeg.

[1] Sections 2 and 3 were computed together by K. Stemerdink and the author, section 4 was mostly computed by K. Stemerdink and section 5 mostly by the author.

[2] Most of the computations in section 2 were performed by D. van de Heisteeg, section 3 was mostly calculated by K. Stemerdink and the author performed most computations in section 4.

Contents

Chapter 1

Introduction

> *While differing widely in the various little bits we know, in our infinite ignorance we are all equal.*
>
> – Karl Popper, *Conjectures and Refutations*

In this work, I will discuss some of the various little bits of research that I have been part of in the last few years. Although all subjects in this work are in some way related to black hole physics, they are all independent of one another. I have found that constantly working on new, unrelated subjects is both challenging and rewarding. Although it requires much effort to work yourself to the necessary level of understanding, there is something enjoyable about learning new ways of looking at things.

There are, besides this introduction, four chapters that each contain a different subject of research. Before we get to those, we will, in this preliminary chapter, first introduce the topics and provide some context. Then, the first chapter considers black holes in the presence of supersymmetry breaking of the background theory. Secondly, we will discuss the embedding of near-horizons of rotating black holes into M-theory. The third chapter concerns a one-dimensional model of Majorana fermions, the Sachdev-Ye-Kitaev model. Lastly, we concern ourselves with magnetohydrodynamics at heavy-ion collisions.

Remarkably, all of these subjects are related to black holes. The first two chapters turn the spotlight onto black holes themselves, while the last two are related to black holes by so-called AdS/CFT and AdS/QCD dualities (which we will explain below). Since parts of this chapter might be read by non-experts, I have written a small section for some of the topics that should be accessible for the layman. I would recommend the first following section on black holes and perhaps the

introduction to string theory and heavy-ion collisions. For each of these sections there is, however, a progressive line of complexity.

1.1 Black Holes and Revelations

What are black holes? What is string theory? How do black holes arise in string theory? It is these questions, plus perhaps some more that we will attempt to answer in the coming sections. We will start by discussing black holes in the classical, general relativistic sense in this section, and in the next section, we introduce string theory to find out how black holes are created using strings.

1.1.1 Dark Stars

The first picture of a black hole was captured only relatively recently, in 2019 [7], it is shown in Figure 1.1. This particular *supermassive black hole* lies at the center of a galaxy called M87. The picture quickly teaches us why blacks holes are called *black*; the black center of the image is where the black hole is located. The accretion disk of matter surrounding the black hole causes the glowing ring around the black hole. The glowing ring around it is caused by emissions from the accretion disk of matter that surrounds the black hole. An example closer to home is Sagittarius A*, a supermassive black hole located in the center of our galaxy. Such supermassive black holes can be found in most, if not all, spiral and elliptical galaxies.
The more ordinary, stellar-mass, black holes come into existence after heavy stars have burned through all their fuel. At this point, provided the star is massive enough, the star will collapse into itself due to gravity, and the extreme densities that build up in the center irreversibly collapse into a black hole.[1]

The existence of these black holes is a critical consequence of Einstein's theory of General Relativity (GR). Gravitational objects are called black holes as soon as light can no longer escape its gravitational potential anymore; no emitted light means they become black, hence the name. Before he published GR, Einstein already figured out that light always travels at the same speed and nothing moves faster than light. Coming back to black holes, when light cannot escape something, nothing can. This point beyond which nothing can escape is usually called the *event horizon*.

[1] The formation of supermassive black holes remains an active field of research, with many hypotheses on the origin of progenitors for the supermassive black holes.

Figure 1.1: *The first picture of a black hole, captured by the Event Horizon Telescope Collaboration [7]. The glowing 'ring' is caused by the accretion disk that spirals around the rotating black hole. The varying brightness is caused by the relativistic beaming of the emission from the rotating plasma.*

The first hints of black holes were already found far before GR was developed in the 18th century. At that time, Michell and Laplace considered objects with gravitational fields that were strong enough to prevent light from escaping [8]. It is because of this fundamental property that Michell named them *dark stars*, the nomenclature of black holes was only introduced in the 60s by Wheeler. Without the full force of general relativity, however, they could not make much progress in understanding these objects. This lack of understanding changed when the first genuine black hole solution, within general relativity, was written down in 1916 by Schwarzschild[2] and independently by Droste four months later, the metric is given by

$$ds^2 = -\left(1 - \frac{r_s}{r}\right) dt^2 + \left(1 - \frac{r_s}{r}\right)^{-1} dr^2 + r^2 d\Omega^2 \ , \tag{1.1}$$

with $r_s = 2GM$, the Schwarzschild radius and $d\Omega^2$ is the metric on a two-sphere.

One way to illustrate the black hole spacetimes more intuitively is with a so-called Penrose diagram. The Penrose diagram corresponding to the Schwarzschild black

[2] Although Schwarzschild wrote it down in 1916, the interpretation as a part of spacetime from which nothing can escape, was only realized by Finkelstein in 1958.

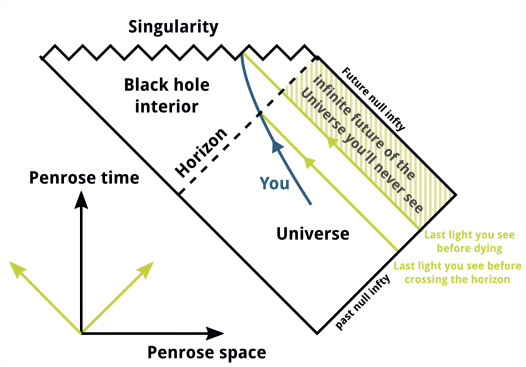

Figure 1.2: *The Penrose diagram for a Schwarzschild black hole. The time and spatial coordinates are shown in the bottom left, along with the yellow lines indicating how light rays move. The horizon is drawn as a dashed line; note that it is also at a 45° angle, meaning light can never escape once it is beyond the horizon. In the diagram, there is also a worldline of an observer that falls into the black hole and ends up in the singularity (which is unavoidable once you cross the horizon, as you may convince yourself from this diagram). Fig. from [10].*

hole is shown in Figure 1.2.[3] In these diagrams, the whole spacetime is put into a compact form, and light always moves on straight lines at angles of 45°.
Since massive objects (such as observers) always move slower than light, they are confined to move within the cone defined by two oppositely moving light rays. The event horizon is shown in the diagram as a line of 45°, such that when light rays move past it, they can never return.

Singularities

Perhaps the most curious feature of black hole solutions in GR arises when we compute their curvature. As we move closer and closer to the center of the black hole, the curvature gets stronger and stronger. In the middle of the black hole, the curvature diverges, a gravitational *singularity*. At this point, Einstein's theory tells us that the curvature is infinite. Needless to say, you would not want to be at this

[3] As a historical note: it is precisely this diagram that Stephen Hawking used at a conference organized by Jack Rosenberg to introduce the so-called information paradox of black holes. Hawking believed to have found that information that fell into the black hole was irretrievably lost. A discussion of this fascinating problem is beyond the scope of this thesis, but I would highly recommend the popular scientific book by Susskind [9].

singularity; from Figure 1.2 it becomes clear that it is, however, impossible to avoid once you move beyond the event horizon.

Usually, singularities signal that the theory is not complete in its explanations. For example, in quantum field theory, we are very used to singularities showing up in the computations and have even thought of a scheme to get rid of them consistently. After doing so, we can match the computations with good agreement to the experiments. That does not mean that quantum field theory is thereby fixed, a better theory would not need such an ad hoc procedure in the first place, and it signals flaws in the theory. However, the gravitational singularities inside the black holes can not be gotten rid of in a similar manner. To make matters worse, if the black hole is rotating, there are also closed timelike curves near the singularity, meaning you could wave to your past self. It is usually thought that a theory of quantum gravity will provide better explanations of what happens inside a black hole and possibly resolve the infinities.

But can they spin?

So far we have discussed only Schwarzschild black holes, which are static non-rotating black holes. In this thesis we will also be interested in certain classes of black holes that rotate. Whereas the Schwarzschild black hole was only characterised by its mass M, the rotating black hole will also have angular momentum J. In four dimensions, the asymptotically flat rotating black holes were discovered by Kerr, and the metric is given by[4]

$$\begin{aligned} ds^2 = &- \left(1 - \frac{r_s r}{\Sigma}\right) dt^2 + \frac{\Sigma}{\Delta} dr^2 + \Sigma d\theta^2 + \left(r^2 + a^2 + \frac{r_s r a^2}{\Sigma} \sin^2\theta\right) \sin^2\theta \; d\phi^2 \\ &- \frac{2 r_s r a \sin^2\theta}{\Sigma} dt \, d\phi \; , \end{aligned} \tag{1.2}$$

where, as before, $r_s = 2GM$ is the Schwarzschild radius, and we have defined

$$\begin{aligned} a &= \frac{J}{M} \; , \\ \Sigma &= r^2 + a^2 \cos^2\theta \; , \\ \Delta &= r^2 - r_s r + a^2 \; . \end{aligned} \tag{1.3}$$

[4]The metric is written in Boyer-Lindquist coordinates, which conforms with conventions we will use later in the thesis.

The rotation of the black hole can be seen from the $dt\,d\phi$ term, which shows there is a coupling between the time and one of the angular coordinates. Furthermore, as we take the angular momentum to zero, this term disappears, as we would expect. The event horizons can be found by considering $\Delta = 0$, which has real solutions provided that $a^2 \leq M^2$ (we took $G = 1$ here). The case in which we take $a = M$ is called *extremal*, which will be an important limit in some of our later chapters. If we were to take the near-horizon limit for the extremal Kerr black hole we would get an AdS_2 term from the time and radial coordinates, along with still the mixing between the time and angular coordinate. Due to this last 'mixing', we often say that the AdS_2 is fibered; in this case over the angular coordinate ϕ.

Apart from rotation, there is one more property we could have given the black hole, an electric charge Q. A static but charged asymptotically flat four-dimensional black hole is known as a Reissner-Nordström black hole, and is given by

$$ds^2 = -\left(1 - \frac{r_s}{r} + \frac{r_Q^2}{r^2}\right) dt^2 + \left(1 - \frac{r_s + \frac{r_Q^2}{r^2}}{r}\right)^{-1} dr^2 + r^2 d\Omega^2 \ , \tag{1.4}$$

where we have defined a length scale

$$r_Q^2 = \frac{Q^2\, G}{4\pi\epsilon_0} \ . \tag{1.5}$$

A natural generalization would be to combine all the above discussed properties and obtain a black hole solution that is both charged and rotating. This is called a Kerr-Newman solution and we will discuss a variant of this later in chapter 3.

What if I throw my wallet in?

Suppose you are near a black hole and throw your wallet into the black hole. Will you still know how much money was in there? What happens with information in general as we throw it into the black hole has a long, interesting history with many viewpoints. It is beyond the scope of this thesis to go into the problem in-depth, and I would happily refer to the book *black hole war* by Susskind [9] for an accessible history. To summarize, the consensus is that information of infalling objects seems to be conserved and is later radiated away by Hawking radiation. So, regarding your wallet: you definitely lose your money, but you can figure out how much it was (by analyzing the Hawking radiation). The presence of radiation already shows us that black holes are thermodynamic objects, and they have their own black hole

thermodynamic laws. The most important for us is the analog of the *second law*, which states that the entropy of isolated systems never decreases. The entropy of a black hole can be computed by the Bekenstein-Hawking entropy [11]

$$S_{\text{BH}} = \frac{A}{4} \ , \tag{1.6}$$

where A is the area of the horizon. This formula shows us that the second law of black hole thermodynamics gets translated to 'the area of a black hole never decreases', i.e. $\mathrm{d}A \geq 0$. Now, if we combine the above entropy along with Boltzmann's understanding that entropy 'measures' the number of microstates, we can wonder, what are the microstates of black holes? Strominger and Vafa gave an answer to this question in [12] for certain five-dimensional black holes. They reproduced the entropy using string theory by considering the distribution of momentum on so-called D1 and D5 branes. In the next section, we will discuss more string theory and how to make black holes within the theory.

1.2 String Theory and Black Holes

The next element in our physics toolbox is string theory, the leading candidate for a theory of quantum gravity. The basic idea of string theory is perfectly well encompassed in its name: instead of considering zero-dimensional point particles, we study one-dimensional objects called *strings*. Other fields, such as gauge fields, will be made from certain strings and excitations that live on these strings. Within string theory, there are two types of strings: open and closed strings. In Figure 1.3 we show two kinds of strings along with another curious feature of string theories, the existence of so-called branes (short for membranes). As it turns out, open strings always have their endpoints confined to higher-dimensional surfaces called D-branes. These D-branes will be extremely vital for our purposes later on; spoiler alert: most of our black holes are made from such D-branes. We will discuss what types of branes exist in which string theories later on in subsection 1.2.5.

So how exactly does this make a theory of quantum gravity? To answer this, we look at the spectrum of string theory. After we have quantized the theory, we can find out what objects exist in the excitations of the strings. As it turns out, the closed string spectrum always has a graviton, which is the force carrier for

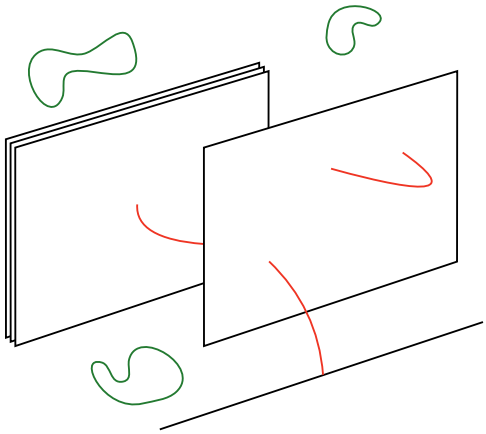

Figure 1.3: *String theories consist of two types of strings, open and closed strings. The closed ones are colored in green, while the open strings are red. A crucial observation in string theories is the existence of D-branes, which are depicted as the black squares here. The open strings always have their endpoints fixed to such branes. Figure from [13].*

gravity.[5] This signals that our quantum theory of strings contains gravity. Apart from the graviton, we can also find gauge fields and others, indicating that we can also describe gauge theories. The presence of gauge fields provided even more enthusiasm for string theory since the current best-corroborated theory of particles in our universe, the standard model, is also a gauge theory. The standard model has a gauge group $\mathrm{SU}(3)\times\mathrm{SU}(2)\times\mathrm{U}(1)$, corresponding to the strong interaction, weak interaction, and electromagnetic interaction, respectively.
One curious feature of string theory[6] is that it requires *ten* dimensions for consistency. Clearly, we only encounter four of these in our daily lives, so the question arises: where did the others go? The best explanation is in terms of *compactification*, whereby the 'extra' dimensions are rolled up to become very small and thus

[5] In quantum field theories, such as the standard model, an indicative feature is the presence of force carriers. These particles, such as the photon for the electromagnetic force, are the fields that mediate interactions. So the presence of the graviton is a good indicator that we are dealing with quantum gravity.

[6] I am assuming here that we are considering *super*string theory, we will show in the next section why purely bosonic string theory is not enough to describe anything remotely related to our universe.

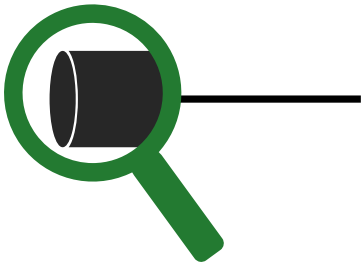

Figure 1.4: *To go from ten dimensions to four, we compactify the extra dimensions. This means we 'roll up' the additional dimensions such that they seem point-like from our four-dimensional point of view. If we were to zoom in closely, we could still find the hidden structure of these additional dimensions. Figure from [13].*

not visible in our seemingly four-dimensional world. An illustration is shown in Figure 1.4. It might help to imagine the drawn line as a power cable seen from far away; it then appears as a one-dimensional object. Suppose now an ant is living on the cable, at his (much smaller) length scales, the wire is not one-dimensional, but the ant can move around the cable in another direction. This analogy encompasses the idea of compactification; at large length scales, the extra dimensions are practically point-like, but they are present on microscopic length scales.

A very reasonable question at this stage would be, are there different ways of compactifying? The answer is yes; in fact, at this stage, it seems appropriate to give the usual estimate of 10^{500} compactifications[7] different possibilities. So, at first sight, it seems that there is an extraordinary amount of freedom to choose here. If we, however, take a closer look at how we can reproduce all aspects of our universe, it seems there is a problem: how can we create de-Sitter spacetimes from string theory. Instead of too much freedom, it seems in this area there is too little. To my knowledge, there exists only one – widely criticized – way to achieve it [14]. The swampland program (see, e.g. [15]) aims to investigate this and other important questions but is beyond the scope of this thesis.
Let me now briefly summarise what we will discuss in the rest of this section. We

[7]This number is more correctly given as an estimate of the possible metastable vacua that can be created in string theory.

will begin with an overview of which types of string theories exist and which we will use in our research later on. Afterward, we will move on to supergravity, which is the low-energy limit of string theory, followed by a short discussion of dualities that exist in string theory. Then we turn to the elusive branes, both from supergravity and string theory points of view. In the penultimate part we discuss how black holes are made in string theory. The last part will shortly discuss holography and the AdS/CFT correspondence since it lies in the motivation of many questions addressed in this thesis.

1.2.1 Supersymmetry and Our Universe

Before we consider the string theories in more detail, we have a short discussion on supersymmetry. The symmetry relates two types of particles: bosons with integer spin and fermions with half-integer spin. Depending on the degree (or amount) of supersymmetry, we can form so-called supermultiplets of different sizes by acting with the different supersymmetries.
For example, consider 4D with $\mathcal{N} = 1$ supersymmetry; in this scenario with one spinor, we can act on, e.g., a spin 0 particle to obtain a spin 1/2, which together form a chiral multiplet. We can build a vector multiplet is built by working on the spin 1/2 particle to get a spin one particle. Similar considerations apply to different dimensions and more extensive amounts of supersymmetry, in which case we can build larger multiplets.
Supersymmetry is also a vital ingredient of superstring theory, and the types of string theories we consider in this thesis will start with the maximal amount of supersymmetry[8]. The question then remains, how much supersymmetry exists in 'our' universe? To answer this question, experiments (including B-physics at LHC, XENON, WIMP, and many more) have sought for the superpartner particles for quite some years; the Particle Data group gives a good overview of experimental results in [16]. Up to now, no superpartners have been found experimentally, and there are strong constraints on the existence of supersymmetry up to the energy scales reached by the LHC.
Due to such results, it has become essential to find ways of ending up in four dimensions with as little or no supersymmetry as possible. These considerations have led to much research into compactifications on manifolds that break supersymmetry.

[8]There is a maximal amount because we only want the multiplets to go up to spin 2 (the graviton); for higher spins, we can't consistently write down renormalizable and interacting actions.

It is also one of the motivations for our work in chapter 2, whereby we construct black hole solutions in supersymmetry breaking backgrounds. Such approaches allow us to use the tools of superstring theory and still try to make contact with our seemingly supersymmetry-less world.

1.2.2 Different Types of String Theories

In this section we will discuss the different types of string theories. To do so, let's make our previous discussion on strings a bit more precise, the action for a point particle in D dimensions is given by

$$S = -m \int \mathrm{d}s = -m \int \mathrm{d}\tau \sqrt{\eta_{\mu\nu}\, \partial_\tau X^\mu \partial_\tau X^\nu} \ , \tag{1.7}$$

where η is the spacetime metric, m is the mass of the particle, μ runs over $0, 1, \ldots, D-1$ and $\mathrm{d}s$ is the line element. The coordinate τ describes the time evolution of the worldline of the particle. This expression can now be generalized to higher dimensional objects, in particular one-dimensional strings, where it is called the *Nambu-Goto* action

$$S = -T \int \mathrm{d}^2\sigma \sqrt{(\dot{X})^2 (X')^2 - (\dot{X} \cdot X')^2} \ , \tag{1.8}$$

where T is now the string tension and since strings are one-dimensional we have introduced a new coordinate σ for the extended spatial direction. Due to the square root in (1.8) it is hard to quantise, but luckily there is another way to write the action, it is the (classically) equivalent *Polyakov* action

$$S = -\frac{T}{2} \int \mathrm{d}^2\sigma \sqrt{g} g^{\alpha\beta} \partial_\alpha X^\mu \partial_\beta X^\nu \eta_{\mu\nu} \ , \tag{1.9}$$

where we have now introduced the auxiliary field g, the metric on the worldsheet. This action is equivalent to the Nambu-Goto one upon substituting the equation of motion for g back into the action. The equation of motion for X reduces to the free wave equation,[9] for which the most general solution is a sum of a left-moving and right-moving wave.

We can complete the quantization for which there are many methods, excellently documented in any string textbook. If we only consider (1.9), however, we will run into a couple of problems. The first problem arises because we only incorporated

[9] Before it takes the form of the free wave equation, we first have to use the reparametrization and Weyl symmetries to fix the worldsheet metric $g^{\alpha\beta} = \eta^{\alpha\beta}$.

bosonic fields in the Polyakov action so far. After the quantization, we will only find bosonic fields; in our universe, all matter is built from fermions, meaning that any remotely realistic theory should reproduce them. Secondly, in the spectrum, we find a *tachyon*, a particle with a negative mass that usually indicates that we are doing perturbation theory in an unstable vacuum. The problem is that we don't know in bosonic string theory what this vacuum is or what we decay into.

Thankfully both problems can be solved by *super*string theory, where we will explicitly introduce fermions and supersymmetry into the Polyakov action. The fermions can be included by simply adding the Dirac action for free massless fermions to the Polyakov action:

$$S = -\frac{T}{2}\int \mathrm{d}^2\sigma \left(\partial_\alpha X^\mu \partial^\alpha X_\mu + \bar{\psi}^\mu \rho^\alpha \partial_\alpha \psi_\mu\right) \ , \tag{1.10}$$

with ψ the worldsheet fermion field and ρ are two-dimensional Dirac matrices satisfying the algebra

$$\{\rho^\alpha, \rho^\beta\} = 2\eta^{\alpha\beta} \ . \tag{1.11}$$

In addition to the action itself, we also need to specify boundary conditions for the fields in order for it to be well defined. We let the σ integral run from 0 to l, where usually l is chosen to be 2π. We then distinguish between closed and open strings.

Closed strings. The boundary points should be identified for the closed strings since it is a closed topology. For the bosonic fields X this means

$$X^\mu(\tau, \sigma + 2\pi) = X^\mu(\tau, \sigma) \ . \tag{1.12}$$

For the fermions, there are two options, which computationally arises because the fermion action has only one derivative. In practice, this means we can choose

$$(\mathrm{R}): \quad \psi^\mu(\tau, \sigma + 2\pi) = \psi^\mu(\tau, \sigma) \ , \tag{1.13}$$

$$(\mathrm{NS}): \quad \psi^\mu(\tau, \sigma + 2\pi) = -\psi^\mu(\tau, \sigma) \ , \tag{1.14}$$

where we call the periodic boundary conditions the Ramond (R) sector and the anti-periodic sector is called the Neveu-Schwarz (NS) sector. Recalling that the most general solutions to the equations of motion were separate for left and right moving waves, we can get four sectors: R-R, R-NS, NS-R, and NS-NS. As a last note, we have to choose the same boundary conditions for all the μ directions, to preserve the spacetime Poincaré invariance.

Open strings. In the open string sector, we have boundary conditions for both endpoints separately since they no longer coincide. The one extra ingredient, which we have mentioned shortly before, is the presence of D-branes. The endpoints of open strings end on these branes, and the presence of them allows us to break the Poincaré invariance in the spacetime, meaning we can have different boundary conditions for different values of the μ index. In Figure 1.3 we can see open strings (drawn in red) that both start and end on the same D-brane, as well as open strings that start and end on different stacks of D-branes (of different dimensions).
Let us consider the bosonic fields X^μ. There are then two different boundary conditions that we can impose at the endpoints $\sigma^* \in \{0, l\}$, Neumann (N) and Dirichlet (D)[10]

$$(\mathrm{N}): \quad \partial_\sigma X^\mu|_{\sigma=\sigma^*} = 0 \ , \tag{1.15}$$

$$(\mathrm{D}): \quad \delta X^\mu|_{\sigma=\sigma^*} = 0 \ , \tag{1.16}$$

where δX^μ indicates the variation of the field X. The Neumann condition is associated with directions in which the open string can move on the D-brane, whilst the Dirichlet condition tells us that the string is fixed in these directions. As an example, if we had open strings ending on a D5-brane, they would have Neumann boundary conditions in the $0, 1, \ldots, 5$ directions (where the brane is located), whilst having Dirichlet in the remaining $6, \ldots, 9$ directions of spacetime.
Similar to the closed strings, the fermions have an R and NS sector, depending on the sign difference we choose at the endpoint of the string. The result for the open strings thus consists of the four possibilities: NN, ND, DN, and DD, within each of which the fermions have the choice between Ramond and Neveu-Schwarz.

Ten Dimensions

The Polyakov action (1.10) has supersymmetry on the two-dimensional worldsheet of the string. We can wonder whether supersymmetry also shows up in the ten-dimensional spacetime that it describes. Before diving into the types of string theories that arise in 10D, we first mention the *orientation* of strings. This orientation of a string is flipped when sending $\sigma \to 2\pi - \sigma$. Strings that are invariant under this operation are called *unoriented*. These properties allows us to classify the first three types of string theories:

[10] The equivalence in the last line follows by realizing that demanding that the variation is zero for all τ is equivalent to saying that X is independent of τ, i.e., the derivative is zero.

	Type I	Type IIA	Type IIB
Strings	Open + Closed	Closed	Closed
Orientation	Unoriented	Oriented	Oriented
Supercharges	16	32	32

All of these theories have supersymmetric spectra. The two Type II theories are distinguished by the particular GSO[11] projections that are performed on the spectrum; we will have more to say about GSO projections in chapter 2. The Type I theory can be constructed from the IIB theory by orientifolding[12] the theory and adding several branes (which break half of the supersymmetry) to cancel anomalies [18].

In the remainder of this work, we will mostly be interested in the Type II theories, so let's shortly discuss their massless spectrum. In the NS-NS sector, both theories contain the same fields: a dilaton Φ, the Kalb-Ramond two-form $B_{\mu\nu}$ and the metric $g_{\mu\nu}$. The dilaton plays an important role in string theory, as the vacuum expectation value determines the coupling strength as

$$g_s = \mathrm{e}^{\langle\Phi\rangle} \ . \tag{1.17}$$

In the R-R sector, the theories differ, IIA has a one-form C_1 and a three-form C_3, while the spectrum of IIB contains a zero-form (also known as the axion) a[13], two-form C_2 and a self-dual four-form C_4. In the fermionic sectors NS-R and R-NS, both have two gravitini (corresponding to 32 supercharges) and dilatini; however, they are of different chiralities. Type IIA is a non-chiral $\mathcal{N} = (1,1)$ theory, and IIB a chiral $\mathcal{N} = (2,0)$ theory. Before moving on, it is important to notice that these theories fix the problems we had with bosonic string theory. There are no tachyons in the spectrum, and we have also found the fermions we were looking for.

So far, we have assumed that we make both the left and right moving sectors of the Polyakov action supersymmetric. If we relax this condition and make only one of these sectors supersymmetric, while leaving the other purely bosonic, we obtain two new theories, called *heterotic* string theories:

[11] Named after the inventors Gliozzi, Scherk and Olive [17].

[12] An orientifold is a generalization of an orbifold, whereby the orbifold group includes the orientation reversing operator $\sigma \to 2\pi - \sigma$.

[13] Here, I use the notation conventions we will use later on, in the literature it is usually written as C_0

- E8 × E8 heterotic string theory
- SO(32) heterotic string theory

The two theories differ in their gauge groups, under which the massless vectors transform. Together all the approaches we have considered make up the five consistent superstring theories.
Apart from these string theories, there is one other player left: *M-theory*. Edward Witten introduced the name[14] at the strings conference in 1995 [19]. The theory is not completely formulated yet, but its low-energy limit is known to be 11D supergravity, which we will discuss in the upcoming section. M-theory is not a string theory in the sense that its constituents are not strings. It is perhaps more accurately described as a membrane theory since it contains two kinds of branes: M2 and M5-branes. In subsection 1.2.4 we will see how M-theory and 11d supergravity are related to the other string theories. Before that, we will discuss supergravity theories.

1.2.3 Low Energy Limits

It is now time to consider the low-energy limit of string theory: supergravity. The supergravities form a correct description when $E \ll l_s^{-1}$, with l_s the string length scale.[15] The supergravities will be of particular importance to us in several places, as we will use the Type IIB supergravity in our Scherk-Schwarz reductions in chapter 2, and 11d supergravity plays a big role in chapter 3. Supergravity has had different roles in its history. Originally, it was envisioned as a fundamental theory, unifying the forces and describing underlying degrees of freedom and free of ultraviolet divergences. It was soon discovered that it could not fulfill these roles. Its modern-day interpretation is better described as an effective field theory of a more fundamental, underlying theory: superstring theory and M-theory.

Local supersymmetry

The fundamental idea of supergravity is to combine the ideas of gravity and supersymmetry. The supersymmetry is promoted to a local gauge symmetry.

[14] Usually said to mean 'mysterious' or 'membrane' of even 'mother', perhaps you can think of a better one even.

[15] The energy E is to be interpreted as the center of mass-energy in a particle experiment. Massive particles can be made from oscillations on strings and have masses $M \approx l_s^{-1}$, when our energy scale is lower than this; we can effectively consider the massless spectrum instead.

A natural question to ask is then: what is the gauge field associated with this symmetry? It is called the *gravitino*, the superpartner of the graviton, and it carries both a spinor and a vector index. The presence of two indices was expected since, unlike 'normal' gauge symmetries, the underlying algebra of supersymmetry is a superalgebra, also containing fermionic generators, the supercharges. Consider now the Lagrangian for a $D \leq 11$ dimensional supergravity; we know that it should at least contain the Einstein-Hilbert term for gravity, but also a description of the gravitino field. As it turns out, these fields are described by the Rarita-Schwinger Lagrangian, supposing we have a single gravitino it is given by

$$\mathcal{L} = \frac{1}{2} e \, \bar{\psi}_\mu \Gamma^{\mu\nu\rho} D_\nu \psi_\rho + \dots \ , \tag{1.18}$$

with e the determinant of the vielbein, ψ is the gravitino field, and Γ^μ form a Clifford algebra[16] by

$$\{\Gamma^\mu, \Gamma^\nu\} = 2\eta^{\mu\nu} \ . \tag{1.19}$$

The $a, b, \dots$ in the Lagrangian denote the tangent space indices needed to describe the spinors, while $\mu\nu, \dots$ are the curved indices; both types run from $0, \dots D-1$. The covariant derivative D is given by

$$D_\mu \psi = \left(\partial_\mu - \tfrac{1}{4} \omega_\mu{}^{ab} \Gamma_{ab}\right) \psi \ , \tag{1.20}$$

where $\omega_\mu{}^{ab}$ is the spin connection associated with the vielbeins.

The degree of supersymmetry differs among the possible supergravity theories, and we can denote them according to the amounts of supercharges in the theory. The maximum number that we consider is 32, as theories with more supercharges automatically get massless fields with a spin larger than two, for which we can't consistently write down interactions.
How these supersymmetries are distributed over the spinors depends on the space-time dimension. The minimum number of components of the spinors relies on the type of spinors we can define; we can always make a Dirac spinor that has $2^{\lfloor D/2 \rfloor}$ complex components. In even dimensions, we can, furthermore, define *Weyl* spinors, and in $D = 2 \bmod 4$ we can combine the Weyl condition with the *Majorana* condition to obtain Majorana-Weyl spinors. Both of the constraints place additional limitations on the spinor, halving its number of degrees of freedom. Spinors

[16] The $\Gamma^{\mu\nu}$ indicate asymmetric combinations of gamma matrices, e.g. $\Gamma^{\mu\nu} = \frac{1}{2}[\Gamma^\mu, \Gamma^\nu]$.

Dimension	Spinor	Components
2	MW	1
3	M	2
4	M	4
5	S	8
6	SW	8
7	S	16
8	M	16
9	M	16
10	MW	16
11	M	32

Table 1.1: *This table shows the minimal real components spinors have in various dimensions. M stands for Majorana, W for Weyl, and S for symplectic. The symplectic condition leaves the number of independent components invariant, but both Majorana and Weyl conditions halve the degrees of freedom of a Dirac spinor. It is also possible to define Weyl spinors in 4D and 8D, but we omitted this from the table.*

can also be symplectic, but this does not yield any restriction on their degrees of freedom. In Table 1.1 we show the different possibilities for the spinors in the various dimensions.

As an example, we can consider the Type II theories in ten dimensions. From the table, we can see that in ten dimensions, we have Majorana-Weyl (MW) spinors, meaning that the 32 complex components of a Dirac spinor get reduced to 16 real components. The Type II theories are maximally supersymmetric, so there will be two of these MW spinors. We can make two choices for the chiralities, one yielding a chiral theory, IIB, and the other a non-chiral theory, IIA. We denote this by writing that IIA is an $\mathcal{N} = (1, 1)$ theory whilst Type IIB is an $\mathcal{N} = (2, 0)$ theory. Apart from the ten- and eleven-dimensional theories, we will also often make use of the six- and five-dimensional spinors in chapter 2.

What does it look like?

Now that we have discussed supersymmetry and spinors, it is time to study some examples of supergravities. As mentioned, the IIB and eleven-dimensional su-

pergravities will play important roles for us. So let us begin with discussing the eleven-dimensional supergravity.

11-dimensional supergravity. The unique, eleven-dimensional supergravity was first written down in [20]; it is maximally supersymmetric, and by considering Table 1.1 we find that there will be one gravitino, whose spinor structures is a 32-component Majorana spinor. The fermionic part of the action will at least contain the Rarita-Schwinger Lagrangian (1.18). In fact, the actions are usually used to make *classical* solutions, in which the fermions always vanish, so the fermionic part of the actions are often omitted. The bosonic action is given by

$$S = \frac{1}{2\kappa_{11}^2} \int R * 1 - \frac{1}{2} F_4 \wedge *F_4 - \frac{1}{6} A_3 \wedge F_4 \wedge F_4 \ , \tag{1.21}$$

where the last term is known as a Chern-Simons term, R denotes the Ricci-scalar, A_3 a three-form, $F_4 = \mathrm{d}A_3$ is its field strength and κ_{11} denotes the gravitational coupling through

$$2\kappa_{11}^2 = 16\,\pi\, G_{11} \ . \tag{1.22}$$

The Bianchi-identity and equation of motion for the three-form are given by

$$\mathrm{d}F_4 = 0 \ , \tag{1.23}$$

$$\mathrm{d} * F_4 = \frac{1}{2} F_4 \wedge F_4 \ . \tag{1.24}$$

Apart from these equations it is often useful to consider the supersymmetry transformations on the action. In particular the variation of the gravitino is considered, since the solutions that set these variations to zero characterise *Killing spinors*. The Killing spinors indicate conserved supersymmetries. The variation, with parameter ϵ, for the gravitino is given by

$$\delta_\epsilon \psi_\mu = D_\mu \epsilon + \frac{1}{288} (\Gamma_\mu^{\nu\rho\sigma\lambda} - 8\delta_\mu^\nu \, \Gamma^{\rho\sigma\lambda}) F_{\nu\rho\sigma\lambda} \epsilon = 0 \ , \tag{1.25}$$

$$D_\mu \epsilon = \left(\partial_\mu + \frac{1}{4} \omega_\mu^{\beta\gamma} \, \Gamma_{\beta\gamma} \right) \epsilon \ . \tag{1.26}$$

Another supergravity theory can be found by reducing the 11d supergravity on a circle. As it turns out this yields exactly the Type IIA supergravity. This remarkable relation is due to the duality of M-theory on a circle to Type IIA string theory, about which we say some more in the next section.

Type IIB. Unlike the IIA theory, IIB cannot be found by reducing the eleven-dimensional theory on a circle. The action for the IIB supergravity schematically looks as

$$S_{\text{IIB}} = S_{\text{NS}} + S_{\text{R}} + S_f \ , \tag{1.27}$$

where the first two terms denote the bosonic actions, arising from NS-NS and R-R sectors of the string theories (see subsection 1.2.2), and the last term denotes the fermions. As mentioned before, the fermionic part will not be of importance for classical solutions, so we focus on the bosonic part. The NS part of the action is given by

$$S_{\text{NS}} = \frac{1}{2\kappa_{10}^2} \int \mathrm{e}^{-2\Phi} \left(R_{10} * 1 - \frac{1}{2} H_3 \wedge * H_3 + 4 \mathrm{d}\Phi \wedge * \mathrm{d}\Phi \right) \ , \tag{1.28}$$

where Φ is the dilaton and $H_3 = \mathrm{d}B_2$ is the field strength of the Kalb-Ramond field B_2. The other bosonic part of the action is found to be

$$S_{\text{R}} = -\frac{1}{4\kappa_{10}^2} \int F_1 \wedge * F_1 + F_3 \wedge * F_3 + \frac{1}{2} F_5 \wedge * F_5 + C_4 \wedge H_3 \wedge F_3 \ , \tag{1.29}$$

where the field strengths are defined as

$$F_1 = \mathrm{d}a \ , \tag{1.30}$$

$$F_3 = \mathrm{d}C_2 - a \, \mathrm{d}B_2 \ , \tag{1.31}$$

$$F_5 = \mathrm{d}C_4 - \frac{1}{2} C_2 \wedge \mathrm{d}B_2 + \frac{1}{2} B_2 \wedge \mathrm{d}C_2 \ . \tag{1.32}$$

The IIB action, as written above, gives rise to all the equations of motion, but we are still missing one more ingredient. As we have mentioned before the five-form field strength is self dual and we need to still manually implement this afterward[17] by demanding alongside the equations of motion

$$F_5 = * F_5 \ . \tag{1.33}$$

The Type IIB supergravity has an important symmetry that is not currently manifest. To find it we change from the string frame to the Einstein frame by a redefinition of the metric, and define two new fields as

$$g^E_{\mu\nu} = \mathrm{e}^{-\Phi/2} g_{\mu\nu} \ , \tag{1.34}$$

$$\tau = a + i\mathrm{e}^{-\Phi} \ , \tag{1.35}$$

$$F_3' = \mathrm{d}C_2 - \tau H_3 \ , \tag{1.36}$$

[17] If it is imposed within the action we find the term $\int F_5 \wedge F_5 = -\int F_5 \wedge F_5 = 0$.

The scalar τ is often referred to as the *axion-dilaton*. Using the above definitions we can rewrite the bosonic IIB action to

$$S_{\text{IIB}} = \frac{1}{2\kappa_{10}^2}\int \Big(R_E * 1 - \frac{1}{4}F_5 \wedge *F_5 - \frac{1}{2(\text{Im}\tau)}F_3' \wedge *\bar{F}_3' \\ - \frac{1}{2(\text{Im}\tau)^2}\text{d}\tau \wedge *\text{d}\bar{\tau} - i\frac{1}{4\,\text{Im}\tau}C_4 \wedge F_3' \wedge \bar{F}_3'\Big)\ , \tag{1.37}$$

where we wrote R_E to indicate that it is now computed in the Einstein frame. In this form there is an SL(2,$\mathbb{R}$) symmetry present, that acts non-trivially two-forms and τ. The two 2-forms transform as a vector[18]

$$\begin{pmatrix} B_2 \\ C_2 \end{pmatrix} = \begin{pmatrix} d & c \\ b & a \end{pmatrix}\begin{pmatrix} B_2 \\ C_2 \end{pmatrix}\ , \tag{1.38}$$

while the scalar τ transforms as

$$\tau \to \frac{a\tau + b}{c\tau + d}\,\tau\ . \tag{1.39}$$

Within this group there is the transformation with $b = 1$, $c = -1$ and the other parameters zero; it sends $\tau \to -1/\tau$. Using the fact that the exponent of the dilaton is the string coupling (1.17), we can see that this maps $g_s \to 1/g_s$. This transformation is better known as *S-duality*, which we will have more to say about in the next section. This concludes for now the discussion on the, for us relevant, supergravities. Later on, in subsection 1.2.5, we will come back to brane solutions of string theory and supergravity. First we turn back to string theory and discuss some important dualities.

1.2.4 The Dual Pictures

This section will have a brief look at some essential dualities for string theory and M-theory. We will not exhaustively discuss all examples of them, but instead, we show the possible dualities and pick a few relevant examples for our purposes.

S-duality The first to consider is called S-duality, which is short for strong-weak duality. This duality is thus concerned with the coupling strength of the theory. It is not only known and used within string theory, but also shows up in quantum field theories. For our purposes, however, let's first consider the Type IIB theory; as it turns out the S-duality here is part of a larger symmetry group SL(2,$\mathbb{Z}$), which

[18] Note that the matrix has to be invertible, real and $ad - bc = 1$.

is the discrete version of the SL(2,$\mathbb{R}$) symmetry of the previous section. The duality sends the string coupling $g_s \to \frac{1}{g_s}$, and in this case, it will map the IIB theory to itself.
For the Type IIA theory, something more intriguing happens. As it turns out, M-theory, when compactified on a circle, is dual to the IIA theory. In the low-energy limit, we already mentioned this, but the duality runs a bit further than this. The radius of the circle is given by

$$R_{11} = \ell_s \, g_s \ ,$$

with ℓ_s the string length and, more importantly, g_s the string coupling. For the perturbative regime of small g_s, the radius will tend to zero, and we have 'ordinary' ten-dimensional string theory. When we now send $g_s \to \frac{1}{g_s}$ we find that the circle radius goes to infinity; it decompactifies. So the S-duality relates the IIA theory to the eleven-dimensional M-theory. There exist other S-dualities between string theories, for example, between Type I and the SO(32) heterotic string theory, but since we will not be using these, we will not go into detail.

T-duality The name is short for target-space duality. This duality arises when we consider theories that are compactified on circles or tori. If we were to consider purely bosonic, closed, string theories, one compactified on a circle with radius R and the other with $\tilde{R} = \alpha'/R$, then T-duality maps these to one another by

$$X_R \to -X_R \quad X_L \to X_L \ , \tag{1.40}$$

where $X_{L,R}$ denote the left and right-movers, respectively. A similar story holds for the Type II string theories when compactified on a circle. When we compactify one of them, say IIA, on a circle with radius R, it turns that T-duality maps it to Type IIB theory compactified on a circle with radius $\frac{\alpha'}{R}$. We already saw that M-theory on a circle was dual to IIA, so combining these facts teaches us that M-theory on a two-torus is dual to IIB.

For compactifications on tori, we usually talk about the T-duality group: this group is, in some sense, the generalization of the $R \to \frac{1}{R}$ symmetry for circles we just mentioned. It acts upon the coordinates, background fluxes and also includes shifts symmetries. When compactifying on a T^n, the resulting T-duality group for Type II theories will be SO(n,n,$\mathbb{Z}$). If we were to consider the O(n,n,$\mathbb{Z}$) group, we can also interchange the Type IIA and Type IIB theories.

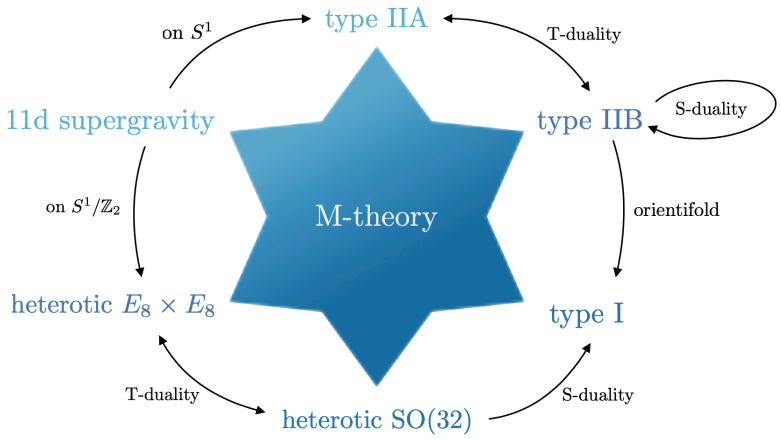

Figure 1.5: *This diagram shows the various dualities and relations between string theories, 11D supergravity, and M-theory. The star indicates that all other theories are certain limits of M-theory. Figure from [21].*

Apart from the Type II theories, there is also a T-duality between the two heterotic string theories. An overview of the different dualities is shown in Figure 1.5.

U-duality The last duality we will shortly mention is the so-called U-duality [22], which unites the previous two dualities into a larger symmetry group. This particular symmetry group is vital for us since we will use it for Scherk-Schwarz reductions in chapter 2. In the specific example that we will consider, we will first be compactifying Type IIB supergravity on a T^4 which has an SO(4,4) T-duality group. The total symmetry (or duality) group for the supergravity is SO(5,5,$\mathbb{R}$), which contains the T-duality group. The U-duality group for string theory is then the discrete version, i.e. SO(5,5,$\mathbb{Z}$).

1.2.5 Branes

String theories describe more than just strings; they also contain non-perturbative, extended objects called *D-branes* or Dp-branes (with p the spatial dimension). These branes are objects upon which open strings can end. The Dirichlet boundary conditions, which we saw in subsection 1.2.2, indicate that the endpoints of an open string are fixed in those spacetime directions; this is the origin of their name: Dirichlet-branes. If we have an open string that has Dirichlet boundary conditions

in p directions and Neumann boundary conditions in the rest, we find that the open string endpoint is confined to a Dp-brane. A major leap in understanding D-branes was made by Polchinski [23], when he realized that the branes carry charge under the RR-fields in string theory. This allowed the identification of the Dp-branes with the supergravity analog called *p-branes*. A p-brane couples to a $(p+1)$-form field by an interaction as

$$S_{\text{int}} = \mu_p \int A_{p+1} \ , \tag{1.41}$$

which can be seen as a generalization of the coupling of a charged particle to a gauge field. We can also consider the worldvolume theory of the brane, which is known as the Dirac-Born-Infeld (DBI) action. The massless bosonic part[19] of this action is given by

$$S = -T_p \int \mathrm{d}^{p+1}\sigma \mathrm{e}^{-\Phi} \sqrt{-\det(G + B_2 + 2\pi\alpha' F)} \ , \tag{1.42}$$

where $F = \mathrm{d}A$ is the field strength of a gauge field, B_2 is the pullback of the Kalb-Ramond form to the brane and G is given as

$$G_{ab} = \eta_{\mu\nu} \partial_a X^\mu \partial_b X^\nu \ , \tag{1.43}$$

with the a, b indices on the worldvolume and μ, ν in the ten-dimensional spacetime. Before we consider how these branes look in supergravity, we consider what happens with the D-branes under T-duality. The duality acts on the open string boundary conditions in the circle direction by interchanging the Neumann and Dirichlet conditions. We can then distinguish two situations: the D-brane is wrapped on the circle or it lies in directions orthogonal to the circle. This results in

$$\begin{aligned} \text{Wrapped} &: \text{D}p\text{-brane} \to \text{D}(p-1)\text{-brane} \ , \\ \text{Unwrapped} &: \text{D}p\text{-brane} \to \text{D}(p+1)\text{-brane} \ , \end{aligned}$$

where the last line follows from the fact that the Dirichlet conditions change to Neumann. To summarize: D-branes that wrap the circle are mapped to those that don't and vice-versa.

From the supergravity point of view

To find the p-branes in supergravity, we can solve the equations of motion that follow from the supergravity actions. First, we will consider the ten-dimensional Type II

[19] There also exist Chern-Simons terms, but they will not be important for us.

theories. Let us consider the spacetime symmetries that exist in the presence of these branes. Before we add the branes, there is an SO(1,9); when introducing a p-dimensional brane, we find

$$\mathrm{SO}(1,9) \to \mathrm{SO}(1,p) \times \mathrm{SO}(9-p) \ . \tag{1.44}$$

The brane breaks the Lorentz-symmetry to its spacetime direction, and the rightmost group arises due to rotations around the directions orthogonal to the brane. We will place one extra demand upon the brane solutions: they are *extremal*, which we require for the preservation of supersymmetry.[20] In particular, the branes will satisfy the Bogomol'ny-Prasad-Sommerfield, or BPS, bound, which relates the mass (or mass density) to the charge of the brane. The extremal branes are 1/2 BPS states, meaning that they preserve half of the supersymmetry. The p-brane solution, in string frame, is found to be[21]

$$\mathrm{d}s^2 = H_p^{-1/2}[-\mathrm{d}x_0^2 + \mathrm{d}x_1^2 + \cdots + \mathrm{d}x_p^2] + H_p^{1/2}[\mathrm{d}r^2 + r^2\mathrm{d}\Omega_{8-p}^2] \ , \tag{1.45}$$

$$\mathrm{e}^{\Phi} = H_p^{\frac{3-p}{4}} \ , \tag{1.46}$$

$$C_{p+1} = (H_p^{-1} - 1)\mathrm{d}x^0 \wedge \cdots \wedge \mathrm{d}x^p \ , \tag{1.47}$$

and all other fields are set to zero. The H_p is a harmonic function given by

$$H_p = 1 + \frac{Q_p}{r^{7-p}} \ , \tag{1.48}$$

and Q_p is the charge of the p-brane. When there are multiple branes present, we can write $Q_p = c_p N_p$, where N_p is the number of branes, and c_p is the charge of a single brane, which we will say more about in chapter 2. So far, we have considered branes charged under RR-fields; what if the brane is charged under the Kalb-Ramond field? When electrically charged, this turns out to be nothing but the fundamental string, and the magnetically charged brane is the so-called NS5-brane.

Looking at M-theory

So far, we have been discussing the ten-dimensional theories, but let's switch over to M-theory for a bit. We saw before, subsection 1.2.2, that the low-energy description

[20] This ensures that the solutions are stable. Also, the solutions are truly 'black', the temperature of the extremal solutions is zero.

[21] When C_{p+1} is one of the form fields present in, say, the IIB theory, the brane is said to be *electrically* charged. If C_{p+1} is, however, the Hodge dual of one of the IIB forms, the brane is said to be *magnetically* charged.

of M-theory, eleven-dimensional supergravity, contains a three-form field A_3. By our previous discussion, we can then conclude there exist two kinds of branes in the theory: M2-branes, which are charged by A_3 electrically, and M5-branes that are charged by the Hodge-star of A_3, hence charged magnetically. The M2-brane solution in the 11d supergravity is

$$\mathrm{d}s^2 = H^{-2/3}\mathrm{d}x^\mu \mathrm{d}x^\nu \eta_{\mu\nu} + H^{1/3}\mathrm{d}x^m \mathrm{d}x^n \delta_{mn} \ , \tag{1.49}$$

$$A_3 = H^{-1}\mathrm{d}t \wedge \mathrm{d}x^1 \mathrm{d}x^2 \ , \tag{1.50}$$

where H is again a harmonic function, dependent on the radial coordinate in the transverse space:

$$H(r) = 1 + \frac{q}{r^6} \ . \tag{1.51}$$

A similar solution can be written down for the M5-brane. Before we move on, we can consider what happens with the M-theory branes when we reduce M-theory on a circle, which yields the IIA theory. The results depend on whether the branes lie on the circle. If the M2-brane is wrapped on the circle, we obtain the fundamental string in IIA, and if it is orthogonal to the circle, we get a D2-brane. The M5-brane on the circle similarly yields a D4-brane, but when it is orthogonal to the circle, we obtain an NS5-brane.

1.2.6 Building Black Holes

The branes we have discussed so far are in some sense 'black'; as we take the limit of $r \to 0$ we find that the solutions have a horizon.[22] There are more things we demand of our black hole solutions, most importantly that they will have a finite, non-zero entropy. By the Bekenstein-Hawking entropy formula, (1.6), a black hole has non-zero entropy if its event-horizon has a non-zero area. This absence of a horizon furthermore implies that black holes with an area of zero have a naked singularity, which are conjectured to not exist in the cosmic censorship conjectures.

So let us use some of the techniques of previous sections to create a physically acceptable black hole. In particular we will consider a five-dimensional black hole, since it will play a role later in chapter 2. One way to construct them is to start with

[22] That the horizon is located at $r = 0$ is a feature of the *isotropic* coordinates that we have used so far.

M-theory on a six-torus and place three orthogonal M2-branes together to obtain a M2⊥M2⊥M2 solution. We can then apply dualities in the following manner

$$\text{M-theory} \xrightarrow{R_{10}} \text{IIA} \xrightarrow{T_{567}} \text{IIB} \tag{1.52}$$

where R_{10} denotes reduction of the tenth spatial dimension, and T_{567} indicates T-dualities in the 5,6 and 7 directions. Note that we end up with Type IIB theory on $T^4 \times S^1$, where we take the circle to be denoted by the x_5 and the torus by y_m with $m = 1, 2, 3, 4$. Denoting an M2-brane that is extended in the (i, j) directions by M2(i, j), the dualities act as follows

$$\begin{aligned} \text{M2}(8,9) &\xrightarrow{R_{10}} \text{D2}(8,9) \xrightarrow{T_{567}} \text{D5}(5,6,7,8,9) \\ \text{M2}(6,7) &\xrightarrow{R_{10}} \text{D2}(6,7) \xrightarrow{T_{567}} \text{D1}(5) \\ \text{M2}(5,10) &\xrightarrow{R_{10}} \text{NS1}(5) \xrightarrow{T_{567}} \text{P}(5) \end{aligned} \tag{1.53}$$

In the last transformation we end up with a gravitational wave in the 5-direction, meaning there is a non-zero amount of momentum present in the resulting D1-D5-P system. The solution in the Type IIB theory is given as

$$\begin{aligned} \mathrm{d}s^2 &= H_1^{-1/2} H_5^{-1/2} [-\mathrm{d}t^2 + \mathrm{d}x_5^2 + K(\mathrm{d}t - \mathrm{d}x_5)^2] + H_1^{1/2} H_5^{1/2} [\mathrm{d}r^2 + r^2 \mathrm{d}\Omega_3^2] \\ &\quad + H_1^{1/2} H_5^{-1/2} [\mathrm{d}y_1^2 + \cdots + \mathrm{d}y_4^2] \ , \\ \mathrm{e}^{-2\phi} &= H_1^{-1} H_5 \\ C_{05} &= H_1^{-1} - 1 \ , \\ (*C)_{056789} &= H_5^{-1} - 1 \ , \end{aligned} \tag{1.54}$$

where we see that, as expected, the D1-brane is charged under C_2 and the D5-brane under the Hodge-dual of C_2. The harmonic functions are given by

$$H_1 = 1 + \frac{Q_1}{r^2} \ , \qquad H_5 = 1 + \frac{Q_5}{r^2} \ , \qquad H_K = 1 + K = 1 + \frac{Q_K}{r^2} \ . \tag{1.55}$$

As we mentioned before the branes are BPS objects, and we can wonder how many supercharges are conserved by this combined configuration. To investigate this, we can investigate the Killing spinors, and how many independent components they have. By considering the starting point with M2-branes (1.53), and realizing that every orthogonal M2-brane breaks half of the supersymmetry, we could already guess that it preserves 1/8. Nevertheless, let us look a bit more formally: Type IIB theory is a chiral $(2, 0)$ theory and contains two spinors of the same 10D chirality,

which we denote by ϵ_L and ϵ_R.[23] The D1 and D5-branes impose the following constraints on the spinors (see e.g. [24])

$$\Gamma^0\Gamma^5\epsilon_L = \epsilon_R \ , \tag{1.56}$$

$$\Gamma^0\Gamma^5\Gamma^6\Gamma^7\Gamma^8\Gamma^9\epsilon_L = \epsilon_R \ . \tag{1.57}$$

The momentum in the x_5 direction imposes the following additional independent constraint

$$\Gamma^0\Gamma^5\epsilon_L = \epsilon_L \ , \tag{1.58}$$

which, when combined with the other constraints, implies the same constraint on the ϵ_R spinor. So, in total, we can see that the independent components in the spinors are halved three times, meaning that the D1-D5-P system is 1/8 BPS.

Down by Five Dimensions

The five-dimensional black hole solution can be found by compactifying over the $T^4 \times S^1$, using the ansatz

$$\mathrm{d}s_{10}^2 = \mathrm{e}^{2\chi}\mathrm{d}y^m\mathrm{d}y_m + \mathrm{e}^{2\psi}(\mathrm{d}x_5^2 + A_\mu \mathrm{d}x^\mu)^2 + \mathrm{e}^{-(8\chi+2\psi+\phi)/3}\mathrm{d}s_5^2 \ , \tag{1.59}$$

where χ, ϕ and ψ are scalar fields, the index μ runs over $1, 2, 3, 4$ and A_μ denote gauge fields in the five-dimensional theory. The prefactor of the five-dimensional metric is found by demanding that it becomes the metric in the Einstein-frame. The 5D-metric is found to be

$$\begin{aligned} \mathrm{d}s_5^2 &= -H^{-2/3}(r)\mathrm{d}t^2 + H^{1/3}(r)(\mathrm{d}r^2 + r^2\mathrm{d}\Omega_3^2) \ , \\ H(r) &= H_1(r)H_5(r)H_K(r) \ . \end{aligned} \tag{1.60}$$

This is the metric of a five-dimensional black hole, and we can now investigate the entropy. To do so we first compute the area of the horizon as $r \to 0$, which gives

$$A = 2\pi^2\sqrt{Q_1Q_5Q_K} \ . \tag{1.61}$$

As we have mentioned before the charges can be written as $Q_i = c_iN_i$, where c_i are the charges of an individual brane, and N_i integers, indicating the number of

[23] The conventional notation for the spinors seems confusing since they have the same chirality in ten dimensions. The L/R denote, however, the two-dimensional worldsheet chirality.

branes or units of momentum. A derivation of the individual charges is found in, for example, [24], the product of the three charges yields

$$\sqrt{c_1 c_5 c_K} = \frac{4G_N^{(5)}}{\pi} \ . \tag{1.62}$$

Using these results we can find that the entropy of the black hole, computed by the Bekenstein-Hawking entropy (1.6), is given by

$$S_{BH} = 2\pi\sqrt{N_1 N_5 N_K} \ . \tag{1.63}$$

The black hole has a non-zero entropy, for which it is vitally important that all N_i are non-zero. This last observation shows us that if we had omitted one of the ingredients, be it one of the D-brane species or the momentum; then the black hole would have been a naked singularity. This particular solution has had quite some attention in the past, as it was also used in [12] to re-derive this entropy from the microscopic string-theory side. This work by Strominger and Vafa provided for the first time a microscopic origin of the black hole entropy. In chapter 2 we will investigate solutions like the D1-D5-P whilst breaking part of the background supersymmetry and then study how this affects the entropy. Let us now turn to another exciting topic: holography.

1.2.7 Holograms

> *the three-dimensional world of ordinary experience —the universe filled with galaxies, stars, planets, houses, boulders, and people— is a hologram, an image of reality coded on a distant two-dimensional surface. This new law of physics, known as the Holographic Principle, asserts that everything inside a region of space can be described by bits of information restricted to the boundary.*
>
> – Leonard Susskind, *The Black Hole War*

The physics world was shocked in 1997 when Maldacena published his paper on the Anti-de Sitter / Conformal Field Theory duality (AdS/CFT) [25]. This proposal was the first string theory-based example of holography: the phenomenon whereby a higher-dimensional theory is equivalently described by a lower-dimensional one, thought of by 't Hooft [26] and popularized by Susskind [27].

The AdS/CFT duality was discovered by looking at stacks of N D3-branes from different perspectives. First, we can consider the D3-branes from a microscopic point of view, where there exist closed strings in the vacuum and open strings that end on the stack of D3-branes. We can consider only the massless excitations if we take the low energy limit, meaning we obtain Type IIB supergravity in 10D Minkowski space in the bulk from the closed strings. For the open string sector we can consider the DBI-action (1.42) which, when expanded in α', yields a maximally supersymmetric Yang-Mills theory. From the first point of view, we thus have two decoupled systems: free IIB supergravity in the bulk, and for the D3-branes, we find an $\mathcal{N} = 4$, $D = 4$ SYM theory.
Now, we also know that D-branes are objects that source fields in the supergravity theory. When considering this perspective at low energies, we get a similar decoupling. The excitations that exist close to the brane, $r \ll R := Q_3^{1/4}$, will be decoupling from those that exist far away, $r \gg R$.[24] In other words, there will be excitations that have such long wavelengths that they will not 'feel' the brane anymore, while the others can't escape the gravity well of the brane. The long-range excitations constitute, once again, IIB supergravity in 10D Minkowski and the short-range ones constitute the near-horizon physics of the branes. The latter consists of an $\mathrm{AdS}_5 \times \mathrm{S}^5$ geometry. We find an equal IIB supergravity in the bulk for both perspectives, so we are now led to identifying the $\mathcal{N} = 4$, $D = 4$ SYM theory with the IIB supergravity in $\mathrm{AdS}_5 \times \mathrm{S}^5$. Since the five-sphere is compact, we usually say that the CFT_4 is dual to AdS_5, and in general that an AdS in $D+1$ dimensions is dual to a D-dimensional CFT.

AdS / CFT Dictionary

Let us be a bit more precise in the couplings and limits that we take. The string coupling constant is g_s, the Yang-Mills coupling is denoted by g_{YM}, L represents the AdS radius. The two theories are then related by

$$g_{YM}^2 = 2\pi g_s \ , \qquad 2\lambda = 2g_{YM}^2 N = \frac{L^4}{\alpha'^2} \ , \tag{1.64}$$

where we introduced the 't Hooft coupling $\lambda = g_{YM}^2 N$. As for the limits: in the weakest form of the AdS/CFT duality, we take limits on the string theory side to

[24] The specific power of Q_3 arises due to the harmonic functions $f = 1 + \frac{Q_3}{r^4}$.

end up in supergravity. The limits consist of first taking the limit $N \to \infty$ and subsequently taking $\lambda \to \infty$, making sure that g_s is small. By (1.64), these limits imply that the string length is much smaller than the AdS radius, meaning we take the point particle limit of string theory and hence obtain supergravity. So this form of the AdS/CFT duality states that $\mathcal{N} = 4$, $D = 4$ Yang-Mills with gauge group SU(N) is dual to Type IIB supergravity with a radius of curvature L along with N units of flux (due to the brane charges). This duality is a strong/weak duality because the gauge theory is strongly coupled, and the supergravity is weakly curved. Stronger forms of the duality are less stringent than the weak form on the limits of N and λ.

Let us now consider the (bosonic) symmetries on both sides. The SYM theory is conformal in four dimensions, and the four-dimensional conformal group is SO(2,4). Furthermore, the R-symmetry in the theory is given by SU(4) $\cong$ SO(6). For AdS_5, the isometry group is SO(2,4) and the isometry group of S^5 is SO(6); the symmetries thus coincide on both ends.
The next important step is to realize how the bulk fields ϕ are related to the operators in the CFT, $\mathcal{O}$. The one-to-one correspondence between these two is realized as[25]

$$\int_{\phi_0} \mathcal{D}\phi \, \mathrm{e}^{-S_{\text{string}}} = \left\langle \mathrm{e}^{\int \mathrm{d}^4 x \, \phi_0 \, \mathcal{O}} \right\rangle_{\text{CFT}} \ , \tag{1.65}$$

where the subscript ϕ_0 means that the paths of ϕ are on-shell and at the boundary of the AdS-space take the value ϕ_0. The partition function of the string theory is thus identified with the generating functional for correlation functions. The identification of objects between the two theories is usually called the *dictionary*. For example, we identify the energy-momentum tensor in the CFT with the metric in the bulk. In this case, the boundary value is the metric on the boundary.[26] A more elaborate introduction to the duality can be found in, for example, [28].
Although we don't explicitly use the correspondence in this thesis often, it motivates much research. The research described in chapter 2 is from the supergravity side of things; an explanation using the AdS/CFT duality would (hopefully) teach us the microscopics of the story. In chapter 3 we discuss the embedding of near horizon limits of rotating black holes into M-theory, which provides the first step towards a gravitational dual of c and $\mathcal{I}$-extremization applicable to rotating geometries. The

[25] Note that we have switched to a Euclidean signature, if

[26] To be precise, it is defined up to a conformal rescaling, so ϕ_0 would correspond to the boundary value of the conformal class of the metric.

models in chapter 5 and chapter 4 can be viewed as duals of black hole physics in some limits, the one-dimensional SYK-model (in certain limits) is thought to be dual to the two-dimensional Jackiw-Teitelboim gravity [29, 30]. The quark-gluon plasma created in heavy-ion collisions can be linked to five-dimensional black hole physics via the AdS/QCD correspondence [31].

1.3 SYK Models

So far, our discussion has concerned string theory and how to build black holes within string theory. We now turn our attention to the Sachdev-Ye-Kitaev (SYK) model [32,33]. Instead of the ten dimensions of string theory, this model has only one: time. In the context of studying black holes, the one-dimensional model is thought to be dual to a two-dimensional gravity model that can contain black holes. There are two reasons why we expect this duality, the first being that there is emergent conformal symmetry in the IR limit. So by the AdS/CFT correspondence, we could learn about the two-dimensional black holes by studying the one-dimensional model. A second relevant property is that the SYK model is *maximally chaotic*. Before we turn to the SYK model, let's shortly review what chaos means and what it has to do with black holes.

Chaos and Scrambling

Black holes are *fast scramblers* , meaning they quickly scramble any information thrown into the black hole. More technically, we can consider a complex, chaotic quantum system with many degrees of freedom N (for example, a black hole) that we initially place into a pure state. After some time, the system evolves in the following sense: if we consider a subsystem of size $m \ll N$, we find that the density matrix approaches a maximally mixed state. Computing the entropy of this mixed state tells us how much entanglement exists between m and m^c (since it is effectively computing the entanglement entropy between the two). In other words, the scrambling tends to send the entanglement entropy of the subsystem to its maximal value. Now, if this last statement is true for any subsystem with size $m < N/2$, we call the system *scrambled*. In practical terms, we need to consider half of the total system to extract information since the data is scrambled over the system. Consider now adding one bit of information to the system. Initially, the system is then no longer scrambled since we can find information by looking only

at one bit. The *scrambling time* is then defined as the time scale until the bit of information is scrambled over the system. What does it have to do with chaos? The chaos, or also called *the butterfly effect*, is thought to be the underlying mechanism by which black holes achieve the scrambling of information. This quantum chaos turns out to be subject to a bound [34], and black holes exactly satisfy this bound, i.e., they are the fastest possible scramblers. So if there is any theory dual to the black hole, we expect it to show this maximal chaos, which the SYK model indeed does.

What does the SYK model look like?

In chapter 4 we will be studying a generalization of the SYK model. We will introduce the 'original' SYK model and its supersymmetric variant here to provide some context for the generalized model. We will introduce the Hamiltonian of the model, the *disorder average* and afterward, we discuss the two-point function for both free Majorana fermions and the complete interacting theory. When we take the large N limit ('t Hooft limit) alongside the IR limit, we can obtain an expression for this full two-point function. Afterward, we will focus on the four-point function, which has a unique role in computing the chaos exponent or Lyapunov exponent. In the next section we discuss the effective action to rewrite the theory in terms of a bilocal action. The last section shortly discusses the supersymmetric SYK model.

The SYK model [35] is a simplified version of the Sachdev-Ye model [32]. The model contains N Majorana fermions that randomly interact with $q \in 2\mathbb{Z}$ other Majorana fermions. In particular, we will first discuss the case $q = 4$ where four fermions interact with each other. The Hamiltonian is then given by:

$$H = \frac{1}{4!} \sum_{ijkl} J_{ijkl}\, \chi_i\, \chi_j\, \chi_k\, \chi_l \ , \tag{1.66}$$

where χ denote the Majorana fermions, which obey the commutation relations

$$\{\chi_i, \chi_j\} = \delta_{ij} \ . \tag{1.67}$$

The coupling J_{ijkl} is completely antisymmetric in all its indices (which follows from H being Hermitian and the anti commutation of the χ fields). From the

Hamiltonian we can also obtain the Lagrangian:

$$L = \frac{1}{2}\,\chi_j\,\frac{d}{d\tau}\,\chi_j - H\ . \tag{1.68}$$

From the Lagrangian we can find that the fermions χ have dimension 0 and the coupling in the Hamiltonian (for any q) has dimension 1, the dimension of an energy scale. The Euler-Lagrange equation for the fermion yields

$$\dot{\chi}_i = \frac{1}{3!}\,J_{iklm}\chi^k\,\chi^l\,\chi^m\ . \tag{1.69}$$

Lastly, the model has quenched disorder where the couplings J_{ijkl} are randomly drawn from a normal distribution [35]

$$P(J_{ijkl}) = \sqrt{\frac{N^3}{12\pi J^2}}\exp\left(\frac{-N^3\,J_{ijkl}^2}{12J^2}\right)\ . \tag{1.70}$$

Where J is the dimension 1 (energy) parameter that characterizes the distribution. To find the average $\langle J_{ijkl}^n\rangle$ ($n \in \mathbb{Z}^+$) we simply integrate over the probability distribution (note that there is no sum in the expression below)

$$\langle J_{ijkl}^n\rangle = \int d(J_{ijkl})\,J_{ijkl}^n\,P(\,J_{ijkl}\,)\ , \tag{1.71}$$

which yields us the two results:

$$\langle J_{ijkl}\rangle = 0\ , \tag{1.72}$$

$$\langle J_{ijkl}^2\rangle = \frac{3!\,J^2}{N^3}\ . \tag{1.73}$$

We will also use $\bar{X}$, for some X dependent on J_{ijkl}, to denote the averaging over the distribution.

One of the nice things about the SYK model is that we can write down explicit results for the n point functions under a large N and strong coupling limit. Let us, as an example, show the results for the two-point function.

1.3.1 Two-Point Functions

The combination of large N and strong coupling limits will severely limit the diagrams that can show up in the loop corrections, and in fact all will be of a type called 'melons'. Let us first see the influence of the large N limit. Consider for

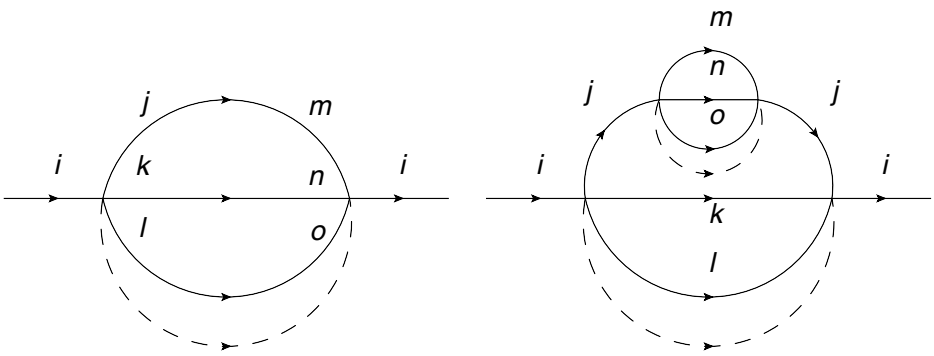

Figure 1.6: These diagrams will contribute to leading order in N. The dotted line indicates the disorder average, which forces the indices to be equal. Note that the indices in the loops are summed over.

example the diagram in Figure 1.6 which will contribute to the leading order in N; the dotted line indicates the disorder average. The expression for the leftmost diagram is:

$$\frac{C}{(4!)^2}\sum_{\substack{jkl\\mno}}\langle J_{ijkl}\,J_{imno}\rangle\,G_{0,jm}\,G_{0,kn}\,G_{0,lo}=J^2G_0(\tau_1,\tau_2)^3\;, \tag{1.74}$$

where we made use of (1.73) and the combinatorial factor $C=\binom{4}{3}\binom{4}{3}3!$. There are, however, also diagrams that don't contribute at this order. For example take the diagrams in Figure 1.7 which can be checked to contribute as $\frac{1}{N^d}$ with $d>0$.

We can now generalize the expression for the self energy by realizing that the only kinds of diagrams that contribute are those similar to (1.74). The diagrams need in general to have a disorder average over their incoming and outgoing lines and the lines must not cross any other lines in the diagram. We can thus construct the full two-point function as shown in (1.8). It then becomes clear that the total expression for the self energy becomes [36, 37]

$$\Sigma(\tau_1,\tau_2)=J^2G(\tau_1,\tau_2)^3\;, \tag{1.75}$$

where G now denotes the full two-point function. Besides the above expression, we can also express the full two-point function as a sum of all the one particle irreducible (1PI) diagrams by

$$\frac{1}{G(\omega)}=-i\omega-\Sigma(\omega)\;. \tag{1.76}$$

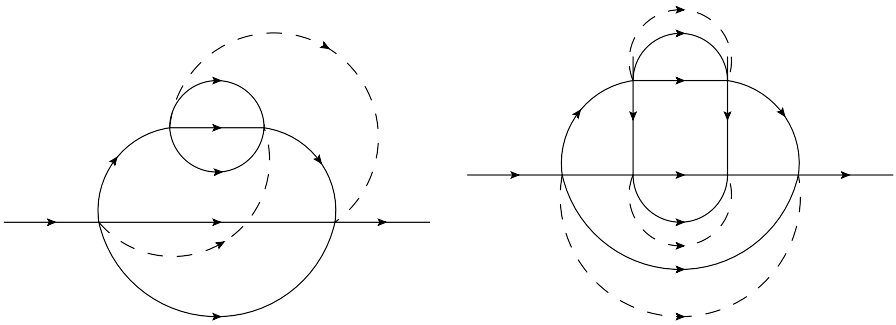

Figure 1.7: Here we show two diagrams that do not contribute at leading order in N the left diagram will contribute at N^{-5} and the right diagram as N^{-1}.

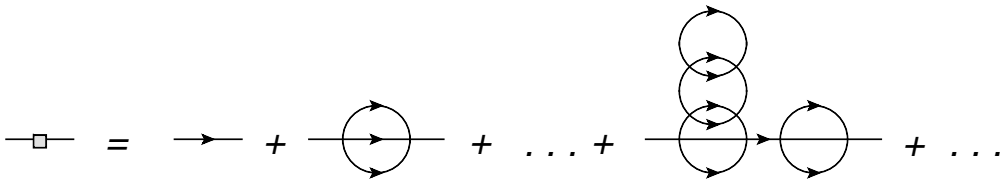

Figure 1.8: The full two-point function is denoted by the line with the box. On the right side, we omitted the dotted lines indicating the disorder averages. They are, however, all implemented in the same manner as shown in Figure 1.6.

When we take (1.75) and (1.76) together, they completely determine the full two-point function. We can solve these equations in the strong coupling (or low energy) limit: $\omega \ll J$.

Cranking the Coupling

In the strong coupling limit we may ignore the first term that appears in (1.76) such that we can obtain the following equation:

$$\int d\tau' G(\tau,\tau')\,\Sigma(\tau',\tau'') = -\delta(\tau-\tau'')\,, \tag{1.77}$$

which, by using (1.75), becomes (notice the familiarity with the Schwinger-Dyson equations)

$$J^2 \int d\tau' G(\tau,\tau')\,G(\tau',\tau'')^3 = -\delta(\tau-\tau'')\,. \tag{1.78}$$

We can now make an ansatz for G by using the conformal symmetry and anticommutativity of fermions

$$G_c(\tau) = A\frac{\mathrm{sgn}(\tau)}{|\tau|^{2\Delta}} , \tag{1.79}$$

where A and Δ are constants and the subscript c denotes the conformal limit. Indeed, it can be checked that the expression is invariant under SL(2,$\mathbb{R}$) transformations. Plugging this into (1.78), we can find that the full two-point function is given by

$$G(\tau) = \left(\frac{1}{4\pi\, J^2}\right)^{\frac{1}{4}} \frac{\mathrm{sgn}(\tau)}{\sqrt{|\tau|}} . \tag{1.80}$$

Similarly, there are techniques for computing four point functions using ladder diagrams, and there are also results for n-point functions [38].

Conformal symmetries and heating up

There is an interesting consequence of taking the IR limit for the equations defining the full two-point function: emergent conformal symmetry. We can see that (1.78) has Conf($\mathbb{R}^1$) $\cong$ Diff($\mathbb{R}^1$) symmetry as follows[27] Suppose that $G(\sigma, \sigma'')$ solves the equation:

$$J^2 \int d\sigma' G(\sigma,\sigma')\, G(\sigma',\sigma'')^3 = -\delta(\sigma - \sigma'') .$$

We now let $\sigma = f(\tau)$ such that we obtain

$$J^2 \int \left|\frac{df}{d\tau'}\right| d\tau' G(f(\tau), f(\tau'))\, G(f(\tau'), f(\tau''))^3 = -\frac{1}{|f'(\tau'')|}\delta(\tau - \tau'') , \tag{1.81}$$

where we used that $\delta(f(x) - f(x_0)) = \frac{1}{|f'(x0)|}\delta(x - x_0)$. It now becomes clear that this is equal to (1.78) if we have

$$G(\tau,\tau') = |f'(\tau)\, f'(\tau')|^{\Delta}\; G(f(\tau), f(\tau')) , \tag{1.82}$$

where, in our current case, $\Delta = \frac{1}{4}$. So we find that (1.78) is invariant under the reparametrisation group Diff($\mathbb{R}$). The symmetry is, however, spontaneously broken by the explicit solution for G in (1.80). This solution no longer has the full symmetry group but instead is only invariant under the subgroup SL(2,$\mathbb{R}$). We can use the conformal symmetry to change the domain to a compact manifold, for

[27] Conf($\mathbb{R}^1$) $\cong$ Diff($\mathbb{R}^1$) follows because there is no notion of an angle in one-dimension, so all smooth transformations are conformal.

example S^1. We pick $f(\tau) = e^{2\pi i t/\beta}$ such that we map the line into the circle, and with this we can obtain a result for finite temperature:

$$G_\beta(\tau) = -\frac{\pi^{\frac{1}{4}}}{\sqrt{2\,\beta\,J}} \frac{1}{\sqrt{\sin(\frac{\pi\tau}{\beta})}} \operatorname{sgn}(\tau) \,. \tag{1.83}$$

1.3.2 Lyapunov and Chaos

As mentioned in the introduction, the SYK model saturates the chaos bound. This chaos bound, introduced in [34], can be found using an Out of Time Order Correlation (OTOC) function. In particular one can consider two Hermitian operators V and W separated by a time distance t. The chaos can then be investigated by the OTOC

$$F(t) = tr\left[y\,W(t)\,y\,V(0)\,y\,W(t)\,y\,V(0)\right] \,, \tag{1.84}$$

where $y = \rho(\beta)^{1/4}$. So the thermal density matrix ρ is split into the four factors of y. One may then furthermore show that for a large N CFT, holographically described by Einstein gravity [34], that

$$F(t) = f_0 - \frac{f_1}{N^2} \exp\left(\frac{2\pi}{\beta}\, t\right) + \mathcal{O}(N^{-4}) \,. \tag{1.85}$$

The conjecture about the bound on chaos then reads: chaos in thermal quantum systems (with many degrees of freedom) can never develop faster than the above holographic result. In chaotic systems the correlators are expected to grow exponentially

$$F_d - F(t) \propto \exp\left(\lambda_L\, t\right) \,, \tag{1.86}$$

where λ_L the Lyapunov exponent and F_d is the product of the disconnected correlators. Furthermore, at some time between the scrambling time, mentioned in the introduction of the SYK section, and the dissipation time, the exponential decay time of two-point functions, we have that $F(t) \approx F_d$. The conjecture is then stated as:

$$\frac{d}{dt}\left(F_d - F(t)\right) \leq \frac{2\pi}{\beta}\left(F_d - F(t)\right) \,. \tag{1.87}$$

Or in terms of the Lyapunov exponent:

$$\lambda_L \leq \frac{2\pi}{\beta} \,. \tag{1.88}$$

As it turns out the SYK saturates this bound. To derive this explicitly requires considering the non-conformal contribution to the four point function in exhaustive detail. In particular we would consider:

$$Tr\ [y\,\chi_i(t)\,y\,\chi_j(0)\,y\,\chi_i(t)\,y\,\chi_j(0)]\ . \tag{1.89}$$

Then, as derived in [37], the non-conformal contribution will yield a factor in the four point function as:

$$C\,\beta\,J\left(1-\frac{\pi}{2}\cosh\frac{2\pi t}{\beta}\right)\ , \tag{1.90}$$

where C is a constant. This indeed shows the exponential behaviour with a Lyapunov exponent $\lambda_L = \frac{2\pi}{\beta}$, such that SYK saturates the chaos bound. In chapter 4 we will use a different, easier, method to find the maximally chaotic behaviour.

1.3.3 Effective Action

Another useful way to understand the model is by a path integral representation over bilocal fields. This can be used to find the free energy, the entropy and might be a good starting point for a holographic interpretation of the theory. We note that the results we discuss below also have a generalization including certain 'flavours' of χ's, see [39]. Now, in order to find the free energy (or action) we would use naively $-\beta F = \log Z$. Due to the disorder averaging, however, we have to consider $\overline{Z}$, and for the free energy $F = \overline{\log Z}$. The problem with our naive assumption is that $\overline{\log Z} \neq \log(\overline{Z})$ in general. The solution to this problem is the so-called replica trick (see [40] for an introduction). This is most intuitively stated as

$$\overline{\log Z} = \lim_{n\to 0}\frac{\overline{Z^n}-1}{n}\ . \tag{1.91}$$

The main idea of this equality is that we now have to calculate the disorder average over n copies of Z instead of the logarithm. This means the disorder average will boil down to doing Gaussian integrals. The replica trick can also be written in a more useful way as

$$\overline{\log Z} = \lim_{n\to 0}\frac{1}{n}\log\left(\overline{Z^n}\right)\ . \tag{1.92}$$

Following the replica idea we will now compute the disorder average of M copies of the partition function.

$$\begin{aligned}\overline{Z^M} = \int \mathcal{D}\chi_i^\alpha \, \mathcal{D}J_{ijkl} \exp\left\{-a \sum_{ijkl} J_{ijkl}^2\right\} \\ \times \exp\left\{-\sum_{\alpha=1}^{M} \int d\tau \, \left(\frac{1}{2}\sum_i \chi_i^\alpha \frac{d}{d\tau}\chi_i^\alpha - \frac{1}{4!}\sum_{ijkl} J_{ijkl}\, \chi_i^\alpha\, \chi_j^\alpha\, \chi_k^\alpha\, \chi_l^\alpha\right)\right\} ,\end{aligned} \tag{1.93}$$

where the bar denotes the disorder average, α denotes the replica index and a is the prefactor in the exponential as in (1.70). We won't show all the details here, but the straightforward computation consists out of first computing the Gaussian integral over J_{ijkl} and afterward introducing, by means of Lagrangian multipliers, bilocal fields

$$\widetilde{G}^{\alpha\beta}(\tau_1, \tau_2) = \frac{1}{N}\sum_{i=1}^{N} \chi_i^\alpha(\tau_1)\, \chi_i^\beta(\tau_2) \, . \tag{1.94}$$

As a last step we can integrate out the fermions and the resulting partition function becomes

$$\overline{Z^M} = \int \mathcal{D}\widetilde{G}\, \mathcal{D}\widetilde{\Sigma} \, \exp\left\{-M\, S_{\text{eff}}\right\} \, , \tag{1.95}$$

where S_{eff} is given by

$$\begin{aligned}S_{\text{eff}} = -\frac{N}{2} \log\det\left(\partial_\tau - \widetilde{\Sigma}\right) \\ + \frac{1}{2}\int d\tau_1\, d\tau_2 \, \left(N\, \widetilde{\Sigma}(\tau_1,\tau_2)\, \widetilde{G}(\tau_1,\tau_2) - \frac{J^2 N}{4}\left(\widetilde{G}(\tau_1,\tau_2)\right)^4\right) \, ,\end{aligned} \tag{1.96}$$

where the $\widetilde{G}$ denotes the bilocal field, and $\widetilde{\Sigma}$ arose as the Lagrangian multiplier. Note that if we vary $\widetilde{\Sigma}$ or $\widetilde{G}$ we obtain (1.76) or (1.75) respectively. This shows us that we have found an exact rewriting of our theory in terms of path integrals over bilocal fields. The computation for a general q-pt interaction is completely analogous to above and yields as a result

$$\begin{aligned}\overline{Z^M} = \int \mathcal{D}\widetilde{G}\, \mathcal{D}\widetilde{\Sigma} \, \exp\left\{M\, \frac{N}{2} \log\det\left(\partial_\tau - \widetilde{\Sigma}\right)\right\} \\ \times \exp\left\{-\frac{M}{2}\int d\tau_1\, d\tau_2 \, \left(N\, \widetilde{\Sigma}(\tau_1,\tau_2)\, \widetilde{G}(\tau_1,\tau_2) - \right.\right. \\ \left.\left. \frac{J^2 N}{q}\left(\widetilde{G}(\tau_1,\tau_2)\right)^q\right)\right\} \, .\end{aligned} \tag{1.97}$$

Lastly, we can now compute the leading order contribution to the free energy by evaluating at the saddle point and using our starting point (1.92) (which exactly divides away the M):

$$\begin{aligned}\frac{-\beta F}{N} = \frac{1}{2}\log\det\left(\partial_\tau - \Sigma\right) - \frac{1}{2}\int d\tau_1\, d\tau_2\, \left[\Sigma(\tau_1,\tau_2)\, G(\tau_1,\tau_2)\right. \\ \left. - \frac{J^2}{q}\, G(\tau_1,\tau_2)^q\right] .\end{aligned} \tag{1.98}$$

Schwarzian

A widely discussed action in relation to the SYK model is the so-called *Schwarzian* action. It arises when we consider the action at its saddle point, and subsequently consider fluctuations around these saddle points, and want an action describing such fluctuations. When we consider the low energy limit, this action has zero modes, exactly the same zero modes as we mentioned during the four point function computations. These zero modes are the fluctuations which are exactly equal to reparametrisations $\tau \to f(\tau)$. The Schwarzian action arises when we consider the non-conformal corrections in the four point function, yielding a finite action for the reparametrisations. The full derivation is involved, but described in [37]. The action is given by

$$\frac{S}{N} = -\frac{\alpha_s}{\mathcal{J}}\int d\tau\, \{f,\tau\} , \tag{1.99}$$

$$\{f,\tau\} = \frac{f'''}{f'} - \frac{3}{2}\left(\frac{f''}{f'}\right)^2 , \tag{1.100}$$

where $\{f,\tau\}$ is called the Schwarzian derivative.

1.3.4 The Supersymmetric SYK Model

In this section, we will shortly discuss the supersymmetric $\mathcal{N}=1$ SYK model, first introduced in [41]. The model we will discuss in chapter 4 will be equivalent to this model at some choice of parameters. We will shortly discuss the Hamiltonian and Lagrangian formulation, followed by the effective action.
To construct the Hamiltonian we start by considering the supercharge

$$Q = \frac{i}{3!}\sum_{ijk=1}^{N} C_{ijk}\, \chi^i\, \chi^j\, \chi^k . \tag{1.101}$$

Following the standard procedures of supersymmetry for quantum mechanics we note that

$$H = \frac{1}{2}\{Q, Q^\dagger\} \ .$$

Of course, in our case, with Majorana fermions, we simply find that $Q^\dagger = Q$ and thus $H = Q^2$. Since H must be Hermitian it follows that also Q must be and C_{ijk} must be an $N \times N \times N$ antisymmetric tensor with fixed real entries. In some analogy with the standard SYK model (see (1.73)) we now take C_{ijk} to be a random Gaussian variables with:

$$\langle C_{ijk} \rangle = 0 \ , \tag{1.102}$$

$$\langle C_{ijk}^2 \rangle = \frac{2!\, J}{N^2} \ . \tag{1.103}$$

After some manipulations we can then write the Hamiltonian as

$$H = E_0 + \frac{1}{4!} \sum_{ijkl=1}^{N} J_{ijkl}\, \chi^i\, \chi^j\, \chi^k\, \chi^l \ , \tag{1.104}$$

where we have defined the constant E_0 and a coupling J_{ijkl} as

$$E_0 = \frac{1}{8}\frac{1}{3!} \sum_{ijk=1}^{N} C_{ijk}^2 = \frac{1}{8} \sum_{1 \le i < j < k \le N} C_{ijk}^2 \ , \tag{1.105}$$

$$J_{ijkl} = -\frac{1}{8} \sum_a C_{a[ij}\, C_{kl]a} \ . \tag{1.106}$$

It is important to note that in this case J_{ijkl} are not the independent Gaussian variables, which constitutes an important difference between the supersymmetric model and the ordinary one.

Superspace and Lagrangian

Now we will obtain the Lagrangian for this supersymmetric model. In particular, we will start by deriving it in the superspace representation following [41], for which we will denote the supercharge with $\mathcal{Q}$. The superspace representation arises by introducing an anticommuting coordinate for each supercharge in the model. So in our case we essentially map (for each t in the domain):

$$t \mapsto (t, \theta) \ ,$$

where now θ is the anticommuting coordinate. In a model where $\mathcal{Q}^\dagger \neq \mathcal{Q}$ (so no Majorana fermions) one would also have the θ^* coordinate. Furthermore, we introduce the superfield

$$\Psi^i = \chi^i + \theta\, b^i \,, \tag{1.107}$$

with b a non-dynamical auxiliary field, that will linearise the supersymmetry transformations. To see this we start by considering the supercharge in this representation

$$\mathcal{Q} = \partial_\theta - \theta\, \partial_\tau \,. \tag{1.108}$$

Note that this supercharge satisfies the expected anticommutation relation $\frac{1}{2}\{\mathcal{Q}, \mathcal{Q}\} = -\partial_\tau = i\partial_t$, yielding the generator of time translations. Related to the supercharge by $t \mapsto -t$ (or taking right derivatives instead of left ones) is the covariant derivative:

$$D_\theta = \partial_\theta + \theta\, \partial_\tau \,. \tag{1.109}$$

Now we can determine how the superfield (and its components) change under supersymmetry transformations, which we will denote by δ_ϵ. For a general superfield Φ we have

$$\delta_\epsilon \Phi = (\epsilon^* \mathcal{Q} + \epsilon \mathcal{Q}^\dagger)\, \Phi \,,$$

where ϵ and ϵ^* are (infinitesimal) anticommuting constant parameters. So in our case we have only the supercharge $\mathcal{Q}$ and the above reduces to

$$\delta_\epsilon\, \Psi^i = \epsilon\, \mathcal{Q}\, \Psi^i = \epsilon b^i + \theta\, \epsilon\, \partial_\tau \chi^i \,. \tag{1.110}$$

So we find that the χ and b fields transform as follows

$$\delta_\epsilon \chi^i = \epsilon b^i \,, \tag{1.111}$$

$$\delta_\epsilon b^i = \epsilon\, \partial_\tau\, \chi^i \,. \tag{1.112}$$

The manifestly supersymmetric Lagrangian is then given by

$$\mathcal{L} = \int d\theta \left(-\frac{1}{2}\, \Psi^i\, D_\theta\, \Psi^i + \frac{i}{3!}\, C_{ijk}\, \Psi^i\, \Psi^j\, \Psi^k \right) \,, \tag{1.113}$$

where $D_\theta = \partial_\theta + \theta\, \partial_\tau$, the covariant derivative, is obtained by taking $t \mapsto -t$ in the supercharge. Instead of writing it in this manifestly symmetric way we can also first fill in the above expressions:

$$\begin{aligned} \mathcal{L} = \int d\theta \Big[& -\frac{1}{2} \left(\chi^i + \theta\, b^i\right) \left(\partial_\theta + \theta\, \partial_\tau\right) \left(\chi^i + \theta\, b^i\right) \\ & + \frac{i}{3!}\, C_{ijk} \left(\chi^i + \theta\, b^i\right) \left(\chi^j + \theta\, b^j\right) \left(\chi^k + \theta\, b^k\right) \Big] \,. \end{aligned} \tag{1.114}$$

Then we can complete the Grassmann integral to obtain

$$\mathcal{L} = \frac{1}{2}\,\chi^i\,\partial_\tau\,\chi^i - \frac{1}{2}\,b^i\,b^i + \frac{i}{2}\,C_{ijk}\,b^i\,\chi^j\,\chi^k\ . \tag{1.115}$$

We see that, as expected, the equation of motion for b^i is algebraic:

$$b_i = \frac{i}{2} C_{ijk}\,\chi^j\,\chi^k\ . \tag{1.116}$$

And since the Lagrangian is quadratic in this non-dynamical field b we can substitute the equation of motion back into the action. When we plug (1.116) into the Lagrangian, (1.115), we see indeed that the second and third term yield the four fermion interaction as seen in (1.104). The dynamics described by this Lagrangian thus indeed reproduce those of the found Hamiltonian.

Effective actions and symmetries

In an analogous process as we followed in subsection 1.3.3 one can integrate out the disorder and derive an effective action for the supersymmetric SYK model [41]

$$\begin{aligned} Z &= \int \mathcal{D}G_{\psi\psi}\mathcal{D}\Sigma_{\psi\psi}\mathcal{D}G_{bb}\mathcal{D}\Sigma_{bb}\,e^{-S_{\text{eff}}}\ , \\ \frac{S_{\text{eff}}}{N} &= -\frac{1}{2}\log\,\det\,[\partial_\tau - \Sigma_{\psi\psi}] + \frac{1}{2}\log\,\det\,[-1-\Sigma_{bb}] \\ &\quad + \frac{1}{2}\int d\tau_1\,d\tau_2\,\left[\Sigma_{\psi\psi}(\tau_1,\tau_2)\,G_{\psi\psi}(\tau_1,\tau_2) + \Sigma_{bb}(\tau_1,\tau_2)\,G_{bb}(\tau_1,\tau_2)\right. \\ &\quad \left. -J\,G_{bb}(\tau_1,\tau_2)\,G_{\psi\psi}(\tau_1,\tau_2)^2\right]\ . \end{aligned} \tag{1.117}$$

Here, just as in the non-supersymmetric SYK, (1.96), the Σ and G are introduced by Lagrange multipliers. In this case there are two types of fields due to the appearance of both a bosonic b and a fermionic ψ. Note also the similar kinetic terms, the lack of a ∂_τ term for b is due to it's lack of dynamics.
The model has a symmetry-breaking pattern analogous to the non-supersymmetric SYK model. However, apart from the Diff($\mathbb{R}$) there is now also supersymmetry. The transformations hence include also the above introduced θ:

$$\tau \mapsto \tau'(\tau,\theta)\ , \tag{1.118}$$

$$\theta \mapsto \theta'(\tau,\theta)\ . \tag{1.119}$$

Together, these make up the so-called SDiff group. The bosonic part of these transformations is simply the group Diff($\mathbb{R}$):

$$\tau \mapsto \tau' = f(\tau) \,, \tag{1.120}$$

$$\theta \mapsto \theta' = \sqrt{\partial_\tau}\theta \,. \tag{1.121}$$

The first line is the symmetry as we had it in the original SYK model, the second line shows its action on θ. There are many more results in supersymmetric SYK models; here, we mention a few, although our list is incomplete. In [42], the notions above are extended to two dimensions, and it discusses the of problems when doing so. The article [43] discusses a bi-local collective superfield theory for both $\mathcal{N} = 1, 2$ supersymmetric SYK models. In [44] the four-point function in $\mathcal{N} = 2$ supersymmetric SYK is computed. This concludes our introduction to the SYK models, and we will continue with the topic in chapter 4.

1.4 Heavy-Ion Collisions

It is now time, once again, to make a complete switch of subjects; this time, we will focus our attention mainly on the depths below Geneva in Switzerland: CERN. About 175 meters below the ground, there is the (at the time of writing) most giant machine in the world, the Large Hadron Collider (LHC). One month a year, two beams of heavy-ions, usually lead, are accelerated to speeds very close to the speed of light, after which they are sent to collide with each other. Understandably, there is loads of energy packed into these collisions, and the resulting plasma has an extremely high temperature (*billions* of degrees in Kelvin). In this introduction we will shortly introduce quantum chromodynamics and point out some relations to the AdS/CFT correspondence. Afterward we expand on heavy-ion collisions and discuss the quark-gluon plasma.

1.4.1 Quantum Chromodynamics

In order to understand what happens at the extreme temperatures of heavy-ion collisions we will need a theory of strong interactions, which govern this regime. The best known explanations are formed by QCD, which is a gauge theory based upon the group SU(3). Its main constituents are the quarks and gluons, which exist in three so-called colors (hence the name). The Lagrangian for this gauge theory is

written as

$$\mathcal{L}_{\text{QCD}} = -\frac{1}{4}\,\text{tr}\,[G_{\mu\nu}\,G^{\mu\nu}] + \sum_{i=1}^{N_f} \bar{q}_i(i\not{D} - m_i)\,q_i \ , \tag{1.122}$$

where we have defined

$$G_{\mu\nu} = \partial_{[\mu}A_{\nu]} + g[A_\mu, A_\nu] \ , \qquad \not{D} = \gamma^\mu\,(i\partial_\mu + gA_\mu) \ . \tag{1.123}$$

The trace over the field strengths G concerns the $N_c = 3$ color indices, and the summation goes over the quark flavours N_f. In the standard model there are six flavours of quarks, denoted by q in the above Lagrangian. Sometimes, for example in holographic applications, the number of colors and flavours are left unspecified; for example in the Veneziano limit both N_f and N_c are assumed to be large, but their ratio is kept fixed.

A remarkable property of QCD concerns the coupling constant g, which we can investigate with the beta function. It turns out that the beta function is negative to the first order in perturbation theory under some reasonable condition on N_c and N_f [45, 46]. This negative beta function leads to the phenomenon known as *asymptotic freedom*, meaning that at high energies, the coupling constant decreases, and the particles become free. This behavior of the coupling constant is also seen in experiment, as shown in Figure 1.9. From the figure we can also see that around 1 GeV the coupling constant is of order one, i.e., we can no longer use perturbation theory.

At the low energy scales, we can thus no longer use the standard, perturbative techniques for understanding the behavior of particles. We won't be very interested in the low energy limit for our purposes, but let us mention one exciting feature: confinement. At low energies, it appears that all quarks confine themselves in groups such that the total color charge is zero. One way this low energy limit of QCD is still studied is using LatticeQCD, whereby the equations of QCD are solved numerically on a small lattice of points.

One last, important aspect of QCD concerns the phase diagram; the expected diagram is shown in Figure 1.10. The phase diagram is plotted with temperature and baryon chemical potential μ_B. The latter quantifies the abundance of quarks over anti-quarks. We can study highly energetic heavy-ion collisions to good approximation with zero chemical potential. In the figure also the accessible parts to LHC and RHIC experiments are shown, along with the beam energies. Note

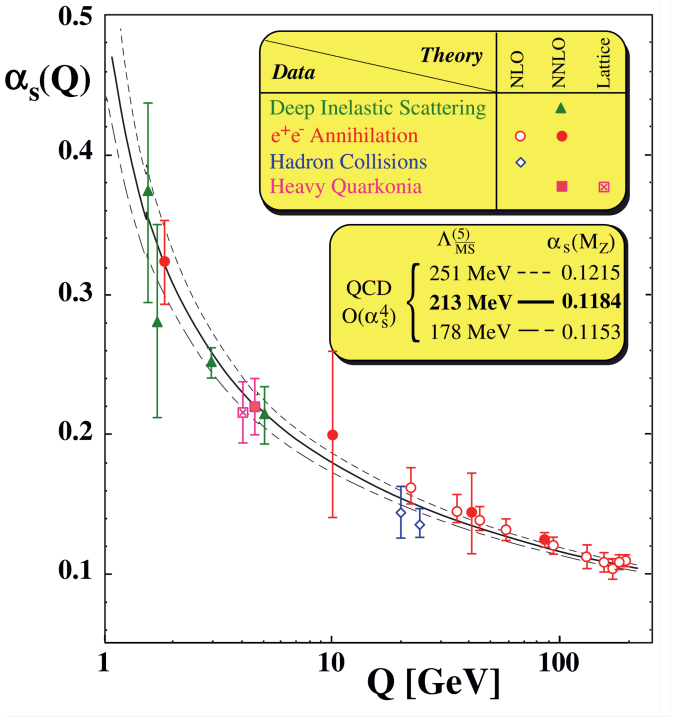

Figure 1.9: *This figure shows the QCD coupling constant, denoted here by α_s, as a function of the energy scale Q. As the energy scale increases, we see indeed that the coupling drops, indicating asymptotic freedom. The figure is taken from [47].*

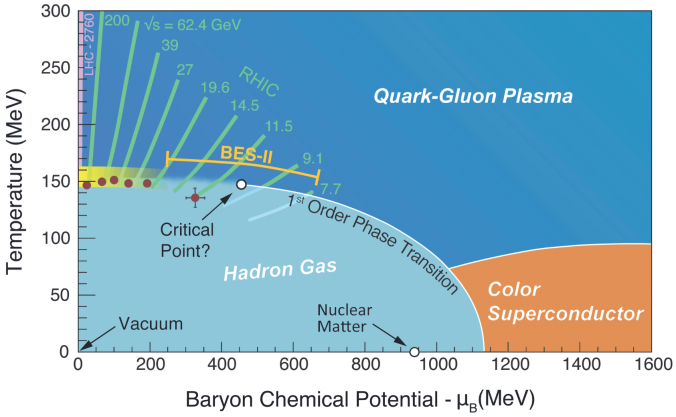

Figure 1.10: *Here, we show the expected phase diagram that follows from quantum chromodynamics; it plots temperature versus chemical potential. At high enough temperatures, a quark-gluon plasma forms. The lines show the regions that are accessible in heavy-ion collisions, along with their beam energies. Note that for increasing beam energy, a baryon chemical of zero becomes a better approximation. The figure was taken from [48].*

that indeed the highly energetic collisions at LHC can be approximated very well with zero chemical potential. The most important takeaway is that there is a phase transition to a Quark-Gluon Plasma (QGP) at high enough temperatures, which we will discuss more below.

One of the main motivations for studying the quark-gluon plasma comes from cosmology. In particular, it has been known since early in the 70's [49, 50] that the early universe was too hot for hadrons, like protons and neutrons, to exist. At these extreme temperatures, microseconds after the big bang, the universe consisted of quark-gluon plasma. The studies of the QGP thus provide us with a peek back at the very early universe. Another interesting situation arises from the AdS/QCD correspondence, which aims to understand (aspects of) QCD by using the AdS/CFT duality from subsection 1.2.7. In [31] it was shown that some aspects of the quark-gluon plasma could be understood by studying five-dimensional black holes.[28] In particular, the ratio of the shear viscosity over the volume density of

[28] And perhaps we can understand aspects of black holes by studying the quark-gluon plasma.

entropy was calculated as

$$\frac{\eta}{s} = \frac{1}{4\pi} \ . \tag{1.124}$$

Recent Bayesian analyses [51, 52] show that the experimentally observed values are consistent with this predicted value.

1.4.2 Quark-Gluon Soup

The question then arises, how can we create the quark-gluon plasma? This is where heavy-ion collisions come in; the collisions produce the right conditions for a quark-gluon plasma to be produced. For the remainder of this section, I will discuss the situation for the ALICE detector at the LHC, although the same principles apply to the Relativistic Heavy Ion Collider (RHIC), albeit with slightly different numbers.

For one month a year, heavy-ions are accelerated in the LHC to tremendous speeds, close to the speed of light. As a result, there are two 'blobs' of heavy-ions, accelerated in opposite directions; when the blobs reach the desired speed, they collide with one another. In Figure 1.11 we show an example of a heavy-ion collision. In this particular example, we can see before the collision the two blobs of heavy-ions. Their shape is elongated due to Lorentz contraction (I usually describe them as pancakes), which is quite extreme at the relativistic velocities of the heavy-ions.

The diameter of the disks of heavy-ions is about 14 fm (femtometer), and their width is Lorentz contracted to $14/\gamma$ fm, where γ is approximately 2500 for the LHC [53]. The energy density just after the collision is roughly 12 GeV/fm^3, which is close to twenty times the energy density of a hadron. At such energy densities, a quark-gluon plasma is created, see also Figure 1.10. As the name suggests, it is a plasma that consists out of quarks and gluons. Normally, under lower temperatures, all the quarks are bound to hadrons, such as protons and neutrons.
As the plasma cools down and expands, we get to a phase called hadronization, whereby the energy densities have dropped enough for hadrons to form again. Understanding this process of hadronization is yet another motivation for performing heavy-ion collisions.

The example collision shown in Figure 1.11 is a *central* one. In heavy-ion collisions, *centrality* measures how aligned the two beams of heavy-ions are, with 0% being the most central and 100% being the most peripheral collisions. A related variable is

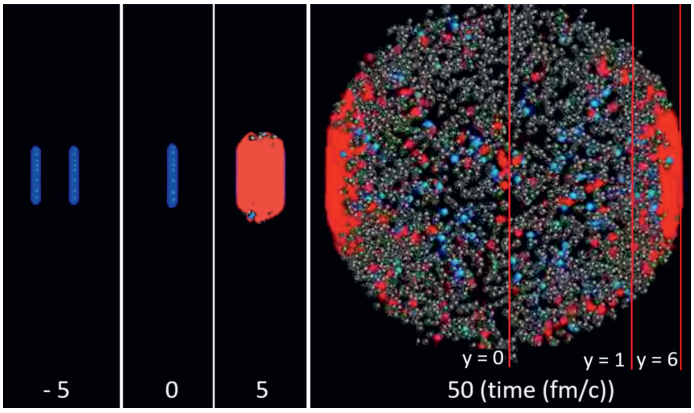

Figure 1.11: *Time snapshots of an animated PbPb heavy-ion collision, as viewed from the side. The situation before, during and after the collision is shown; red color indicates the presence of the quark-gluon plasma. The last time snapshot shows the hadronization taking place. Figure taken from [53], which adapted it from [54].*

the *impact parameter* b, which is defined as the distance between the two centers of the heavy-ion disks. The ions that participate in the collision are called *participants* and those that don't are called *spectators*, since they only 'spectate' the collision; the latter will turn out to be very important for us. The situation is illustrated in Figure 1.12, where the dotted circles indicate spectators and the solid lines the participants.

Coordinate systems

In the field of particle physics, there are some conventions for coordinates, which we briefly review. Due to the detector layouts, it is useful to measure not 'ordinary' momentum but *transverse* momentum. This transverse momentum thus lies in the plane orthogonal to the beam direction ($\hat{z}$), so it lies in the xy-plane. More importantly, however, the transverse momentum is caused completely by the collision and contains all the important information. The azimuthal angle ϕ is defined as the angle in the transverse plane. Next up, the pseudorapidity, η, which is a spatial coordinate describing the angle of the particle relative to the beam-axis (not to be

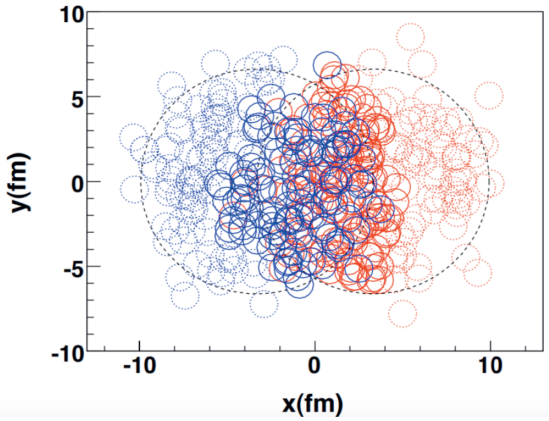

Figure 1.12: *Here we show a view transverse to the beams, red circles indicate nucleons from one beam and blue from the other. Solid circles indicate nucleons that participate in the collision, while the dotted circles are the spectators. The more central a collision is, the more participants will be in a collision. Figure taken from [55].*

confused with ϕ), by

$$\eta = -\ln \tan\left(\frac{\theta}{2}\right) \ . \tag{1.125}$$

Lastly we define the rapidity Y, which is not a coordinate but an alternative way to describe speed as

$$Y = \tanh^{-1}\left(\frac{v_z}{c}\right) \ , \tag{1.126}$$

where v_z is the speed in the beam direction and thus the rapidity maps the speed $-c < v_z < c$ to $-\infty < Y < \infty$. The Lorentz factor $\gamma = 1/\sqrt{1 - \frac{v^2}{c^2}}$ can be rewritten with the rapidity as $\cosh(Y)$.

Anisotropic flow

One of the main observations that lead to a whole host of new research ideas was the observation of large elliptic flow. This flow is an example of anisotropic flow in the expansion of the quark-gluon plasma. In addition to this elliptic flow, there are different forms of anisotropic flow, which provide information on the bulk properties of the matter and the initial geometry of the collision. The most important anisotropic flows we will consider are the directed and the elliptic flow,

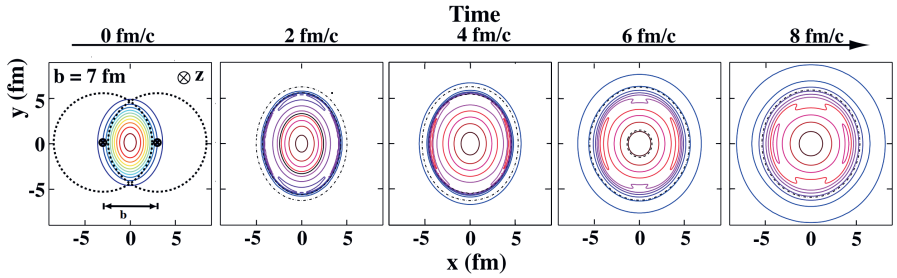

Figure 1.13: Shown here is the elliptic flow and its time dependence. One can see the characteristic elliptic shape of the expansion, which defines elliptic flow. Note that the z-direction is the beam direction, and here the x-axis is defined by the impact parameter. Figure from Ref. [23].

denoted by v_1 and v_2 respectively. These flow components can be found from a Fourier expansion of the differential azimuthal distribution of the particles, given by

$$E\frac{\mathrm{d}^3N}{\mathrm{d}p^3} = \frac{1}{2\pi}\frac{\mathrm{d}^2N}{\mathrm{d}p_T\,\mathrm{d}Y}\left(1+2\sum_{n=1}^{\infty}v_n\,\cos[n(\phi-\psi_{\mathrm{RP}})]\right)\,, \tag{1.127}$$

where E is the energy of the particle, p the momentum, p_T the transverse momentum, Y the rapidity, ϕ the azimuthal angle, ψ_{RP} the angle with the reaction plane[29] and v_n are the Fourier coefficients or flow components, defined by

$$v_n = \langle\cos[n(\phi-\psi_{\mathrm{RP}})]\rangle\,, \tag{1.128}$$

where the brackets define an average over all particles and all events (for a certain (p_T,Y) bin). As mentioned before, we will look mostly at the first few Fourier coefficients, called the directed flow, v_1, the elliptic flow, v_2 and the triangular flow v_3. The directed flow is the flow directed along transverse axes with respect to the beam axis. The elliptic/triangular flow is the elliptic/triangular expansion of the plasma in the transverse plane, the elliptic flow is shown in Figure 1.13.

1.4.3 Electromagnetic fields

In this thesis, we shall be looking at the quark-gluon plasma in the presence of vast electromagnetic fields. These fields have various origins, which we will study in

[29]The reaction plane is the plane formed by the collision geometry, and lies in the x and z directions if we follow the conventions of Figure 1.13

chapter 5. The magnitude of these fields, at LHC, has been estimated to be of order $e|\vec{B}|/m_\pi^2 \approx 10-15$ [56]. [30] Our goal is to obtain the influence of the electromagnetic fields on the expansion of the QGP and, in particular, the influence on the first few flow coefficients. We will approach this by first using a numerical realistic hydrodynamic background for the quark-gluon expansion without electromagnetic fields. After obtaining the background velocity u, we want to get the velocity $\vec{v}$ caused by the electromagnetic field. To get this, however, we will need to boost to the local fluid rest frame where we have $\vec{u}' = 0$. In this *primed* frame (with $\vec{v}'$), all the components of $\vec{E}'$ and $\vec{B}'$ are non-zero. To compute the velocity $\vec{v}'$ we will solve the equation of motion with the Lorentz force law and using stationary currents

$$m\,\frac{d\vec{v}'}{dt} = q\vec{E}' + q\vec{v}' \times \vec{B}' - \mu\, m\, \vec{v}' = 0\ , \tag{1.129}$$

where m denotes the mass, q the charge, μ is the drag coefficient, and the last term denotes the drag force on a fluid element with mass m. Note that the above Lorentz equation is a non-relativistic equation, which is only applicable in the case that $|\vec{v}| << |\vec{u}|$. We shall see later, chapter 5, that this is a good assumption. The calculation of μm for light quarks is not trivial, and it is not exactly analytically known at this moment. We use holographic results from [57]; currently, there are only precise results known for heavy quarks in the $\mathcal{N} = 4$ SYM theory (which we also mentioned in subsection 1.2.7)

$$\mu m = \frac{1}{2}\,\pi\,\sqrt{\lambda}\,T^2\ , \tag{1.130}$$

where $\lambda = g_{\rm YM}^2\, N_c$ is the t' Hooft coupling. Here g is the gauge coupling and N_c the number of colors, see also [58, 59]. We will pick, just as in [56], $\lambda = 6\pi$ and further assume μm to be constant. Having obtained our four-velocity in the fluid rest frame, we shall boost back to the center of mass frame and obtain $V^{\pm\mu}$, the total four-velocity. This four-velocity then incorporates the expansion as found by the hydrodynamic model and the effects due to the electromagnetic field. With the four-velocity at hand, we can get the spectra of particles (protons and pions in our case), and by using (1.127) we can compute the different flow components, the details of which we will show in the later chapters.

[30] In units of Tesla, this estimate is of order 10^{15} T.

1.5 This thesis

Although we have mentioned various bits throughout the introduction, let us briefly discuss the topics in this thesis. In the first chapter, chapter 2 we will discuss black holes in string theory with duality twists. In particular, we start off using a supergravity setup and then perform Scherk-Schwarz twists (of which the string counterpart is called a duality twist). The starting point is Type IIB supergravity, which we then compactify on $T^4 \times S^1$, where the compactification on the circle is a Scherk-Schwarz twist. The Scherk-Schwarz twist can, as we will see, break the supersymmetry of the supergravity theory. This breaking provides one of the primary motivations for this research: to study black holes from string theory under the breaking of supersymmetry. The relevance of this study is clear since there appears to be no supersymmetry in our universe (at currently accessible energy scales). Thus, we will use black holes, like the ones we created in subsection 1.2.6, and investigate them under the Scherk-Schwarz twists. We will describe the Type IIB action in an SO(5,5) covariant manner, introduce the relevant Scherk-Schwarz twists, discuss the implications for the black hole solutions, and, finally, describe how the twists can be uplifted to string theory. Certain classes of duality twists can be alternatively described as orbifolds, which provide a more complete picture of the duality twists, including all the possible string states.

In the second chapter, chapter 3, we investigate the near-horizons of rotating supersymmetric black holes, in particular how we can uplift these to the eleven-dimensional M-theory. The rotating black holes always have some fibered AdS_2 structure in the near-horizon, which we also saw in our discussion of the Kerr black hole in (1.2). We will allow for the most general fibration over the AdS_2 and keep a flux configuration that allows for rotating M2-branes. As an example, we will provide the uplift of the asymptotically AdS_4 Kerr-Newman black hole into the classification. The last part of the chapter concerns the conditions of rotating black strings in Type IIB using dualities with the aforementioned eleven-dimensional theory.

The third chapter, chapter 4, concerns a generalization of the 'standard' SYK model that we discussed in section 1.3. Apart from the N Majorana fermions, we also add in M auxiliary bosons; when $M = N$ the model coincides with the supersymmetric SYK model. The disorder average gets changed in this model, which results in different dynamics. When solving the model with assumptions that

the two-point functions are conformal, similar to what we did in (1.79), we find two solutions. Based on their behavior when $M/N = 1$, we name them 'rational' and 'irrational'. Afterward we determine numerically which of these appears to be the dominant saddle, and lastly, we investigate the chaos of the model using the OTOC correlators.

Finally, in the last chapter, chapter 5, we will study heavy-ion collisions and the quark-gluon plasma, which we introduced in section 1.4. In particular, we will examine the electromagnetic fields that are present in the heavy-ion collisions and what influence they have on the charge-dependent expansion of the quark-gluon plasma, beside its 'normal' thermodynamic growth. First, we first numerically model the evolution of a cooling droplet in the strongly coupled plasma and subsequently add in the electromagnetic fields. We find that there are charge-odd, parity-odd, contributions to the directed flow v_1 and the triangular flow v_3, arising due to a combination of Lorentz, Faraday, and Coulomb forces. Furthermore, we find a parity even contribution to the elliptic flow v_2, which arises from the plasma's charged participants. We conclude by analyzing of the influence of parameters used in the computations.

Conventions

In this thesis we will always use natural units with $\hbar = c = k_b = G = 1$ unless otherwise stated. For metrics we work in the mostly plus convention such that $\eta = \text{diag}(-1, 1, 1, \ldots, 1)$.

Part I

Black Holes in String Theory

In this first part there are two chapters, each with a specific focus on black hole solutions. The first chapter, black holes in string theory with duality twists, focusses on black hole solutions in string theory whereby part of the spacetime supersymmetry is broken. We will investigate whether several ten-dimensional brane solutions are preserved under the supersymmetry breaking compactifications. In the second chapter we discuss how the near-horizon geometries of rotating black holes can be embedded into M-theory. We will allow for a general AdS_2 fibration structure, with fluxes allowing rotating M2-brane setups. As an example, we show how the AdS_4 Kerr-Newman black hole fits into the classification.

Chapter 2

Black Holes in String Theory with Duality Twists

> *Of all the conceptions of the human mind from unicorns to gargoyles to the hydrogen bomb perhaps the most fantastic is the black hole: a hole in space with a definite edge over which anything can fall and nothing can escape; a hole with a gravitational field so strong that even light is caught and held in its grip; a hole that curves space and warps time.*
>
> – Kip Thorne, *Cosmology + 1*

In this first chapter we will discuss black holes in the presence of supersymmetry breaking backgrounds. From a phenomenological point of view this has interest since there appears to be no supersymmetry present in our universe at our energy scales. The method we use can in principle be used to break all of the supersymmetry, which could provide insights into creating black hole objects from string theory whilst simultaneously breaking the supersymmetry. In this work we will mostly consider cases where only part of the supersymmetry is broken, as to maintain the various advantages of the symmetry, e.g. the stability of the vacuum that we end up in. The set-up we consider will be Type IIB theory on $T^4 \times S^1$, whereby the reduction on the circle will be a so-called *Scherk-Schwarz* reduction, which we will introduce in section 2.2.[1] Since Type IIB is ten-dimensional, our resulting black holes will live in five dimensions.

In order to study such BPS black holes in five dimensions both macroscopically and microscopically, we can use a set-up of the D1-D5-P system in Type IIB string

[1] We could also have used $K3$ instead of T^4.

theory. The black hole can be described as an asymptotically flat three-charge 1/8 BPS black hole solution of 5D $\mathcal{N} = 8$ supergravity (or 1/4 BPS in $\mathcal{N} = 4$ supergravity). The entropy can be computed microscopically from a 2D $(4, 4)$ CFT dual to the near horizon geometry of the black hole [12]. This system has U-dual formulations in terms of F1 and NS5-branes, and in terms of intersecting D3-branes.

Black holes in compactifications preserving eight supersymmetries in five dimensions can be constructed in M-theory on CY_3 [60] or in F-theory on $CY_3 \times S^1$ [61, 62]. In these cases, the microscopic field theory dual to the black hole horizon geometry is a 2D $(0, 4)$ CFT. These CFTs are considerably more complicated than the $(4, 4)$ CFTs on the symmetric product of T^4 (or $K3$) as they have less supersymmetry [12].

In this chapter, we consider a different way to reduce supersymmetry, namely string compactifications with a duality twist [63], which are the lifts to string theory of Scherk-Schwarz reductions in supergravity [64, 65]. Such compactifications allow for partial supersymmetry breaking and include string vacua preserving no supersymmetry at all (though this won't be the focus in this work). This gives rise to 5D Minkowski vacua preserving $\mathcal{N} = 6, 4, 2, 0$ supersymmetry. We investigate 5D supersymmetric black holes in these theories that lift to 10D systems of branes in the string theory picture. An important point is that we choose the twist inducing the supersymmetry breaking to be a duality transformation that leaves the original system of branes invariant, and so the 5D black hole solution of the untwisted theory remains a solution of the twisted theory. The fields sourcing the system of branes are invariant under the twist, so that the fields appearing in the solution remain massless and the same solution remains as a solution of the twisted theory. This makes it possible to consider the effect of the twist on the corresponding CFT and so to investigate the microscopic aspects of these black holes.

This work is a follow-up to the ideas proposed earlier in [66] in an M-theory setting in which supersymmetry is completely broken. Completely broken supersymmetry is not a well controlled situation, and for that reason we will focus on the twists preserving some supersymmetry. The current work studies string vacua with partial supersymmetry breaking and the macroscopic supergravity description of black holes in such vacua. The microscopic description of the dual CFTs is left for future study.

Scherk-Schwarz reduction of supergravity theories has been extensively studied in the literature; see e.g. [63–65, 67–75] and references therein. IIB supergravity compactified on T^4 gives maximal $\mathcal{N} = (2, 2)$ supergravity in six dimensions which has a Spin$(5, 5)$ duality symmetry. The maximal compact subgroup of this global symmetry is Spin$(5) \times$Spin(5); we shall refer to this as the R-symmetry group. (Note that this global R-symmetry should not be confused with the Spin$(5) \times$Spin(5) local symmetry that is introduced in some formulations of the theory.) The 6D scalar fields take values in the coset Spin$(5, 5)$/Spin$(5) \times$ Spin(5). We will be interested in the Scherk-Schwarz reduction of this theory to five dimensions, which has been considered previously in [69,70]. This uses ansätze of the type $\hat{\psi}(x^\mu, z) = g(z)\,\psi(x^\mu)$ where z is the S^1 coordinate and $g(z)$ is a local element of Spin$(5, 5)$. On going round the circle $z \to z + 2\pi R$, the fields pick up a monodromy $\mathcal{M} = g(2\pi R) \in$ Spin$(5, 5)$. Such a reduction gives a consistent truncation to a 5D gauged supergravity theory for the fields $\psi(x^\mu)$, in which there is a Scherk-Schwarz potential for the scalar fields and mass terms are generated for all fields charged under the monodromy.

If the twist $g(z)$ is compact, i.e. it is an element of the R-symmetry group, then the potential is non-negative and has stable five-dimensional Minkowski vacua [63]. Such a twist can be specified by four parameters m_1, m_2, m_3, m_4 which become mass parameters in the reduced theory. The amount of supersymmetry that is preserved in the vacuum depends on the number of parameters m_i that are equal to zero: if r of the parameters m_i are zero, then $\mathcal{N} = 2r$ supersymmetry is preserved. This yields 5D supergravities with $\mathcal{N} = 8, 6, 4, 2, 0$ Minkowski vacua [70] (where the case $r = 4$ is the untwisted reduction to 5D $\mathcal{N} = 8$ supergravity, and the case $r = 0$ is the twisted reduction that breaks all supersymmetry). This reduction is a straightforward generalization of the Scherk-Schwarz reduction of 5D $\mathcal{N} = 8$ supergravity to 4D with four mass parameters and $\mathcal{N} = 8, 6, 4, 2, 0$ vacua [67].

The lift of these supergravity reductions to full compactifications of string theory involves a number of subtle features [63]. These have been worked out in detail for compactifications of IIA string theory on K3 or the heterotic string on T^4 followed by a reduction on a circle with a duality twist in [74,75]. Here we draw on these and the results of [63] for our construction, which is IIB string theory compactified on $T^4 \times S^1$ with a U-duality twist around the circle. Type IIB on T^4 has a Spin$(5, 5)$ supergravity duality symmetry that, on the level of the full string theory, is broken to the discrete U-duality subgroup Spin$(5, 5; \mathbb{Z})$ by quantum corrections [22]. The moduli space is the scalar coset space Spin$(5, 5)/[($Spin$(5) \times$ Spin$(5))/\mathbb{Z}_2]$

identified under the action of $\mathrm{Spin}(5,5;\mathbb{Z})$. A key requirement for there to be a lift to string theory is that the Scherk-Schwarz monodromy lies in the U-duality group $\mathrm{Spin}(5,5;\mathbb{Z})$, imposing a 'quantization' condition on the twist parameters m_i [63, 76].

There is still an action of the continuous group $\mathrm{Spin}(5,5)$ on the theory, but only the subgroup $\mathrm{Spin}(5,5;\mathbb{Z})$ is a symmetry. Reduction of the theory on a circle with a duality twist introduces a monodromy $\mathcal{M}$ which is required to be an element of $\mathrm{Spin}(5,5;\mathbb{Z})$. If the monodromy acts as a diffeomorphism of T^4, which requires that it is in a $\mathrm{GL}(4;\mathbb{Z})$ subgroup of $\mathrm{Spin}(5,5;\mathbb{Z})$, then this corresponds to compactification of the IIB string on a T^4 bundle over S^1. If the monodromy acts as a T-duality of T^4, which requires that it is in an $\mathrm{SO}(4,4;\mathbb{Z})$ subgroup of $\mathrm{Spin}(5,5;\mathbb{Z})$, then this constructs a T-fold background, while for general U-duality monodromies this is a U-fold [77].

A point in the scalar coset will be a minimum of the scalar potential giving a stable Minkowski vacuum if and only if it is a fixed point under the action of the monodromy $\mathcal{M} \in \mathrm{Spin}(5,5;\mathbb{Z})$ [63]. The monodromy will then generate a $\mathbb{Z}_p$ subgroup of $\mathrm{Spin}(5,5;\mathbb{Z})$ for some integer p. Furthermore, at this critical point the construction becomes a $\mathbb{Z}_p$ generalized orbifold of IIB string theory on T^5, where the theory is quotiented by the $\mathbb{Z}_p$ generated by $\mathcal{M}$ acting on the IIB string on T^4 combined with a shift by $2\pi R/p$ on the circle. When the monodromy is a T-duality, this is a $\mathbb{Z}_p$ asymmetric orbifold.

Regarded as an element of $\mathrm{Spin}(5,5)$, the monodromy is conjugate to an R-symmetry transformation: $\mathcal{M} = kRk^{-1}$ for some $R \in \mathrm{Spin}(5) \times \mathrm{Spin}(5)$ and $k \in \mathrm{Spin}(5,5)$ [63]. The rotation R conjugate to a given monodromy is specified by four angles, which are given by the four parameters m_i. For $\mathcal{N} = 2$ supersymmetry to be preserved, one of the parameters must be zero so that R in fact lies in an $\mathrm{SU}(2) \times \mathrm{Spin}(5)$ subgroup. For $\mathcal{N} = 4$ supersymmetry to be preserved, two of the parameters must be zero so that R lies either in a $\mathrm{Spin}(5)$ subgroup or a $\mathrm{SU}(2) \times \mathrm{SU}(2)$ subgroup (with one $SU(2)$ factor in each $\mathrm{Spin}(5)$). These two options lead to theories that have the same massless sector, but differ in their massive sectors. We use the notation $(0,2)$ and $(1,1)$ to distinguish these two $\mathcal{N} = 4$ theories, reflecting whether the massive states are in $(0,2)$ or $(1,1)$ BPS supermultiplets, using the terminology of [78]. Lastly, for $\mathcal{N} = 6$ supersymmetry to be preserved, three of the parameters must be zero so that R lies in an $\mathrm{SU}(2)$ subgroup of the R-symmetry.

As mentioned above, if $\mathcal{M}$ is a perturbative symmetry (i.e. a T-duality) in $\mathrm{Spin}(4,4;\mathbb{Z})$, the theory in the Minkowski vacuum is an asymmetric orbifold. In general this will not be modular invariant, and further modifications are needed to achieve modular invariance. For perturbative monodromies, the shift in the circle coordinate z must be accompanied by a shift in the coordinate of the T-dual circle [75, 79, 80]. Put differently, the quotient introduces phases dependent on both the momentum and the winding number on the circle, and on the charges of the state under the action of $\mathcal{M}$ [75]. For non-perturbative monodromies, the arguments of [75, 81] lead to phases dependent on other brane wrapping numbers.

Quantum effects can lead to corrections to the coefficients of the five-dimensional Chern-Simons terms $A \wedge F \wedge F$ at the two-derivative level and $A \wedge R \wedge R$ at the four-derivative level. There have been indications in the literature (see e.g. [82]) that the $A \wedge R \wedge R$ term can be supersymmetrized in the $\mathcal{N} = 4$ $(0,2)$ theory but not in the $\mathcal{N} = 4$ $(1,1)$ theory, nor in the $\mathcal{N} = 6$ theory. In the $\mathcal{N} = 2$ theory the supersymmetrization is known [83]. Our results are in agreement with these claims. That is, we find corrections only in the cases where supersymmetric Chern-Simons terms are expected. The corrections to the Chern-Simons coefficients modify the black hole solutions in supergravity [84, 85] and therefore also the entropy. We compute the quantum corrections to the Chern-Simons coefficients and the resulting modifications to the black hole entropies from supergravity and the Kaluza-Klein modes from the circle compactification, using results in the literature for 5D $\mathcal{N} = 2$ supergravity [84, 85]. Similar calculations have been done in different setups, see [86, 87].

As a by-product of our analysis, we present in detail the supergravity reduction of type IIB on T^4. While the general techniques and results are known in the literature [88], the explicit relation between the 10D and 6D fields has not been given, to the best of our knowledge. We present this calculation in section 2.1; the results are relevant for understanding which black holes survive which twist in subsequent sections.

In section 2.2, we perform the Scherk-Schwarz reduction to five dimensions, starting from the maximally supersymmetric 6D $(2,2)$ supergravity. We construct mass matrices and decompose the 5D field content into massless and massive multiplets. By simply truncating to the massless sector, we can embed known BPS black holes in these five dimensional theories. In section 2.3, we work out which choices of

Scherk-Schwarz twist preserve the D1-D5-P black hole, the F1-NS5-P black hole and the D3-D3-P black hole. By tuning the mass parameters, we can find twists that preserve more than one black hole solution (e.g. we find the twists that preserve both the D1-D5-P and the F1-NS5-P black holes). In section 2.4, we study one-loop effects by integrating out the massive fields. We compute the corrections to the Chern-Simons terms and to the entropy of 5D BPS black holes. Finally, in section 2.5, we discuss how to embed our supergravity model in string theory and discuss the quantization conditions on the parameters m_i of the twist.

2.1 Duality invariant formulation of IIB supergravity on a four-torus

Reducing type IIB supergravity on a four-torus gives six-dimensional maximal supergravity. This theory has $\mathcal{N} = (2,2)$ supersymmetry and a $\mathrm{Spin}(5,5)$ duality symmetry group. The goal of this section is to write this supergravity theory in a form in which both the type IIB origin of the six-dimensional fields and the $\mathrm{Spin}(5,5)$ symmetry are manifest. We do this explicitly for the scalar and tensor fields.

2.1.1 Ansätze for reduction to 6D

We start from type IIB supergravity. Written in Einstein frame, the bosonic terms in the Lagrangian read

$$\begin{aligned}\mathscr{L}_{\text{IIB}} = \Big(& R^{(10)} - \frac{1}{2}|\mathrm{d}\Phi|^2 - \frac{1}{2}\, e^{-\Phi} \left|H_3^{(10)}\right|^2 - \frac{1}{2}\, e^{2\Phi} \left|\mathrm{d}a\right|^2 - \frac{1}{2}\, e^{\Phi} \left|F_3^{(10)}\right|^2 \\ & - \frac{1}{4}\left|F_5^{(10)}\right|^2 \Big) * 1 - \frac{1}{2}\, C_4^{(10)} \wedge H_3^{(10)} \wedge F_3^{(10)}\,,\end{aligned} \tag{2.1}$$

where the field strengths are given by

$$\begin{aligned} H_3^{(10)} &= \mathrm{d}B_2^{(10)}\,, \\ F_3^{(10)} &= \mathrm{d}C_2^{(10)} - a\,\mathrm{d}B_2^{(10)}\,, \\ F_5^{(10)} &= \mathrm{d}C_4^{(10)} - \frac{1}{2}C_2^{(10)} \wedge \mathrm{d}B_2^{(10)} + \frac{1}{2}B_2^{(10)} \wedge \mathrm{d}C_2^{(10)}\,. \end{aligned} \tag{2.2}$$

The superscripts (10) indicate that the fields live in 10 dimensions. The field equations are supplemented by the self-duality constraint

$$F_5^{(10)} = *F_5^{(10)} \ . \tag{2.3}$$

In our compactification to six dimensions, the coordinates split up as $X^M = (\hat{x}^{\hat{\mu}}, y^m)$ with $M = 0, \ldots, 9$, $\hat{\mu} = 0, \ldots, 5$ and $m = 1, \ldots, 4$. We now present the ansätze that we use in our reduction. In order to arrive in Einstein frame in 6D, we decompose the ten-dimensional metric as

$$g_{MN} = \begin{pmatrix} g_4^{-1/4}\, g_{\hat{\mu}\hat{\nu}} + g_{mn}\, \mathcal{A}^m_{\hat{\mu}} \mathcal{A}^n_{\hat{\nu}} & g_{mn}\, \mathcal{A}^m_{\hat{\mu}} \\ g_{mn}\, \mathcal{A}^n_{\hat{\nu}} & g_{mn} \end{pmatrix} , \tag{2.4}$$

where $g_4 = \det(g_{mn})$. The compact part of the metric, g_{mn}, we parametrize in terms of scalar fields ϕ_i $(i = 1, \ldots, 4)$ and A_{mn} $(m < n)$ by

$$g_{mn} = \begin{cases} e^{\vec{b}_m \cdot \vec{\phi}} + \sum\limits_{k<m} e^{\vec{b}_k \cdot \vec{\phi}}\, (A_{km})^2 & \text{for } m = n \\ e^{\vec{b}_m \cdot \vec{\phi}}\, A_{mn} + \sum\limits_{k<m} e^{\vec{b}_k \cdot \vec{\phi}}\, A_{km} A_{kn} & \text{for } m < n \\ g_{nm} & \text{for } m > n \, . \end{cases} \tag{2.5}$$

Here $\vec{\phi} = (\phi_1, \phi_2, \phi_3, \phi_4)$ and the vectors $\vec{b}_m$ are given by

$$\begin{aligned} \vec{b}_1 &= (-\tfrac{1}{\sqrt{2}}, -\tfrac{1}{\sqrt{2}}, -\tfrac{1}{\sqrt{2}}, \tfrac{1}{2}) \, , \\ \vec{b}_2 &= (-\tfrac{1}{\sqrt{2}}, \tfrac{1}{\sqrt{2}}, \tfrac{1}{\sqrt{2}}, \tfrac{1}{2}) \, , \\ \vec{b}_3 &= (\tfrac{1}{\sqrt{2}}, \tfrac{1}{\sqrt{2}}, -\tfrac{1}{\sqrt{2}}, \tfrac{1}{2}) \, , \\ \vec{b}_4 &= (\tfrac{1}{\sqrt{2}}, -\tfrac{1}{\sqrt{2}}, \tfrac{1}{\sqrt{2}}, \tfrac{1}{2}) \, . \end{aligned} \tag{2.6}$$

From this, it can be computed that $g_4 = e^{2\phi_4}$, so the scalar ϕ_4 parametrizes the volume of the T^4.

We reduce the 10D form-valued fields by simply splitting into components with different numbers of indices on the torus. For example, the Kalb-Ramond field

$B_2^{(10)}$ decomposes as

$$\begin{aligned} B_2^{(10)} &= \frac{1}{2} B_{MN}\, \mathrm{d}X^M \wedge \mathrm{d}X^N \\ &= \frac{1}{2} B_{\hat{\mu}\hat{\nu}}\, \mathrm{d}x^{\hat{\mu}} \wedge \mathrm{d}x^{\hat{\nu}} + B_{\hat{\mu}m}\, \mathrm{d}x^{\hat{\mu}} \wedge \mathrm{d}y^m + \frac{1}{2} B_{mn}\, \mathrm{d}y^m \wedge \mathrm{d}y^n \\ &= B_2^{(6)} + B_{1,m}^{(6)} \wedge \mathrm{d}y^m + \frac{1}{2} B_{mn}\, \mathrm{d}y^m \wedge \mathrm{d}y^n \,, \end{aligned} \tag{2.7}$$

where $B_2^{(6)}$, $B_{1,m}^{(6)}$ and B_{mn} are 2, 1 and 0-forms defined on the six-dimensional non-compact space. The ten-dimensional scalars are simply equal to their six-dimensional descendants, e.g. $\Phi^{(10)} = \Phi^{(6)} = \Phi$. For this reason, we usually drop the superscript (D) for scalar fields.

Reduction of the self-dual five-form field strength

To find the fields that descend from the RR four-form $C_4^{(10)}$ we need to be a bit careful, since it has a self-dual field strength: $*F_5^{(10)} = F_5^{(10)}$. Because of this self-duality, the action (2.1) does not properly describe the dynamics of the RR four-form. So instead of reducing the action, we should reduce the corresponding field equations along with the self-duality constraint. The action (2.1) with field strengths (2.2) yields the following equation of motion and Bianchi identity

$$\mathrm{d}\big(*\, F_5^{(10)}\big) = \mathrm{d}B_2^{(10)} \wedge \mathrm{d}C_2^{(10)} \,, \tag{2.8}$$

$$\mathrm{d}F_5^{(10)} = \mathrm{d}B_2^{(10)} \wedge \mathrm{d}C_2^{(10)} \,. \tag{2.9}$$

We see that, because of the self-duality of $F_5^{(10)}$, these two equations are identical, so we only have to reduce one of them. In what follows, we choose to reduce the Bianchi identity (2.9). Subsequently, we reduce the self-duality equation and use it to rewrite the six-dimensional Bianchi identities to a system of Bianchi identities and equations of motion. By integrating this system of equations to an action, we find the proper result of the reduction of $C_4^{(10)}$. Below, we work out this reduction in detail for the scalars and the two-forms.

First, we consider the scalars. In 6D, massless four-forms can be dualized to scalars, so we need to consider the components of $F_5^{(10)}$ that have either zero or four legs on the torus. The Bianchi identities for these components following from (2.9) read

$$\begin{aligned} \mathrm{d}P_1^{(6)} &= \frac{1}{2!\,2!}\, \varepsilon^{mnpq}\, \mathrm{d}B_{mn} \wedge \mathrm{d}C_{pq} \,, \\ \mathrm{d}P_5^{(6)} &= \mathrm{d}B_2^{(6)} \wedge \mathrm{d}C_2^{(6)} \,. \end{aligned} \tag{2.10}$$

Here we have introduced the notation $P_1^{(6)} = \frac{1}{4!}\,\varepsilon^{mnpq}\,F^{(6)}_{1,mnpq}$ and $P_5^{(6)} = F_5^{(6)}$. Next, we write down the relevant components that follow from the reduction of the self-duality constraint. By using the metric ansatz (2.4), and ignoring interactions with the graviphotons $\mathcal{A}^m_{\hat{\mu}}$, we find

$$P_5^{(6)} = \frac{1}{g_4} * P_1^{(6)}\,. \tag{2.11}$$

We now use this constraint to eliminate $P_5^{(6)}$ from (2.10). In this way, we find the following Bianchi identity and equation of motion for the one-form field strength $P_1^{(6)}$

$$\begin{aligned} \mathrm{d}P_1^{(6)} &= \frac{1}{2!\,2!}\,\varepsilon^{mnpq}\,\mathrm{d}B_{mn}\wedge\mathrm{d}C_{pq}\,,\\ \mathrm{d}\big(e^{-2\phi_4} * P_1^{(6)}\big) &= \mathrm{d}B_2^{(6)}\wedge\mathrm{d}C_2^{(6)}\,. \end{aligned} \tag{2.12}$$

From the first equation, we can find an expression for $P_1^{(6)}$ in terms of the corresponding scalar field that we denote by b. The second equation can be integrated to an action that contains both the kinetic term for b and interaction terms between b and other scalar and two-forms fields. These expressions can be found in (2.16) and (2.17).

Next, we look at the two-forms coming from $C_4^{(10)}$. We are interested in the action for the six-dimensional two-form fields and their interactions with scalar fields. We will ignore interactions with six-dimensional one-forms. The relevant components that follow from the reduction of (2.9) read

$$\begin{aligned} \mathrm{d}F^{(6)}_{3,mn} &= \mathrm{d}B_{mn}\wedge\mathrm{d}C_2^{(6)} + \mathrm{d}B_2^{(6)}\wedge\mathrm{d}C_{mn}\\ &= \mathrm{d}\big(B_{mn}\,\mathrm{d}C_2^{(6)} - C_{mn}\,\mathrm{d}B_2^{(6)}\big)\,. \end{aligned} \tag{2.13}$$

These are Bianchi identities for six tensors in six dimensions. We want to eliminate half of these fields in exchange for equations of motion for the residual ones. We choose to retain the components $F^{(6)}_{3,mn}$ for $mn = 12, 13, 14$ and to eliminate the ones with indices $mn = 23, 24, 34$. For this, we again use the reduced self-duality constraint. The relevant components are

$$F^{(6)}_{3,mn} = \frac{1}{2}\sqrt{g_4}\,\varepsilon_{mnpq}\,g^{pr}g^{qs} * F^{(6)}_{3,rs}\,. \tag{2.14}$$

Due to the summations over the r and s indices, each component of this equation contains a linear combination of all the dual field strengths $*F^{(6)}_{3,rs}$ (recall that the

metric on T^4 is given by (2.5)). Consequently, solving (2.14) for three of the six field strengths results in unwieldy expressions. We choose not to write down these expressions here, but instead to give a step-by-step outline of the way we use them to find an action for the 6D tensors.

First, we introduce a new notation for the field strengths that we plan on retaining: $P^{(6)}_{3;\,1} = F^{(6)}_{3,12}$, $P^{(6)}_{3;\,2} = F^{(6)}_{3,14}$ and $P^{(6)}_{3;\,3} = F^{(6)}_{3,13}$. Here the first subscript indicates that these are three-forms, and the second subscript labels the three distinct field strengths (we will sometimes drop this label when we are talking about all three of them). The expressions for these field strengths in terms of the corresponding two-form fields can be deduced from (2.13). For example,

$$P^{(6)}_{3;\,1} = \mathrm{d}R^{(6)}_{2;\,1} + B_{12}\,\mathrm{d}C^{(6)}_2 - C_{12}\,\mathrm{d}B^{(6)}_2\,, \tag{2.15}$$

where $R^{(6)}_{2;\,1}$ is then one of the two-forms that arise from compactifying the ten-dimensional 4-form. Similar expressions can be found for $P^{(6)}_{3;\,2}$ and $P^{(6)}_{3;\,3}$ in terms of fields that we call $R^{(6)}_{2;\,2}$ and $R^{(6)}_{2;\,3}$ respectively.

Next, we solve the six equations in (2.14) for $F^{(6)}_{3,mn}$ and $*F^{(6)}_{3,mn}$ (for $mn = 23, 24, 34$) in terms of the field strengths $P^{(6)}_3$ and their duals $*P^{(6)}_3$. By substituting these expressions in the components of (2.13) for $mn = 23, 24, 34$, we find the equations of motion for the tensor fields $R^{(6)}_2$ purely in terms of the (dual) field strengths $P^{(6)}_3$ and $*P^{(6)}_3$, and fields that don't descend from the RR four-form $C^{(10)}_4$. These field equations are quite unwieldy, but with some careful bookkeeping they can be integrated to an action. We will not write down this awkward version of the action here. Instead, we write down a more elegant version of the action for the six-dimensional tensor fields and their interactions with scalar fields in subsection 2.1.3.

2.1.2 6D scalars

The field content of maximal six-dimensional supergravity contains 25 scalars. In terms of their origin in type IIB, these are Φ, ϕ_i, A_{mn}, B_{mn}, C_{mn}, a and b. We find the action for these scalar fields by using the methods and ansätze described in the previous section. This yields

$$\begin{aligned} e^{-1}_{(6)}\,\mathscr{L}_{\mathrm{s}} \;=\; & -\frac{1}{2}\,|\mathrm{d}\Phi|^2 - \frac{1}{4}\,|\mathrm{d}\phi_4|^2 - \frac{1}{2}\,|\mathrm{d}g_{mn}|^2 - \frac{1}{2}\,e^{-\Phi}\,\left|H^{(6)}_{1,mn}\right|^2 \\ & - \frac{1}{2}\,e^{2\Phi}\,|\mathrm{d}a|^2 - \frac{1}{2}\,e^{\Phi}\,\left|F^{(6)}_{1,mn}\right|^2 - \frac{1}{2}\,e^{-2\phi_4}\,\left|P^{(6)}_1\right|^2 . \end{aligned} \tag{2.16}$$

Note that the absolute values apply both to the 6D Lorentz indices and to the indices on the torus. For example, $|H^{(6)}_{1,mn}|^2 = \frac{1}{2!}\, H_{\hat{\mu}mn} H^{\hat{\mu}mn} = \frac{1}{2!}\, H_{\hat{\mu}mn}\, g^{mp} H^{\hat{\mu}}{}_{pq}\, g^{pn}$. The field strengths in (2.16) are given by

$$\begin{aligned} H^{(6)}_{1,mn} &= \mathrm{d}B_{mn}\,, \\ F^{(6)}_{1,mn} &= \mathrm{d}C_{mn} - a\,\mathrm{d}B_{mn}\,, \\ P^{(6)}_{1} &= \mathrm{d}b + \frac{1}{8}\,\varepsilon^{mnpq}\,(B_{mn}\,\mathrm{d}C_{pq} - C_{mn}\,\mathrm{d}B_{pq})\,. \end{aligned} \tag{2.17}$$

These 25 scalar fields together parametrize the coset $\mathrm{Spin}(5,5)/(\mathrm{Spin}(5)\times\mathrm{Spin}(5))$ [88]. The action above has a global $\mathrm{Spin}(5,5)$ and a local $\mathrm{Spin}(5)\times\mathrm{Spin}(5)$ symmetry. In its current form, these symmetries are not visible, so we will now write this action in a form that makes both symmetries manifest.

In order to do this, we construct a generalized vielbein (or coset representative) $\mathcal{V}$ from the scalar fields. This vielbein is an element of $\mathrm{Spin}(5,5)$ and it transforms as $\mathcal{V} \to U\,\mathcal{V}\,W(\hat{x})$, with $U \in \mathrm{Spin}(5,5)$ and $W(\hat{x}) \in \mathrm{Spin}(5)\times\mathrm{Spin}(5)$. We now define the $\mathrm{Spin}(5)\times\mathrm{Spin}(5)$ invariant field $\mathcal{H} = \mathcal{V}\,\mathcal{V}^T$, that transforms as $\mathcal{H} \to U\,\mathcal{H}\,U^T$ under global $\mathrm{Spin}(5,5)$ transformations[2]. We can now write the scalar Lagrangian in terms of $\mathcal{H}$ as

$$e^{-1}_{(6)}\,\mathscr{L}_{\mathrm{s}} \;=\; \frac{1}{8}\,\mathrm{Tr}\big[\partial_{\hat{\mu}}\mathcal{H}^{-1}\partial^{\hat{\mu}}\mathcal{H}\big]\,. \tag{2.18}$$

In this formulation, the Lagrangian is manifestly invariant under the U-duality group $\mathrm{Spin}(5,5)$.

We now specify the way we build $\mathcal{V}$ from the 25 scalar fields so that the two Lagrangians (2.16) and (2.18) are equal to one another. We choose to build $\mathcal{V} \in \mathrm{Spin}(5,5)$ in τ-frame, i.e. it satisfies $\mathcal{V}^T\tau\,\mathcal{V} = \tau$ (for the definition of τ, see Appendix 2.B.1). The exact construction is as follows:

$$\begin{aligned} \mathcal{V} \;=\; &\exp\big[b\,T^b\big] \times \exp\Big[\sum_{1\le m<n\le 4}\big(B_{mn}\,T^B_{mn} + C_{mn}\,T^C_{mn}\big)\Big] \times \exp\big[a\,T^a\big] \\ &\times \Big(\prod_{1\le m<n\le 4}\exp\big[A_{mn}\,T^A_{mn}\big]\Big) \times \exp\Big[\Phi\,H_0 + \sum_{i=1}^{4}\phi_i\,H_i\Big]\,. \end{aligned} \tag{2.19}$$

[2]In this section we suppress $\mathrm{Spin}(5,5)$ indices, but we will need them later on. With indices, $\mathcal{H}$ is written as $\mathcal{H}_{AB}$ and it transforms as $\mathcal{H}_{AB} \to U_A{}^C\,\mathcal{H}_{CD}\,\big(U^T\big)^D{}_B$. The inverse of $\mathcal{H}$ is written with upper indices: $\mathcal{H}^{-1} = \mathcal{H}^{AB}$.

Here the T's and the H's are generators of $\mathfrak{so}(5,5)$ that span the subspace of $\mathfrak{so}(5,5)$ that generates the coset $\mathrm{Spin}(5,5)/(\mathrm{Spin}(5)\times\mathrm{Spin}(5))$. The precise expressions for these generators are given in Appendix 2.B.1. All the scalar fields appear under the same name as in (2.16).

Because we construct our vielbein (2.19) in τ-frame[3], the transformation matrices U and W are also written in τ-frame. Henceforth, we use this frame whenever $\mathrm{Spin}(5,5)$ and $\mathrm{Spin}(5)\times\mathrm{Spin}(5)$ groups appear (unless mentioned otherwise).

2.1.3 6D tensors

The field content of maximal supergravity in six dimensions contains five 2-form tensor gauge fields. Collectively, we denote these fields by $A^{(6)}_{2,a}$ $(a=1,\ldots,5)$, and their field strengths by $G^{(6)}_{3,a}=\mathrm{d}A^{(6)}_{2,a}$. The Lagrangian for these fields reads [88, 89]

$$\mathscr{L}_{\mathrm{t}}=-\frac{1}{2}\,K^{ab}\,G^{(6)}_{3,a}\wedge *\,G^{(6)}_{3,b}-\frac{1}{2}\,L^{ab}\,G^{(6)}_{3,a}\wedge G^{(6)}_{3,b}\,. \tag{2.20}$$

Here K^{ab} and L^{ab} are functions of the scalar fields. We define a set of dual field strengths $\tilde{G}^{(6)a}_3=K^{ab}*G^{(6)}_{3,b}+L^{ab}\,G^{(6)}_{3,b}$ so that we can write the Lagrangian in the more compact form

$$\mathscr{L}_{\mathrm{t}}=-\frac{1}{2}\,G^{(6)}_{3,a}\wedge\tilde{G}^{(6)a}_3\,. \tag{2.21}$$

In this notation, we write the Bianchi identities and the equations of motion as $\mathrm{d}G^{(6)}_{3,a}=0$ and $\mathrm{d}\tilde{G}^{(6)a}_3=0$. We can combine these in the more compact notation $\mathrm{d}G^{(6)}_{3,A}=0$, where $G^{(6)}_{3,A}$ is defined as

$$G^{(6)}_{3,A}=\begin{pmatrix}G^{(6)}_{3,a}\\ \tilde{G}^{(6)a}_3\end{pmatrix}\,. \tag{2.22}$$

The $\mathrm{Spin}(5,5)$ duality symmetry acts on this ten-component vector as

$$G^{(6)}_{3,A}\;\rightarrow\;U_A{}^B\,G^{(6)}_{3,B}\,,\qquad\qquad U_A{}^B\in\mathrm{Spin}(5,5)\,. \tag{2.23}$$

Only the subgroup $\mathrm{GL}(5)\subset\mathrm{Spin}(5,5)$ is a symmetry of the action. The full symmetry group is only manifest on the level of the field equations.

[3]For the convenience of the reader, it might be useful to mention how this convention is related to those of other authors. The following relations hold: $\mathcal{V}=X\,U_{[\mathrm{Tanii}]}X$ where $U_{[\mathrm{Tanii}]}$ is the vielbein that is used in [88], and $\mathcal{V}=\mathcal{V}_{[\mathrm{BSS}]}X$ where $\mathcal{V}_{[\mathrm{BSS}]}$ is the vielbein that is used in [89]. The matrix X is a conjugation matrix that is defined in Appendix 2.B.1.

When we decompose our coset representative in 5×5 blocks as $\mathcal{V} = \left(\begin{smallmatrix} a & b \\ c & d \end{smallmatrix}\right)$, we can write the matrices K^{ab} and L^{ab} as

$$\begin{aligned} K &= \tfrac{1}{2}((c+d)(a+b)^{-1} - (c-d)(a-b)^{-1})\,, \\ L &= \tfrac{1}{2}((c+d)(a+b)^{-1} + (c-d)(a-b)^{-1})\,. \end{aligned} \tag{2.24}$$

Now, by making the identification

$$A^{(6)}_{2,a} = \left(R^{(6)}_{2;\,1}\,,\, R^{(6)}_{2;\,2}\,,\, R^{(6)}_{2;\,3}\,,\, C^{(6)}_{2}\,,\, -B^{(6)}_{2}\right), \tag{2.25}$$

the Lagrangian (2.21) is exactly equal to the one that we find by explicit reduction from type IIB supergravity using the ansätze given in subsection 2.1.1. The advantage of (2.21) is that we have made the duality symmetry manifest.

Doubled formalism

It is a common feature of supergravity actions in even dimensions that only a subgroup of the duality group is a symmetry of the action. In such cases, one can use the so-called doubled formalism [90] to construct an action that realizes the full symmetry group. In order to do this, one needs to introduce twice the original amount of form-valued fields as well as a constraint that makes sure that the doubled theory does not contain more degrees of freedom than the original theory.

We apply this formalism to our 6D tensor fields. We promote the $\tilde{G}^{(6)a}_3$ to field strengths that correspond to the doubled fields, i.e. we write them as $\tilde{G}^{(6)a}_3 = \mathrm{d}\tilde{A}^{(6)a}_2$. These doubled fields $\tilde{A}^{(6)a}_2$ are now treated as independent fields. We write down the doubled Lagrangian as

$$\mathscr{L}^{(\mathrm{doubled})}_{\mathrm{t}} = -\frac{1}{4}\,\mathcal{H}^{AB}\,G^{(6)}_{3,A} \wedge * G^{(6)}_{3,B}\,. \tag{2.26}$$

In this formulation we have ten field strengths $G^{(6)}_{3,A}$ that satisfy the Bianchi identities $\mathrm{d}G^{(6)}_{3,A} = 0$ and the equations of motion $\mathrm{d}\big(\mathcal{H}^{AB} * G^{(6)}_{3,B}\big) = 0$. Furthermore, these fields are subject to the self-duality constraint

$$G^{(6)}_{3,A} = \tau_{AB}\,\mathcal{H}^{BC} * G^{(6)}_{3,C}\,. \tag{2.27}$$

By imposing this constraint on the field equations, we see that they reduce to the ones that correspond to the undoubled action. Thus we have found a proper

doubled version of (2.21). Both the action (2.26) and the constraint (2.27) are invariant under the full Spin(5, 5) duality group. This can be seen directly from the way that these transformations work on the fields:

$$\mathcal{H}^{AB} \;\to\; \left(U^{-T}\right)^{A}{}_{C}\, \mathcal{H}^{CD}\, \left(U^{-1}\right)_{D}{}^{B}, \qquad G^{(6)}_{3,A} \;\to\; U_{A}{}^{B}\, G^{(6)}_{3,B}\,, \tag{2.28}$$

where $U_A{}^B \in \mathrm{Spin}(5,5)$ and we use the notation $U^{-T} = (U^{-1})^T$.

2.2 Scherk-Schwarz reduction to five dimensions

In a Scherk-Schwarz reduction, one considers a $(D+1)$-dimensional supergravity theory with a global symmetry given by a Lie group G that is compactified to D dimensions. The difference between 'ordinary' Kaluza-Klein and Scherk-Schwarz reduction lies in the compactification ansatz. Consider a field $\hat{\psi}$ in the $(D+1)$-dimensional theory that transforms as $\hat{\psi} \to g\hat{\psi}$ with $g \in G$ (for scalars, this is typically a non-linear realization, while some fields such as the metric in Einstein frame will be invariant). The Scherk-Schwarz ansatz then gives $\hat{\psi}$ a dependence on the coordinate z on the circle, which has periodicity $z \simeq z + 2\pi R$, given by

$$\hat{\psi}(x^\mu, z) = \exp\left(\frac{Mz}{2\pi R}\right)\, \psi(x^\mu)\,, \tag{2.29}$$

where M lies in the Lie algebra of G. This ansatz is not periodic around the circle, but picks up a monodromy $\mathcal{M} = e^M \in G$. The Lie algebra element M is sometimes called the mass matrix because it appears in mass terms in the D-dimensional theory. For more details, see [63–65, 67–75, 91] and references therein. A conjugate mass matrix

$$M' = gMg^{-1}\,, \tag{2.30}$$

with $g \in G$, gives a conjugate monodromy

$$\mathcal{M}' = g\mathcal{M}g^{-1}\,. \tag{2.31}$$

This conjugated monodromy gives a massive theory that is related to the one for the monodromy $\mathcal{M}$ by a field redefinition, so that it defines an equivalent theory. Thus the possible Scherk-Schwarz reductions are classified by the conjugacy classes of the duality group [63].

In our case, we reduce from 6D to 5D on a circle with a Scherk-Schwarz twist. We denote the coordinates on the five-dimensional Minkowski space by x^μ and the

coordinate on the circle by z. The compact coordinate is periodic with periodicity $z \simeq z + 2\pi R$. The metric (in Einstein frame) is inert under the duality group, so we choose the conventional Kaluza-Klein metric ansatz:

$$g_{\hat{\mu}\hat{\nu}} = \begin{pmatrix} e^{-\sqrt{1/6}\,\phi_5}\, g_{\mu\nu} + e^{\sqrt{3/2}\,\phi_5}\, \mathcal{A}^5_\mu \mathcal{A}^5_\nu & e^{\sqrt{3/2}\,\phi_5}\, \mathcal{A}^5_\mu \\ e^{\sqrt{3/2}\,\phi_5}\, \mathcal{A}^5_\nu & e^{\sqrt{3/2}\,\phi_5} \end{pmatrix} . \tag{2.32}$$

The factors in the exponents are chosen so that we arrive in Einstein frame in five dimensions and the scalar field ϕ_5 is canonically normalized [92].

The result of our reduction is a gauged $\mathcal{N} = 8$ supergravity theory in five dimensions in which a non-semi-simple subgroup of $\mathrm{Spin}(5,5)$ is gauged. The gauge group contains an important $\mathrm{U}(1)$ subgroup for which $\mathcal{A}^5_\mu$ is the corresponding gauge field. For each twist, the theory has a vacuum (partially) breaking the supersymmetry where it can be described by an $\mathcal{N} < 8$ effective field theory. This reduction from 6D to 5D has been considered previously in [69, 70]. An important feature is that reducing self-dual 2-form gauge fields in 6D can result in massive self-dual 2-form fields in 5D [69]. See [72, 91] for further details.

2.2.1 Monodromies and masses

In six dimensions the global symmetry is $G = \mathrm{Spin}(5,5)$, so in principle we can choose the mass matrix to be any element of the Lie algebra of G. However, our goal is to obtain a Minkowski vacuum with partially broken supersymmetry, so, as discussed in the introduction, we restrict our twist to be conjugate to an element of the R-symmetry group

$$\mathrm{USp}(4)_{\mathrm{L}} \times \mathrm{USp}(4)_{\mathrm{R}} \;=\; \mathrm{Spin}(5)_{\mathrm{L}} \times \mathrm{Spin}(5)_{\mathrm{R}}\,, \tag{2.33}$$

that preserves the identity in $\mathrm{Spin}(5,5)$. We take then a monodromy

$$\mathcal{M} = g\tilde{\mathcal{M}}g^{-1}\,, \quad g \in \mathrm{Spin}(5,5)\,, \quad \tilde{\mathcal{M}} \in \mathrm{USp}(4)_{\mathrm{L}} \times \mathrm{USp}(4)_{\mathrm{R}} \subset \mathrm{Spin}(5,5)\,. \tag{2.34}$$

By a further conjugation, we can bring $\tilde{\mathcal{M}}$ to an element $\bar{\mathcal{M}}$ of a maximal torus $\mathbb{T} = \mathrm{U}(1)^4$ of the R-symmetry group $\mathrm{USp}(4)_{\mathrm{L}} \times \mathrm{USp}(4)_{\mathrm{R}}$

$$\tilde{\mathcal{M}} = h\bar{\mathcal{M}}h^{-1}\,, \quad h \in \mathrm{USp}(4)_{\mathrm{L}} \times \mathrm{USp}(4)_{\mathrm{R}}\,, \quad \bar{\mathcal{M}} \in \mathbb{T} \subset \mathrm{USp}(4)_{\mathrm{L}} \times \mathrm{USp}(4)_{\mathrm{R}}\,. \tag{2.35}$$

The element $\bar{\mathcal{M}}$ of a maximal torus $\mathbb{T} = \mathrm{U}(1)^4$ is then specified by four angles, which we denote m_1, m_2, m_3, m_4; we take $0 \le m_i < 2\pi$. Writing

$$\bar{\mathcal{M}} = (\mathcal{M}_{\mathrm{L}}^{\mathfrak{usp}(4)}, \mathcal{M}_{\mathrm{R}}^{\mathfrak{usp}(4)})\,, \qquad \mathcal{M}_{\mathrm{L/R}}^{\mathfrak{usp}(4)} \in \mathrm{USp}(4)_{\mathrm{L/R}}\,, \tag{2.36}$$

we can take the monodromies to be in the $\mathrm{SU}(2) \times \mathrm{SU}(2)$ subgroup of $\mathrm{USp}(4)$ for both the left and right factors (note that $\mathrm{SU}(2) \cong \mathrm{USp}(2)$):

$$\mathrm{SU}(2)_{\mathrm{L}_1} \times \mathrm{SU}(2)_{\mathrm{L}_2} \times \mathrm{SU}(2)_{\mathrm{R}_1} \times \mathrm{SU}(2)_{\mathrm{R}_2} \subset \mathrm{USp}(4)_{\mathrm{L}} \times \mathrm{USp}(4)_{\mathrm{R}} \,. \tag{2.37}$$

We can then take, for example,

$$\mathcal{M}_{\mathrm{L}}^{\mathfrak{usp}(4)} = e^{m_1\sigma_3} \otimes e^{m_2\sigma_3} \,, \qquad \mathcal{M}_{\mathrm{R}}^{\mathfrak{usp}(4)} = e^{m_3\sigma_3} \otimes e^{m_4\sigma_3} \,, \tag{2.38}$$

where σ_3 is the usual Pauli matrix. Other choices of the monodromy are related to this by $\mathrm{USp}(4)_{\mathrm{L}} \times \mathrm{USp}(4)_{\mathrm{R}}$ conjugation.

The six-dimensional supergravity fields fit into the following representations under the R-symmetry group (see e.g. [70, 88]):

$$\begin{aligned} \text{scalars}: &\quad (\mathbf{5},\mathbf{5}) \,, \\ \text{vectors}: &\quad (\mathbf{4},\mathbf{4}) \,, \\ \text{tensors}: &\quad (\mathbf{5},\mathbf{1}) + (\mathbf{1},\mathbf{5}) \,, \\ \text{gravitini}: &\quad (\mathbf{4},\mathbf{1}) + (\mathbf{1},\mathbf{4}) \,, \\ \text{dilatini}: &\quad (\mathbf{5},\mathbf{4}) + (\mathbf{4},\mathbf{5}) \,. \end{aligned} \tag{2.39}$$

We have an equal number of self-dual and anti-self-dual 2-form tensor fields, and an equal number of fermions of positive and negative chirality. In terms of the R-symmetry representations above, the self-dual tensors B_2^+ transform in the $(\mathbf{5},\mathbf{1})$ and the anti-self-dual tensors B_2^- transform in the $(\mathbf{1},\mathbf{5})$. The positive chiral gravitini ψ_μ^+ and dilatini χ^+ transform in the $(\mathbf{4},\mathbf{1})$ and $(\mathbf{5},\mathbf{4})$ respectively, and the negative chiral gravitini ψ_μ^- and dilatini χ^- transform in the $(\mathbf{1},\mathbf{4})$ and $(\mathbf{4},\mathbf{5})$.

These representations determine the charges (e_1, e_2, e_3, e_4) of each field under $\mathrm{U}(1)^4 \subset \mathrm{USp}(4)_{\mathrm{L}} \times \mathrm{USp}(4)_{\mathrm{R}}$. A field with charges (e_1, e_2, e_3, e_4) will then be an eigenvector of the mass matrix with eigenvalue $i\mu$ and will have z-dependence $e^{i\mu z/2\pi R}$ where

$$\mu = \sum_{i=1}^{4} e_i m_i \,. \tag{2.40}$$

The resulting mass for the field will turn out to be $|\mu|/2\pi R$.

2.2.2 Supersymmetry breaking and massless field content

The R-symmetry representations (2.39) decompose into the following representations under the $\mathrm{SU}(2)^4$ subgroup (2.37):

$$\begin{aligned}
\text{scalars}: \quad & (\mathbf{5},\mathbf{5}) && \to\ (\mathbf{2},\mathbf{2},\mathbf{2},\mathbf{2}) + (\mathbf{2},\mathbf{2},\mathbf{1},\mathbf{1}) + (\mathbf{1},\mathbf{1},\mathbf{2},\mathbf{2}) + (\mathbf{1},\mathbf{1},\mathbf{1},\mathbf{1})\,,\\
\text{vectors}: \quad & (\mathbf{4},\mathbf{4}) && \to\ (\mathbf{2},\mathbf{1},\mathbf{2},\mathbf{1}) + (\mathbf{2},\mathbf{1},\mathbf{1},\mathbf{2}) + (\mathbf{1},\mathbf{2},\mathbf{2},\mathbf{1}) + (\mathbf{1},\mathbf{2},\mathbf{1},\mathbf{2})\,,\\
\text{tensors}: \quad & (\mathbf{5},\mathbf{1}) + (\mathbf{1},\mathbf{5}) && \to\ (\mathbf{2},\mathbf{2},\mathbf{1},\mathbf{1}) + (\mathbf{1},\mathbf{1},\mathbf{2},\mathbf{2}) + 2\,(\mathbf{1},\mathbf{1},\mathbf{1},\mathbf{1})\,,\\
\text{gravitini}: \quad & (\mathbf{4},\mathbf{1}) + (\mathbf{1},\mathbf{4}) && \to\ (\mathbf{2},\mathbf{1},\mathbf{1},\mathbf{1}) + (\mathbf{1},\mathbf{2},\mathbf{1},\mathbf{1}) + (\mathbf{1},\mathbf{1},\mathbf{2},\mathbf{1}) + (\mathbf{1},\mathbf{1},\mathbf{1},\mathbf{2})\,,\\
\text{dilatini}: \quad & (\mathbf{5},\mathbf{4}) + (\mathbf{4},\mathbf{5}) && \to\ (\mathbf{2},\mathbf{2},\mathbf{2},\mathbf{1}) + (\mathbf{2},\mathbf{2},\mathbf{1},\mathbf{2}) + (\mathbf{2},\mathbf{1},\mathbf{2},\mathbf{2}) + (\mathbf{1},\mathbf{2},\mathbf{2},\mathbf{2})\\
& && \quad + (\mathbf{2},\mathbf{1},\mathbf{1},\mathbf{1}) + (\mathbf{1},\mathbf{2},\mathbf{1},\mathbf{1}) + (\mathbf{1},\mathbf{1},\mathbf{2},\mathbf{1}) + (\mathbf{1},\mathbf{1},\mathbf{1},\mathbf{2})\,.
\end{aligned} \tag{2.41}$$

This then determines the four charges e_i under the $\mathrm{U}(1)^4$ subgroup: each doublet gives charges ± 1 and each singlet gives charge 0. For example, the sixteen vector fields in the

$$(\mathbf{4},\mathbf{4}) \ \to\ (\mathbf{2},\mathbf{1},\mathbf{2},\mathbf{1}) + (\mathbf{2},\mathbf{1},\mathbf{1},\mathbf{2}) + (\mathbf{1},\mathbf{2},\mathbf{2},\mathbf{1}) + (\mathbf{1},\mathbf{2},\mathbf{1},\mathbf{2}) \tag{2.42}$$

have charges

$$\begin{aligned}
(e_1,e_2,e_3,e_4) = {} & (\pm 1,0,\pm 1,0) + (\pm 1,0,0,\pm 1) + (0,\pm 1,\pm 1,0)\\
& + (0,\pm 1,0,\pm 1)\,.
\end{aligned} \tag{2.43}$$

These charges then determine the masses through (2.40). The eight gravitini (symplectic Weyl spinors) in the $(\mathbf{4},\mathbf{1}) + (\mathbf{1},\mathbf{4})$ representation of the R-symmetry group $\mathrm{USp}(4)_{\mathrm{L}} \times \mathrm{USp}(4)_{\mathrm{R}}$ decompose into four pairs, each of which has a different mass $|m_i|/2\pi R$, with $i = 1,2,3,4$. The number $\mathcal{N}$ of unbroken supersymmetries is then given by the number of massless gravitini, which is $\mathcal{N} = 2r$ where r is the number of parameters m_i that are zero. The different values of r give rise to 5D supergravities with $\mathcal{N} = 8,6,4,2,0$ Minkowski vacua, corresponding to twisting in $4 - r$ of the SU(2) factors in (2.37).

In general, all fields that are charged, with at least one of the $e_i \neq 0$ corresponding to an $m_i \neq 0$, become massive in 5D. Below we give the massless field content of reductions with twists that preserve $\mathcal{N} = 8,6,4,2,0$ supersymmetry in the Minkowski vacuum and check that they fit into the relevant supermultiplets of 5D supergravities [93].

- $\mathcal{N} = 8$

  We start with the untwisted case, $m_i = 0$, where all fields remain massless. Apart from the 5D graviton, the spectrum contains 8 gravitini, 27 vectors, 48 dilatini and 42 scalars (all massless). As expected, these fields make up a single gravity multiplet of maximal 5D supergravity.

- $\mathcal{N} = 6$

  In order to end up with $\mathcal{N} = 6$ supergravity, we take only one of the four mass parameters to be non-zero so that we twist in only one of the four SU(2) subgroups. The massless spectrum from such a reduction contains a graviton, 6 gravitini, 15 vectors, 20 dilatini and 14 scalars. These fields form the gravity multiplet of the $\mathcal{N} = 6$ theory.

- $\mathcal{N} = 4$

  We obtain $\mathcal{N} = 4$ supergravity by twisting in two SU(2) groups, with two mass parameters zero. This can be done in two qualitatively different ways: either with a chiral twist, say in $\mathrm{SU}(2)_{\mathrm{R}_1}$ and $\mathrm{SU}(2)_{\mathrm{R}_2}$ with $m_1 = m_2 = 0$, or with a non-chiral twist, for example in $\mathrm{SU}(2)_{\mathrm{L}_2}$ and $\mathrm{SU}(2)_{\mathrm{R}_2}$ with $m_1 = m_3 = 0$. Both types of twists result in the same massless spectrum: the graviton, 4 gravitini, 7 vectors, 8 dilatini and 6 scalars, although as we shall see, they result in different massive spectra.

  In the $\mathcal{N} = 4$ theory, the gravity multiplet contains the graviton, 4 gravitini, 6 vectors, 4 dilatini and a single scalar field, and the vector multiplet contains 1 vector, 4 dilatini and 5 scalars [94]. We see that our massless spectrum consists of the gravity multiplet coupled to one vector multiplet.

- $\mathcal{N} = 2$

  We end up with minimal 5D supergravity by twisting in three of the four SU(2) subgroups, with just one of the mass parameters zero. The massless field content after such a twist contains the graviton, 2 gravitini, 3 vectors, 4 dilatini and 2 scalars.

  For $\mathcal{N} = 2$ supersymmetry, the gravity multiplet contains the graviton, 2 gravitini, and 1 vector field, and the vector multiplet contains 1 vector, 2

dilatini and 1 scalar field. Thus, the field content that we find from this reduction forms a gravity multiplet coupled to two vector multiplets.

- $\mathcal{N} = 0$

  By twisting in all four SU(2) groups, with all four mass parameters non-zero, we break all supersymmetry. The only fields that are not charged under such a twist are the graviton and the singlets which are completely uncharged, with all $e_i = 0$. As a result, the massless spectrum in 5D consists of the graviton, 3 vectors and 2 scalars. Note that all fermions become massive.

2.2.3 Massive field content

The charges (e_1, e_2, e_3, e_4) following from (2.41) determine the massive spectrum for the reduced theory in five dimensions. This spectrum is summarized in Table 2.1. The spectrum of Table 2.1 has been previously derived from Scherk-Schwarz reduction in [70] and corresponds to a gauging of $\mathcal{N} = 8$ five-dimensional supergravity.

We now give the supermultiplet structure of the massive spectra that follow from the various twists preserving different amounts of supersymmetry. All fields that acquire mass also become charged under the graviphoton $\mathcal{A}_1^5$ with covariant derivatives of the form

$$D_\mu \;=\; \partial_\mu - iq\, g\, \mathcal{A}_\mu^5 \,. \tag{2.44}$$

Here the gauge coupling is $g = 1/R$, and the charge q of each 5D field is equal to $1/g = R$ times its mass. Because the massive fields are charged, the real fields that follow from the reduction have to combine into complex fields. In the spectra that we give below, we list the number of complex fields (unless stated otherwise). Furthermore, when we give the mass of a field or collection of fields we only write down $|\mu|$. In order to find the actual mass, this needs to be divided by $2\pi R$.

The massive multiplets we find are all BPS multiplets in five dimensions; these multiplets were analyzed and classified in [78] and are labeled by two integers (p, q). For $\mathcal{N}$ supersymmetries in five dimensions (with $\mathcal{N}$ even), the R-symmetry is $\mathrm{USp}(\mathcal{N})$. For a (p, q) massive multiplet, the choice of central charge breaks the R-symmetry to a subgroup $\mathrm{USp}(2p) \times \mathrm{USp}(2q)$, i.e. the subgroup of $\mathrm{USp}(\mathcal{N})$ preserving the central charge, where $2p + 2q = \mathcal{N}$. The nomenclature was chosen such that a massless supermultiplet of (p, q) supersymmetry in six-dimensions has, after reducing on a circle, Kaluza-Klein modes that fit into (p, q) massive

Fields	Representation	$\lvert\mu\rvert$ = Mass (multiplied by $2\pi R$)
Scalars	$(\mathbf{5},\mathbf{5})$	$\lvert\pm m_1 \pm m_2 \pm m_3 \pm m_4\rvert$
		$\lvert\pm m_1 \pm m_2\rvert$
		$\lvert\pm m_3 \pm m_4\rvert$
		0
Vectors	$(\mathbf{4},\mathbf{4})$	$\lvert\pm m_{1,2} \pm m_{3,4}\rvert$
Tensors	$(\mathbf{5},\mathbf{1})$	$\lvert\pm m_1 \pm m_2\rvert$, 0
	$(\mathbf{1},\mathbf{5})$	$\lvert\pm m_3 \pm m_4\rvert$, 0
Gravitini	$(\mathbf{4},\mathbf{1})$	$\lvert\pm m_{1,2}\rvert$
	$(\mathbf{1},\mathbf{4})$	$\lvert\pm m_{3,4}\rvert$
Dilatini	$(\mathbf{5},\mathbf{4})$	$\lvert\pm m_1 \pm m_2 \pm m_{3,4}\rvert$
		$\lvert\pm m_{3,4}\rvert$
	$(\mathbf{4},\mathbf{5})$	$\lvert\pm m_{1,2} \pm m_3 \pm m_4\rvert$
		$\lvert\pm m_{1,2}\rvert$

Table 2.1: *This table gives the value of $|\mu(m_i)|$ for the 5D fields coming from the different types of 6D fields. The mass of the field is then $|\mu(m_i)|/2\pi R$. The notation $m_{i,j}$ indicates that both m_i and m_j occur. There is no correlation between the $\pm$ signs and the $_{ij}$ indices, so that e.g. $(\pm m_1 \pm m_2)$ denotes 4 different combinations of mass parameters, and $(\pm m_{1,2} \pm m_{3,4})$ denotes 16 different combinations. For example, the 5 tensors in the $(\mathbf{5},\mathbf{1})$ representation consist of two with mass $|m_1+m_2|$, two with mass $|m_1-m_2|$ and one with mass* 0.

supermultiplets in five dimensions. The physical states of a (p,q) massive multiplet in five dimensions then fit into representations of

$$\mathrm{SU}(2)\times\mathrm{SU}(2)\times\mathrm{USp}(2p)\times\mathrm{USp}(2q)\ , \tag{2.45}$$

where $\mathrm{SU}(2)\times\mathrm{SU}(2)\sim\mathrm{SO}(4)$ is the little group for massive representations in five dimensions. The representations of the little group $\mathrm{SU}(2)\times\mathrm{SU}(2)$ that arise include $(3,2)$ and $(2,3)$ for massive gravitini and $(2,2)$ for massive vector fields.

The representation $(3,1)$ corresponds to a massive self-dual two-form field satisfying the five-dimensional duality condition

$$\mathrm{d}B_2 = -im * B_2 \ , \tag{2.46}$$

while the $(1,3)$ representation corresponds to the anti-self dual case with $\mathrm{d}B_2 = im * B_2$. In the following, we consider the cases in which the Scherk-Schwarz reduction breaks the supersymmetry to $\mathcal{N} = 6, 4, 2$. The massless states are in the $\mathcal{N}$ supersymmetry representations given in the previous subsection, and we now give the $\mathcal{N}$ supersymmetry representations of the massive fields. It was already pointed out in subsection 2.2.2 that there are two qualitatively different twists that result in a theory with $\mathcal{N} = 4$ supersymmetry: a chiral one and a non-chiral one. Both theories have the same massless spectrum (see subsection 2.2.2), but their massive spectra are different. The non-chiral twist gives massive fields fitting into $(1,1)$ multiplets and we will refer to this as the $(1,1)$ theory. The chiral twist leads to $(0,2)$ supermultiplets and we will refer to this as the $(0,2)$ (or $(2,0)$) theory.

- $\mathcal{N} = 6$

  In order to break to $\mathcal{N} = 6$, we twist with just one of the four mass parameters non-zero. Without loss of generality, we take $m_1 \neq 0$ and the other three parameters equal to zero. The physical states will then fall into representations of

  $$\mathrm{SU}(2) \times \mathrm{SU}(2) \times \mathrm{USp}(2) \times \mathrm{USp}(4) \, . \tag{2.47}$$

  The massive field content from such a twist contains 1 gravitino, 2 self-dual tensors, 4 vectors, 13 dilatini and 10 scalars. All these fields are complex, and their mass is equal to $|m_1|$. This is a $(1,2)$ BPS supermultiplet with the representations

  $$(3,2;1,1)+(3,1;2,1)+(2,2;1,4)+(1,2;1,5)+(2,1;2,4)+(1,1;2,5) \, . \tag{2.48}$$

- $\mathcal{N} = 4$ $(0,2)$

  We obtain the $(0,2)$ theory by taking chiral twist with $m_1, m_2 \neq 0$ and $m_3, m_4 = 0$. The physical states will then fall in representations of

  $$\mathrm{SU}(2) \times \mathrm{SU}(2) \times \mathrm{USp}(4) \ . \tag{2.49}$$

From the reduction we find two massive $(0,2)$ spin-$\frac{3}{2}$ multiplets, one with mass $|m_1|$, and the other with mass $|m_2|$. Each consists of 1 gravitino, 4 vectors and 5 dilatini, which are in the representations

$$(3,2;1)+(2,2;4)+(1,2;5)\ . \tag{2.50}$$

Furthermore, we find two massive $(0,2)$ tensor multiplets with masses $|m_1+m_2|$ and $|m_1-m_2|$. Each of these contains one self-dual 2-form satisfying (2.46), 4 dilatini and 5 scalars [78], fitting in the representations

$$(3,1;1)+(2,1;4)+(1,1;5)\ . \tag{2.51}$$

We note at this point that a part of the massive spectrum above can be made massless by tuning the mass parameters. That is, if we choose $m_1=\pm m_2$, one of the two (complex) tensor multiplets becomes massless. This gives two additional real vector multiplets in the massless sector of the $\mathcal{N}=4$ theory (see subsection 2.2.2).

- $\mathcal{N}=4$ $(1,1)$

  For the non-chiral twist, we choose $m_1,m_3\neq 0$ and $m_2,m_4=0$ in order obtain the $(1,1)$ theory. There are two massive $(1,1)$ vector multiplets, one with mass $|m_1+m_3|$ and one with mass $|m_1-m_3|$. Each consists of 1 vector, 4 dilatini and 4 scalars [78] corresponding to a representation of

  $$\mathrm{SU}(2)\times\mathrm{SU}(2)\times\mathrm{USp}(2)\times\mathrm{USp}(2)\,, \tag{2.52}$$

  given by

  $$(2,2;1,1)+(2,1;2,1)+(1,2;1,2)+(1,1;2,2)\,. \tag{2.53}$$

  In addition, there are two massive $(1,1)$ spin-$\frac{3}{2}$ multiplets, one with mass $|m_1|$, and one with mass $|m_3|$. Each consists of 1 gravitino, 2 (anti-)self-dual tensors, 2 vectors, 5 dilatini and 2 scalars. The one with mass $|m_1|$ is in the representation

  $$(3,2;1,1)+(3,1;2,1)+(2,2;1,2)+(1,2;1,1)+(2,1;2,2)+(1,1;2,1)\,, \tag{2.54}$$

  and the one with mass $|m_3|$ is in the representation

  $$(2,3;1,1)+(1,3;1,2)+(2,2;2,1)+(2,1;1,1)+(1,2;2,2)+(1,1;1,2)\,. \tag{2.55}$$

As in the $(0,2)$ theory, we can tune the mass parameters in such a way that a part of this spectrum becomes massless. For $m_1 = \pm m_3$, one of the massive vector multiplets becomes massless, and so we get two more real vector multiplets in the massless sector of the theory (again see subsection 2.2.2). Note that, even though the massive tensor multiplet of the $(0,2)$ theory and the massive vector multiplet of the $(1,1)$ theory contain different fields, they give the same field content in the massless limit.

- $\mathcal{N} = 2$

  We choose $m_1, m_2, m_3 \neq 0$ and $m_4 = 0$ to obtain the $\mathcal{N} = 2$ case with massive $(0,1)$ multiplets in representations of

  $$\mathrm{SU}(2) \times \mathrm{SU}(2) \times \mathrm{USp}(2) \ . \tag{2.56}$$

  There are four massive hypermultiplets with masses $|m_1 \pm m_2 \pm m_3|$ consisting of 1 complex dilatino and 2 complex scalars in the

  $$(2,1;1) + (1,1;2) \tag{2.57}$$

  representation. The four vector multiplets with masses $|m_{1,2} \pm m_3|$ consist of 1 vector and 2 dilatini in the

  $$(2,2;1) + (1,2;2) \tag{2.58}$$

  representation. Furthermore, we find two tensor multiplets (1 self-dual tensor, 2 dilatini, 1 scalar) with masses $|m_1 \pm m_2|$ in the following representation of (2.56):

  $$(3,1;1) + (2,1;2) + (1,1;1) \ . \tag{2.59}$$

  There are also two spin-$\frac{3}{2}$ multiplets, one with mass $|m_1|$ and one with mass $|m_2|$, containing 1 gravitino, 2 vectors and 1 dilatino in the

  $$(3,2;1) + (2,2;2) + (1,2;1) \tag{2.60}$$

  representation. We also find another multiplet containing a spin-$\frac{3}{2}$ field: 1 gravitino, 2 anti-self-dual tensors, 1 dilatino and 2 scalars with mass $|m_3|$. This is reducible, giving one massive hypermultiplet consisting of 1 dilatino and 2 scalars with the representation (2.57) and one multiplet consisting of 1 gravitino and 2 anti-self-dual tensors in the representation:

  $$(2,3;1) + (1,3;2) \ . \tag{2.61}$$

As for the $\mathcal{N}=4$ theories, we can tune the mass parameters in order to obtain extra massless fields. Choosing $m_1 = \pm m_2$ or $m_{1,2} = \pm m_3$ would make either a tensor multiplet or a vector multiplet massless. Both of these would give two real massless vector multiplets. Another choice would be to set $m_1 = \pm m_2 \pm m_3$ so that one of the massive hypermultiplets becomes massless.

2.2.4 Mass matrices

The monodromies $\mathcal{M}_{\rm L}^{\mathfrak{usp}(4)} \in \mathrm{USp}(4)_{\rm L}$ and $\mathcal{M}_{\rm R}^{\mathfrak{usp}(4)} \in \mathrm{USp}(4)_{\rm R}$ in (2.36) are the exponentials of mass matrices in the Lie algebra of USp(4):

$$\mathcal{M}_{\rm L}^{\mathfrak{usp}(4)} = \exp(M_{\rm L}^{\mathfrak{usp}(4)})\,, \qquad \mathcal{M}_{\rm R}^{\mathfrak{usp}(4)} = \exp(M_{\rm R}^{\mathfrak{usp}(4)})\,. \tag{2.62}$$

For the monodromies (2.38), the mass matrices are given by

$$M_{\rm L}^{\mathfrak{usp}(4)} = m_1\sigma_3 \oplus m_2\sigma_3\,, \qquad M_{\rm R}^{\mathfrak{usp}(4)} = m_3\sigma_3 \oplus m_4\sigma_3\,. \tag{2.63}$$

By conjugating, as in (2.35), by an element h of the $\mathrm{SU}(2)^4$ subgroup (2.37), we can bring this to the form

$$\begin{aligned} M_{\rm L}^{\mathfrak{usp}(4)} &= m_1(n_1\cdot\sigma) \oplus m_2(n_2\cdot\sigma)\,,\\ M_{\rm R}^{\mathfrak{usp}(4)} &= m_3(n_3\cdot\sigma) \oplus m_4(n_4\cdot\sigma)\,, \end{aligned} \tag{2.64}$$

for any four unit 3-vectors n_i. Here σ is the 3-vector of Pauli matrices.

The Lie algebra of USp(4) consists of anti-hermitian 4×4 matrices $M_A{}^B$ ($M^\dagger = -M$) such that $M^{AB} = \Omega^{AC}M_C{}^B$ is symmetric ($M^{AB} = M^{BA}$), where $\Omega^{AB} = -\Omega^{BA}$ is the symplectic invariant; see Appendix 2.B.2 for more details. In a basis in which $\Omega = \sigma_2 \oplus \sigma_2$ and the subgroup (2.37) is block diagonal, we have the 4×4 matrix representation

$$M_{\rm L}^{\mathfrak{usp}(4)} = \begin{pmatrix} m_1(n_1\cdot\sigma) & 0 \\ 0 & m_2(n_2\cdot\sigma) \end{pmatrix}\,, \qquad \Omega^{AB} = \begin{pmatrix} \sigma_2 & 0 \\ 0 & \sigma_2 \end{pmatrix}\,. \tag{2.65}$$

However, for our purposes, it will be useful to have mass matrices in a basis in which

$$\Omega^{AB} = \begin{pmatrix} 0 & \mathbb{1}_2 \\ -\mathbb{1}_2 & 0 \end{pmatrix}\,. \tag{2.66}$$

In this basis, we can take for example

$$M_{\mathrm{L}}^{\mathfrak{usp}(4)} = \begin{pmatrix} 0 & 0 & -m_1 & 0 \\ 0 & 0 & 0 & -m_2 \\ m_1 & 0 & 0 & 0 \\ 0 & m_2 & 0 & 0 \end{pmatrix}, \tag{2.67}$$

and a similar expression for $M_{\mathrm{R}}^{\mathfrak{usp}(4)}$ that can be found by replacing $m_1 \to m_3$ and $m_2 \to m_4$. The monodromy for the above mass matrix is given by

$$\mathcal{M}_{\mathrm{L}}^{\mathfrak{usp}(4)} = \begin{pmatrix} \cos(m_1) & 0 & -\sin(m_1) & 0 \\ 0 & \cos(m_2) & 0 & -\sin(m_2) \\ \sin(m_1) & 0 & \cos(m_1) & 0 \\ 0 & \sin(m_2) & 0 & \cos(m_2) \end{pmatrix}, \tag{2.68}$$

and there is a similar expression for $\mathcal{M}_{\mathrm{R}}^{\mathfrak{usp}(4)}$. We can use the isomorphism $\mathfrak{usp}(4) \cong \mathfrak{so}(5)$ to map (2.67) to the corresponding generator in the Lie algebra of SO(5). This yields

$$M_{\mathrm{L}} = \begin{pmatrix} 0 & -(m_1+m_2) & 0 & 0 & 0 \\ m_1+m_2 & 0 & 0 & 0 & 0 \\ 0 & 0 & 0 & 0 & -(m_1-m_2) \\ 0 & 0 & 0 & 0 & 0 \\ 0 & 0 & m_1-m_2 & 0 & 0 \end{pmatrix}, \tag{2.69}$$

and a similar expression for M_{R} where we replace $m_1 \to m_3$ and $m_2 \to m_4$ (see Appendix 2.B.2 for more information on the isomorphism $\mathfrak{usp}(4) \cong \mathfrak{so}(5)$). The corresponding SO(5) monodromy is given by

$$\mathcal{M}_{\mathrm{L}} = \begin{pmatrix} \cos(m_1+m_2) & -\sin(m_1+m_2) & 0 & 0 & 0 \\ \sin(m_1+m_2) & \cos(m_1+m_2) & 0 & 0 & 0 \\ 0 & 0 & \cos(m_1-m_2) & 0 & -\sin(m_1-m_2) \\ 0 & 0 & 0 & 1 & 0 \\ 0 & 0 & \sin(m_1-m_2) & 0 & \cos(m_1-m_2) \end{pmatrix}.$$

The USp(4) monodromy is of course a double cover of the SO(5) monodromy: taking e.g. $m_1 = m_2 = \pi$ gives $\mathcal{M}_{\mathrm{L}} = \mathbb{1}$ but $\mathcal{M}_{\mathrm{L}}^{\mathfrak{usp}(4)} = -\mathbb{1}$.

We can use the mass matrices M_{L} and M_{R} in the algebras of $\mathrm{SO}(5)_{\mathrm{L}}$ and $\mathrm{SO}(5)_{\mathrm{R}}$ to create an $\mathfrak{so}(5,5)$ mass matrix. In the basis in which the SO(5, 5) metric takes

the form

$$\tau_{AB} = \begin{pmatrix} 0 & \mathbb{1}_5 \\ \mathbb{1}_5 & 0 \end{pmatrix} , \tag{2.70}$$

(see Appendix 2.B.1) this $\mathfrak{so}(5,5)$ mass matrix is given by

$$\mathbb{M}_A{}^B = \frac{1}{2} \begin{pmatrix} (M_{\mathrm{L}} + M_{\mathrm{R}})_a{}^b & (M_{\mathrm{L}} - M_{\mathrm{R}})_{ab} \\ (M_{\mathrm{L}} - M_{\mathrm{R}})^{ab} & (M_{\mathrm{L}} + M_{\mathrm{R}})^a{}_b \end{pmatrix} \in \mathfrak{so}(5,5) . \tag{2.71}$$

It is this matrix that appears explicitly in the bosonic action, as we shall see in the following subsections.

In section 2.3, we consider various brane configurations that result in five-dimensional black holes. For each of these systems, we choose M_{L} and M_{R} in such a way that the fields that charge the black hole remain massless in 5D. All of these are conjugate to the ones given here. In particular, they all have the same eigenvalues and so give the same mass spectrum.

2.2.5 5D scalars

In this section, we go through the reduction of the 6D scalar fields in detail. The goal is to compute the mass that each of the 25 scalar fields obtains in 5D. For notational convenience, we set $R = \frac{1}{2\pi}$ here and in the next subsection where we reduce the 6D tensors. Consequently, the masses that we compute here carry an 'invisible' factor $\frac{1}{2\pi R}$ that can be reinstated by checking the mass dimensions.

The scalar Lagrangian in six dimensions reads (see subsection 2.1.2)

$$e_{(6)}^{-1} \mathscr{L}_{\mathrm{s}} = \frac{1}{8} \operatorname{Tr}\left[\partial_{\hat{\mu}} \mathcal{H}^{-1} \partial^{\hat{\mu}} \mathcal{H}\right] . \tag{2.72}$$

The global $\mathrm{Spin}(5,5)$ transformations act as $\mathcal{H} \to U \mathcal{H} U^T$ with $U \in \mathrm{Spin}(5,5)$. This leads us to the following Scherk-Schwarz ansatz:

$$\mathcal{H}(\hat{x}^{\hat{\mu}}) = e^{\mathbb{M} z} \mathcal{H}(x^{\mu}) e^{\mathbb{M}^T z} , \tag{2.73}$$

where $\mathbb{M}$ is the mass matrix defined in (2.71). By substituting this ansatz in (2.72), we find the five-dimensional Lagrangian

$$e_{(5)}^{-1} \mathscr{L}_{\mathrm{s}} = \frac{1}{8} \operatorname{Tr}\left[D_{\mu} \mathcal{H}^{-1} D^{\mu} \mathcal{H}\right] - V(\mathcal{H}) . \tag{2.74}$$

Matter that is charged under the monodromy becomes charged under the U(1) symmetry corresponding to the graviphoton $\mathcal{A}_1^5$ in 5D. The covariant derivative on $\mathcal{H}$ is given by

$$D_\mu \mathcal{H} = \partial_\mu \mathcal{H} - \mathcal{A}_\mu^5 \left(\mathbb{M}\, \mathcal{H} + \mathcal{H}\, \mathbb{M}^T \right). \tag{2.75}$$

The potential in (2.74) is given by

$$V(\mathcal{H}) = \frac{1}{4}\, e^{-\sqrt{8/3}\,\phi_5}\ \mathrm{Tr}\big[\mathbb{M}^2 + \mathbb{M}^T \mathcal{H}^{-1} \mathbb{M}\, \mathcal{H}\big]\,. \tag{2.76}$$

For an R-symmetry twist, such potentials must be non-negative [63]; consequently, a global minimum can be found by solving $V = 0$. We find such a minimum by putting all 25 scalar fields to zero, so that $\mathcal{H} = \mathbb{1}$. By realizing that our mass matrix is anti-symmetric, $\mathbb{M}^T = -\,\mathbb{M}$, we immediately see that this gives $V = 0$.

We now compute the masses of the scalar fields in this minimum. We denote the collection of all 25 scalar fields by σ^i, with $i = 1, \ldots, 25$, and compute the mass matrix as[4]

$$m_{ij} = \left. \frac{\partial^2 V}{\partial \sigma^i \partial \sigma^j} \right|_{\sigma^k = 0}\,. \tag{2.77}$$

We diagonalize this mass matrix as $m_{ij} = Q_i{}^k\, m^{\mathrm{diag}}_{kl}\, Q^l{}_j$, where m^{diag} is a diagonal matrix and Q is a conjugation matrix built from an orthonormal basis of eigenvectors. In this way, we find the mass that corresponds to each of the redefined fields $\tilde{\sigma}^i = Q^i{}_j \sigma^j$.

We have computed these masses explicitly for the mass matrices that preserve the various 6D black string configurations that we consider in section 2.3. Tables are provided in section 2.C.

2.2.6 5D tensors

In this section we work out the reduction of the six-dimensional tensor fields in detail, following [69, 91]. Just like in the previous subsection, we set $R = \frac{1}{2\pi}$ and neglect the Kaluza-Klein towers for notational convenience.

The Lagrangian for the six-dimensional tensor fields reads

$$\mathscr{L}_{\mathrm{t}}^{(\mathrm{doubled})} = -\frac{1}{4}\, \mathcal{H}^{AB}\, G^{(6)}_{3,A} \wedge * G^{(6)}_{3,B}\,. \tag{2.78}$$

[4] The kinetic term of the sigma model is diagonal at the minimum of the potential, i.e. it takes the form $-\frac{1}{2} g_{ij}(\sigma^k)\, \partial_\mu \sigma^i \partial^\mu \sigma^j$ with $g_{ij}(0) = \delta_{ij}$.

The ten three-form field strengths $G^{(6)}_{3,A}$ transform as in (2.28), so we choose our Scherk-Schwarz ansatz to be

$$G^{(6)}_{3,A}(\hat{x}^{\hat{\mu}}) = \left(e^{\mathbb{M}z}\right)_A{}^B \left(G^{(5)}_{3,B}(x^\mu) + G^{(5)}_{2,B}(x^\mu) \wedge \left(\mathrm{d}z + \mathcal{A}^5_1\right)\right), \tag{2.79}$$

where $G^{(5)}_{3,A}$ and $G^{(5)}_{2,A}$ are five-dimensional field strengths that are independent of the circle coordinate z. As usual for self-dual tensor fields, we don't compactify the Lagrangian of the theory but rather its field equations. We start by reducing the six-dimensional Bianchi identities $\mathrm{d}G^{(6)}_{3,A} = 0$. We find

$$\begin{aligned} \mathrm{d}G^{(5)}_{3,A} + \mathrm{d}\big(G^{(5)}_{2,A} \wedge \mathcal{A}^5_1\big) &= 0\,, \\ \mathrm{d}G^{(5)}_{2,A} - \mathbb{M}_A{}^B\big(G^{(5)}_{3,B} + G^{(5)}_{2,B} \wedge \mathcal{A}^5_1\big) &= 0\,. \end{aligned} \tag{2.80}$$

From these we deduce expressions for the five-dimensional field strengths in terms of the corresponding two-form and one-form potentials:

$$\begin{aligned} G^{(5)}_{3,A} &= \mathrm{d}A^{(5)}_{2,A} - G^{(5)}_{2,A} \wedge \mathcal{A}^5_1\,, \\ G^{(5)}_{2,A} &= \mathrm{d}A^{(5)}_{1,A} + \mathbb{M}_A{}^B\, A^{(5)}_{2,B}\,. \end{aligned} \tag{2.81}$$

Normally at this point, we would like to shift $A^{(5)}_{2,A} \to A^{(5)}_{2,A} - (\mathbb{M}^{-1})_A{}^B\, \mathrm{d}A^{(5)}_{1,B}$ so that the field strengths in (2.81) would lose their dependence on $A^{(5)}_{1,A}$. This is not possible, however, because our mass matrix $\mathbb{M}_A{}^B$ is not invertible. We therefore need to diagonalize $\mathbb{M}_A{}^B$ and split the indices that correspond to zero and non-zero eigenvalues. In the most general case where the combinations $m_1 \pm m_2$ and $m_3 \pm m_4$ are non-zero, this splitting goes like $A \to (\alpha, \dot{\alpha})$ with $\dot{\alpha} \in \{i, i+5\}$, where i is the index that corresponds to the row and column that we set to zero in M_{L} and M_{R}. For example, for the reduction of the D1-D5 system (see (2.112)) we have $\dot{\alpha} \in \{4, 9\}$. The index α takes the other eight values of the original index A. The second equation in (2.81) now separates into

$$\begin{aligned} G^{(5)}_{2,\alpha} &= \mathrm{d}A^{(5)}_{1,\alpha} + \mathbb{M}_\alpha{}^\beta\, A^{(5)}_{2,\beta}\,, \\ G^{(5)}_{2,\dot{\alpha}} &= \mathrm{d}A^{(5)}_{1,\dot{\alpha}}\,. \end{aligned} \tag{2.82}$$

The matrix $\mathbb{M}_\alpha{}^\beta$ is invertible, so now we can shift $A^{(5)}_{2,\alpha} \to A^{(5)}_{2,\alpha} - (\mathbb{M}^{-1})_\alpha{}^\beta\, \mathrm{d}A^{(5)}_{1,\beta}$. After this shift, the five-dimensional field strengths read

$$\begin{aligned} G^{(5)}_{3,\alpha} &= \mathrm{d}A^{(5)}_{2,\alpha} - G^{(5)}_{2,\alpha} \wedge \mathcal{A}^5_1\,, & G^{(5)}_{3,\dot{\alpha}} &= \mathrm{d}A^{(5)}_{2,\dot{\alpha}} - G^{(5)}_{2,\dot{\alpha}} \wedge \mathcal{A}^5_1\,, \\ G^{(5)}_{2,\alpha} &= \mathbb{M}_\alpha{}^\beta\, A^{(5)}_{2,\beta}\,, & G^{(5)}_{2,\dot{\alpha}} &= \mathrm{d}A^{(5)}_{1,\dot{\alpha}}\,. \end{aligned} \tag{2.83}$$

The six-dimensional field strengths are subject to the self-duality constraint

$$G^{(6)}_{3,A} = \tau_{AB}\, \mathcal{H}^{BC} * G^{(6)}_{3,C}\,. \tag{2.84}$$

We now compactify this constraint. First, we need to reduce the six-dimensional Hodge star to five dimensions. By using the metric decomposition (2.32), we find

$$\begin{aligned} *^{(6)} G^{(6)}_{3,A} \;&=\; \big(e^{\mathbb{M}z}\big)_A{}^B\, *^{(6)} \big(G^{(5)}_{3,B} \,+\, G^{(5)}_{2,B} \wedge \big(\mathrm{d}z + \mathcal{A}^5_1\big)\big) \\ &=\; \big(e^{\mathbb{M}z}\big)_A{}^B \big(e^{\sqrt{2/3}\,\phi_5}\; *^{(5)} G^{(5)}_{3,B} \wedge \big(\mathrm{d}z + \mathcal{A}^5_1\big) \;-\; e^{-\sqrt{2/3}\,\phi_5}\; *^{(5)} G^{(5)}_{2,B}\big)\,. \end{aligned} \tag{2.85}$$

This result allows us to write down the 5D self-duality constraint that follows from (2.84) as

$$G^{(5)}_{3,A} = -\, e^{-\sqrt{2/3}\,\phi_5}\, \tau_{AB}\, \mathcal{H}^{BC} * G^{(5)}_{2,C}\,. \tag{2.86}$$

Recall for the derivation of this result that $\mathcal{H}^{AB}$ with raised indices is the inverse of the matrix $\mathcal{H}$ as defined in subsection 2.1.2. Consequently, we use the inverse of (2.73) as Scherk-Schwarz ansatz.

Mass spectrum

In order to find the mass spectrum of the fields that descend from $G^{(6)}_{3,A}$, we put all other fields in (2.86) to zero. In particular, this means that $\mathcal{H}^{AB} = \delta^{AB}$. We find

$$\mathrm{d}A^{(5)}_{2,\alpha} = -\,\tau_\alpha{}^\beta\, \mathbb{M}_\beta{}^\gamma * A^{(5)}_{2,\gamma}\,, \qquad \mathrm{d}A^{(5)}_{2,\dot\alpha} = -\,\tau_{\dot\alpha}{}^{\dot\beta} * \mathrm{d}A^{(5)}_{1,\dot\beta}\,, \tag{2.87}$$

where we use the notation $\tau_\alpha{}^\beta = \tau_{\alpha\gamma}\,\delta^{\gamma\beta}$ and an analogous expression for the dotted indices. These are massive and massless five-dimensional self-duality conditions. From these, we can deduce the equations of motion for the corresponding fields (following [95]). They read

$$\mathrm{d}\big(*\,\mathrm{d}A^{(5)}_{2,\alpha}\big) = -\,\big(\tau\mathbb{M}\tau\mathbb{M}\big)_\alpha{}^\beta * A^{(5)}_{2,\beta}\,, \qquad \mathrm{d}\big(*\,\mathrm{d}A^{(5)}_{1,\dot\alpha}\big) = 0\,. \tag{2.88}$$

So in 5D, we end up with eight massive tensors and two massless vectors (again, this is for the case where $m_1 \pm m_2$ and $m_3 \pm m_4$ are non-zero). The self-duality constraint (2.86) eliminates the massless tensors $A^{(5)}_{2,\dot\alpha}$ and makes sure that the massive tensors $A^{(5)}_{2,\alpha}$ carry only half their usual degrees of freedom. The masses of the fields $A^{(5)}_{2,\alpha}$ are determined by the mass matrix $-\big(\tau\mathbb{M}\tau\mathbb{M}\big)_\alpha{}^\beta$. By diagonalizing this matrix, we find the mass corresponding to each field.

Just as for the scalar fields, we have computed these masses explicitly for the mass matrices that we use for the reduction of the D1-D5 system and the dual brane configurations in section 2.3. These masses can be found in section 2.C.

Graviphoton interactions

We now pay some extra attention to the interactions between the graviphoton and the vector and tensor fields that we find in this subsection. They will prove to be very important in section 2.4. As it turns out, there is a difference in the result that we find for the reduction of a self-dual 6D tensor and an anti-self-dual 6D tensor. We illustrate this difference with two simple examples.

Consider a six-dimensional (anti-)self-dual tensor field $\hat{B}_2$ with field strength $\hat{H}_3 = \hat{\mathrm{d}}\hat{B}_2$ (here hats denote 6D quantities). The field equations and self-duality constraint for this field read

$$\hat{\mathrm{d}}\hat{H}_3 = 0\,, \qquad \hat{*}\,\hat{H}_3 = \pm\,\hat{H}_3\,. \tag{2.89}$$

By decomposing this field (strength) as $\hat{H}_3 = H_3 + H_2 \wedge (\mathrm{d}z + \mathcal{A}_1)$, and by using straightforward reduction techniques and the conventions of this chapter, we find the following 5D Lagrangian:

$$\mathscr{L} = -\tfrac{1}{2}\, H_2 \wedge * H_2 \,\pm\, \tfrac{1}{2}\, \mathcal{A}_1 \wedge H_2 \wedge H_2\,, \tag{2.90}$$

with $H_2 = \mathrm{d}B_1$. We see that a self-dual and an anti-self-dual tensor give a Chern-Simons interaction term with the graviphoton with an opposite sign.

Now take a real doublet of (anti-)self-dual tensor fields, that we Scherk-Schwarz reduce from 6D to 5D with the ansatz

$$\hat{H}_3 = \exp\left[\begin{pmatrix} 0 & -m \\ m & 0 \end{pmatrix} z\right] \big(H_3 + H_2 \wedge (\mathrm{d}z + \mathcal{A}_1)\big), \tag{2.91}$$

(apart from the ansatz and the fact that we are considering a doublet this set-up is similar to the previous one). Going through this reduction gives a complex massive tensor B_2 in five dimensions subject to the self-duality equation

$$\mathrm{d}B_2 \,-\, im\, \mathcal{A}_1 \wedge B_2 \,\pm\, im * B_2 = 0\,. \tag{2.92}$$

Again, the $\pm$ sign indicates the difference between the result for the reduction of a self-dual and an anti-self-dual tensor from six dimensions. Now, this sign is not in

front of the interaction with the graviphoton, but we can still flip it by redefining $\mathcal{A}_1 \to -\mathcal{A}_1$. To see this, recall that the field B_2 is complex so that we also have the complex conjugate of (2.92). By flipping the sign of the graviphoton, we effectively switch the particle and the anti-particle $B_2 \leftrightarrow \bar{B}_2$ in order to protect the sign in the covariant derivative. The $\pm$ sign in the mass term of the equation for $\bar{B}_2$ is flipped with respect to (2.92), and so we see that redefining $\mathcal{A}_1 \to -\mathcal{A}_1$ effectively interchanges the result for a self-dual and an anti-self-dual tensor.

2.2.7 Conjugate monodromies

We have so far considered monodromies in the R-symmetry group $\mathrm{Spin}(5)_{\mathrm{L}} \times \mathrm{Spin}(5)_{\mathrm{R}}$ preserving the identity in the coset $\mathrm{Spin}(5,5)/\mathrm{Spin}(5)_{\mathrm{L}} \times \mathrm{Spin}(5)_{\mathrm{R}}$, which is the point in the moduli space at which all scalar fields vanish. Then this point in moduli space is a fixed point under the action of the $\mathrm{Spin}(5,5)$ transformation $\psi \to \mathcal{M}\psi$ given by the monodromy, and as we have seen this point is a minimum of the Scherk-Schwarz potential giving a Minkowski vacuum. Conjugating by an element of the R-symmetry group

$$\mathcal{M} \to h\bar{\mathcal{M}}h^{-1}\,, \qquad h \in \mathrm{USp}(4)_{\mathrm{L}} \times \mathrm{USp}(4)_{\mathrm{R}} \tag{2.93}$$

will then preserve the fixed point in the moduli space and the minimum will remain at the origin.

However, for the embedding in string theory (see subsection 2.5.1), we will need to consider monodromies that are related to an R-symmetry transformation by conjugation by an element of $\mathrm{Spin}(5,5)$

$$\mathcal{M} = g\tilde{\mathcal{M}}g^{-1}\,, \quad g \in \mathrm{Spin}(5,5)\,, \quad \tilde{\mathcal{M}} \in \mathrm{USp}(4)_{\mathrm{L}} \times \mathrm{USp}(4)_{\mathrm{R}} \subset \mathrm{Spin}(5,5)\,. \tag{2.94}$$

This change of monodromy can be thought of as the result of acting on the theory twisted with monodromy $\tilde{\mathcal{M}}$ by a transformation $\psi \to g\psi$. For the supergravity theory, this is just a field redefinition giving an equivalent theory, but as we shall see later this has consequences for the embedding in string theory. The fixed point is now at the coset containing g, $[g] = \{gh \mid h \in \mathrm{Spin}(5)_{\mathrm{L}} \times \mathrm{Spin}(5)_{\mathrm{R}}\}$, and this is now the location of the minimum of the potential [63]. At this point, the kinetic terms of the various fields are not conventionally normalized. On bringing these to standard form, the masses become precisely the ones given earlier for the theory with monodromy $\tilde{\mathcal{M}}$. This was of course to be expected: a field redefinition cannot change physical parameters such as masses.

2.2.8 Gauged supergravity and gauge group

The result of the Scherk-Schwarz reduction is a gauged $\mathcal{N} = 8$ supergravity theory in which a subgroup of the E_6 duality symmetry of the ungauged 5D theory is promoted to a gauge symmetry. In this subsection we discuss this gauged supergravity and its gauge group.

We start with the case in which the twist is a T-duality transformation in the T-duality subgroup Spin(4, 4) of Spin(5, 5). Consider first the bosonic NS-NS sector of the ten-dimensional supergravity theory, consisting of the metric, B-field and dilaton. Compactifying on T^4 gives a 6D theory with SO(4, 4) symmetry. There is a 6D metric, B-field and dilaton, together with 8 vector fields $A^A_{\hat{\mu}}$ in the **8** of SO(4, 4) (with $A = 1, \ldots, 8$ labelling the vector representation of SO(4, 4)) and scalars in the coset space $\mathrm{SO}(4,4)/\mathrm{SO}(4) \times \mathrm{SO}(4)$. The Scherk-Schwarz compactification of this on a circle with an SO(4, 4) twist with mass matrix $N_A{}^B$ was given in detail in [72]. In 5D, there are then 10 gauge fields: eight A^A_μ arising from the 6D vector fields, the graviphoton vector field $\mathcal{A}^5_\mu$ from the metric and a vector field $\mathcal{B}^5_\mu$ from the reduction of the 6D B-field. Then $(A^A_\mu, \mathcal{A}^5_\mu, \mathcal{B}^5_\mu)$ are the gauge fields for a gauge group with 10 generators $T_A, T_z, T_{\tilde{z}}$ respectively. After the field redefinitions given in [72] to obtain tensorial fields transforming covariantly under duality transformations, the gauge algebra is [72]

$$[T_z, T_A] = N_A{}^B\, T_B\,, \qquad [T_A, T_B] = N_{AB}\, T_{\tilde{z}}\,, \tag{2.95}$$

with all other commutators vanishing. Here $N_{AB} = N_A{}^C \eta_{CB}$ where η_{AB} is the SO(4, 4)-invariant metric, so that $N_{AB} = -N_{BA}$ as the mass matrix is in the Lie algebra of SO(4, 4). This then represents a gauging of a 10-dimensional subgroup of SO(4, 4), which has a $\mathrm{U}(1)^2$ subgroup generated by $T_z, T_{\tilde{z}}$. A further U(1) factor can be obtained by dualising the 2-form $b_{\mu\nu}$ to give an extra gauge field and the generator t of this U(1) factor commutes with all other generators.

Next, consider reintroducing the R-R sector. In six dimensions, there are a further 8 one-form gauge fields $C^\alpha_{\hat{\mu}}$ transforming as a Weyl spinor of Spin(4, 4) ($\alpha = 1, \ldots, 8$), which combine with the 8 NS-NS one-form gauge fields to form the **16** of Spin(5, 5). There are also a further 4 two-form gauge fields, which split into four self-dual ones and four anti-self dual ones that transform as an **8** of SO(4, 4). These combine with the degrees of freedom of the NS-NS 2-form to form the **10** of Spin(5, 5). The mass matrix acts on the spinor representation through $N_\alpha{}^\beta$ which is given as usual

by $N_{\alpha\beta} = \frac{1}{4} N_{AB} (\gamma^{AB})_{\alpha\beta}$ where $N_{\alpha\beta} = N_\alpha{}^\gamma \eta_{\gamma\beta}$ and $\eta_{\alpha\beta}$ is the symmetric charge conjugation matrix. The structure in the spinor representation is related to that in the vector representation by SO(4, 4) triality. The gauge algebra then gains the terms

$$[T_z, T_\alpha] = N_\alpha{}^\beta T_\beta \,, \qquad [T_\alpha, T_\beta] = N_{\alpha\beta} T_{\tilde{z}} \,, \tag{2.96}$$

to give an 18-dimensional gauge group. This corresponds to gauging an 18-dimensional subgroup of E_6. For generic values of the parameters m_i, the two-form gauge fields in the **8** of SO(4, 4) become massive, while the 5D NS-NS two-form remains massless and can again be dualized to give a further U(1) factor with generator t. For special values of the parameters, some of the two-forms in the **8** of SO(4, 4) can become invariant under the twist and so become massless as well. These can be dualized to give further U(1) factors.

The gauge algebra can now be written

$$[T_z, T_a] = M_a{}^b T_b \,, \qquad [T_a, T_b] = M_{ab} T_{\tilde{z}} \,, \tag{2.97}$$

with all other commutators vanishing, where $T_a = (T_A, T_\alpha)$ and

$$M_a{}^b = \begin{pmatrix} N_A{}^B & 0 \\ 0 & N_\alpha{}^\beta \end{pmatrix} . \tag{2.98}$$

There is a $U(1)^3$ subgroup generated by t (if the NS-NS two-form is dualized) with possible further U(1) factors coming in if some of the R-R two-forms remain massless.

In the generic case in which $M_a{}^b$ has no zero eigenvalues, then the vector fields A^a corresponding to the generators T_a all become massive, while the gauge fields corresponding to the generators $T_z, T_{\tilde{z}}, t$ remain massless. Then the gauge group is spontaneously broken to the $U(1)^3$ subgroup generated by $T_z, T_{\tilde{z}}, t$. For special values of the parameters m_i such that $M_a{}^b$ has some zero eigenvalues, there will be more massless gauge fields and the unbroken gauge group will be larger.

In subsection 2.3.2, we will consider a twist of this kind in the compact Spin(4) × Spin(4) subgroup of the Spin(4, 4) T-duality group. The other twists we will consider are all related to this one by conjugation (see subsection 2.2.7 and 2.3.2) and will give isomorphic gauge groups.

One can argue what part of the matter content is charged under each of these generators of the gauge group by Scherk-Schwarz reducing the 6D gauge transformations and seeing how the 5D fields transform under these reduced transformations. The 6D gauge transformations can be found in [88, 89]. The generators T_a come from the gauge transformations corresponding to the 16 vector fields in 6D. These transform the 6D vectors and the 6D tensors, so the 5D descendants of these fields can become charged under generators T_a. The generators $T_{\tilde{z}}$ and t come from the gauge transformation that correspond to the 6D tensor field that is a singlet under the twist. This transformation acts only on this tensor field, so after reduction no matter becomes charged under the resulting 5D transformations $T_{\tilde{z}}$ and t. The generator T_z (corresponding to the graviphoton $\mathcal{A}_1^5$) comes from 6D diffeomorphisms in the circle direction. By explicit reduction of these diffeomorphisms, we find that all fields that become massive in 5D carry U(1) charge under T_z.

2.2.9 Kaluza-Klein towers

In the previous subsections, we have constructed 5D theories with both massless and massive fields from Scherk-Schwarz reduction. However, this is not the whole story: if we consider a compactification on S^1, then each field picks up an infinite Kaluza-Klein tower[5]. We choose Scherk-Schwarz ansätze including Kaluza-Klein towers on the S^1 of the form

$$\psi(x^\mu, z) = \exp\left(\frac{Mz}{2\pi R}\right) \sum_{n\in\mathbb{Z}} e^{inz/R}\, \psi_n(x^\mu)\,, \tag{2.99}$$

where we use ψ as a schematic notation for any field in the theory that transforms in some representation of the R-symmetry group. Then if ψ has charges e_i, it is an eigenvector of M with eigenvalue $i\mu$ given by (2.40), $M\psi = i\mu\,\psi$, so that

$$\psi(x^\mu, z) = \sum_{n\in\mathbb{Z}} \exp\left(i\left(\frac{\mu}{2\pi} + n\right)\frac{z}{R}\right) \psi_n(x^\mu)\,. \tag{2.100}$$

Clearly, shifting $\frac{\mu}{2\pi}$ by an integer r can be absorbed into a shift $n \to n - r$ and so corresponds to changing the n'th Kaluza-Klein mode to the $(n-r)$'th one while leaving the sum unchanged. From Table 2.1, we see that shifting the m_i by $2\pi r_i$ for

[5] Of course, even this is not the whole story. There are also Kaluza-Klein modes that come from the reduction from 10D to 6D on the four-torus, plus stringy degrees of freedom. We will return to these in section 2.5, where we discuss the full string theory.

any integers r_i shifts all the $\frac{\mu}{2\pi}$ by an integer and so leaves the above sum (2.100) unchanged. For this reason, there is no loss of generality in taking $m_i \in [0, 2\pi)$.

Without loss of generality, we can restrict the m_i's further by realizing that all eigenvalues $i\mu$ appear with a $\pm$ sign in front of them. By taking into account two towers of the form (2.100), one of them with a minus sign in front of μ, we see that the *combination* of these towers is unchanged under $\frac{\mu}{2\pi} \to 1 - \frac{\mu}{2\pi}$. Consequently, we can take $m_i \in [0, \pi]$ without loss of generality.

The Scherk-Schwarz ansatz is a truncation of (2.100) to the $n = 0$ mode. This gives a consistent truncation to a gauged five-dimensional supergravity theory, which is sufficient for e.g. determining which twists preserve which brane configuration in section 2.3. The full string theory requires keeping all these modes, together with stringy modes and degrees of freedom from branes wrapping the internal space.

The mass of the n'th KK-mode is given by

$$\left| \frac{\mu}{2\pi R} + \frac{n}{R} \right| , \qquad n \in \mathbb{Z} , \tag{2.101}$$

and the value of $\mu(m_i)$ for each field can be read off from Table 2.1. As an example, we check this for the reduction of the 6D tensors. If the whole tower is taken into account, the Scherk-Schwarz ansatz (2.79) is extended to

$$G_3^{(6)}(\hat{x}^{\hat{\mu}}) = \exp\left(\frac{\mathbb{M}z}{2\pi R}\right) \sum_{n\in\mathbb{Z}} e^{inz/R} \left(G_{3,n}^{(5)}(x^\mu) + G_{2,n}^{(5)}(x^\mu) \wedge \left(\mathrm{d}z + \mathcal{A}_1^5\right)\right) . \tag{2.102}$$

Note that we have restored the circle radius R in this ansatz; from now on, we will keep it manifest in all our equations. Furthermore, in (2.102) the Spin$(5,5)$ indices are suppressed for clarity. It can be seen directly that this extended ansatz essentially changes the mass matrix $\mathbb{M}$ as we used it in subsection 2.2.6 to

$$\left(\frac{\mathbb{M}}{2\pi R} + \frac{in\mathbb{1}}{R} \right) , \qquad n \in \mathbb{Z} . \tag{2.103}$$

We can now use that the eigenvalue of $\mathbb{M}$ is $i\mu$ with μ given by (2.40) to see that the masses of the Kaluza-Klein modes are given by (2.101).

Note that the modes with $n = 0$ that are kept in the Scherk-Schwarz reduction are not necessarily the lightest modes in the tower. In particular, if the parameters m_i

are chosen so that $\frac{\mu(m_i)}{2\pi}$ is an integer, $\frac{\mu(m_i)}{2\pi} = N$, then the mode with $n = -N$ will be massless. As an example of this, we can choose

$$m_1 = m_2 = \tfrac{\pi}{2}\,,\ m_3 = \pi\,,\ m_4 = 0\,. \tag{2.104}$$

By using Table 2.1, we can see which additional massless fields arise. In this case, there are four scalars and two spin-$\frac{1}{2}$ fermions that become massless, which form a hypermultiplet of $\mathcal{N} = 2$ supergravity. For further discussion of such accidental massless modes, see [63, 74].

2.3 Five-dimensional black hole solutions

In this section, we consider several 10D brane configurations that we compactify to give black holes in 5D. We do this in two steps. First, we reduce the brane configuration to a black string solution of $(2, 2)$ supergravity in six dimensions. This solution will not be invariant under the whole Spin$(5, 5)$ duality group, but will be preserved by a stabilizing subgroup. If we then do a standard (untwisted) compactification of this on a circle with the black string wrapped along the circle, we obtain a BPS black hole solution of $\mathcal{N} = 8$ supergravity in five dimensions. This reduction can be modified by including a duality twist on the circle. If the duality twist is in the stabilizing subgroup, the same black hole solution will remain a solution of the gauged supergravity resulting from the Scherk-Schwarz reduction, and of its truncation to an effective $\mathcal{N} < 8$ supergravity describing the massless sector. This is because the only fields that become massive as a result of the Scherk-Schwarz twist are the ones that are trivial (zero) in the black hole solution. As a consequence, the black hole will also be BPS and preserving (at least) four supercharges. Indeed, it descends from a BPS black string solution in six dimensions, and the duality twist preserves the supercharges and Killing spinors of the truncated theory that has the black hole as a solution.

Primarily, we focus on the D1-D5 system, but later in this section we also consider the dual F1-NS5 and D3-D3 systems.

2.3.1 The D1-D5-P system

The D1-D5 system, sometimes more accurately called the D1-D5-P system, consists of D1-branes, D5-branes and waves carrying momentum. The ten-dimensional configuration is as follows:

	$\mathbb{R}^{1,4}$					S^1	T^4			
	t	r	θ	φ_1	φ_2	z	y_1	y_2	y_3	y_4
D1	–	·	·	·	·	–	···	···	···	···
D5	–	·	·	·	·	–	–	–	–	–
P	–	·	·	·	·	–	···	···	···	···

Here a line (−) denotes an extended direction, a dot (·) denotes a pointlike direction, and multiple dots (· · ·) denote a direction in which the brane or wave is smeared.

We start from the ten-dimensional solution and reduce it to 5D with the ansätze that are given in previous sections. The D1-D5 solution of type IIB supergravity in Einstein frame reads

$$\begin{cases} \mathrm{d}s^2_{(10)} = H_1^{-\frac{3}{4}} H_5^{-\frac{1}{4}} \left[-\mathrm{d}t^2 + \mathrm{d}z^2 + K(\mathrm{d}t - \mathrm{d}z)^2 \right] + H_1^{\frac{1}{4}} H_5^{\frac{3}{4}} \left[\mathrm{d}r^2 + r^2 \mathrm{d}\Omega_3^2 \right] \\ \qquad\qquad + H_1^{\frac{1}{4}} H_5^{-\frac{1}{4}} \left[\mathrm{d}y_1^2 + \mathrm{d}y_2^2 + \mathrm{d}y_3^2 + \mathrm{d}y_4^2 \right] \\ e^{\Phi} = H_1^{\frac{1}{2}} H_5^{-\frac{1}{2}} \\ C_2^{(10)} = (H_1^{-1} - 1)\, \mathrm{d}t \wedge \mathrm{d}z + Q_5 \cos^2\theta \, \mathrm{d}\varphi_1 \wedge \mathrm{d}\varphi_2 \,, \end{cases} \tag{2.105}$$

where $\mathrm{d}\Omega_3^2 = \mathrm{d}\theta^2 + \sin^2\theta \, \mathrm{d}\varphi_1^2 + \cos^2\theta \, \mathrm{d}\varphi_2^2$ is the metric on the three-sphere written in Hopf coordinates. The harmonic functions corresponding to the D1-branes, the D5-branes and the momentum modes can be written in terms of their total charges as

$$H_1 = 1 + \frac{Q_1}{r^2} \,, \qquad H_5 = 1 + \frac{Q_5}{r^2} \,, \qquad H_K = 1 + K = 1 + \frac{Q_K}{r^2} \,. \tag{2.106}$$

Reduction to six dimensions

We compactify the metric in (2.105) to 6D using the ansatz (2.4). The metric on the torus, g_{mn}, is diagonal in (2.105) so we find that

$$e^{\vec{b}_m \cdot \vec{\phi}} = H_1^{\frac{1}{4}} H_5^{-\frac{1}{4}} \,, \qquad m = 1, \ldots, 4 \,. \tag{2.107}$$

By using the expressions for the vectors $\vec{b}_m$ given in (2.6), we can solve for the individual scalar fields ϕ_i. We find that only one of them is non-zero in the 6D solution:

$$e^{\phi_4} = H_1^{\frac{1}{2}} H_5^{-\frac{1}{2}} \,, \qquad \phi_1 = \phi_2 = \phi_3 = 0 \,. \tag{2.108}$$

The rest of the reduction is straightforward. The six-dimensional Einstein frame metric is related to the ten-dimensional one by a Weyl rescaling with $g_4^{1/4} = H_1^{\frac{1}{4}} H_5^{-\frac{1}{4}}$, which is incorporated in the ansatz (2.4). The dilaton Φ and the R-R two-form $C_2^{(10)}$ have no non-zero components on the torus, so they reduce trivially. The result reads

$$\begin{cases} \mathrm{d}s^2_{(6)} = H_1^{-\frac{1}{2}} H_5^{-\frac{1}{2}} \left[-\mathrm{d}t^2 + \mathrm{d}z^2 + K(\mathrm{d}t - \mathrm{d}z)^2 \right] + H_1^{\frac{1}{2}} H_5^{\frac{1}{2}} \left[\mathrm{d}r^2 + r^2 \mathrm{d}\Omega_3^2 \right] \\ e^{\phi_+} = H_1^{\sqrt{\frac{1}{2}}} H_5^{-\sqrt{\frac{1}{2}}} \\ C_2^{(6)} = (H_1^{-1} - 1)\, \mathrm{d}t \wedge \mathrm{d}z + Q_5 \cos^2\theta\, \mathrm{d}\varphi_1 \wedge \mathrm{d}\varphi_2 \,. \end{cases} \tag{2.109}$$

Here, we have defined the scalar field $\phi_+ = \frac{1}{\sqrt{2}}(\phi_4 + \Phi)$. This solution describes a black string in six dimensions.

When we use the doubled formalism (see subsection 2.1.3) we can rewrite the solution above in terms of the doubled tensor fields. To derive the contributions of these doubled fields to the black string solution, recall that the dual field strengths are defined as $\tilde{G}_3^{(6)a} = K^{ab} * G_{3,b}^{(6)} + L^{ab} G_{3,b}^{(6)}$. By putting all scalar fields except ϕ_+ to zero, this reduces to $\tilde{G}_3^{(6)a} = K^{ab} * G_{3,b}^{(6)}$ with $K^{ab} = \mathrm{diag}\,(1, 1, 1, e^{\sqrt{2}\,\phi_+}, 1)$. Hence, we find that the doubled tensors to which the black string solution couples are given by

$$\begin{aligned} C_2^{(6)} &= (H_1^{-1} - 1)\, \mathrm{d}t \wedge \mathrm{d}z + Q_5 \cos^2\theta\, \mathrm{d}\varphi_1 \wedge \mathrm{d}\varphi_2 \,, \\ \tilde{C}_2^{(6)} &= (H_5^{-1} - 1)\, \mathrm{d}t \wedge \mathrm{d}z + Q_1 \cos^2\theta\, \mathrm{d}\varphi_1 \wedge \mathrm{d}\varphi_2 \,. \end{aligned} \tag{2.110}$$

In the doubled formalism, the degrees of freedom of both these fields are halved by the self-duality constraint (2.27) so the total number of degrees of freedom of the fields that the black string couples to remain unchanged.

Scherk-Schwarz reduction to five dimensions

The last step is to Scherk-Schwarz reduce the six-dimensional black string solution, which results in a black hole in five dimensions. We choose the twist matrices to be in the stabilizing subgroup of the R-symmetry group, i.e. the subgroup of the R-symmetry that preserves the solution. As a result, all the fields that are non-constant in the black hole remain massless.

For the D1-D5 system, we choose the following $\mathfrak{usp}(4)$ mass matrices:

$$M_{\mathrm{L}}^{\mathfrak{usp}(4)} = \begin{pmatrix} 0 & 0 & -m_1 & 0 \\ 0 & 0 & 0 & -m_2 \\ m_1 & 0 & 0 & 0 \\ 0 & m_2 & 0 & 0 \end{pmatrix}, \qquad M_{\mathrm{R}}^{\mathfrak{usp}(4)} = \begin{pmatrix} 0 & 0 & -m_3 & 0 \\ 0 & 0 & 0 & -m_4 \\ m_3 & 0 & 0 & 0 \\ 0 & m_4 & 0 & 0 \end{pmatrix}. \tag{2.111}$$

Here m_1, m_2, m_3 and m_4 are real mass parameters, each corresponding to one SU(2) in the R-symmetry subgroup (2.37). The isomorphism $\mathfrak{usp}(4) \cong \mathfrak{so}(5)$ of Appendix 2.B.2 maps these to $\mathfrak{so}(5)$ mass matrices. We find

$$M_{\mathrm{L}} = \begin{pmatrix} 0 & -(m_1+m_2) & 0 & 0 & 0 \\ m_1+m_2 & 0 & 0 & 0 & 0 \\ 0 & 0 & 0 & 0 & -(m_1-m_2) \\ 0 & 0 & 0 & 0 & 0 \\ 0 & 0 & m_1-m_2 & 0 & 0 \end{pmatrix}, \qquad M_{\mathrm{R}} = \begin{pmatrix} 0 & -(m_3+m_4) & 0 & 0 & 0 \\ m_3+m_4 & 0 & 0 & 0 & 0 \\ 0 & 0 & 0 & 0 & -(m_3-m_4) \\ 0 & 0 & 0 & 0 & 0 \\ 0 & 0 & m_3-m_4 & 0 & 0 \end{pmatrix}. \tag{2.112}$$

The embedding of these $\mathfrak{so}(5)$ matrices in the $\mathfrak{so}(5,5)$ mass matrix $\mathbb{M}_A{}^B$ is given in (2.71).

We can now follow the techniques of subsection 2.2.5 and 2.2.6 to determine the masses that each of the scalar and tensor fields acquires due to this twist. The results of these calculations for the mass matrices (2.112) are presented in Appendix 2.C. In particular, we find that the fields that appear in the six-dimensional black string solution (ϕ_+, $C_2^{(6)}$ and $\tilde{C}_2^{(6)}$) do not become massive in this Scherk-Schwarz reduction, as required. This means that the reduction of the solution (2.109) to a 5D black hole is the same as in the untwisted case.

The two self-dual tensors that charge the black string solution, $C_2^{(6)}$ and $\tilde{C}_2^{(6)}$, yield two tensors and two vector fields in 5D. We denote these by $C_2^{(5)}$, $C_1^{(5)}$, $\tilde{C}_2^{(5)}$, $\tilde{C}_1^{(5)}$. We now consider the self-duality conditions for these fields from (2.86), where we only take along fields that are non-zero in the 5D black hole solution. We find that they are pairwise dual by the relations

$$\begin{aligned} \mathrm{d}C_1^{(5)} &= e^{\sqrt{2/3}\,\phi_5}\, e^{-\sqrt{2}\,\phi_+} * \mathrm{d}\tilde{C}_2^{(5)} \,, \\ \mathrm{d}\tilde{C}_1^{(5)} &= e^{\sqrt{2/3}\,\phi_5}\, e^{\sqrt{2}\,\phi_+} * \mathrm{d}C_2^{(5)} \,. \end{aligned} \tag{2.113}$$

We use these to write the contributions of $C_2^{(5)}$ and $\tilde{C}_2^{(5)}$ to the black hole solution in terms of the dual one-forms. In doing so, we move to an undoubled formalism. The full five-dimensional black hole solution is then given by

$$\begin{cases} \mathrm{d}s^2_{(5)} = -(H_1 H_5 H_K)^{-\frac{2}{3}}\,\mathrm{d}t^2 + (H_1 H_5 H_K)^{\frac{1}{3}}\left[\mathrm{d}r^2 + r^2 \mathrm{d}\Omega_3^2\right] \\ e^{\phi_+} = H_1^{\sqrt{\frac{1}{2}}} H_5^{-\sqrt{\frac{1}{2}}} \\ e^{\phi_5} = H_1^{-\sqrt{\frac{1}{6}}} H_5^{-\sqrt{\frac{1}{6}}} H_K^{\sqrt{\frac{2}{3}}} \\ C_1^{(5)} = (H_1^{-1} - 1)\,\mathrm{d}t \\ \tilde{C}_1^{(5)} = (H_5^{-1} - 1)\,\mathrm{d}t \\ \mathcal{A}_1^5 = (H_K^{-1} - 1)\,\mathrm{d}t \,. \end{cases} \tag{2.114}$$

Here $C_1^{(5)}$ and $\tilde{C}_1^{(5)}$ are full vector fields, meaning that they are not subject to a self-duality constraint and carry the usual number of degrees of freedom. Note that this compactification can be generalized by adding angular momentum in directions transverse to the 10D branes to give a rotating black hole in five dimensions.

This three-charge black hole has been well studied in the literature. Its charges are quantized as $Q_i = c_i N_i$, where N_i are integers and the the basic charges are given by [24]

$$c_1 = \frac{4G_N^{(5)} R}{\pi \alpha' g_s} \,, \qquad c_5 = \alpha' g_s \,, \qquad c_K = \frac{4G_N^{(5)}}{\pi R} \,. \tag{2.115}$$

The entropy of this black hole can be computed with the Bekenstein-Hawking formula, which yields

$$S_{\mathrm{BH}} = \frac{A}{4G_N^{(5)}} = \frac{\pi^2}{2G_N^{(5)}} \sqrt{Q_1 Q_5 Q_K} = 2\pi \sqrt{N_1 N_5 N_K} \,. \tag{2.116}$$

2.3.2 Dual brane configurations

The F1-NS5-P system

We now study the F1-NS5-P system, which consists of F1 and NS5-branes arranged as follows:

	t	r	θ	φ_1	φ_2	z	y_1	y_2	y_3	y_4
F1	–	·	·	·	·	–	···	···	···	···
NS5	–	·	·	·	·	–	–	–	–	–

Again there are waves with momentum in the z-direction. This system is related to the D1-D5 system via S-duality. As in the previous case, we start by considering the supergravity solution in ten dimensions. It can be written in Einstein frame as

$$\begin{cases} \mathrm{d}s^2_{(10)} = H_F^{-\frac{3}{4}} H_N^{-\frac{1}{4}} \left[-\mathrm{d}t^2 + \mathrm{d}z^2 + K(\mathrm{d}t - \mathrm{d}z)^2 \right] + H_F^{\frac{1}{4}} H_N^{\frac{3}{4}} \left[\mathrm{d}r^2 + r^2 \mathrm{d}\Omega_3^2 \right] \\ \qquad\qquad + H_F^{\frac{1}{4}} H_N^{-\frac{1}{4}} \left[\mathrm{d}y_1^2 + \mathrm{d}y_2^2 + \mathrm{d}y_3^2 + \mathrm{d}y_4^2 \right] \\ e^{\Phi} = H_F^{-\frac{1}{2}} H_N^{\frac{1}{2}} \\ B_2^{(10)} = (H_F^{-1} - 1)\, \mathrm{d}t \wedge \mathrm{d}z + Q_N \cos^2\theta\, \mathrm{d}\varphi_1 \wedge \mathrm{d}\varphi_2 \,, \end{cases} \tag{2.117}$$

where we have the harmonic functions

$$H_F = 1 + \frac{Q_F}{r^2} \,, \qquad H_N = 1 + \frac{Q_N}{r^2} \,, \tag{2.118}$$

and H_K is as before. Note that this solution can be obtained from the D1-D5 solution (2.105) by an S-duality transformation, which sends $\Phi \to -\Phi$ and $C_2^{(10)} \to B_2^{(10)}$. After reduction on T^4, we obtain a very similar six-dimensional solution, given by (2.109) with the replacements $\phi_+ \to \phi_- = \frac{1}{\sqrt{2}}(\phi_4 - \Phi)$ and $C_2^{(6)} \to B_2^{(6)}$. In the doubled formalism, the black string couples to the two-forms

$$\begin{aligned} B_2^{(6)} &= (H_F^{-1} - 1)\, \mathrm{d}t \wedge \mathrm{d}z + Q_N \cos^2\theta\, \mathrm{d}\varphi_1 \wedge \mathrm{d}\varphi_2 \,, \\ \tilde{B}_2^{(6)} &= (H_N^{-1} - 1)\, \mathrm{d}t \wedge \mathrm{d}z + Q_F \cos^2\theta\, \mathrm{d}\varphi_1 \wedge \mathrm{d}\varphi_2 \,. \end{aligned} \tag{2.119}$$

Again these fields carry only half their usual degrees of freedom due to the self-duality constraint (2.27).

To reduce to five dimensions, we need to specify the mass matrices. We choose the Scherk-Schwarz twist to be in the stabilizing subgroup of the R-symmetry group. Since the F1-NS5 system couples to B_2 instead of C_2, the twist is chosen to preserve B_2. We choose the $\mathfrak{so}(5)$ matrices

$$M_{\mathrm{L}} = \begin{pmatrix} 0 & -(m_1+m_2) & 0 & 0 & 0 \\ m_1+m_2 & 0 & 0 & 0 & 0 \\ 0 & 0 & 0 & -(m_1-m_2) & 0 \\ 0 & 0 & m_1-m_2 & 0 & 0 \\ 0 & 0 & 0 & 0 & 0 \end{pmatrix}, \tag{2.120}$$

and M_{R} similar with $m_1 \to m_3$ and $m_2 \to m_4$. By using the isomorphism in Appendix 2.B.2, these map to $\mathfrak{usp}(4)$ generators of the form

$$M_{\mathrm{L}}^{\mathfrak{usp}(4)} = \begin{pmatrix} 0 & 0 & -\frac{m_1+m_2}{2} & \frac{m_1-m_2}{2} \\ 0 & 0 & \frac{m_1-m_2}{2} & -\frac{m_1+m_2}{2} \\ \frac{m_1+m_2}{2} & \frac{-m_1+m_2}{2} & 0 & 0 \\ \frac{-m_1+m_2}{2} & \frac{m_1+m_2}{2} & 0 & 0 \end{pmatrix}. \tag{2.121}$$

The masses of the scalar and tensor fields that follow from the reduction with these mass matrices are given in Appendix 2.C.

The resulting five-dimensional black hole is given by (2.114) with the field redefinitions $\phi_+ \to \phi_-$, $C_2^{(5)} \to B_2^{(5)}$ and $\tilde{C}_2^{(5)} \to \tilde{B}_2^{(5)}$. It is not surprising that these black holes are related by field redefinitions. After all, the D1-D5 and F1-NS5 systems are related by U-duality, and the corresponding mass matrices are related by conjugation

$$\mathbb{M}_{\text{F1-NS5}} = C\,\mathbb{M}_{\text{D1-D5}}\,C^{-1}, \qquad C \in \mathrm{Spin}(5,5). \tag{2.122}$$

This conjugation matrix C is given by

$$C = \begin{pmatrix} c & 0 \\ 0 & c \end{pmatrix}, \qquad c = \begin{pmatrix} 1 & 0 & 0 & 0 & 0 \\ 0 & 1 & 0 & 0 & 0 \\ 0 & 0 & 1 & 0 & 0 \\ 0 & 0 & 0 & 0 & 1 \\ 0 & 0 & 0 & 1 & 0 \end{pmatrix}. \tag{2.123}$$

Essentially this conjugation matrix interchanges the fourth and fifth row and column and the ninth and tenth row and column in the mass matrix (and monodromy).

The D3-D3-P systems

Finally, we consider the reduction of the D3-D3-P system of branes. We specify the brane configuration:

	t	r	θ	φ_1	φ_2	z	y_1	y_2	y_3	y_4
D3	–	·	·	·	·	–	–	–	···	···
D3′	–	·	·	·	·	–	···	···	–	–

As before, we also have momentum in the z-direction. We start with the supergravity solution in ten dimensions, in Einstein frame it can be written as

$$\begin{cases} \mathrm{d}s^2_{(10)} = H_3^{-\frac{1}{2}} H_{3'}^{-\frac{1}{2}} \left[-\mathrm{d}t^2 + \mathrm{d}z^2 + K(\mathrm{d}t - \mathrm{d}z)^2 \right] + H_3^{\frac{1}{2}} H_{3'}^{\frac{1}{2}} \left[\mathrm{d}r^2 + r^2 \mathrm{d}\Omega_3^2 \right] \\ \qquad\qquad + H_3^{-\frac{1}{2}} H_{3'}^{\frac{1}{2}} \left[\mathrm{d}y_1^2 + \mathrm{d}y_2^2 \right] + H_3^{\frac{1}{2}} H_{3'}^{-\frac{1}{2}} \left[\mathrm{d}y_3^2 + \mathrm{d}y_4^2 \right] \\ C_4^{(10)} = (H_3^{-1} - 1)\, \mathrm{d}t \wedge \mathrm{d}z \wedge \mathrm{d}y_1 \wedge \mathrm{d}y_2 + (H_{3'}^{-1} - 1)\, \mathrm{d}t \wedge \mathrm{d}z \wedge \mathrm{d}y_3 \wedge \mathrm{d}y_4 \,, \end{cases} \tag{2.124}$$

where the harmonic functions are given by

$$H_3 = 1 + \frac{Q_3}{r^2} \,, \qquad H_{3'} = 1 + \frac{Q_{3'}}{r^2} \,. \tag{2.125}$$

On compactifying to six dimensions on T^4 by taking the coordinates $y_1, \ldots, y_4$ periodic, this brane configuration is related to the D1-D5 system by T-duality. This means that the black string solution for the D3-D3 system can be obtained from that for the D1-D5 system (2.109) by a field redefinition. We find this field redefinition as $C_2^{(6)} \to R_{2;\,1}^{(6)}$ and $\phi_+ \to \phi_1$. In the doubled formalism, the six-dimensional black string arising from the D3-D3 system couples to the two-forms

$$\begin{aligned} R_{2;\,1}^{(6)} &= (H_3^{-1} - 1)\, \mathrm{d}t \wedge \mathrm{d}z + Q_{3'} \cos^2\theta\, \mathrm{d}\varphi_1 \wedge \mathrm{d}\varphi_2 \,, \\ \tilde{R}_{2;\,1}^{(6)} &= (H_{3'}^{-1} - 1)\, \mathrm{d}t \wedge \mathrm{d}z + Q_3 \cos^2\theta\, \mathrm{d}\varphi_1 \wedge \mathrm{d}\varphi_2 \,. \end{aligned} \tag{2.126}$$

Different D3-D3 systems can be constructed by arranging the D3-branes differently on the torus. These would be charged under the two-forms coming from the reduction of $C_4^{(10)}$ in such systems. All of these systems are related by T-duality.

In the last step of the reduction we need to ensure the fields that are non-trivial in the black hole solution remain massless in 5D. For this twisted reduction we choose

$\mathfrak{so}(5)$ mass matrices of the form

$$M_{\rm L} = \begin{pmatrix} 0 & 0 & 0 & 0 & 0 \\ 0 & 0 & 0 & -(m_1+m_2) & 0 \\ 0 & 0 & 0 & 0 & -(m_1-m_2) \\ 0 & m_1+m_2 & 0 & 0 & 0 \\ 0 & 0 & m_1-m_2 & 0 & 0 \end{pmatrix}, \tag{2.127}$$

which results in $R^{(6)}_{2;\,1}$ remaining massless. In $\mathfrak{usp}(4)$ this mass matrix reads

$$M_{\rm L}^{\mathfrak{usp}(4)} = \begin{pmatrix} 0 & 0 & -\frac{m_1-m_2}{2} & \frac{i(m_1+m_2)}{2} \\ 0 & 0 & \frac{i(m_1+m_2)}{2} & \frac{m_1-m_2}{2} \\ \frac{m_1-m_2}{2} & \frac{i(m_1+m_2)}{2} & 0 & 0 \\ \frac{i(m_1+m_2)}{2} & -\frac{m_1-m_2}{2} & 0 & 0 \end{pmatrix}. \tag{2.128}$$

The scalar and tensor masses that follow from the reduction with these mass matrices are given in Appendix 2.C. The resulting five-dimensional black hole is given by making the field redefinitions $\phi_+ \to \phi_1$, $C^{(5)}_2 \to R^{(5)}_{2;\,1}$ and $\tilde{C}^{(5)}_2 \to \tilde{R}^{(5)}_{2;\,1}$ in the solution (2.114). The mass matrices are again conjugate to those of the dual D1-D5 and F1-NS5 solutions. The relation is similar to the F1-NS5 result in (2.122), except now the matrix C switches the first and fourth rows and columns instead of the fourth and fifth ones.

2.3.3 Preserving further black holes by tuning mass parameters

In the previous subsection, we chose twist matrices with four arbitrary real parameters m_i. For each black hole solution (D1-D5, F1-NS5, D3-D3), we chose this matrix in such a way that the fields that source the black hole are left unchanged by the Scherk-Schwarz twist. Consequently, the black hole remains a valid solution of the 5D theory for all values of the mass parameters.

Here, we treat the special cases in which the mass parameters can be tuned in such a way that, in addition to the original black hole, other black hole solutions are also preserved by the same twist. For example, we consider twists that preserve both the D1-D5 and F1-NS5 black holes. As it turns out, this can only be done in the $\mathcal{N} = 4$ $(0,2)$ theory and in the $\mathcal{N} = 0$ theory. Since we are interested mostly in partial supersymmetry breaking, we treat an example of the $\mathcal{N} = 4$ $(0,2)$ case in detail below.

Preserving D1-D5 with T-duality twist in $\mathcal{N} = 4(0,2)$

For this example, we consider mass matrices of the form given in (2.120) that preserve the F1-NS5 black hole solution. In order to twist to the $\mathcal{N} = 4\ (0,2)$ theory, we choose $m_1, m_2 \neq 0$ and $m_3, m_4 = 0$.

Suppose that, in addition to the F1-NS5 solution, we also want to preserve the D1-D5 solution with this twist. Then the fields

$$\left\{\phi_+ = \tfrac{1}{\sqrt{2}}(\phi_4 + \Phi)\,,\, C_2^{(5)},\, \tilde{C}_2^{(5)}\right\} \tag{2.129}$$

have to remain massless as well. The masses of these fields for this twist matrix can be found in Appendix 2.C. By setting $m_3, m_4 = 0$, we see that each field either becomes massive with mass $|m_1 - m_2|$ or remains massless. It is therefore straightforward to tune the mass parameters in such a way that all of these fields remain massless by taking $m_1 = m_2$.

We thus see that the D1-D5 solution can be preserved in a reduction to $\mathcal{N} = 4\ (0,2)$ with the twist matrix that was originally proposed to preserve the F1-NS5 solution, simply by taking the two mass parameters to be equal. This particular example offers some interesting possibilities. On the one hand, we note that the twist that preserves the F1-NS5 solution lies in the perturbative $\mathrm{SO}(4,4)$ subgroup of the duality group. From the perspective of the full string theory this is a T-duality twist. Since T-duality is a perturbative symmetry, we can in principle work out the corresponding orbifold compactification of the perturbative string theory explicitly. On the other hand, the microscopic description of the D1-D5 black hole, the D1-D5 CFT, is understood reasonably well. Therefore, it should be possible to study this particular reduction thoroughly both from the perspective of the full string theory, and from the perspective of the black hole microscopics. We will return to this elsewhere.

Other possibilities in $\mathcal{N} = 4\ (0,2)$

By taking $m_1 = m_2$ in the example above, we managed to keep the fields that couple to the D1-D5 black hole massless, and so we could preserve this particular solution. It turns out, however, that this choice kept more fields massless than just the ones that charge the D1-D5 solution. In particular, the fields

$$\left\{\phi_3\,,\, R_{2;3}^{(5)}\,,\, \tilde{R}_{2;3}^{(5)}\right\} \tag{2.130}$$

also remain massless (as can be checked from the tables in Appendix 2.C). These are exactly the fields that are non-trivial in one of the three possible D3-D3 black holes. So not only the D1-D5 and F1-NS5 black holes, but also one of the D3-D3 black holes is preserved in this reduction.

Suppose now that, instead of $m_1 = m_2$, we choose $m_1 = -m_2$ in this reduction to $\mathcal{N} = 4$ $(0, 2)$. This choice does not preserve the D1-D5 solution and the D3-D3 solution charged under $R^{(5)}_{2;3}$, but instead other solutions are preserved. Now the fields coupling to the two other D3-D3 black holes remain massless:

$$\{\phi_1\,,\, R^{(5)}_{2;1}\,,\, \tilde{R}^{(5)}_{2;1}\} \quad \text{and} \quad \{\phi_2\,,\, R^{(5)}_{2;2}\,,\, \tilde{R}^{(5)}_{2;2}\}\,. \tag{2.131}$$

These are all the possibilities for preserving multiple black hole solutions with a T-duality twist to the $\mathcal{N} = 4$ $(0, 2)$ theory. The same game can be played, however, with the other twist matrices given in subsection 2.3.1 and 2.3.2. For each case, we find that taking either $m_1 = m_2$ or $m_1 = -m_2$ in the reduction to $\mathcal{N} = 4$ $(0, 2)$ results in the preservation of two additional black hole solutions.

Preserving further black holes in $\mathcal{N} = 0$

The only other theory in which we can preserve several black hole solutions by tuning mass parameters is the one in which we break all supersymmetry: the $\mathcal{N} = 0$ case. Now all four mass parameters are non-zero. As an example, let's consider the geometric F1-NS5 twist (2.120) again. If we take $m_1 = m_2$ and $m_3 = m_4$ in this reduction, all fields (2.129) that are non-trivial in the D1-D5 black hole solution remain massless. Consequently, the D1-D5 solution is preserved. Other examples can be worked out for similar reductions to $\mathcal{N} = 0$.

2.4 Quantum corrections

So far, we have considered five-dimensional supergravity theories with both massless and massive fields. For the purpose of finding black hole solutions in these theories, we truncated (consistently) to the $n = 0$ modes of the Kaluza-Klein towers and identified black hole solutions in the massless sector after this truncation.

Under certain conditions, which we discuss in the next section, the black hole solutions we have been considering lift to solutions of the full string theory. In the string theory, the effective supergravity theory receives quantum corrections. In

particular, there are quantum corrections to the coefficients of the 5D Chern-Simons terms which in turn lead to modifications of the black hole solutions and hence to quantum corrections to their entropy.

In this section, we consider corrections to the coefficients of the 5D Chern-Simons terms that result from integrating out the massive spectrum. It is a little unusual that it is *m*assive fields that contribute to these parity-violating terms. This is because in five dimensions massive fields can be in chiral representations of the little group $\mathrm{SU}(2) \times \mathrm{SU}(2)$ and so can contribute to the parity-violating Chern-Simons terms. First, we consider these quantum corrections in a general setting and then discuss their origins and consequences for the entropy of the black holes solutions of section 2.3. Subsequently, we compute the quantum corrections to the Chern-Simons terms from integrating out massive supergravity fields. This is of course not the full story: there are in principle further corrections from stringy modes; these will be considered elsewhere.

2.4.1 Corrections to Chern-Simons terms

In five dimensions massive fields can be *c*hiral as they are in representations (s, s') of the little group $\mathrm{SU}(2) \times \mathrm{SU}(2)$, and we will refer to them as chiral if $s \neq s'$. In the supergravity theory we have been discussing, the chiral massive field content consists of the gravitino in the $(3, 2)$ representation, the self-dual two-form field in the $(3, 1)$ representation and the spin-half dilatino in the $(2, 1)$ representation (together with their anti-chiral counterparts $(2, 3)$, $(1, 3)$ and $(1, 2)$). As we have seen in subsection 2.2.3, these massive fields fit into (p, q) BPS supermultiplets. By integrating out this chiral matter, we can obtain corrections to the 5D Chern-Simons terms [96]. In principle, one would need to integrate out the entire chiral massive spectrum; the fields that we found in our supergravity calculation, as well as massive stringy modes. We focus on the supergravity fields here.

From the fields that we obtain in our duality-twisted compactification of 6D supergravity, only the self-dual tensors, gravitini (spin-$\frac{3}{2}$ fermions) and dilatini (spin-$\frac{1}{2}$ fermions) contribute to the Chern-Simons terms. Integrating out other types of massive fields does not yield Chern-Simons couplings [96]. The origin of this lies in parity: since the Chern-Simons terms violate parity, they can only be generated by integrating out parity-violating fields.

The non-abelian gauge symmetry of the 5-dimensional gauged supergravity is spontaneously broken to an abelian subgroup with massless abelian gauge field one-forms A^I with field strengths $F^I = \mathrm{d}A^I$, with the index I running over the number of massless vector fields in the theory. The pure gauge and the mixed gauge-gravitational Chern-Simons terms involving these fields are of the form

$$\begin{aligned} S_{AFF} &= \frac{-g^3}{48\pi^2}\int k_{IJK} A^I \wedge F^J \wedge F^K \ , \\ S_{ARR} &= \frac{-g}{48\pi^2}\int k_I A^I \wedge \mathrm{tr}\,(R\wedge R) \ , \end{aligned} \tag{2.132}$$

for some coefficients k_{IJK}, k_I. Here g denotes the gauge coupling and R denotes the curvature two-form. Integrating out the chiral massive fields yields quantum corrections to the coefficients k_{IJK}, k_I.

Consider first the Chern-Simons terms in the classical 5D supergravity obtained by Scherk-Schwarz reduction from maximal 6D supergravity. By explicit reduction, we find that there are no $A\wedge R\wedge R$ terms. There are $A\wedge F\wedge F$ terms present however. For example, in the reduction with the Scherk-Schwarz twist that preserves the D1-D5 black hole, we find the term

$$\frac{1}{2\kappa^2_{(5)}}\int \mathcal{A}^5_1 \wedge \mathrm{d}C^{(5)}_1 \wedge \mathrm{d}\tilde{C}^{(5)}_1 \ , \tag{2.133}$$

so that we have $k_{IJK} = -\frac{4\pi^2}{\kappa^2_{(5)}g^3}$ for the indices I, J, K corresponding to the three gauge fields in (2.133). This Chern-Simons term (and other similar terms) can be found from the reduction of the 6D tensor fields (following subsection 2.2.6). There are also Chern-Simons terms coming from the reduction of the 6D vectors.

Quantum corrections to the Chern-Simons terms are only allowed for certain amounts of unbroken supersymmetry. The coefficients of the $A\wedge F\wedge F$ term are fixed for $\mathcal{N} > 2$ supersymmetry, so corrections to this terms are only allowed in the $\mathcal{N} = 2$ (and 0) theories. For $\mathcal{N} = 2$, the supersymmetric completion of the $A\wedge R\wedge R$ term exists and is known [83], but this is not the case for theories with more supersymmetry. However, in the chiral $\mathcal{N} = 4$ $(0,2)$ theory a $A\wedge R\wedge R$ term is generated by quantum corrections, leading to the conjecture that a supersymmetric completion of this term should exist [82]. There is no such quantum $A\wedge R\wedge R$ term for the non-chiral $\mathcal{N} = 4$ $(1,1)$ theory, nor for the $\mathcal{N} = 8, 6$ theories. We will see in subsection 2.4.3 that the corrections that we find from integrating

out the massive fields that come from our duality-twisted compactification of 6D supergravity (including the Kaluza-Klein towers from the circle compactification) are in agreement with the above: we find corrections to the $A \wedge F \wedge F$ term only for $\mathcal{N} = 2$ supersymmetry and a quantum $A \wedge R \wedge R$ term is induced only for $\mathcal{N} = 2$ and the chiral $\mathcal{N} = 4$ $(0, 2)$ theory.

For our purposes, we will focus on the Chern-Simons terms $\mathcal{A}^5 \wedge \mathrm{d}\mathcal{A}^5 \wedge \mathrm{d}\mathcal{A}^5$ and $\mathcal{A}^5 \wedge R \wedge R$ that involve the graviphoton $\mathcal{A}^5$. This is because the black holes that we consider couple only to the graviphoton and to vectors descending from the 6D tensors (see section 2.3). The chiral massive field content that we find from duality-twisted compactification is not charged under the gauge symmetries corresponding to the vectors that descend from 6D tensors, so for the purposes of studying corrections to the black hole solutions we only need to consider couplings of this chiral matter to the graviphoton; these then lead to corrections to the coefficients of the $\mathcal{A}^5 \wedge \mathrm{d}\mathcal{A}^5 \wedge \mathrm{d}\mathcal{A}^5$ and $\mathcal{A}^5 \wedge R \wedge R$ terms.

We introduce the notation k_{AFF} for the coefficient of the $\mathcal{A}^5 \wedge \mathrm{d}\mathcal{A}^5 \wedge \mathrm{d}\mathcal{A}^5$ term and k_{ARR} for the coefficient of the $\mathcal{A}^5 \wedge R \wedge R$ term. Neither of these terms are present in the classical theory – there is no $\mathcal{A}^5 \wedge \mathrm{d}\mathcal{A}^5 \wedge \mathrm{d}\mathcal{A}^5$ term for the graviphoton. As a result, both k_{AFF} and k_{ARR} have no classical contributions and arise only from quantum corrections.

2.4.2 Corrections to black hole entropy

We now study the effect that the corrections to the Chern-Simons terms have on the black holes that we studied in section 2.3. As it turns out, both the coefficients k_{AFF} and k_{ARR} affect the black hole solutions. In particular, the entropy of these black holes is modified by the corrections to these coefficients.

In [84, 85] general BPS black hole solutions were found for $\mathcal{N} = 2$ supergravity with both pure gauge and gauge-gravitational Chern-Simons terms (2.132). These general results then give BPS black hole solutions for our $\mathcal{N} = 2$ supergravity models, with the specific values of the Chern-Simons coefficients obtained in the next subsection. In particular, these BPS black holes are preserved by four supersymmetries, and these are the black holes for which we compute the entropy.

We can also apply this to the black holes in the $\mathcal{N} = 4$ $(0, 2)$ theory. As discussed in the previous subsection, the $\mathcal{N} = 2$ and $\mathcal{N} = 4$ $(0, 2)$ theories are the only ones

for which corrections to the Chern-Simons coefficients are allowed, and so these are the only theories in which we find corrected black hole solutions.

Consider the $\mathcal{N} = 4$ $(0, 2)$ theory. By integrating out the massive field content we obtain a non-zero coefficient k_{ARR} for the gauge-gravitational Chern-Simons term. In order to compute corrected BPS black hole solutions in this theory, we use the framework of [84, 85] for $\mathcal{N} = 2$ supergravity. We can consistently truncate this $\mathcal{N} = 4$ theory to an $\mathcal{N} = 2$ theory by decomposing fields into representations of an $\mathrm{USp}(2) \times \mathrm{USp}(2)$ subgroup of the R-symmetry group and removing all fields that transform non-trivially under one of these $\mathrm{USp}(2)$'s. For each of the black hole solutions we have considered, we make a corresponding choice of the embedding of the $\mathrm{USp}(2) \times \mathrm{USp}(2)$ subgroup so that all the fields that are non-trivial in the black hole solution survive the truncation. As a result, the black hole solutions of the effective theory with an $A \wedge R \wedge R$ term given in [84, 85] will also be solutions of the quantum-corrected $\mathcal{N} = 4$ $(0, 2)$ theory that we have been considering here.

We now briefly review the procedure to compute the entropy of BPS black holes in these quantum corrected theories. It is given by the formula [84, 85]

$$S = \frac{\pi}{6} k_{IJK} X^I X^J X^K , \tag{2.134}$$

where X^I are the (rescaled) moduli corresponding to the three gauge fields A^I that couple to the black hole charges and k_{IJK} are the Chern-Simons coefficients from (2.132). The values of these moduli in the solution are found by solving the attractor equation, which in the near-horizon limit is

$$-\frac{1}{2} k_{IJK} X^J X^K = \frac{\pi}{2g G_N^{(5)}} Q_I + 2 k_I , \tag{2.135}$$

More comprehensive studies of these solutions can be found in [84, 85].

We now apply this to our setup. When we solve (2.135) and compute (2.134) for general coefficients k_{AFF} and k_{ARR} (to the Chern-Simons terms that contain the graviphoton $\mathcal{A}^5$), we find the entropy of the corrected D1-D5-P black hole solution in terms of its three charges to be

$$S_{\mathrm{BH}} = \frac{2\pi^2}{4G_N^{(5)}} \sqrt{Q_1 Q_5 \hat{Q}_K \frac{2\left(1 + \sqrt{1 + k_{AFF} \frac{4G_N^{(5)}}{\pi R^3} \frac{Q_1 Q_5}{\hat{Q}_K^2}} + k_{AFF} \frac{4G_N^{(5)}}{3\pi R^3} \frac{Q_1 Q_5}{\hat{Q}_K^2}\right)^2}{\left(1 + \sqrt{1 + k_{AFF} \frac{4G_N^{(5)}}{\pi R^3} \frac{Q_1 Q_5}{\hat{Q}_K^2}}\right)^3}} . \tag{2.136}$$

Here the charge arising from momentum in the z direction is shifted

$$\hat{Q}_K \;=\; Q_K + \frac{4G_N^{(5)}}{\pi R}\, k_{ARR}\,. \tag{2.137}$$

It can easily be checked that for $k_{AFF} = k_{ARR} = 0$ this expression for the black hole entropy reduces to the uncorrected result

$$S_{\rm BH} \;=\; \frac{\pi^2}{2G_N^{(5)}}\,\sqrt{Q_1 Q_5 Q_K}\,. \tag{2.138}$$

Just as was done for the uncorrected expression for the entropy, we can express the three charges in terms of integers N_i times the basic charges as $Q_i = c_i N_i$ with the basic charges c_i as given in (2.115). This yields

$$S_{\rm BH} \;=\; 2\pi\,\sqrt{N_1 N_5 \hat{N}_K\,\frac{2\left(1+\sqrt{1+k_{AFF}\,\frac{N_1N_5}{\hat{N}_K^2}}+\frac{1}{3}\,k_{AFF}\,\frac{N_1N_5}{\hat{N}_K^2}\right)^2}{\left(1+\sqrt{1+k_{AFF}\,\frac{N_1N_5}{\hat{N}_K^2}}\right)^3}}\,, \tag{2.139}$$

where the shifted momentum charge number is given by

$$\hat{N}_K \;=\; N_K + k_{ARR}\,. \tag{2.140}$$

The expression (2.139) can be expanded for small k_{AFF} as

$$S_{\rm BH} \;=\; 2\pi\sqrt{N_1 N_5 \hat{N}_K} + \frac{\pi}{12}\,k_{AFF}\left(\frac{N_1N_5}{\hat{N}_K}\right)^{\frac{3}{2}} + \mathcal{O}\big(k_{AFF}^2\big)\,. \tag{2.141}$$

The first term is equal to the uncorrected black hole entropy (2.116) and the second term is the correction to first order in k_{AFF}.

2.4.3 One-loop calculation of the Chern-Simons coefficients

In this section we compute the contributions to k_{AFF} and k_{ARR} that come from integrating out chiral massive fields arising from the duality-twisted compactification of 6D supergravity. While this is a well-defined calculation, some caution is needed since there will also be contributions from the chiral spectrum of stringy modes to the Chern-Simons coefficients. The coefficients that we compute here come purely from the supergravity modes.

Contributions are only obtained from integrating out massive self-dual tensors, gravitini (spin-$\frac{3}{2}$ fermions) and dilatini (spin-$\frac{1}{2}$ fermions). The relevant diagrams

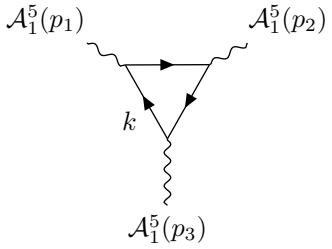

Figure 2.1: *This diagram generates corrections to the $A \wedge F \wedge F$ Chern-Simons coupling. The external lines represent the graviphoton whilst the solid internal lines represent a massive self-dual tensor, gravitino or dilatino running in the loop.*

for corrections to the couplings (2.132) have been computed in [96]. As an example, we show the diagram that contributes to the $A \wedge F \wedge F$ term in Figure 2.1. The diagrams that contribute to the $A \wedge R \wedge R$ term can be found in [96]. The results of these computations are shown in the table below.

	self-dual tensor B_2	gravitino ψ_μ	dilatino χ
k_{AFF}	$-4\, c_B\, q^3$	$5\, c_\psi\, q^3$	$c_\chi\, q^3$
k_{ARR}	$c_B\, q$	$-\frac{19}{8}\, c_\psi\, q$	$\frac{1}{8}\, c_\chi\, q$

We see that the contribution of a massive field to each of the Chern-Simons couplings consists of three parts: a prefactor that depends on the field type, a constant c_{field} (equal to ± 1) that depends on the field's representation under the massive little group, and the field's U(1) charge q under the graviphoton $\mathcal{A}_1^5$.

In order to find the corrections to the Chern-Simons terms that are induced by the massive spectra of our 5D theories, we need to know two things about each of the massive fields: the sign of c_{field} and the charge q. We always take $q \geq 0$ and absorb any minus signs into the corresponding c_{field}.

The conventions in this work are such that 5D tensors that descend from 6D self-dual tensors and 5D fermions that descend from 6D positive chiral fermions have $c_{\text{field}} = -1$, while tensors descending from 6D anti-self-dual tensors and fermions descending from 6D negative chiral fermions have $c_{\text{field}} = +1$. In terms of the

six-dimensional R-symmetry representations, the signs of c_{field} of the corresponding five-dimensional massive fields are

$$\begin{aligned}
&(\mathbf{5},\mathbf{1}): \quad c_B = -1\,, && (\mathbf{1},\mathbf{5}): \quad c_B = +1\,,\\
&(\mathbf{4},\mathbf{1}): \quad c_\psi = -1\,, && (\mathbf{1},\mathbf{4}): \quad c_\psi = +1\,,\\
&(\mathbf{5},\mathbf{4}): \quad c_\chi = -1\,, && (\mathbf{4},\mathbf{5}): \quad c_\chi = +1\,.
\end{aligned} \tag{2.142}$$

We know from subsection 2.2.9 that each 6D field produces a Kaluza-Klein tower of 5D fields for which the sum of the charges is given by

$$\sum_{n=-\infty}^{\infty} \left| \frac{\mu(m_i)}{2\pi} + n \right| . \tag{2.143}$$

We need to regularize such sums (and similar sums in which we take the sum of the cube of the charges). Following [97], the regularized expressions are

$$s_1[m] = \sum_{n=-\infty}^{\infty} \left| \frac{m}{2\pi} + n \right| = \left| \frac{m}{2\pi} \right| (2k+1) - k(k+1) - \frac{1}{6}\,, \tag{2.144}$$

$$\begin{aligned}
s_3[m] = \sum_{n=-\infty}^{\infty} \left| \frac{m}{2\pi} + n \right|^3 &= \left| \frac{m}{2\pi} \right|^3 (2k+1) - 3\left(\frac{m}{2\pi}\right)^2 \left(k(k+1) + \frac{1}{6}\right) \\
&\quad + 3\left|\frac{m}{2\pi}\right| \left(\frac{k(k+1)(2k+1)}{3} \right) - \frac{k^2(k+1)^2}{2} + \frac{1}{60}\,.
\end{aligned} \tag{2.145}$$

Here we use the notation

$$k \equiv \left\lfloor \left| \tfrac{m}{2\pi} \right| \right\rfloor\,,$$

where $\lfloor x \rfloor$ is the integer part of x.

We now have all the information that we need to compute the corrections to the Chern-Simons terms (2.132) that are generated by integrating out our massive five-dimensional spectra. Now, for a general twist (i.e. all twist parameters are

turned on) we find the correction to the pure gauge term

$$\begin{aligned} k_{AFF} \;=\; & 4\big(-s_3[m_1]-s_3[m_2]+s_3[m_3]+s_3[m_4] \\ & \quad +s_3[m_1+m_2]+s_3[m_1-m_2]-s_3[m_3+m_4]-s_3[m_3-m_4]\big) \\ & -s_3[m_1+m_2+m_3]-s_3[m_1+m_2-m_3]-s_3[m_1-m_2+m_3] \\ & -s_3[m_1-m_2-m_3]-s_3[m_1+m_2+m_4]-s_3[m_1+m_2-m_4] \\ & -s_3[m_1-m_2+m_4]-s_3[m_1-m_2-m_4]+s_3[m_1+m_3+m_4] \\ & +s_3[m_1+m_3-m_4]+s_3[m_1-m_3+m_4]+s_3[m_1-m_3-m_4] \\ & +s_3[m_2+m_3+m_4]+s_3[m_2+m_3-m_4]+s_3[m_2-m_3+m_4] \\ & +s_3[m_2-m_3-m_4]\,, \end{aligned} \tag{2.146}$$

and the correction to the mixed gauge-gravitational term

$$\begin{aligned} k_{ARR} \;=\; & \tfrac{5}{2}\big(s_1[m_1]+s_1[m_2]-s_1[m_3]-s_1[m_4]\big) \\ & -s_1[m_1+m_2]-s_1[m_1-m_2]+s_1[m_3+m_4]+s_1[m_3-m_4] \\ & +\tfrac{1}{8}\big(-s_1[m_1+m_2+m_3]-s_1[m_1+m_2-m_3]-s_1[m_1-m_2+m_3] \\ & \quad -s_1[m_1-m_2-m_3]-s_1[m_1+m_2+m_4]-s_1[m_1+m_2-m_4] \\ & \quad -s_1[m_1-m_2+m_4]-s_1[m_1-m_2-m_4]+s_1[m_1+m_3+m_4] \\ & \quad +s_1[m_1+m_3-m_4]+s_1[m_1-m_3+m_4]+s_1[m_1-m_3-m_4] \\ & \quad +s_1[m_2+m_3+m_4]+s_1[m_2+m_3-m_4]+s_1[m_2-m_3+m_4] \\ & \quad +s_1[m_2-m_3-m_4]\big)\,. \end{aligned} \tag{2.147}$$

The above formulae give the contributions from summing over all Kaluza Klein modes arising from the reduction from 6D to 5D. The Scherk-Schwarz reduction to 5D supergravity keeps only the $n = 0$ modes and not the whole KK-towers, and on restricting to the $n = 0$ modes the functions s_1 and s_3 reduce to

$$s_1[m] = \left|\tfrac{m}{2\pi}\right| , \qquad s_3[m] = \left|\tfrac{m}{2\pi}\right|^3 . \tag{2.148}$$

Then the quantum corrections to the Chern-Simons coefficients k_{AFF} and k_{ARR} from integrating out only the massive modes of the 5D supergravity that arises from Scherk-Schwarz reduction are given by (2.146) and (2.147) with the simpler expressions (2.148) for s_1, s_3.

The expressions (2.146) and (2.147) are the quantum corrections for general values of the mass parameters. The results for twists that preserve supersymmetry can be found by taking certain parameters in (2.146) and (2.147) equal to zero. We work out some interesting cases below.

- $\mathcal{N} = 8$, $\mathcal{N} = 6$ and $\mathcal{N} = 4$ $(1,1)$

  By twisting to any of these cases we find that $k_{AFF} = 0$ and $k_{ARR} = 0$, as can be checked straightforwardly by setting the appropriate mass parameters equal to zero in (2.146) and (2.147). This is consistent with expectations based on supersymmetry and chirality, as was explained earlier in this section.

- $\mathcal{N} = 4$ $(0,2)$

  For the case where we choose a chiral twist to the $\mathcal{N} = 4$ theory, say with $m_1, m_2 \neq 0$ and $m_3 = m_4 = 0$, we find that k_{AFF} vanishes but k_{ARR} does not. For such a twist, we find the correction from the $n = 0$ modes to be

  $$k_{ARR} \;=\; \tfrac{1}{2\pi}\left(3\,|m_1| + 3\,|m_2| - \tfrac{3}{2}\,|m_1 + m_2| - \tfrac{3}{2}\,|m_1 - m_2|\right)\,, \qquad (2.149)$$

  and by taking into account the Kaluza-Klein towers as well we find

  $$k_{ARR} \;=\; \tfrac{1}{2} + 3\,s_1[m_1] + 3\,s_1[m_2] - \tfrac{3}{2}\,s_1[m_1 + m_2] - \tfrac{3}{2}\,s_1[m_1 - m_2]\,. \qquad (2.150)$$

- $\mathcal{N} = 2$ $(0,1)$

  In the minimal $\mathcal{N} = 2$ theory corrections to both the Chern-Simons coefficients are allowed, and the supersymmetric extension of the $A \wedge R \wedge R$ term is known [83]. The coefficients k_{AFF} and k_{ARR} can be computed from the general formulas (2.146) and (2.147) by taking $m_4 = 0$ and the other parameters non-zero. The general expressions are quite unwieldy, but if we take $m_1 = m_2 = m_3 = m$ they simplify substantially. For this choice of mass parameters the corrections due to the $n = 0$ modes are

  $$k_{AFF} \;=\; 36\left|\frac{m}{2\pi}\right|^3\,, \qquad k_{ARR} \;=\; \frac{9}{4}\left|\frac{m}{2\pi}\right|\,, \qquad (2.151)$$

  and the corrections due to both the $n = 0$ modes and the Kaluza-Klein towers read

  $$k_{AFF} \;=\; \tfrac{1}{6} - 15\,s_3[m] + 6\,s_3[2m] - s_3[3m]\,, \qquad (2.152)$$

  $$k_{ARR} \;=\; \tfrac{13}{24} + \tfrac{33}{8}\,s_1[m] - \tfrac{3}{4}\,s_1[2m] - \tfrac{1}{8}\,s_1[3m]\,. \qquad (2.153)$$

The expressions for the coefficients k_{AFF} and k_{ARR} that we found in this subsection are computed from the supergravity fields that come from the duality-twisted

compactification. A more thorough calculation would be needed to include all the stringy modes as well. The embedding into string theory is discussed in the next section. The full string theory calculation of the coefficients k_{AFF} and k_{ARR}, however, is beyond the scope of this research and left for future study.

2.5 Embedding in string theory

So far we have considered a supergravity setup in which we studied BPS black holes in a Scherk-Schwarz reduced theory. In some cases, Scherk-Schwarz reductions can be lifted to string theory as compactifications with a duality twist. We study such lifts in this section.

2.5.1 Quantization of the twist parameters

The Scherk-Schwarz reductions we have been considering have lifts to string theory (or M-theory) only for special values of the parameters m_i. We now investigate the lifts of Scherk-Schwarz reductions to full string theory constructions. The supergravity duality symmetry is broken to the discrete U-duality symmetry $\mathrm{Spin}(5,5;\mathbb{Z})$ [22], and the Scherk-Schwarz monodromy has to be restricted to be in this discrete subgroup [63, 76].

We then have three conditions on the monodromy, similar to the three conditions in [74, 75].

1. The monodromy is a U-duality

$$\mathcal{M} \in \mathrm{Spin}(5,5;\mathbb{Z})\,. \tag{2.154}$$

2. The monodromy is conjugate to an R-symmetry

$$\mathcal{M} = g\tilde{\mathcal{M}}g^{-1}, \quad g \in \mathrm{Spin}(5,5), \quad \tilde{\mathcal{M}} \in \mathrm{USp}(4)_{\mathrm{L}} \times \mathrm{USp}(4)_{\mathrm{R}}\,. \tag{2.155}$$

   This ensures that there is a Minkowski vacuum and implies that the monodromy is in fact conjugate to an element of a maximal torus (2.35) parameterised by four angles m_i. Note that the conjugation is by an element g of the *c*ontinuous group $\mathrm{Spin}(5,5)$.

3. At least one of the parameters m_i is zero, so that the monodromy is conjugate to a subgroup of the R-symmetry

$$\tilde{\mathcal{M}} \in \mathrm{SU}(2) \times \mathrm{USp}(4) \in \mathrm{USp}(4) \times \mathrm{USp}(4)\,. \tag{2.156}$$

   This condition ensures that some supersymmetry is preserved.

Conditions (1) and (2) imply that $\mathcal{M}$ satisfies $\mathcal{M}^p = \mathbb{1}$ for some integer p, so that $\mathcal{M}$ generates a cyclic group $\mathbb{Z}_p$ [63]. As a a result, the phases e^{im_i} are all p'th roots of unity, so that

$$m_i = \frac{2\pi n_i}{p}\,, \qquad i = 1, \ldots, 4\,, \tag{2.157}$$

for some integers n_i. This can be thought of as a quantization of the parameters m_i.

The point in the moduli space given by the coset $[g]$ of the group element $g \in \mathrm{Spin}(5,5)$ in (2.155) is a fixed point under the action of the $\mathbb{Z}_p$ generated by $\mathcal{M}$, and this is the point at which the scalar potential has its minimum [63]. The corresponding low energy supergravity description is as described in subsection 2.2.7.

The general solution to these three requirements is not known. Consider, however, the special case in which

$$\mathcal{M} \in \mathrm{SL}(2;\mathbb{Z}) \times \mathrm{SL}(2;\mathbb{Z}) \times \mathrm{SL}(2;\mathbb{Z}) \times \mathrm{SL}(2;\mathbb{Z}) \subset \mathrm{Spin}(5,5;\mathbb{Z})\,. \tag{2.158}$$

This subgroup arises from considering

$$\mathrm{Spin}(2,2) \times \mathrm{Spin}(2,2) \subset \mathrm{Spin}(4,4) \subset \mathrm{Spin}(5,5)\,, \tag{2.159}$$

and the isomorphism

$$\mathrm{Spin}(2,2) \;\cong\; \mathrm{SL}(2;\mathbb{R}) \times \mathrm{SL}(2;\mathbb{R})\,. \tag{2.160}$$

Then taking

$$\mathcal{M} = M_1 \times M_2 \times M_3 \times M_4 \in \mathrm{SL}(2;\mathbb{Z}) \times \mathrm{SL}(2;\mathbb{Z}) \times \mathrm{SL}(2;\mathbb{Z}) \times \mathrm{SL}(2;\mathbb{Z})\,, \tag{2.161}$$

there are solutions in which each $M_i \in \mathrm{SL}(2;\mathbb{Z})$ is an element of an elliptic conjugacy class of $\mathrm{SL}(2;\mathbb{Z})$ [63]. Each M_i is then conjugate to a rotation:

$$M_i = k_i\, R(m_i)\, k_i^{-1}\,, \tag{2.162}$$

where

$$k_i \in SL(2;\mathbb{R})\,, \qquad R(m_i) = \begin{pmatrix} \cos m_i & -\sin m_i \\ \sin m_i & \cos m_i \end{pmatrix}\,. \tag{2.163}$$

The angles m_i must each take one of the values

$$m_i \in \left\{0, \tfrac{\pi}{3}, \tfrac{\pi}{2}, \tfrac{2\pi}{3}, \pi\right\}, \tag{2.164}$$

and each M_i generates a $\mathbb{Z}_{n_i}$ subgroup of $\mathrm{SL}(2;\mathbb{Z})$ with each n_i being one of $1, 2, 3, 4, 6$ (the lowest number such that $R(m_i)^{n_i} = \mathbb{1}$). The monodromy $\mathcal{M}$ then generates a $\mathbb{Z}_p$ where p is the least common multiple of the n_i $(i = 1, \ldots, 4)$ and so is equal to $2, 3, 4, 6$ or 12 (excluding the trivial case $\mathcal{M} = \mathbb{1}$).

The quantization condition on the parameters m_i then provides a condition on the corrections to the coefficients of the Chern-Simons terms. We have checked that for the values of the m_i given by (2.164), the corrections to the coefficients of the Chern-Simons terms satisfy the appropriate quantization conditions.

2.5.2 Orbifold picture and modular invariance

The point in moduli space at which there is a minimum of the scalar potential is a fixed point under the action of the $\mathbb{Z}_p$ generated by the U-duality transformation $\mathcal{M}$. At this point, the construction can be realized as a generalized orbifold of IIB string theory compactified on $T^4 \times S^1$ [63]. The full string construction is then IIB string theory on $T^4 \times S^1$ quotiented by the $\mathbb{Z}_p$ generated by the monodromy $\mathcal{M}$ combined with a shift on the S^1 given by $z \to z + 2\pi R/p$.

The T-duality subgroup of the U-duality group is a particular embedding of $\mathrm{Spin}(4,4;\mathbb{Z}) \subset \mathrm{Spin}(5,5;\mathbb{Z})$, and when the monodromy is a T-duality, this orbifold construction becomes a conventional asymmetric orbifold [79, 80]. However, this asymmetric orbifold is not modular invariant in general. The remedy is straightforward [75, 79, 80]: modular invariance can be achieved if the shift in the circle coordinate z is accompanied by a shift in the coordinate of the T-dual circle. The T-dual circle has radius α'/R, and its coordinate $\tilde{z}$ undergoes a shift $\tilde{z} \to \tilde{z} + 2\pi n\alpha'/pR$ for a particular integer n which is determined as in [75, 80]. This can also be understood in momentum space. The quotient introduces phases dependent on both the momentum and the winding number on the circle, and dependent on the charges e_i under the action of $\mathcal{M}$; see [75] for further discussion. This then gives an exact

conformal field theory formulation of the duality twisted theory in its Minkowski vacuum [63].

Acting on this asymmetric orbifold with a U-duality transformation will take the monodromy to a conjugate U-duality monodromy that will in general not be a T-duality. It will then take the phase depending on the winding number to a phase depending on brane wrapping numbers, giving a non-perturbative construction similar to the ones given in [75, 81].

2.6 Conclusion

In this chapter we have studied duality twists and their effect on black holes in string theory. Our set-up was type IIB string theory compactified on T^4 and then further compactified on S^1 with a duality twist along the circle. If the twist is with a diffeomorphism of T^4, this gives T^4 bundle over S^1, but for a U-duality twist this gives a U-fold, which is a non-geometric generalization of this bundle [77].

We have given the relations between the 6D fields of the duality-invariant formulation of 6D $\mathcal{N} = 8$ supergravity and the 10D fields of type IIB supergravity on a four-torus explicitly. We then reduced this six-dimensional theory on a circle with a duality twist. For this reduction we have chosen a monodromy in the R-symmetry, depending on four independent twist parameters. This reduction yields gauged 5D $\mathcal{N} = 8$ supergravity, with Minkowski vacua preserving $\mathcal{N} = 6, 4, 2, 0$ supersymmetry. The amount of supersymmetry that is preserved depends on the number of the twist parameters that are equal to zero.

This Scherk-Schwarz reduction in supergravity can be embedded in string theory as a compactification with a duality twist. For such an embedding to exist, the monodromy must be an element of the discrete U-duality group $\mathrm{Spin}(5, 5; \mathbb{Z})$. As a consequence, the twist parameters were constrained to take certain discrete values, and could hence be thought of as being quantized. The minimum of the Scherk-Schwarz potential in such compactifications is a fixed point under the action of the monodromy. When the duality twist is a T-duality, the theory arising at the minimum of the potential is an asymmetric orbifold of the type IIB string theory and so has an exact CFT description. In this case, the stringy quantum corrections can be calculated exactly. For more general twists in which the twist is

a non-perturbative symmetry, the result is a generalized orbifold of the type IIB string theory in which it is quotiented by a U-duality symmetry.

One of our main objectives was to study black holes in this set-up with partially broken supersymmetry. Here we considered several brane configurations – D1-D5, F1-NS5 and D3-D3 – that result in five-dimensional black holes after standard (untwisted) dimensional reduction. In each case, we compactified on T^4 to a 6D solution and then chose the twist in such a way that all the fields that source the 6D solution remain massless in 5D. This ensures that the original black hole solution remains a solution of the twisted theory with partially broken supersymmetry.

Our reduction scheme yielded a rich spectrum of massive modes. In 5D, massive BPS multiplets can be chiral. For twists that yield chiral BPS multiplets, integrating out the chiral fields gives quantum corrections to the coefficients of the pure gauge and mixed gauge-gravitational Chern-Simons terms. This gives an EFT with both pure gauge and mixed gauge-gravitational Chern-Simons terms and these terms led to modifications of the BPS black hole solutions and in particular modifies the expression for the black hole entropy.

Several interesting directions for follow-up research remain. One is to investigate the microscopic side of the macroscopic story laid out in this work. This would involve studying the effects of the duality twist on the CFT dual of the black holes in our set-up. Of these, the D1-D5 CFT has been studied the most in the literature and therefore seems to be the most practical option for this. In general, one might expect that similar supersymmetry breaking patterns arise in the dual superconformal CFT, from (4,4) supersymmetry to e.g. (4,2), (2,2) or (4,0) supersymmetry. D-branes and their world-volume theories in backgrounds with a duality twist have been discussed in [98] and it will be interesting to apply the results found there to the configurations discussed here.

Another open question is the computation of the Chern-Simons coefficients in the full string theory. That is, including modes that we don't see from the supergravity point of view (such as winding modes). For twists that lie in the T-duality group, this can be worked out in detail as an asymmetric orbifold compactification of perturbative string theory. As we have seen in this work, it is possible to choose a T-duality twist that preserves the D1-D5-P black hole in reductions to the $\mathcal{N} = 4$ $(0, 2)$ theory. In this reduction it may be possible to combine the detailed study of the full string theory with the microscopic calculation.

Finally, it would be interesting to extend this work to the study of four-dimensional black holes in string compactifications with duality twists. For this, one could take for example the four-charge D2-D6-NS5-P black hole of type IIA string theory or a dual brane configuration.

Appendices

2.A Conventions and notation

Throughout this work, we set $c = \hbar = k_B = 1$, and we work in the 'mostly plus' convention for the metric, i.e. $\eta_{\mu\nu} = \mathrm{diag}(-, +, \ldots, +)$. The notations that we use for the coordinates and indices in various dimensions are summarized in the table below.

Space	Coordinate	Indices
$D = 10$	$X^M = (\hat{x}^{\hat{\mu}}, y^m)$	$M, N, \ldots = 0, 1, \ldots, 9$
$D = 6$	$\hat{x}^{\hat{\mu}} = (x^\mu, z)$	$\hat{\mu}, \hat{\nu}, \ldots = 0, 1, \ldots, 5$
$D = 5$	x^μ	$\mu, \nu, \ldots = 0, 1, \ldots, 4$
T^4	y^m	$m, n, \ldots = 1, \ldots, 4$

In general, we denote form-values fields as $A_p^{(d)}$, where p is the rank of the form and d is the dimension in which it lives. We define the Hodge star operator on forms as

$$*A_p^{(d)} = \frac{1}{p!(d-p)!}\sqrt{g_{(d)}}\,\varepsilon_{\mu_1\ldots\mu_p\nu_1\ldots\nu_{d-p}}\,A^{\mu_1\cdots\mu_p}\,\mathrm{d}x^{\nu_1}\wedge\ldots\wedge\mathrm{d}x^{\nu_{d-p}}\,. \tag{2.165}$$

We use the subscript or superscript (d) more often to indicate the number of spacetime dimensions where necessary, e.g. $R^{(d)}$, $e_{(d)}$, etc. In all dimensions, we normalize Lagrangians such that the corresponding actions are given by

$$S^{(d)} = \frac{1}{2\kappa_{(d)}^2}\int \mathscr{L}^{(d)}\,, \tag{2.166}$$

where $\kappa_{(d)}^2 = 8\pi G_N^{(d)}$ is the d-dimensional Newton's constant.

We use $A, B, \ldots = 1, \ldots, 10$ to denote $\mathrm{Spin}(5,5)$ indices that transform in τ-frame (as explained in Appendix 2.B.1), and we use $a, b, \ldots = 1, \ldots, 5$ for indices

transforming under the subgroup $\mathrm{GL}(5) \subset \mathrm{Spin}(5,5)$. For example, in 6D we have ten tensor fields (subject to a self-duality constraint), whose field strengths we write as

$$G^{(6)}_{3,A} = \begin{pmatrix} G^{(6)}_{3,a} \\ \tilde{G}^{(6)a}_{3} \end{pmatrix} . \tag{2.167}$$

The GL(5) subgroup works on the index a of the (dual) field strengths $G^{(6)}_{3,a}$ and $\tilde{G}^{(6)a}_{3}$. For more information on how this subgroup works, see Appendix 2.B.1.

2.B Group theory

2.B.1 The group $\mathrm{SO}(5,5)$ and its algebra

In this appendix we discuss some details and our conventions concerning the group $\mathrm{SO}(5,5)$ and its algebra $\mathfrak{so}(5,5)$. In particular, we construct two bases in which $\mathrm{SO}(5,5)$ can be written down; we call these the η-frame and the τ-frame. Furthermore, we build an explicit basis for the algebra that we use to construct a vielbein $\mathcal{V} \in \mathrm{SO}(5,5)$ in the main text.

Canonically, an element $g \in \mathrm{SO}(5,5)$ is represented by a 10×10 matrix, satisfying the conditions

$$g^T \eta\, g \,=\, \eta\,, \qquad \eta = \begin{pmatrix} \mathbb{1}_5 & 0 \\ 0 & -\mathbb{1}_5 \end{pmatrix} , \tag{2.168}$$

and $\det(g) = 1$. Henceforth, we refer to group elements satisfying these conditions as being written in the η-frame of $\mathrm{SO}(5,5)$. In the η-frame, a generator of the Lie algebra $M \in \mathfrak{so}(5,5)$ can be written in 5×5 blocks as

$$M = \begin{pmatrix} a & b \\ b^T & c \end{pmatrix} , \tag{2.169}$$

where a and c are antisymmetric and b is unconstrained.

There is another (isomorphic) way of writing down the group $\mathrm{SO}(5,5)$. We construct this other basis by conjugating the group elements as $\tilde{g} = X^{-1} g X$, where X is the matrix

$$X = \frac{1}{\sqrt{2}} \begin{pmatrix} \mathbb{1}_5 & \mathbb{1}_5 \\ \mathbb{1}_5 & -\mathbb{1}_5 \end{pmatrix} . \tag{2.170}$$

Note that $X = X^{-1} = X^T$. We can now rewrite (2.168) in terms of $\tilde{g}$, which yields the following conditions on the conjugated group elements:

$$\tilde{g}^T \tau \tilde{g} = \tau\,, \qquad \tau = \begin{pmatrix} 0 & \mathbb{1}_5 \\ \mathbb{1}_5 & 0 \end{pmatrix}. \tag{2.171}$$

We see that the conjugated matrices $\tilde{g}$ preserve the matrix τ (instead of η), and therefore we refer to these matrices as being written in the τ-frame of $\mathrm{SO}(5,5)$. It is clear from the conjugation relation $\tilde{g} = X^{-1} g X$ that the two frames are isomorphic. The general block structure for generators of the Lie algebra $\mathfrak{so}(5,5)$ in the τ-frame is of the form

$$\tilde{M} = \begin{pmatrix} A & B \\ C & -A^T \end{pmatrix}. \tag{2.172}$$

Here A is unconstrained and B and C are antisymmetric.

There is a subgroup $\mathrm{GL}(5) \subset \mathrm{SO}(5,5)$ that is embedded diagonally in the τ-frame matrices $\tilde{g}$. Generators of $\mathrm{GL}(5)$ can be represented by unconstrained 5×5 matrices, and these can be embedded diagonally in the block structure (2.172) by taking $B = C = 0$ and A equal to the $\mathfrak{gl}(5)$ generator. By exponentiating, we find the corresponding group element to be of the form

$$\begin{pmatrix} P & 0 \\ 0 & (P^T)^{-1} \end{pmatrix} \in \mathrm{GL}(5) \subset \mathrm{SO}(5,5)\,, \tag{2.173}$$

where P is an invertible five by five matrix. The embedding in the η-frame can be found by conjugating (2.173) with the matrix X given in (2.170).

A basis for the algebra $\mathfrak{so}(5,5)$

Using the general form of M, we build a basis of generators. Since $\mathfrak{so}(5,5)$ has rank five, we have five Cartan generators, denoted by H_n ($n = 0, \ldots, 4$). We choose the Cartan subalgebra to be block-diagonal in the τ-frame, so that when written in the form (2.172), they all have $B = C = 0$. Furthermore, for convenience we choose

the following form for the A matrices for the H_n:

$$\begin{aligned} A_{H_0} &= \frac{1}{2}\,\mathrm{diag}\,(0,0,0,-1,1) \\ A_{H_1} &= \frac{1}{\sqrt{2}}\,\mathrm{diag}\,(-1,0,0,0,0)\ , \\ A_{H_2} &= \frac{1}{\sqrt{2}}\,\mathrm{diag}\,(0,-1,0,0,0)\ , \\ A_{H_3} &= \frac{1}{\sqrt{2}}\,\mathrm{diag}\,(0,0,-1,0,0)\ , \\ A_{H_4} &= \frac{1}{2}\,\mathrm{diag}\,(0,0,0,-1,-1)\ . \end{aligned}$$

Apart from these Cartan generators, there are 20 root generators with $B = C = 0$. We denote them by $E^{A,+}_{nm}$ and $E^{A,-}_{nm}$ ($n, m = 1, \ldots, 5$ and $n < m$). The $E^{A,+}_{nm}$ together fill the upper triangular part of A and the $E^{A,-}_{nm}$ fill the lower-triangular part. They do so in such a way that $\left(E^{A,+}_{nm}\right)^T = E^{A,-}_{nm}$. For example, we have

$$A_{E^{A,+}_{12}} = \begin{pmatrix} 0 & -1 & 0 & 0 & 0 \\ 0 & 0 & 0 & 0 & 0 \\ 0 & 0 & 0 & 0 & 0 \\ 0 & 0 & 0 & 0 & 0 \\ 0 & 0 & 0 & 0 & 0 \end{pmatrix} \qquad \text{and} \qquad A_{E^{A,-}_{12}} = \begin{pmatrix} 0 & 0 & 0 & 0 & 0 \\ -1 & 0 & 0 & 0 & 0 \\ 0 & 0 & 0 & 0 & 0 \\ 0 & 0 & 0 & 0 & 0 \\ 0 & 0 & 0 & 0 & 0 \end{pmatrix} \tag{2.174}$$

Finally, there are ten root generators E^B_{nm} with $A = C = 0$, and ten root generators E^C_{nm} with $A = B = 0$. The generators E^B_{nm} have

$$B_{E^B_{12}} = \begin{pmatrix} 0 & 1 & 0 & 0 & 0 \\ -1 & 0 & 0 & 0 & 0 \\ 0 & 0 & 0 & 0 & 0 \\ 0 & 0 & 0 & 0 & 0 \\ 0 & 0 & 0 & 0 & 0 \end{pmatrix} \ , \quad B_{E^B_{13}} = \begin{pmatrix} 0 & 0 & 1 & 0 & 0 \\ 0 & 0 & 0 & 0 & 0 \\ -1 & 0 & 0 & 0 & 0 \\ 0 & 0 & 0 & 0 & 0 \\ 0 & 0 & 0 & 0 & 0 \end{pmatrix} \ , \quad \text{etc.} \tag{2.175}$$

The generators E^C_{nm} are constructed in the same way as E^B_{nm}, but now we have $B = 0$ and $C \neq 0$. The matrix C that corresponds to E^C_{nm} is equal to the matrix B that defined E^B_{nm} in the construction above. Note that this implies that $\left(E^B_{nm}\right)^T = -\,E^C_{nm}$.

The set of matrices defined above $\left\{H_n,\, E^{A,+}_{nm},\, E^{A,-}_{nm},\, E^B_{nm},\, E^C_{nm}\right\}$ gives a complete basis of generators of $\mathfrak{so}(5,5)$. When we mention E^A_{mn} below we always mean $E^{A,+}_{mn}$.

Let us now discuss the notation T^F_{ij} used in the text. These matrices T are certain generators of the $\mathfrak{so}(5,5)$ algebra described above. In particular if we let $\vec{T}^F_{ij} := (T^F_{12}, T^F_{13}, \ldots, T^F_{34})$, then we have the following definitions for T:

$$\begin{aligned}
\vec{T}^A_{ij} &= \big(E^C_{23},\, E^C_{12},\, -E^C_{13},\, -(E^A_{13})^T,\, -(E^A_{12})^T,\, -E^A_{23} \big) \\
\vec{T}^B_{ij} &= \big(E^A_{14},\, E^A_{34},\, E^A_{24},\, -E^C_{24},\, E^C_{34},\, -E^C_{14} \big) \\
\vec{T}^C_{ij} &= \big(E^A_{15},\, E^A_{35},\, E^A_{25},\, -E^C_{25},\, E^C_{35},\, -E^C_{15} \big) \\
T^a &= E^A_{45} \\
T^b &= E^C_{45}
\end{aligned} \tag{2.176}$$

2.B.2 The isomorphism $\mathfrak{usp}(4) \cong \mathfrak{so}(5)$

The group USp(4) is the group of 4×4 matrices g satisfying

$$g^\dagger = g^{-1} \,, \qquad \Omega\, g\, \Omega^{-1} = \big(g^{-1}\big)^T \tag{2.177}$$

where Ω is the symplectic metric, given by the block matrix

$$\Omega^{AB} = \begin{pmatrix} 0_{2\times 2} & \mathbb{1}_{2\times 2} \\ -\mathbb{1}_{2\times 2} & 0_{2\times 2} \end{pmatrix} \,. \tag{2.178}$$

The Lie algebra $\mathfrak{usp}(4)$ is represented by 4×4 matrices $M_A{}^B$ satisfying

$$M^\dagger = -M, \qquad \Omega\, M\, \Omega^{-1} = -M^T \,, \tag{2.179}$$

The isomorphism $\mathrm{USp}(4) \cong \mathrm{Spin}(5)$ can be made explicit by introducing five 4×4 gamma matrices, that satisfy the Euclidean Clifford algebra

$$\{\Gamma_a, \Gamma_b\}_A{}^B = 2\, \delta_{ab}\, \delta^B_A. \tag{2.180}$$

Here $a, b = 1, \ldots, 5$ are the indices corresponding to Spin(5), and $A, B = 1, \ldots, 4$ are the indices corresponding to USp(4). An explicit basis of (Hermitian and traceless) gamma matrices, that satisfies (2.180), is given by

$$\Gamma_1 = \begin{pmatrix} 0 & i & 0 & 0 \\ -i & 0 & 0 & 0 \\ 0 & 0 & 0 & -i \\ 0 & 0 & i & 0 \end{pmatrix}, \qquad \Gamma_2 = \begin{pmatrix} 0 & 0 & 0 & i \\ 0 & 0 & -i & 0 \\ 0 & i & 0 & 0 \\ -i & 0 & 0 & 0 \end{pmatrix}, \qquad \Gamma_3 = \begin{pmatrix} 0 & 0 & 0 & 1 \\ 0 & 0 & -1 & 0 \\ 0 & -1 & 0 & 0 \\ 1 & 0 & 0 & 0 \end{pmatrix},$$

$$\Gamma_4 = \begin{pmatrix} 1 & 0 & 0 & 0 \\ 0 & -1 & 0 & 0 \\ 0 & 0 & 1 & 0 \\ 0 & 0 & 0 & -1 \end{pmatrix}, \qquad \Gamma_5 = \begin{pmatrix} 0 & 1 & 0 & 0 \\ 1 & 0 & 0 & 0 \\ 0 & 0 & 0 & 1 \\ 0 & 0 & 1 & 0 \end{pmatrix}. \tag{2.181}$$

It can easily be checked that the gamma matrices with upper indices, defined as $(\tilde{\Gamma}_a)^{AB} = \Omega^{AC}(\Gamma_a)_C{}^B$, are antisymmetric[6], i.e. $(\tilde{\Gamma}_a)^T = -\tilde{\Gamma}_a$. Using this, we deduce that

$$(\Gamma_a)^T = (\Omega^{-1}\tilde{\Gamma}_a)^T = -\tilde{\Gamma}_a\,(\Omega^{-1})^T = \Omega\,\Gamma_a\,\Omega^{-1}. \tag{2.182}$$

Hence, the symplectic metric Ω acts on the gamma matrices as a charge conjugation matrix. We now define $\Gamma_{ab} = \frac{1}{2}[\Gamma_a, \Gamma_b]$. From (2.182) and the Hermitian property of the Dirac matrices, it follows directly that Γ_{ab} satisfies the conditions (2.179). Furthermore, using the Clifford algebra, it is straightforward to check that the commutator of Γ_{ab} reads

$$\big[\Gamma_{ab}, \Gamma_{cd}\big] = -2\,\delta_{ac}\Gamma_{bd} + 2\,\delta_{ad}\Gamma_{bc} + 2\,\delta_{bc}\Gamma_{ad} - 2\,\delta_{bd}\Gamma_{ac}. \tag{2.183}$$

This is exactly the commutator of the basis elements of the $\mathfrak{so}(5)$ algebra. We conclude that the ten matrices Γ_{ab} form a set of generators of $\mathrm{USp}(4) \cong \mathrm{Spin}(5)$. Using these gamma matrices the explicit form of the isomorphism between the algebras can be derived [99]

$$M_{ab} = -\frac{1}{2}\,\mathrm{tr}\big[M_A{}^B(\Gamma_{ab})_B{}^C\big]\,. \tag{2.184}$$

The special orthogonal Lie algebra $\mathfrak{so}(5)$ consists of real antisymmetric matrices. We can check these properties for the found generators (2.184). The antisymmetry follows immediately from the antisymmetry in the gamma matrices $\Gamma_{ab} = -\Gamma_{ba}$. To prove the reality condition we use that both $M_A{}^B$ and $(\Gamma_{ab})_A{}^B$ satisfy the conditions (2.179). Using these constraints we find

$$\begin{aligned} (M_{ab})^* &= -\frac{1}{2}\,\mathrm{tr}\left[M^*(\Gamma_{ab})^*\right] \\ &= -\frac{1}{2}\,\mathrm{tr}\left[\Omega\,M\,\Omega^{-1}\,\Omega\,\Gamma_{ab}\,\Omega^{-1}\right] \\ &= -\frac{1}{2}\,\mathrm{tr}\left[M\,\Gamma_{ab}\right] \;=\; M_{ab}. \end{aligned} \tag{2.185}$$

[6] This property is used in what follows, but it is not generally true for other choices of Ω and Γ_a.

Thus we find that M_{ab}, as given in (2.184), is a real antisymmetric matrix, and therefore a suitable generator of SO(5). For completeness we also mention the inverse of the isomorphism (2.184) which maps $\mathfrak{so}(5)$ to $\mathfrak{usp}(4)$:

$$M^A{}_B = \frac{1}{4} M_{ab} \, (\Gamma^{ab})^A{}_B \ . \tag{2.186}$$

2.C Scalar and tensor masses after Scherk-Schwarz reduction

In this appendix we show the masses of the fields for the various set-ups we discussed. In particular, we show the scalar and tensor masses for the D1-D5 system discussed in subsection 2.3.1, and the dual NS5-F1 and D3-D3 systems discussed in subsection 2.3.2.

Field $\tilde{\sigma}^i$	Mass
$\frac{1}{\sqrt{2}}(\phi_4 + \Phi)$	0
$\frac{1}{2}(\phi_4 - \Phi + \sqrt{2}\,\phi_3)$	$\lvert m_1 - m_2 - m_3 + m_4 \rvert$
$\frac{1}{2}(\phi_4 - \Phi - \sqrt{2}\,\phi_3)$	$\lvert m_1 - m_2 + m_3 - m_4 \rvert$
$\frac{1}{\sqrt{2}}(\phi_1 + \phi_2)$	$\lvert m_1 + m_2 - m_3 - m_4 \rvert$
$\frac{1}{\sqrt{2}}(\phi_1 - \phi_2)$	$\lvert m_1 + m_2 + m_3 + m_4 \rvert$
$\frac{1}{2}(A_{12} + A_{34} + C_{12} + C_{34})$	$\lvert m_1 + m_2 - m_3 + m_4 \rvert$
$\frac{1}{2}(A_{12} + A_{34} - C_{12} - C_{34})$	$\lvert m_1 + m_2 + m_3 - m_4 \rvert$
$\frac{1}{2}(A_{12} - A_{34} + C_{12} - C_{34})$	$\lvert m_1 - m_2 + m_3 + m_4 \rvert$
$\frac{1}{2}(A_{12} - A_{34} - C_{12} + C_{34})$	$\lvert m_1 - m_2 - m_3 - m_4 \rvert$
$\frac{1}{2}(A_{14} + A_{23} + C_{14} - C_{23})$	$\lvert m_1 - m_2 + m_3 + m_4 \rvert$
$\frac{1}{2}(A_{14} + A_{23} - C_{14} + C_{23})$	$\lvert m_1 - m_2 - m_3 - m_4 \rvert$
$\frac{1}{2}(A_{14} - A_{23} + C_{14} + C_{23})$	$\lvert m_1 + m_2 - m_3 + m_4 \rvert$
$\frac{1}{2}(-A_{14} + A_{23} + C_{14} + C_{23})$	$\lvert m_1 + m_2 + m_3 - m_4 \rvert$
A_{13}	$\lvert m_1 + m_2 - m_3 - m_4 \rvert$
A_{24}	$\lvert m_1 + m_2 + m_3 + m_4 \rvert$
C_{13}	$\lvert m_1 - m_2 + m_3 - m_4 \rvert$
C_{24}	$\lvert m_1 - m_2 - m_3 + m_4 \rvert$
$\frac{1}{\sqrt{2}}(B_{12} + B_{34})$	$\lvert m_1 + m_2 \rvert$
$\frac{1}{\sqrt{2}}(B_{12} - B_{34})$	$\lvert m_3 + m_4 \rvert$
$\frac{1}{\sqrt{2}}(B_{13} + B_{24})$	$\lvert m_3 - m_4 \rvert$
$\frac{1}{\sqrt{2}}(B_{13} - B_{24})$	$\lvert m_1 - m_2 \rvert$
$\frac{1}{\sqrt{2}}(B_{14} + B_{23})$	$\lvert m_1 + m_2 \rvert$
$\frac{1}{\sqrt{2}}(B_{14} - B_{23})$	$\lvert m_3 + m_4 \rvert$
$\frac{1}{\sqrt{2}}(a + b)$	$\lvert m_1 - m_2 \rvert$
$\frac{1}{\sqrt{2}}(a - b)$	$\lvert m_3 - m_4 \rvert$

Table 2.2: *The D1-D5 scalar masses.*

Field $A^{(5)}_{2,A}$	Mass
$C^{(5)}_2$	0
$\tilde{C}^{(5)}_2$	0
$\frac{1}{\sqrt{2}}\left(B^{(5)}_2 + \tilde{B}^{(5)}_2\right)$	$\lvert m_1 - m_2\rvert$
$\frac{1}{\sqrt{2}}\left(B^{(5)}_2 - \tilde{B}^{(5)}_2\right)$	$\lvert m_3 - m_4\rvert$
$\frac{1}{\sqrt{2}}\left(R^{(5)}_{2;\,1} + \tilde{R}^{(5)}_{2;\,1}\right)$	$\lvert m_1 + m_2\rvert$
$\frac{1}{\sqrt{2}}\left(R^{(5)}_{2;\,1} - \tilde{R}^{(5)}_{2;\,1}\right)$	$\lvert m_3 + m_4\rvert$
$\frac{1}{\sqrt{2}}\left(R^{(5)}_{2;\,2} + \tilde{R}^{(5)}_{2;\,2}\right)$	$\lvert m_1 + m_2\rvert$
$\frac{1}{\sqrt{2}}\left(R^{(5)}_{2;\,2} - \tilde{R}^{(5)}_{2;\,2}\right)$	$\lvert m_3 + m_4\rvert$
$\frac{1}{\sqrt{2}}\left(R^{(5)}_{2;\,3} + \tilde{R}^{(5)}_{2;\,3}\right)$	$\lvert m_1 - m_2\rvert$
$\frac{1}{\sqrt{2}}\left(R^{(5)}_{2;\,3} - \tilde{R}^{(5)}_{2;\,3}\right)$	$\lvert m_3 - m_4\rvert$

Table 2.3: *The D1-D5 tensor masses.*

Field $\tilde{\sigma}^i$	Mass
$\frac{1}{\sqrt{2}}(\phi_4 - \Phi)$	0
$\frac{1}{2}(\phi_4 + \Phi + \sqrt{2}\,\phi_3)$	$\lvert m_1 - m_2 - m_3 + m_4\rvert$
$\frac{1}{2}(\phi_4 + \Phi - \sqrt{2}\,\phi_3)$	$\lvert m_1 - m_2 + m_3 - m_4\rvert$
$\frac{1}{\sqrt{2}}(\phi_1 + \phi_2)$	$\lvert m_1 + m_2 - m_3 - m_4\rvert$
$\frac{1}{\sqrt{2}}(\phi_1 - \phi_2)$	$\lvert m_1 + m_2 + m_3 + m_4\rvert$
$\frac{1}{2}(A_{12} + A_{34} + B_{12} + B_{34})$	$\lvert m_1 + m_2 - m_3 + m_4\rvert$
$\frac{1}{2}(A_{12} + A_{34} - B_{12} - B_{34})$	$\lvert m_1 + m_2 + m_3 - m_4\rvert$
$\frac{1}{2}(A_{12} - A_{34} + B_{12} - B_{34})$	$\lvert m_1 - m_2 + m_3 + m_4\rvert$
$\frac{1}{2}(A_{12} - A_{34} - B_{12} + B_{34})$	$\lvert m_1 - m_2 - m_3 - m_4\rvert$
$\frac{1}{2}(A_{14} + A_{23} + B_{14} - B_{23})$	$\lvert m_1 - m_2 + m_3 + m_4\rvert$
$\frac{1}{2}(A_{14} + A_{23} - B_{14} + B_{23})$	$\lvert m_1 - m_2 - m_3 - m_4\rvert$
$\frac{1}{2}(A_{14} - A_{23} + B_{14} + B_{23})$	$\lvert m_1 + m_2 - m_3 + m_4\rvert$
$\frac{1}{2}(-A_{14} + A_{23} + B_{14} + B_{23})$	$\lvert m_1 + m_2 + m_3 - m_4\rvert$
A_{13}	$\lvert m_1 + m_2 - m_3 - m_4\rvert$
A_{24}	$\lvert m_1 + m_2 + m_3 + m_4\rvert$
B_{13}	$\lvert m_1 - m_2 + m_3 - m_4\rvert$
B_{24}	$\lvert m_1 - m_2 - m_3 + m_4\rvert$
$\frac{1}{\sqrt{2}}(C_{12} + C_{34})$	$\lvert m_1 + m_2\rvert$
$\frac{1}{\sqrt{2}}(C_{12} - C_{34})$	$\lvert m_3 + m_4\rvert$
$\frac{1}{\sqrt{2}}(C_{13} + C_{24})$	$\lvert m_3 - m_4\rvert$
$\frac{1}{\sqrt{2}}(C_{13} - C_{24})$	$\lvert m_1 - m_2\rvert$
$\frac{1}{\sqrt{2}}(C_{14} + C_{23})$	$\lvert m_1 + m_2\rvert$
$\frac{1}{\sqrt{2}}(C_{14} - C_{23})$	$\lvert m_3 + m_4\rvert$
$\frac{1}{\sqrt{2}}(a + b)$	$\lvert m_3 - m_4\rvert$
$\frac{1}{\sqrt{2}}(a - b)$	$\lvert m_1 - m_2\rvert$

Table 2.4: *The NS5-F1 scalar masses.*

Field $A^{(5)}_{2,A}$	Mass
$B^{(5)}_2$	0
$\tilde{B}^{(5)}_2$	0
$\frac{1}{\sqrt{2}}\left(C^{(5)}_2 + \tilde{C}^{(5)}_2\right)$	$\lvert m_1 - m_2\rvert$
$\frac{1}{\sqrt{2}}\left(C^{(5)}_2 - \tilde{C}^{(5)}_2\right)$	$\lvert m_3 - m_4\rvert$
$\frac{1}{\sqrt{2}}\left(R^{(5)}_{2;\,1} + \tilde{R}^{(5)}_{2;\,1}\right)$	$\lvert m_1 + m_2\rvert$
$\frac{1}{\sqrt{2}}\left(R^{(5)}_{2;\,1} - \tilde{R}^{(5)}_{2;\,1}\right)$	$\lvert m_3 + m_4\rvert$
$\frac{1}{\sqrt{2}}\left(R^{(5)}_{2;\,2} + \tilde{R}^{(5)}_{2;\,2}\right)$	$\lvert m_1 + m_2\rvert$
$\frac{1}{\sqrt{2}}\left(R^{(5)}_{2;\,2} - \tilde{R}^{(5)}_{2;\,2}\right)$	$\lvert m_3 + m_4\rvert$
$\frac{1}{\sqrt{2}}\left(R^{(5)}_{2;\,3} + \tilde{R}^{(5)}_{2;\,3}\right)$	$\lvert m_1 - m_2\rvert$
$\frac{1}{\sqrt{2}}\left(R^{(5)}_{2;\,3} - \tilde{R}^{(5)}_{2;\,3}\right)$	$\lvert m_3 - m_4\rvert$

Table 2.5: *The NS5-F1 tensor masses.*

Field $\tilde{\sigma}^i$	Mass
ϕ_1	0
$\frac{1}{2}(\Phi + \sqrt{2}\,\phi_2 + \phi_4)$	$\lvert m_1 + m_2 - m_3 - m_4\rvert$
$\frac{1}{2}(\Phi + \sqrt{2}\,\phi_3 - \phi_4)$	$\lvert m_1 - m_2 + m_3 - m_4\rvert$
$\frac{1}{2}(\Phi - \sqrt{2}\,\phi_3 - \phi_4)$	$\lvert m_1 - m_2 - m_3 + m_4\rvert$
$\frac{1}{2}(\Phi - \sqrt{2}\,\phi_2 + \phi_4)$	$\lvert m_1 + m_2 + m_3 + m_4\rvert$
$\frac{1}{2}(b + a + A_{12} - A_{34})$	$\lvert m_1 - m_2 - m_3 - m_4\rvert$
$\frac{1}{2}(b - a - A_{12} - A_{34})$	$\lvert m_1 + m_2 + m_3 - m_4\rvert$
$\frac{1}{2}(b - a + A_{12} + A_{34})$	$\lvert m_1 + m_2 - m_3 + m_4\rvert$
$\frac{1}{2}(b + a - A_{12} + A_{34})$	$\lvert m_1 - m_2 + m_3 + m_4\rvert$
$\frac{1}{2}(C_{23} - C_{14} - B_{24} + B_{13})$	$\lvert m_1 - m_2 - m_3 - m_4\rvert$
$\frac{1}{2}(C_{23} + C_{14} + B_{24} + B_{13})$	$\lvert m_1 + m_2 + m_3 - m_4\rvert$
$\frac{1}{2}(C_{23} + C_{14} - B_{24} - B_{13})$	$\lvert m_1 + m_2 - m_3 + m_4\rvert$
$\frac{1}{2}(C_{23} - C_{14} + B_{24} - B_{13})$	$\lvert m_1 - m_2 + m_3 + m_4\rvert$
B_{14}	$\lvert m_1 + m_2 + m_3 + m_4\rvert$
B_{23}	$\lvert m_1 + m_2 - m_3 - m_4\rvert$
C_{13}	$\lvert m_1 - m_2 + m_3 - m_4\rvert$
C_{24}	$\lvert m_1 - m_2 - m_3 + m_4\rvert$
$\frac{1}{\sqrt{2}}(C_{12} + C_{34})$	$\lvert m_3 - m_4\rvert$
$\frac{1}{\sqrt{2}}(C_{12} - C_{34})$	$\lvert m_1 - m_2\rvert$
$\frac{1}{\sqrt{2}}(A_{13} + A_{24})$	$\lvert m_3 + m_4\rvert$
$\frac{1}{\sqrt{2}}(A_{13} - A_{24})$	$\lvert m_1 + m_2\rvert$
$\frac{1}{\sqrt{2}}(A_{14} + A_{23})$	$\lvert m_1 - m_2\rvert$
$\frac{1}{\sqrt{2}}(A_{14} - A_{23})$	$\lvert m_3 - m_4\rvert$
$\frac{1}{\sqrt{2}}(B_{12} + B_{34})$	$\lvert m_3 + m_4\rvert$
$\frac{1}{\sqrt{2}}(B_{12} - B_{34})$	$\lvert m_1 + m_2\rvert$

Table 2.6: *The D3-D3 scalar masses.*

Field $A^{(5)}_{2,A}$	Mass
$R^{(5)}_{2;\,1}$	0
$\tilde{R}^{(5)}_{2;\,1}$	0
$\frac{1}{\sqrt{2}}\left(C^{(5)}_2 + \tilde{C}^{(5)}_2\right)$	$\lvert m_1 + m_2\rvert$
$\frac{1}{\sqrt{2}}\left(C^{(5)}_2 - \tilde{C}^{(5)}_2\right)$	$\lvert m_3 + m_4\rvert$
$\frac{1}{\sqrt{2}}\left(B^{(5)}_2 + \tilde{B}^{(5)}_2\right)$	$\lvert m_1 - m_2\rvert$
$\frac{1}{\sqrt{2}}\left(B^{(5)}_2 - \tilde{B}^{(5)}_2\right)$	$\lvert m_3 - m_4\rvert$
$\frac{1}{\sqrt{2}}\left(R^{(5)}_{2;\,2} + \tilde{R}^{(5)}_{2;\,2}\right)$	$\lvert m_1 + m_2\rvert$
$\frac{1}{\sqrt{2}}\left(R^{(5)}_{2;\,2} - \tilde{R}^{(5)}_{2;\,2}\right)$	$\lvert m_3 + m_4\rvert$
$\frac{1}{\sqrt{2}}\left(R^{(5)}_{2;\,3} + \tilde{R}^{(5)}_{2;\,3}\right)$	$\lvert m_1 - m_2\rvert$
$\frac{1}{\sqrt{2}}\left(R^{(5)}_{2;\,3} - \tilde{R}^{(5)}_{2;\,3}\right)$	$\lvert m_3 - m_4\rvert$

Table 2.7: *The D3-D3 tensor masses.*

Chapter 3

Rotating black holes in M-theory

There are more things in heaven and earth, Horatio, than are dreamt of in your philosophy.

– William Shakespeare, *Hamlet*

In the previous chapter we investigated black hole solutions, in particular the D1-D5-P solution, in the presence of supersymmetry-breaking backgrounds. We now turn our attention to rotating black holes. This chapter will focus on the near-horizons of rotating black holes and how to uplift them into M-theory. Before we dive into the story, we will use several principles of complex geometry in this chapter, and we have given a very short review in section 3.A.

One of the motivations for the project is related to a gravitational extremization principle. The idea of extremizationd principles playing a fundamental role in physics has a long history since the advent of the Lagrangian and the principle of least action. More recently extremal problems have also been shown to play a role in both quantum field theory and supergravity. On the field theory side the so-called a-maximization [100], F-maximization [101], c-extremization [102, 103] and $\mathcal{I}$-extremization [104] have been successfully used to compute observables in SCFTs in 4, 3, 2 and 1 dimension(s) respectively. Via AdS/CFT it is natural to conjecture that there are dual extremization principles on the gravity side. Indeed, such geometric extremization principles have been found for all of the field theory principles mentioned above. In [105, 106] a geometric dual to a-maximization and F-maximization was given whilst in [107] an analogous proposal for c-extremization and $\mathcal{I}$-extremization was given for certain classes of theories. The classes of solutions tackled in [107] and in the later works [108–114] are AdS_3 solutions in Type IIB and

AdS_2 solutions in 11d supergravity. Subclasses of these arise as the near-horizon of static black strings and black holes embedded in the respective theories.[1]

For example, the near-horizon limit of a static asymptotically AdS_4 extremal black hole in 4d gauged supergravity contains an AdS_2 factor, see the review [116] and references therein. The staticity of the black hole requires that the transverse directions of the geometry are not fibered over AdS_2 but merely form a warped product. If one further restricts to magnetically charged black holes and uplifts the near-horizon solution to 11d supergravity, one obtains a supersymmetric solution with an AdS_2 factor and electric four-form charge. Solutions of this form were classified in [117] and later extended in [118, 119] to include additional magnetic flux. The geometries are a warped product of AdS_2 with a nine-dimensional internal manifold which is locally a U(1) bundle over a conformally Kähler space. To construct these geometries one places M2-branes in an asymptotic geometry of $\mathbb{R} \times CY_5$ and wraps them on a curve inside the Calabi–Yau five-fold. The near-horizon of this setup then gives rise to the AdS_2 geometry which in turn is seen to be the near-horizon of a black hole.

In order to obtain an AdS_2 solution it was important that the 4d black hole was both static and only magnetically charged. Adding rotation to the four-dimensional black hole leads to the internal space being fibered over the AdS_2 in the near-horizon, which will clearly persist in the uplift. Though not as obvious, if the 4d black hole has electric charges which are identified as arising from gauged flavour symmetries, this will also lead to a fibered AdS_2 in the 11d uplift. A gauge field in the truncation can have two sources, either it comes from gauging an isometry of the compactification manifold, or from the expansion of a p-form potential on $(p-1)$-cycles of the compactification manifold. The former gauge fields are dual to flavour symmetries whilst the latter are dual to baryonic symmetries. For the flavour symmetries the uplift will lead to the isometries being fibered over AdS_2 in the 11d solution. In summary, in order to incorporate more general black holes which rotate and have electric charges, one *must* relax the product structure of the 11d solution and allow for the internal manifold to be fibered over AdS_2. In contrast, one of the essential ingredients used in the works [117, 119], and more generally in AdS classifications, is that the AdS factor is a direct product in the metric.

[1] See also [115] for an extremization principle for $\mathcal{N} = (0,4)$ AdS_2 solutions in Type IIB.

In this chapter we will lay the groundwork for extending the geometric dual of $\mathcal{I}$-extremization and c-extremization to theories arising from the near-horizon of rotating black holes and black strings respectively. Concretely we will classify a large class of supersymmetric solutions of 11d supergravity containing an internal manifold arbitrarily fibered over AdS_2. With such a general ansatz we cover the black holes considered in [120–124]. We find that the 9d internal manifold is a U(1) fibration over an 8d space admitting a balanced metric. The balanced metric satisfies a master equation which is the analogue of the one found in the non-rotating case [117, 125], see also [118, 126–128] for further generalizations of these master equations. Through dualities we also classify a class of rotating black string near-horizons in Type IIB.

The outline of this chapter is as follows. In section 3.1 we study the necessary and sufficient conditions for a supersymmetric solution with time fibered over the transverse directions and consistent with preserving an $\mathrm{SO}(2,1)$ symmetry. In section 3.2 we give an action from which the equations of motion found in section 3.1 may be derived. In particular we show that when supersymmetry is imposed on the action it reduces to a simple form which computes the entropy of the black hole/string. In section 3.3 we exemplify how the electrically charged AdS_4 Kerr-Newman black hole is embedded in the classification. Section 3.4 discusses the conditions on the geometry of rotating black strings in Type IIB by using dualities with the 11d geometry. We conclude in section 3.5. A discussion on general black hole near-horizons and computing observables of the solutions is presented in appendix 3.B.

3.1 Setup

In this section we will explain the general procedure for obtaining the conditions for preserving supersymmetry of near-horizon solutions of rotating black holes. In general the conditions we find are necessary and sufficient conditions that must be satisfied by the near-horizon of any rotating black hole in 11d supergravity arising from rotating M2-branes. We will determine these conditions by using the results in [129] which classified all 11d supergravity backgrounds preserving supersymmetry and admitting a timelike Killing vector. Using [129] we can reduce the 11d supersymmetry conditions into differential conditions on a 10d base space. This base space must be non-compact and upon imposing the natural condition

that the 10d space is a cone we can reduce the conditions further to a compact 9d base, Y_9. This 9d base is a U(1) fibration over an 8d base, $\mathcal{B}$. In general the 8d base is not conformally Kähler, which *is* true for the non-rotating AdS_2 case studied in [117], but instead is a conformally balanced space.

One of the guiding principles that we will use is to impose that the near-horizon solution possesses an $SO(2,1)$ symmetry dual to the conformal group in the 1d superconformal quantum mechanical theory. Generally the ansatz that we will use when reducing the supersymmetry conditions does not possess this full symmetry but only a subset of it. However, from the point of view of imposing supersymmetry it is more convenient to work with this more general setup and then further constrain the geometry to preserve the full conformal group later. We will find that the additional constraints that we need to impose for the existence of an $SO(2,1)$ symmetry are specified by giving a constant vector with entries corresponding to each of the Killing vectors of the metric. These constants are related to the near-horizon angular velocities of the black hole along the Killing directions.

We begin this section by reviewing the conditions for a supersymmetric geometry in 11d supergravity to admit a timelike Killing vector following [129]. We discuss in detail the ansatz we will use in performing the reduction and subsequently reduce the conditions to an 8d base space. Up until this point we have not imposed the existence of an $SO(2,1)$ symmetry and in the final part of this section we discuss the additional constraints one must impose for such a symmetry using the results in appendix 3.B.

3.1.1 Timelike structures in 11d supergravity

In [129] the conditions for a solution of 11d supergravity to admit a timelike Killing spinor were derived. Here we summarize the most important results for our purposes. The metric takes the general form

$$\mathrm{d}s_{11}^2 = -\Delta^2(\mathrm{d}t + a)^2 + \Delta^{-1}\mathrm{e}^{2\phi}\mathrm{d}s_{10}^2 \tag{3.1}$$

where Δ and $\mathrm{e}^{2\phi}$ are functions defined on the 10d base. Note that we use a rescaling $\mathrm{e}^{2\phi}$ of the 10d metric compared to [129]. The 10d base admits a canonical SU(5)

structure which we denote by (j,ω)[2]. We normalize this structure such that

$$\omega \wedge \bar{\omega} = (-2i)^5 \frac{j^5}{5!}\,. \tag{3.2}$$

The exterior derivatives of the structure forms satisfy

$$\mathrm{d}j = \frac{1}{8} w_1 \lrcorner \mathrm{Im}[\omega] + w_3 + \frac{1}{4} w_4 \wedge j\,, \tag{3.3}$$

$$\mathrm{d}\,\mathrm{Re}[\omega] = \frac{1}{3} w_1 \wedge \frac{j^2}{2!} + w_2 \wedge j - \frac{1}{8} w_5 \wedge \mathrm{Re}[\omega]\,. \tag{3.4}$$

Here the w_i are the torsion modules of the SU(5) structure: w_1 is a real $(2,0)+(0,2)$-form, w_2 a real primitive $(3,1)+(1,3)$-form, w_3 a real primitive $(2,1)+(1,2)$-form and w_4 and w_5 are real one-forms. The 11d four-form flux is decomposed into 10d fluxes as

$$\mathcal{G}_4 = (\mathrm{d}t + a) \wedge f_3 + h_4\,. \tag{3.5}$$

Following the results of [129], imposing supersymmetry yields the following conditions relating the fluxes to the structure forms

$$\mathrm{d}(\mathrm{e}^{2\phi} j) = f_3\,, \tag{3.6}$$

$$\mathrm{d}\big(\Delta^{-3/2}\mathrm{e}^{5\phi}\,\mathrm{Re}[\omega]\big) = \mathrm{e}^{2\phi} \star_{10} h_4 - \mathrm{e}^{2\phi}\, h_4 \wedge j - \mathrm{e}^{4\phi}\,\mathrm{d}a \wedge \frac{j^2}{2}\,. \tag{3.7}$$

Moreover it follows that the 11d flux takes the form

$$\begin{aligned}\mathcal{G}_4 = {} & (\mathrm{d}t + a) \wedge \mathrm{d}(\mathrm{e}^{2\phi} j) - \Big[\frac{3}{4}\,\mathrm{d}a^{(0)} j + \mathrm{d}a^{(2,0)} + \mathrm{d}a^{(0,2)} + \frac{1}{3}\,\mathrm{d}a_0^{(1,1)}\Big] \wedge \mathrm{e}^{2\phi} j \\ & + \frac{1}{2}\mathrm{e}^{-2\phi} \star_{10} \mathrm{d}\big(\Delta^{-3/2}\mathrm{e}^{5\phi}\,\mathrm{Re}[\omega]\big) - \frac{1}{2}\mathrm{e}^{-2\phi} \star_{10} \Big[j \wedge \mathrm{d}\big(\Delta^{-3/2}\mathrm{e}^{5\phi}\,\mathrm{Re}[\omega]\big)\Big] \wedge j \\ & - \frac{1}{16}\Delta^{-3/2}\mathrm{e}^{3\phi} \star_{10} \left([w_5 + 4w_4 - 8\mathrm{d}\phi] \wedge \mathrm{Re}[\omega]\right) + h_0^{(2,2)}\,,\end{aligned} \tag{3.8}$$

where $\mathrm{d}a$ decomposes as $\mathrm{d}a = \mathrm{d}a^{(0)} j + \mathrm{d}a_0^{(1,1)} + \mathrm{d}a^{(2,0)} + \mathrm{d}a^{(0,2)}$, and $h_0^{(2,2)}$ is the primitive $(2,2)$ part of h_4 and is unconstrained by supersymmetry. Additionally the torsion module w_5 is fixed by supersymmetry to be

$$w_5 = -12\,\mathrm{d}\log\Delta + 40\,\mathrm{d}\phi\,. \tag{3.9}$$

[2] In comparison to [129] one should identify $(a, \mathrm{e}^{2\phi} j, \mathrm{e}^{5\phi}\omega, \mathrm{e}^{5\phi}\,\mathrm{Re}[\omega])_{\text{here}} \leftrightarrow (\omega, \Omega, \theta, \chi)_{\text{there}}$. In particular this transforms the torsion modules as $(\mathrm{e}^{\phi} w_1, \mathrm{e}^{3\phi} w_2, \mathrm{e}^{2\phi} w_3, w_4 + 8\,\mathrm{d}\phi, w_5 - 40\,\mathrm{d}\phi)_{\text{here}} \leftrightarrow (w_1, w_2, w_3, w_4, w_5)_{\text{there}}$.

For a supersymmetric solution to exist these conditions must be supplemented by the Bianchi identity and Maxwell equation

$$\mathrm{d}h_4 = -\mathrm{d}a \wedge \mathrm{d}(\mathrm{e}^{2\phi} j)\,, \tag{3.10}$$

$$\mathrm{d}\big(\Delta^{-3}\mathrm{e}^{4\phi} \star_{10} \mathrm{d}(\mathrm{e}^{2\phi} j)\big) = \mathrm{e}^{2\phi}\, \mathrm{d}a \wedge \star_{10} h_4 + \frac{1}{2} h_4 \wedge h_4\,. \tag{3.11}$$

The set of equations as given above are both necessary and sufficient for a solution to admit a timelike Killing spinor.

Our main motivation is to obtain the near-horizon geometries of rotating M2-branes wrapped on Riemann surfaces, which may give rise to the near-horizon of rotating black holes. It is also possible to engineer black holes using M5-branes, see for example [124, 130–133] however we will not consider this possibility in this work and restrict exclusively to solutions without M5 branes. This implies that we must make some assumptions about the form of the solution. It would be interesting in the future to relax these assumptions. To engineer such solutions one should place the rotating M2-branes in an asymptotic geometry of the form $\mathbb{R}_t \ltimes CY_5$ and then wrap the M2-brane on a Riemann surface inside the Calabi–Yau five-fold. Note that the rotation of the M2-brane leads to the non-trivial fibration of the 11d spacetime, with the time direction fibered over the five-fold. Since the asymptotic geometry is Calabi–Yau it is natural to expect that our 10d base space is complex, which requires that $w_1 = w_2 = 0$. This is indeed how the rotating M2-brane solution is embedded in the classification of [129] however we have not been able to prove that restricting to just M2-branes implies the complex condition. We will be satisfied with using the complex condition as a well-motivated ansatz in the following though it would certainly be interesting to lift this restriction. In addition to requiring the complex condition we also want to eliminate the possibility of having flux sourcing M5-branes. For this reason we will remove any terms appearing in the flux which are of Hodge type $(4,0)+(0,4)$, since these would not come from M2-branes wrapped on a Riemann surface.[3] From (3.8) and (3.9) we see that this assumption implies $w_4 = 3\,\mathrm{d}\log\Delta - 8\,\mathrm{d}\phi$.

[3]Lifting this assumption would open up the possibility of studying the near-horizon of rotating asymptotically AdS_7 black holes [130] arising from wrapping M5-branes on SLAG five-cycles in the Calabi–Yau five-fold. This would give the 11d geometric setting for the computations performed in [124, 131–133].

Under these assumptions the 10d torsion conditions are

$$\begin{aligned} \mathrm{d}(\mathrm{e}^{2\phi}\, j) &= f_3\,, \\ \mathrm{d}(\Delta^{-3}\mathrm{e}^{8\phi}\, j^4) &= 0\,, \\ \mathrm{d}(\Delta^{-3/2}\mathrm{e}^{5\phi}\, \omega) &= 0\,. \end{aligned} \tag{3.12}$$

The last unspecified torsion module is given by the primitive part of the three-form flux: $w_3 = \mathrm{e}^{-2\phi}\, f_{3,0}$. The 11d flux can now be succinctly written as

$$\begin{aligned} \mathcal{G}_4 &= (\mathrm{d}t + a) \wedge \mathrm{d}(\mathrm{e}^{2\phi} j) - \Big[\frac{3}{4}\,\mathrm{d}a^{(0)} j + \mathrm{d}a^{(2,0)} + \mathrm{d}a^{(0,2)} + \frac{1}{3}\,\mathrm{d}a_0^{(1,1)}\Big] \wedge \mathrm{e}^{2\phi} j + h_0^{(2,2)} \\ &= -\,\mathrm{d}\big[(\mathrm{d}t + a) \wedge \mathrm{e}^{2\phi} j\big] + \tilde{h}^{(2,2)}\,, \end{aligned} \tag{3.13}$$

where we define the shifted four-form flux

$$\begin{aligned} \tilde{h}^{(2,2)} &= h_4 + \mathrm{d}a \wedge \mathrm{e}^{2\phi} j\,, \\ &= h_0^{(2,2)} + \frac{1}{2}\,\mathrm{e}^{2\phi}\,\mathrm{d}a^{(0)}\,\frac{j^2}{2!} + \frac{2}{3}\,\mathrm{e}^{2\phi}\,\mathrm{d}a_0^{(1,1)} \wedge j\,. \end{aligned} \tag{3.14}$$

The Bianchi identity (3.10) and Maxwell equation (3.11) can now be rewritten in terms of $\tilde{h}^{(2,2)}$ as

$$\mathrm{d}\tilde{h}^{(2,2)} = 0\,, \tag{3.15}$$

$$\mathrm{d}\big(\Delta^{-3}\mathrm{e}^{4\phi} \star_{10} \mathrm{d}(\mathrm{e}^{2\phi} j)\big) = \frac{1}{2}\tilde{h}^{(2,2)} \wedge \tilde{h}^{(2,2)}\,. \tag{3.16}$$

For future reference, we give a few useful identities containing $\tilde{h}^{(2,2)}$:

$$\star_{10}\,\tilde{h}^{(2,2)} = \tilde{h}^{(2,2)} \wedge j - \mathrm{e}^{2\phi}\,\mathrm{d}a^{(0)}\,\frac{j^3}{3!} - 2\,\mathrm{e}^{2\phi}\,\mathrm{d}a_0^{(1,1)} \wedge \frac{j^2}{2!}\,, \tag{3.17}$$

$$j \lrcorner\, \tilde{h}^{(2,2)} = 2e^{2\phi}\,\mathrm{d}a^{(1,1)}\,. \tag{3.18}$$

Here $\mathrm{d}a^{(1,1)} = \mathrm{d}a^{(0)} j + \mathrm{d}a_0^{(1,1)}$, i.e. we omit the $(0,2)$ and $(2,0)$ contributions.

3.1.2 Ansatz

To proceed we must now insert an ansatz for the 10d base space. It was shown in [129] that the base is necessarily non-compact (the argument uses some smoothness conditions but these should hold in the present setting), and so we impose that the base is conformally a cone. The metric we take is

$$\mathrm{d}s_{11}^2 = -\Delta^2(\mathrm{d}t + a)^2 + \Delta^{-1}\mathrm{e}^{2\phi}\big(\mathrm{d}r^2 + r^2\mathrm{d}s_9^2\big)\,. \tag{3.19}$$

Next we need to specify how the scalar fields Δ, ϕ, connection one-form a and fluxes scale with respect to the radial coordinate. Ultimately we want to be able to recover a warped AdS_2 factor and an r-independent 9d space. This fixes the scaling of Δ and ϕ to be

$$\Delta = \frac{\mathrm{e}^{B+C}}{r}\,, \qquad \mathrm{e}^{2\phi} = \frac{\mathrm{e}^{3B+C}}{r^3}\,, \tag{3.20}$$

where we have introduced two new scalars B and C which are independent of the radial coordinate. For general scalar C this will not lead to a geometry admitting an $\mathrm{SO}(2,1)$ isometry generating the conformal group in 1d. As discussed earlier one must impose additional constraints. Rather than imposing them now it is more convenient to impose them later and leave the scalar C unconstrained for the moment.

The conical geometry naturally gives rise to an R-symmetry vector ξ defined by

$$\xi = j \cdot (r\partial_r)\,. \tag{3.21}$$

As can be easily checked by explicit computation the norm squared of the vector is r^2. On the link of the cone at $r = 1$ this translates to the existence of a unit-norm vector generating a holomorphic foliation over an 8d base admitting an SU(4) structure inherited from the parent SU(5) structure. We denote this 8d base by $\mathcal{B}$. Introducing coordinates for this vector

$$\xi = \partial_z\,, \tag{3.22}$$

we can write the dual one-form as

$$\eta = \mathrm{d}z + P\,, \tag{3.23}$$

where P is a one-form on $\mathcal{B}$. We may now decompose the SU(5) structure (j, ω) in terms of the SU(4) structure, which we denote by (J, Ω), as

$$\begin{aligned} j &= r\eta \wedge \mathrm{d}r + r^2\,\mathrm{e}^{-3B-C/3}\,J\,,\\ \omega &= r^4\,\mathrm{e}^{-6B-2C/3}\,\mathrm{e}^{\mathrm{i}z}(\mathrm{d}r - \mathrm{i}r\eta) \wedge \Omega\,. \end{aligned} \tag{3.24}$$

Here we include a scaling $\mathrm{e}^{-3B-C/3}$ of the 8d base, and a phase along the z-direction. The choice of scaling has been chosen so that the two form is balanced rather than conformally balanced as will become clear in the following section. While the phase is required by supersymmetry and implies that the holomorphic volume form has unit charge under the vector ξ.

The scaling of the connection one-form appearing in the time-fibration is fixed to be

$$a = r(\alpha\,\eta + A)\,, \tag{3.25}$$

where α and A denote an 8d scalar and one-form respectively. Note that we did not include a term with a leg on $\mathrm{d}r$ in this decomposition because such a term could be absorbed by redefinitions and coordinate changes for a near-horizon geometry. It will turn out that imposing the $\mathrm{SO}(2,1)$ symmetry will further constrain the one-form a and scalar C however we postpone this discussion to later. The field strength $\mathrm{d}a$ is

$$\mathrm{d}a = \alpha\,\mathrm{d}r\wedge\eta + \mathrm{d}r\wedge A - r\,\eta\wedge\mathrm{d}\alpha + r\,(\alpha\,\mathrm{d}\eta + \mathrm{d}A)\,. \tag{3.26}$$

With these ansätze the 11d metric becomes

$$\mathrm{d}s_{11}^2 = \mathrm{e}^{2B}\Big[-\mathrm{e}^{2C}\Big(\frac{\mathrm{d}t}{r} + \alpha\,\eta + A\Big)^2 + \frac{\mathrm{d}r^2}{r^2} + \eta^2 + \mathrm{e}^{-3B-C/3}\,\mathrm{d}s_8^2\Big]\,. \tag{3.27}$$

We recover the non-rotating case by setting $\alpha = 0$, $A = 0$ and $\mathrm{e}^{2C} = 1$.[4]

Finally we must fix the r-scaling of the flux. The scaling is fixed by regularity as $r \to 0$ and preserving the $\mathrm{SO}(2,1)$ symmetry which requires the radial dependence to only appear in the one-forms

$$\frac{\mathrm{d}t}{r} \quad \text{and} \quad \frac{\mathrm{d}r}{r}\,. \tag{3.28}$$

It follows that the 10d fluxes f_3 and $\tilde{h}^{(2,2)}$ decompose in terms of 8d fluxes as

$$f_3 = r^{-1}\Big[\frac{\mathrm{d}r}{r}\wedge\eta\wedge F_1 + \frac{\mathrm{d}r}{r}\wedge F_2 + F_3\Big]\,, \tag{3.29}$$

$$\begin{aligned}\tilde{h}^{(2,2)} = {} & H^{(2,2)} + \frac{\mathrm{d}r}{r}\wedge(H^{(2,1)} + H^{(1,2)}) + \eta\wedge\mathrm{i}(H^{(2,1)} - H^{(1,2)}) \\ & + \frac{\mathrm{d}r}{r}\wedge\eta\wedge H^{(1,1)}\,.\end{aligned} \tag{3.30}$$

In principle one could include a piece of f_3 with one leg on η and two legs on $\mathcal{B}$, but we omit it here because it will be put to zero by supersymmetry. Note that we keep track of the Hodge type of the components of $\tilde{h}^{(2,2)}$, where the holomorphic and anti-holomorphic one-form associated with $\mathrm{d}r$ and η are given by $e^1 = \mathrm{d}r - \mathrm{i}r\eta$ and its conjugate respectively.

[4] In comparison to [117] we identify $B_{\text{here}} \leftrightarrow A_{\text{there}}$, and comparing with [134] we identify $B_{\text{here}} \leftrightarrow -B_{\text{there}}/3$.

3.1.3 8d supersymmetry conditions

We can now derive the 8d conditions by reducing their 10d counterparts using the ansätze presented in the previous section. Let us begin by reducing the SU(5) structure torsion conditions to SU(4) structure conditions. From decomposing (3.12) we find

$$F_1 = -\,\mathrm{d}\mathrm{e}^{3B+C}\,, \tag{3.31}$$

$$F_2 = \mathrm{e}^{3B+C}\,\mathrm{d}\eta - \mathrm{e}^{2C/3}\,J\,, \tag{3.32}$$

$$F_3 = \mathrm{d}(\mathrm{e}^{2C/3}\,J)\,, \tag{3.33}$$

$$\mathrm{d}J^3 = 0\,, \tag{3.34}$$

$$\mathrm{d}\eta \wedge \frac{J^3}{3!} = \mathrm{e}^{-3B-C/3}\,\frac{J^4}{4!}\,, \tag{3.35}$$

$$\mathrm{d}\mathrm{e}^{-3B-C/3} \wedge J^4 = 0\,, \tag{3.36}$$

$$\mathrm{d}\Omega = \mathrm{i}\big(P + \tfrac{1}{3}\mathrm{d}^c C\big) \wedge \Omega\,. \tag{3.37}$$

Recall that Ω has unit charge under the vector ∂_z which is evident from (3.24). From these equations we can deduce the SU(4) torsion modules W_i. From (3.37) we immediately see that the 8d base is complex: $W_1 = W_2 = 0$. Furthermore, from (3.34) we see that $W_4 = 0$, i.e. the base is balanced. Fixing the two-form to be balanced as opposed to conformally balanced fixed the choice of scaling of the 8d base in (3.24). In particular the base is not Kähler: the third torsion module is related to the primitive part of F_3 as $W_3 = \mathrm{e}^{-2C/3}\,F_{3,0}$. However, for the Kerr–Newman electrically charged black hole that we consider in section 3.3 this part of the flux vanishes, and the 8d base is therefore Kähler. From (3.37) we find $W_5 = -4J \cdot P - \frac{4}{3}\mathrm{d}C$ and this fixes the Ricci-form of the base in terms of the connection P and the scalar C as we show below. Before proceeding it is useful to rewrite the three-form flux f_3 as

$$f_3 = r^{-1}\Big[\frac{\mathrm{d}r}{r} \wedge \hat{F} - \mathrm{d}\hat{F}\Big]\,, \quad \text{where} \quad \hat{F} = -\mathrm{e}^{2C/3}J + \mathrm{d}(\mathrm{e}^{3B+C}\eta) \tag{3.38}$$

which puts it into a form more reminiscent of the non-rotating case [117].

Let us turn our attention to the other identities following from (3.31)-(3.37). Firstly, from (3.36) we find

$$\mathcal{L}_\xi \mathrm{e}^{-3B-C/3} = 0\,. \tag{3.39}$$

In fact, we will take ξ to be a symmetry of each of the scalars B, C individually, though supersymmetry does not require this. This assumption is natural since we want ξ to play the role of the R-symmetry vector of the solution. Note that these conditions imply that it is a Killing vector of the 10d space and by imposing $\mathcal{L}_\xi \alpha = 0$, it is in fact a Killing vector for the full 11d metric. Taking the exterior derivative of (3.37) implies

$$\mathrm{d}\eta \wedge \Omega = 0\,, \tag{3.40}$$

hence $\mathrm{d}\eta$ is a $(1,1)$-form on the base. Moreover from (3.35) we find that

$$J \lrcorner \mathrm{d}\eta = \mathrm{e}^{-3B-C/3}\,. \tag{3.41}$$

Finally from (3.37) we can read off the Ricci form ρ on the 8d space to be

$$\rho = \mathrm{d}\eta + \tfrac{1}{3}\mathrm{d}\mathrm{d}^c C\,. \tag{3.42}$$

Note that the second term is exact since we require the scalar C to be globally well-defined.
This in turn allows us to compute the Chern–Ricci scalar[5]

$$R_C \equiv 2J \lrcorner \rho = 2e^{-3B-C/3} - \tfrac{2}{3}\Box C\,. \tag{3.43}$$

The Chern–Ricci scalar is related to the more common 8d Ricci scalar via[6]

$$R_8 = R_C - \tfrac{1}{2}|\mathrm{d}J|^2\,. \tag{3.44}$$

It is clear from the above relation that the two scalars coincide when the manifold is Kähler.

So far we have only imposed supersymmetry and not the equations of motion. Integrability of the Killing spinor equations implies that the Einstein equations are satisfied so long as the Bianchi identity (3.15) and Maxwell equation (3.16) are imposed. Imposing these gives us additional constraints on the geometry and fluxes.

[5]Here we find the d'Alembertian operator through the short computation:

$$J \lrcorner \mathrm{d}\mathrm{d}^c C = *(\mathrm{d}\mathrm{d}^c C \wedge *J) = *\,\mathrm{d}\,(\mathrm{d}^c C \wedge *J) = *\,\mathrm{d} * (\mathrm{d}^c C \lrcorner J) = - * \mathrm{d} * \mathrm{d} C = -\Box C\,,$$

where we use that $\frac{1}{3!}\mathrm{d}J^3 = \mathrm{d} * J = 0$.
[6]Note that this is equivalent to the identity $R_8 = R_C - \frac{1}{2}|\mathrm{d}^c J|^2$ that is also used in the literature.

From reducing the Bianchi identity we find

$$\begin{aligned} &\mathrm{d}H^{(2,2)} = -\mathrm{i}\mathrm{d}\eta \wedge (H^{(2,1)} - H^{(1,2)})\,, \\ &\partial H^{(2,1)} = \bar{\partial} H^{(1,2)} = 0\,, \\ &\bar{\partial} H^{(2,1)} = \partial H^{(1,2)} = -\tfrac{1}{2}\,\mathrm{d}\eta \wedge H^{(1,1)}\,, \\ &\mathrm{d}H^{(1,1)} = 0\,. \end{aligned} \tag{3.45}$$

From this decomposition it is simple to show that the R-symmetry vector ξ is not just a symmetry of the metric, but also for the 10d flux $\tilde{h}^{(2,2)}$, i.e.

$$\mathcal{L}_\xi \tilde{h}^{(2,2)} = 0\,. \tag{3.46}$$

In fact, we find that ξ is a symmetry for the full 11d flux G_4 as well, since by using (3.26) and that the scalar α has vanishing Lie-derivative along ξ one can show that

$$\mathcal{L}_\xi G_4 = 0\,. \tag{3.47}$$

This is then consistent with our interpretation of ξ as being the Killing vector dual to the R-symmetry of a putative dual field theory.
From the 10d Maxwell equation we find the set of equations

$$-\mathrm{d} *_8 \mathrm{d}\mathrm{e}^{-3B-C} + \mathrm{e}^{-2C/3}\,\mathrm{d}\eta \wedge \mathrm{d}\eta \wedge \frac{J^2}{2!} = \frac{1}{2} H^{(2,2)} \wedge H^{(2,2)}\,, \tag{3.48}$$

$$\mathrm{e}^{-4C/3}\,\mathrm{d}\eta \wedge *_8\,\mathrm{d}(\mathrm{e}^{2C/3} J) = H^{(2,2)} \wedge (H^{(2,1)} + H^{(1,2)})\,, \tag{3.49}$$

$$-\mathrm{d}\eta \wedge \mathrm{d}\Big(\mathrm{e}^{-2C/3}\,\frac{J^2}{2!}\Big) = H^{(2,2)} \wedge \mathrm{i}(H^{(2,1)} - H^{(1,2)})\,, \tag{3.50}$$

$$-\mathrm{d}\mathrm{d}^c\Big(\mathrm{e}^{-2C/3}\frac{J^2}{2!}\Big) = H^{(2,2)} \wedge H^{(1,1)} + 2\mathrm{i} H^{(2,1)} \wedge H^{(1,2)}\,. \tag{3.51}$$

It can be shown that the second and third equation are equivalent by acting with the operator $J\cdot$ which acts by contracting the complex structure into each index of the form. For a (p,q)-form this acts by multiplying the form by i^{p-q}. By applying the 8d Hodge star to (3.48), and by inserting (3.42) and (3.43), we can rewrite it as

$$\begin{aligned} \mathrm{e}^{2C/3} *_8 (H^{(2,2)} \wedge H^{(2,2)}) = &-\mathrm{e}^{2C/3}\Box\big(\mathrm{e}^{-2C/3}(R_C + \tfrac{2}{3}\Box C)\big) \\ &+ \tfrac{1}{2}\big(R_C + \tfrac{2}{3}\Box C\big)^2 - 2\big|\rho - \tfrac{1}{3}\mathrm{d}\mathrm{d}^c C\big|^2 \end{aligned} \tag{3.52}$$

This is the rotating version of the master equation [117, 125]. It reduces to the familiar non-rotating master equation of [117] by setting $e^{2C} = 1$, $H^{(2,2)} = 0$ and $\mathrm{d}J = 0$ (so that $R_C = R_8$).

One can be slightly more explicit with the form of the flux terms and determine them up to primitive pieces. From (3.26) and by decomposing $\mathrm{d}a$ in term of its Hodge type we find

$$\begin{aligned}
\mathrm{d}a^{(0)} &= \tfrac{4}{5}\, r^{-1}\mathrm{e}^{3B+C/3}\,\mathrm{d}A^{(0)}\,,\\
\mathrm{d}a^{(2,0)} &= \tfrac{1}{2}e^1\wedge(A^{(1,0)}-\mathrm{i}\partial\alpha)+r\,\mathrm{d}A^{(2,0)}\,,\\
\mathrm{d}a^{(0,2)} &= \tfrac{1}{2}\bar{e}^1\wedge(A^{(0,1)}+\mathrm{i}\bar{\partial}\alpha)+r\,\mathrm{d}A^{(0,2)}\,,\\
\mathrm{d}a_0^{(1,1)} &= \mathrm{d}r\wedge\eta\left(\alpha+\tfrac{4}{5}\,\mathrm{e}^{3B+C/3}\,\mathrm{d}A^{(0)}\right)+r\left(\alpha\,\mathrm{d}\eta+\tfrac{1}{5}\,\mathrm{d}A^{(0)}J+\mathrm{d}A_0^{(1,1)}\right)\\
&\quad+\tfrac{1}{2}\mathrm{d}r\wedge(A-\mathrm{d}^c\alpha)+\tfrac{1}{2}r\eta\wedge(J\cdot A-\mathrm{d}\alpha)\,.
\end{aligned}\tag{3.53}$$

We can use these decompositions to reduce (3.18) which implies:

$$\begin{aligned}
e^{-2C/3}\,J\lrcorner\,H^{(1,1)} &= 2\alpha\,,\\
e^{-2C/3}\,J\lrcorner\,H^{(2,1)} &= \mathrm{i}\partial\alpha+A^{(1,0)}\,,\\
e^{-2C/3}\,J\lrcorner\,H^{(2,2)}-e^{-3B-C}\,H^{(1,1)} &= 2\mathrm{d}A^{(1,1)}+2\alpha\mathrm{d}\eta\,.
\end{aligned}\tag{3.54}$$

Therefore we may rewrite the fluxes as

$$\begin{aligned}
H^{(1,1)} &= \tfrac{1}{2}e^{2C/3}\alpha J+H_0^{(1,1)}\,,\\
H^{(2,1)} &= \tfrac{1}{3}e^{2C/3}J\wedge(i\partial\alpha+A^{(1,0)})+H_0^{(2,1)}\,,\\
H^{(2,2)} &= \tfrac{1}{2}J\wedge\left(e^{-3B-C/3}H^{(1,1)}+2e^{2C/3}(\mathrm{d}A^{(1,1)}+\alpha\mathrm{d}\eta)\right)\\
&\quad-\tfrac{1}{3}(2e^{2C/3}\mathrm{d}A^{(0)}+e^{-3B+C/3}\alpha)J^2+H_0^{(2,2)}\,,
\end{aligned}\tag{3.55}$$

where $H_0^{(p,q)}$ denotes the primitive piece. In principle one could now substitute these expressions into the Bianchi identities and Maxwell equations however this is not particularly enlightening and so we refrain from presenting them here. Note that the primitive pieces are essential for satisfying the Bianchi identities.

3.1.4 Imposing the SO(2,1) isometry

So far our analysis has been for general scalars C, α and one-form A. However, in order to construct the near-horizon of a black hole we need to impose that there is an $\mathrm{SO}(2,1)$ isometry, which leads to constraints on these fields. In appendix 3.B we have given the general metric for the near-horizon of a rotating black hole with a manifest AdS_2 factor over which the internal manifold is fibered and seen the constraints that this imposes on the geometry. In particular the fibration is governed by a vector of constants k^i associated to each Killing vector of the internal

manifold fibered over AdS_2. As we reviewed in the appendix the necessity for these parameters to be constant arises in order that there is an $\mathrm{SO}(2,1)$ isometry. From the analysis of appendix 3.B we find that the scalar and one-form take the form[7]

$$\alpha\eta + A = -k^i g(\partial_{\phi_i}, \cdot)\,, \qquad \mathrm{e}^{-2C} = 1 + |\alpha\eta + A|^2_9\,, \tag{3.56}$$

where ∂_{ϕ_i} are the Killing vectors of the internal manifold and the metric g_{ij} is the metric on $\mathrm{d}s^2_9$, as defined in (3.19), restricted to the angular coordinates. Denoting by

$$\eta_i \equiv g(\partial_{\phi_i}, \cdot)\,, \tag{3.57}$$

the dual one-form of the Killing vector ∂_{ϕ_i} using the metric on $\mathrm{d}s^2_9$. Then the one-form a is simply

$$a \equiv r(\alpha\eta + A) = -rk^i\eta_i\,. \tag{3.58}$$

In the remainder of this section let us assume that the 8d base is Kähler since this will allow for more explicit expressions. In addition we will assume that the base is toric, with the 9d space Y_9 admitting a $\mathrm{U}(1)^5$ action with Killing vectors ∂_{ϕ_i}.[8] We may write the one form η as[9]

$$\eta = 2\sum_i w_i \mathrm{d}\phi_i\,, \tag{3.59}$$

where the w_i are the moment map coordinates of the cone restricted to Y_9. Moreover the Kähler two-form on the base may be expanded as

$$J = \sum_i \mathrm{d}x_i \wedge \mathrm{d}\phi_i\,, \tag{3.60}$$

where x_i are global functions on Y_9 since $b_1(Y_9) = 0$ for a toric contact structure. Note that

$$\partial_{\phi_i} \lrcorner\, J = -\mathrm{d}x_i\,. \tag{3.61}$$

[7] We use the math literature notation such that $g(\partial_{\phi_i}, \cdot)$ is a one-form.

[8] We need not require the full space to be toric for our arguments to hold, we merely do so for simplicity of exposition. An interesting case to consider, which requires a minor generalization, is to consider a Riemann surface embedded into Y_9 as $Y_9 \equiv O(\vec{n})_{\Sigma_g} \times_{U(1)^4} Y_7$ with $\vec{n}$ a four-vector of constant twist parameters which are the Chern numbers of the U(1) bundle over the Riemann surface [108].

[9] We follow the toric geometry notational conventions of [108].

With this short (and very incomplete) review of toric geometry we may proceed with writing the scalars and one-form in terms of the global functions of the toric geometry defined above. It follows that

$$\alpha = -k^i \partial_{\phi_i} \lrcorner \, \eta = -2k^i w_i \,. \tag{3.62}$$

Next consider A, we find the simple result

$$A = -\mathrm{e}^{-3B-C/3} k^i \mathrm{d}^c x_i \,. \tag{3.63}$$

Finally we may evaluate (3.56) which implies

$$\mathrm{e}^{-2C} = 1 + (2k^i w_i)^2 + \mathrm{e}^{-3B-C/3} |k^i \mathrm{d}^c x_i|_8^2 \,, \tag{3.64}$$

where $|\cdot|_8^2$ is the norm with respect to the Kähler metric. In principle one could try to solve this for the scalar C, however this is a sextic equation to solve. One could use (3.64) as defining the combination $\mathrm{e}^{-3B-C/3}$ which appears ubiquitously in the geometry.

Note that this last comment only applies when the gauge field A is non-zero. When it vanishes and the fibration is only along the R-symmetry direction, it turns out that C is constant. To see this it is more insightful to use the parametrization employed in appendix 3.B where the z-coordinate is assigned its own constant k^z, i.e. we do not use the basis ∂_{ϕ_i} used previously in this section. In this basis the Killing vectors are the four U(1) isometries of the base and the R-symmetry vector ∂_z. It is then clear that for A to vanish each of the four constants associated to the U(1)'s of the base must be zero. It follows from (3.176) that α is precisely the constant $-k^z$. Moreover e^{-2C} takes the constant value,

$$\mathrm{e}^{-2C} = 1 + (k^z)^2 \,. \tag{3.65}$$

The natural interpretation of this subcase is that of the near-horizon of a non-rotating black hole equipped with an electric component for the graviphoton and possibly including magnetic charges for each of the gauge fields in the 4d theory.

3.2 Action for the theory

One of the essential ingredients for performing the extremization in [107] was the existence of an action which gave rise to the equations of motion of the theory. This

action was derived in [134] for the near-horizon geometry of static black holes and strings in M-theory and Type IIB respectively. As a first step towards performing the extremization in the rotating case we will construct the analogous rotating action. Thereafter we impose the supersymmetry constraints on this action and show that it reduces to a simple and familiar form. The action computes the entropy of these black holes.

3.2.1 Non-supersymmetric action

The simplest method for constructing an action for the 9d geometry is to reduce the 11d action using our ansätze. By construction the equations of motion of the resulting 9d action will match the ones obtained in the section 3.1.3. We start from the action of eleven-dimensional supergravity

$$S_{11} = \frac{1}{2\kappa_{11}^2} \int R_{11} *_{11} 1 - \frac{1}{2} \mathcal{G}_4 \wedge *_{11} \mathcal{G}_4 - \frac{1}{6} \mathcal{C}_3 \wedge \mathcal{G}_4 \wedge \mathcal{G}_4 \,. \tag{3.66}$$

Here $\mathcal{C}_3$ is the three-form potential and $\mathcal{G}_4 = \mathrm{d}\mathcal{C}_3$ is its field strength. Using the ansätze

$$\begin{aligned} \mathrm{d}s_{11}^2 &= -\Delta^2 (\mathrm{d}t + a)^2 + \Delta^{-1} e^{2\phi} \, \mathrm{d}s_{10}^2 \,, \\ \mathcal{G}_4 &= \Delta^{-1} e^0 \wedge f_3 + h_4 \,, \end{aligned} \tag{3.67}$$

we reduce this action to 10d. The Bianchi identity $\mathrm{d}\mathcal{G}_4 = 0$ implies that

$$\mathrm{d}f_3 = 0 \,, \qquad \mathrm{d}h_4 + \mathrm{d}a \wedge f_3 = 0 \,. \tag{3.68}$$

We write these field strengths in terms of their potentials as

$$f_3 = \mathrm{d}c_2 \,, \qquad h_4 = \mathrm{d}c_3 - \mathrm{d}a \wedge c_2 \,. \tag{3.69}$$

Now we can write $\mathcal{G}_4$ into the convenient form

$$\mathcal{G}_4 = -\,\mathrm{d}\big[(\mathrm{d}t + a) \wedge c_2\big] + \tilde{h}^{(2,2)} \,, \tag{3.70}$$

where we introduce the shifted four-form field strength

$$\tilde{h}^{(2,2)} = h_4 + \mathrm{d}a \wedge c_2 = \mathrm{d}c_3 \,. \tag{3.71}$$

Note that although we add a superscript to indicate that upon imposing supersymmetry this field strength is a $(2,2)$-form, at the moment we have not imposed

supersymmetry yet so we have to treat $\tilde{h}^{(2,2)}$ as a general four-form. The 11d potential $\mathcal{C}_3$ can now be expressed in terms of the 10d potentials as

$$\mathcal{C}_3 = -(\mathrm{d}t + a) \wedge c_2 + c_3 \,. \tag{3.72}$$

By using these ansätze and definitions, we find the 10d Lagrangian

$$\begin{aligned}
\mathscr{L}_{10} = \Delta^{-3} e^{8\phi} \big(& R_{10} - 72(\partial_\mu \phi)^2 - 18\, \nabla^2 \phi \\
& - 12(\partial_\mu \log \Delta)^2 + 7\, \nabla^2 \log \Delta + 56\, \partial_\mu \phi\, \partial^\mu \log \Delta \big) *_{10} 1 \\
& + \tfrac{1}{2}\, e^{6\phi}\, \mathrm{d}a \wedge *_{10} \mathrm{d}a + \tfrac{1}{2}\, \Delta^{-3} e^{4\phi}\, f_3 \wedge *_{10} f_3 - \tfrac{1}{2}\, e^{2\phi}\, \tilde{h}^{(2,2)} \wedge *_{10} \tilde{h}^{(2,2)} \\
& + e^{2\phi}\, c_2 \wedge \mathrm{d}a \wedge *_{10} \tilde{h}^{(2,2)} - \tfrac{1}{2}\, e^{2\phi}\, c_2 \wedge \mathrm{d}a \wedge *_{10} (c_2 \wedge \mathrm{d}a) \\
& + \tfrac{1}{2}\, c_2 \wedge \tilde{h}^{(2,2)} \wedge \tilde{h}^{(2,2)} - \tfrac{1}{2}\, (c_2)^2 \wedge \mathrm{d}a \wedge \tilde{h}^{(2,2)} + \tfrac{1}{6} (c_2)^3 \wedge (\mathrm{d}a)^2 \,.
\end{aligned} \tag{3.73}$$

Next we want to consider the reduction of this Lagrangian to 9d, by using the cone ansatz presented in (3.1.2). In addition, we want to split off the η-direction from the 8d space $\mathcal{B}$ so that we end up with a 9d Lagrangian density of the form $\mathscr{L}_9 = \eta \wedge (\ldots)$ where the dots represent an expression in terms of fields defined on $\mathcal{B}$. The relevant ansätze for this reduction are[10]

$$\begin{aligned}
\mathrm{d}s_{10}^2 &= \mathrm{d}r^2 + r^2 \eta^2 + r^2\, \mathrm{e}^{-3B - C/3}\, \mathrm{d}s_8^2 \,, \\
\mathrm{e}^{2\phi} &= r^{-3}\, \mathrm{e}^{3B + C} \,, \\
\Delta &= r^{-1}\, \mathrm{e}^{B + C} \,, \\
\mathrm{d}a &= r\, (\alpha\, \mathrm{d}\eta + \mathrm{d}A) + \mathrm{d}r \wedge A - r\, \eta \wedge \mathrm{d}\alpha + \alpha\, \mathrm{d}r \wedge \eta \,, \\
c_2 &= r^{-1}\, C_2 + r^{-1}\, \eta \wedge C_1 + r^{-2}\, C_0\, \mathrm{d}r \wedge \eta \,, \\
f_3 &= r^{-1}\, F_3 + r^{-2}\, \mathrm{d}r \wedge F_2 + r^{-1}\, \eta \wedge \hat{F}_2 + r^{-2}\, \mathrm{d}r \wedge \eta \wedge F_1 \,, \\
\tilde{h}^{(2,2)} &= H^{(2,2)} + r^{-1} \mathrm{d}r \wedge (H^{(2,1)} + H^{(1,2)}) + i\eta \wedge (H^{(2,1)} - H^{(1,2)}) \,, \\
&\quad + r^{-1} \mathrm{d}r \wedge \eta \wedge H^{(1,1)} \,.
\end{aligned} \tag{3.74}$$

[10] Note that we omitted the part of c_2 that has one leg on $\mathrm{d}r$ and one leg on $\mathcal{B}$ only. The reason for this is that such a term can be absorbed in C_2 by a gauge transformation.

Performing this reduction is a lengthy but in principle straightforward calculation. We find the 9d Lagrangian[11]

$$
\begin{aligned}
\mathscr{L}_9 = \eta \wedge \Big[& \big(R_8 - \tfrac{9}{2}(\partial_\mu B)^2 - \tfrac{7}{6}(\partial_\mu C)^2 - 3\,\partial_\mu B\,\partial^\mu C - 2\,e^{-3B-C/3}\big) *_8 1 - \tfrac{1}{2}\,e^{3B+C/3}\,\mathrm{d}\eta \wedge *_8 \mathrm{d}\eta \\
& + \tfrac{1}{2}\,e^{-3B+5C/3}\alpha^2 *_8 1 + \tfrac{1}{2}\,e^{2C} A \wedge *_8 A + \tfrac{1}{2}\,e^{2C}\mathrm{d}\alpha \wedge *_8 \mathrm{d}\alpha + \tfrac{1}{2}\,e^{3B+7C/3}(\alpha\,\mathrm{d}\eta + \mathrm{d}A) \wedge *_8 (\alpha\,\mathrm{d}\eta + \mathrm{d}A) \\
& + \tfrac{1}{2}\,e^{-6B-2C} F_1 \wedge *_8 F_1 + \tfrac{1}{2}\,e^{-3B-5C/3} F_2 \wedge *_8 F_2 + \tfrac{1}{2}\,e^{-3B-5C/3}\hat{F}_2 \wedge *_8 \hat{F}_2 + \tfrac{1}{2}\,e^{-4C/3} F_3 \wedge *_8 F_3 \\
& - \tfrac{1}{2}\,e^{3B+C} H^{(2,2)} \wedge *_8 H^{(2,2)} - 2e^{2C/3} H^{(2,1)} \wedge *_8 H^{(1,2)} - \tfrac{1}{2}\,e^{-3B+C/3} H^{(1,1)} \wedge *_8 H^{(1,1)} \\
& + e^{3B+C}\,C_2 \wedge (\alpha\,\mathrm{d}\eta + \mathrm{d}A) \wedge *_8 H^{(2,2)} + i e^{2C/3}\big(C_1 \wedge (\alpha\,\mathrm{d}\eta + \mathrm{d}A) - C_2 \wedge \mathrm{d}\alpha\big) \wedge *_8 (H^{(2,1)} - H^{(1,2)}) \\
& + e^{2C/3} C_2 \wedge A \wedge *_8 (H^{(2,1)} + H^{(1,2)}) + e^{-3B+C/3}\big(\alpha\,C_2 + C_1 \wedge A + C_0\,(\alpha\,\mathrm{d}\eta + \mathrm{d}A)\big) \wedge *_8 H^{(1,1)} \\
& - \tfrac{1}{2}\,e^{3B+C}\,C_2 \wedge (\alpha\,\mathrm{d}\eta + \mathrm{d}A) \wedge *_8 (C_2 \wedge (\alpha\,\mathrm{d}\eta + \mathrm{d}A)) - \tfrac{1}{2}\,e^{2C/3} C_2 \wedge A \wedge *_8 (C_2 \wedge A) \\
& - \tfrac{1}{2}\,e^{2C/3}\big(C_1 \wedge (\alpha\,\mathrm{d}\eta + \mathrm{d}A) - C_2 \wedge \mathrm{d}\alpha\big) \wedge *_8 \big(C_1 \wedge (\alpha\,\mathrm{d}\eta + \mathrm{d}A) - C_2 \wedge \mathrm{d}\alpha\big) \\
& - \tfrac{1}{2}\,e^{-3B+C/3}\big(\alpha\,C_2 + C_1 \wedge A + C_0\,(\alpha\,\mathrm{d}\eta + \mathrm{d}A)\big) \wedge *_8 \big(\alpha\,C_2 + C_1 \wedge A + C_0\,(\alpha\,\mathrm{d}\eta + \mathrm{d}A)\big) \\
& - C_2 \wedge H^{(2,2)} \wedge H^{(1,1)} - 2iC_2 \wedge H^{(2,1)} \wedge H^{(1,2)} - \tfrac{1}{2}\,C_0\,H^{(2,2)} \wedge H^{(2,2)} - C_1 \wedge H^{(2,2)} \wedge (H^{(2,1)} + H^{(1,2)}) \\
& + \tfrac{1}{2}\,(C_2)^2 \wedge \alpha\,H^{(2,2)} - \tfrac{1}{2}\,(C_2)^2 \wedge \mathrm{d}\alpha \wedge (H^{(2,1)} + H^{(1,2)}) - \tfrac{1}{2}\,i(C_2)^2 \wedge A \wedge (H^{(2,1)} - H^{(1,2)}) \\
& + \tfrac{1}{2}\,(C_2)^2 \wedge (\alpha\,\mathrm{d}\eta + \mathrm{d}A) \wedge H^{(1,1)} + C_0\,C_2 \wedge (\alpha\,\mathrm{d}\eta + \mathrm{d}A) \wedge H^{(2,2)} + C_2 \wedge C_1 \wedge A \wedge H^{(2,2)} \\
& + C_2 \wedge C_1 \wedge (\alpha\,\mathrm{d}\eta + \mathrm{d}A) \wedge (H^{(2,1)} + H^{(1,2)}) - (C_2)^2 \wedge C_1 \wedge A \wedge (\alpha\,\mathrm{d}\eta + \mathrm{d}A) \\
& - \tfrac{1}{3}(C_2)^3 \wedge \alpha\,(\alpha\,\mathrm{d}\eta + \mathrm{d}A) - \tfrac{1}{3}(C_2)^3 \wedge A \wedge \mathrm{d}\alpha - \tfrac{1}{2}\,C_0\,(C_2)^2 \wedge (\alpha\,\mathrm{d}\eta + \mathrm{d}A)^2 \Big] .
\end{aligned}
\tag{3.75}
$$

From this action one can derive the equation of motions that define the solutions discussed in the previous section 3.1.3. Note that we have not imposed any supersymmetry in deriving this action.

3.2.2 Supersymmetric action

Here we consider the restriction of the Lagrangian obtained above to off-shell supersymmetric geometries. We say these 9d geometries are off-shell because we do not impose the equations of motion such as (3.52), and supersymmetric since we do impose the supersymmetry constraints discussed in section 3.1. We will see that the Lagrangian (3.75) becomes quite simple once supersymmetry has been imposed. The simplest method is to impose supersymmetry in 10d and subsequently reduce to 9d, instead of starting from the 9d Lagrangian (3.75). We begin with the 10d non-supersymmetric Lagrangian in (3.73). There we can readily plug in the susy conditions

$$
c_2 = \mathrm{e}^{2\phi}\,j\,, \qquad\qquad f_3 = \mathrm{d}(\mathrm{e}^{2\phi}\,j)\,. \tag{3.76}
$$

[11] We split off the r-coordinate as $\mathscr{L}_{10} = \mathscr{L}_9 \wedge r^{-2}\mathrm{d}r$. Splitting off $\mathrm{d}r$ on the left side would give an overall minus sign.

Furthermore, we use the decompositions

$$\mathrm{d}a = \mathrm{d}a^{(0)}\, j + \mathrm{d}a_0^{(1,1)} + \mathrm{d}a^{(2,0)} + \mathrm{d}a^{(0,2)}\,, \tag{3.77}$$

$$\tilde{h}^{(2,2)} = \tilde{h}_0^{(2,2)} + \tfrac{1}{2}\,\mathrm{e}^{2\phi}\,\mathrm{d}a^{(0)}\,\frac{j^2}{2!} + \tfrac{2}{3}\,\mathrm{e}^{2\phi}\,\mathrm{d}a_0^{(1,1)} \wedge j\,, \tag{3.78}$$

to write out the Hodge stars

$$*_{10}\,\mathrm{d}a = \mathrm{d}a^{(0)}\,\frac{j^4}{4!} - \mathrm{d}a_0^{(1,1)} \wedge \frac{j^3}{3!} + \big(\mathrm{d}a^{(2,0)} + \mathrm{d}a^{(0,2)}\big) \wedge \frac{j^3}{3!}\,, \tag{3.79}$$

$$*_{10}\,(j \wedge \mathrm{d}a) = 2\,\mathrm{d}a^{(0)}\,\frac{j^3}{3!} - \mathrm{d}a_0^{(1,1)} \wedge \frac{j^2}{2!} + \big(\mathrm{d}a^{(2,0)} + \mathrm{d}a^{(0,2)}\big) \wedge \frac{j^2}{2!}\,, \tag{3.80}$$

$$*_{10}\,\tilde{h}^{(2,2)} = \tilde{h}^{(2,2)} \wedge j - \mathrm{e}^{2\phi}\,\mathrm{d}a^{(0)}\,\frac{j^3}{3!} - 2\,\mathrm{e}^{2\phi}\,\mathrm{d}a_0^{(1,1)} \wedge \frac{j^2}{2!}\,. \tag{3.81}$$

By combining all these results, we find the 10d supersymmetric Lagrangian

$$\begin{aligned}\mathscr{L}_{10}^{\mathrm{SUSY}} = \Delta^{-3}\mathrm{e}^{8\phi}\big(&R_{10} - 80(\partial_\mu\phi)^2 - 12(\partial_\mu \log\Delta)^2 + 62\,\partial_\mu\phi\,\partial^\mu \log\Delta \\ &- \nabla^2(18\,\phi - 7\,\log\Delta)\big) *_{10} 1 + \tfrac{1}{2}\,\Delta^{-3}\mathrm{e}^{8\phi}\,\mathrm{d}j \wedge *_{10}\,\mathrm{d}j\,.\end{aligned} \tag{3.82}$$

Here we also used that $w_4 = j \lrcorner\, \mathrm{d}j = 3\,\mathrm{d}\log\Delta - 8\,\mathrm{d}\phi$.

We reduce this Lagrangian to 9d using the ansätze

$$\begin{aligned}\mathrm{d}s_{10}^2 &= \mathrm{d}r^2 + r^2\eta^2 + r^2\,\mathrm{e}^{-3B-C/3}\,\mathrm{d}s_8^2\,,\\ \mathrm{e}^{2\phi} &= r^{-3}\,\mathrm{e}^{3B+C}\,,\\ \Delta &= r^{-1}\,\mathrm{e}^{B+C}\,,\\ j &= r\,\eta \wedge \mathrm{d}r + r^2\,e^{-3B-C/3}\,J\,,\end{aligned} \tag{3.83}$$

and find (again using $\mathscr{L}_{10} = \mathscr{L}_9 \wedge r^{-2}\mathrm{d}r$)

$$\begin{aligned}\mathscr{L}_9^{\mathrm{SUSY}} = \eta \wedge \Big[&\big(R_8 - \tfrac{3}{2}(\partial_\mu(3B + \tfrac{1}{3}C))^2 - 11\,\mathrm{e}^{-3B-C/3}\big) *_8 1 + 2\,J \wedge *_8\,\mathrm{d}\eta \\ &+ 2\,\mathrm{e}^{-3B-C/3}\,J \wedge *_8 J + \tfrac{1}{2}\,\mathrm{e}^{6B+2C/3}\,\mathrm{d}(\mathrm{e}^{-3B-C/3}\,J) \wedge *_8\,\mathrm{d}(\mathrm{e}^{-3B-C/3}\,J)\Big]\,.\end{aligned} \tag{3.84}$$

We simplify this expression using the supersymmetry conditions

$$\begin{aligned}J \lrcorner\,\mathrm{d}\eta &= \mathrm{e}^{-3B-C/3}\,,\\ W_4 = J \lrcorner\,\mathrm{d}J &= 0\,,\\ R_C &= 2\,\mathrm{e}^{-3B-C/3} - \tfrac{2}{3}\,\Box C\,,\end{aligned} \tag{3.85}$$

as well as the relation between the Ricci and the Chern–Ricci scalar

$$R_C = R_8 + \tfrac{1}{2}\,|\mathrm{d}J|^2\,. \tag{3.86}$$

This yields the surprisingly simple result

$$\begin{aligned}\mathscr{L}_9^{\mathrm{SUSY}} &= \eta \wedge \mathrm{e}^{-3B-C/3} *_8 1 \\ &= \eta \wedge \mathrm{d}\eta \wedge \frac{J^3}{3!}\,.\end{aligned} \tag{3.87}$$

Note that this is the same expression for the 9d supersymmetric action as was obtained in the non-rotating case in [107]. A subtle difference is that $\mathrm{d}\eta \neq \rho$ here, but rather $\rho = \mathrm{d}\eta + \frac{1}{3}\mathrm{d}\mathrm{d}^c C$. However since the forms ρ and $\mathrm{d}\eta$ are in the same cohomology class this distinction does not matter. Observe that

$$\int_{Y_9} \eta \wedge \mathrm{d}\mathrm{d}^c C \wedge \frac{J^3}{3!} = \int_{Y_9} \eta \wedge \left(\mathrm{d}\Big(\mathrm{d}^c C \wedge \frac{J^3}{3!}\Big) + \mathrm{d}^c C \wedge \frac{\mathrm{d}J^3}{3!}\right) = 0\,, \tag{3.88}$$

where the first term equality uses the fact that $J, \mathrm{d}J$ and $\mathrm{d}^c C$ are basic[12] with respect to to the R-symmetry vector ξ, and the second equality follows since the first term is a total derivative and the second vanishes because J is balanced. We conclude that we may replace $\mathrm{d}\eta$ by ρ in expression (3.87) and therefore the integrals for computing the supersymmetric action, and therefore the entropy

$$S_{\mathrm{BH}} = \frac{1}{4G_{11}} \int_{Y_9} \mathscr{L}_9^{\mathrm{SUSY}}\,, \tag{3.89}$$

in both the rotating and non-rotating cases are exactly the same.

Later in section 3.4 we will discuss how one can obtain near-horizon geometries of rotating black strings in Type IIB from the 11d setup considered so far. In anticipation of this, let us reduce the 9d action for geometries on the M-theory side to a 7d action for geometries on the Type IIB side. These 7d geometries can be obtained from the 9d geometries by requiring that the 9d geometry admits a two-torus. By using the ansatz (3.132) we find the supersymmetric Lagrangian for the 7d geometry to be

$$\mathscr{L}_7^{\mathrm{SUSY}} = \eta \wedge \mathrm{d}\eta \wedge \frac{J_{(6)}^2}{2!}\,. \tag{3.90}$$

Let us point out that one can replace $\mathrm{d}\eta$ by $\rho_{(6)}$ in the 7d Lagrangian only when τ is constant. Namely, for a non-trivial axio-dilaton profile the term $\mathrm{d}Q$ appearing in

[12] A form β is basic with respect to ξ if it satisfies both $\xi \lrcorner \beta = 0$ and $\mathcal{L}_\xi \beta = 0$.

(3.136) is only locally exact, and therefore cannot be interpreted as a total derivative term as was the case for the $\mathrm{d}\mathrm{d}^c C$ term. As studied in [114] it is more convenient to view these near-horizon geometries from an 11d perspective rather than a 10d one. The central charge of the dual 2d SCFT is given by

$$c = \frac{3}{(2\pi)^6 \mathrm{g}_s^2 \ell_s^8} \int_{Y_7} \eta \wedge \mathrm{d}\eta \wedge \frac{J_{(6)}^2}{2!} \,. \tag{3.91}$$

3.3 Embedding of the AdS$_4$ Kerr–Newman black hole

Here we study the embedding of the supersymmetric limit of the AdS$_4$ Kerr–Newman (KN) black hole solution found in [135] and further studied in [136, 137] into our classification by using the uplift of minimal gauged supergravity on an arbitrary 7d Sasaki–Einstein manifold. Note that we could have taken one out of the zoo of supersymmetric rotating AdS$_4$ solutions, e.g. [130, 138–140]. We choose the KN solution since it is the simplest yet contains all the necessary ingredients. Note that the Kerr–Newman black hole is one of two classes of possible black holes [141], the other being the magnetic black holes. We have checked that an example of the second class also fits into the classification however we will not present the results here.[13] In future work we will investigate how the 11d solution differentiates between the two classes of solution in 4d.

3.3.1 Kerr–Newman solution

We begin by first considering the black hole in four dimensions before studying the full eleven-dimensional solution. The four-dimensional black hole is given by

$$\begin{aligned} \mathrm{d}s^2 &= -\frac{\Delta_r}{W}\left(\mathrm{d}t - \frac{\gamma \sin^2\theta}{\Xi}\mathrm{d}\phi\right)^2 + W\left(\frac{\mathrm{d}r^2}{\Delta_r} + \frac{\mathrm{d}\theta^2}{\Delta_\theta}\right) + \frac{\Delta_\theta \sin^2\theta}{W}\left(\gamma \mathrm{d}t - \frac{\tilde{r}^2+\gamma^2}{\Xi}\mathrm{d}\phi\right)^2, \\ A &= \frac{2m\tilde{r}\sinh^2\delta}{W}\left(\mathrm{d}t - \frac{\gamma\sin^2\theta}{\Xi}\mathrm{d}\phi\right) + \alpha_{\text{gauge}}\mathrm{d}t \,, \end{aligned} \tag{3.92}$$

[13] We thank K. Hristov and S. Hosseini for discussions on this point.

where

$$\begin{aligned} \tilde{r} &= r + 2m\sinh^2\delta\,, \\ \Delta_r &= r^2 + \gamma^2 - 2mr + \tilde{r}^2(\tilde{r}^2+\gamma^2)\,, \\ \Delta_\theta &= 1 - \gamma^2\cos^2\theta\,, \\ W &= \tilde{r}^2 + \gamma^2\cos^2\theta\,, \\ \Xi &= 1-\gamma^2\,. \end{aligned} \tag{3.93}$$

The solution is characterised by three constants (γ, δ, m) whilst the parameter α_{gauge} is related to a pure gauge transformation and is therefore not a parameter of the solution. The solution describes a non-extremal black hole provided that $\gamma^2 < 1$ and m is bounded from below. The exact value of the bound is not important for our purposes, but it is derived in [142]. Without loss of generality we have $m, \delta, \gamma > 0$. The black hole is characterized by its energy E, electric charge Q and momentum J:

$$E = \frac{m}{G_{(4)}\Xi^2}\cosh 2\delta\,, \qquad Q = \frac{m}{G_{(4)}\Xi}\sinh 2\delta\,, \qquad J = \frac{m\gamma}{G_{(4)}\Xi^2}\cosh 2\delta\,. \tag{3.94}$$

The Bekenstein-Hawking entropy of the black hole can be found by computing the area of the outer horizon, resulting in

$$S = \left.\frac{\pi(\tilde{r}^2+\gamma^2)}{G_{(4)}\Xi}\right|_{r=r_+}\,, \tag{3.95}$$

where r_+ denotes the largest positive root of $\Delta_r = 0$, and therefore describes the location of the outer horizon. For arbitrary values of the parameters (γ, δ, m), the black hole is neither extremal nor supersymmetric. The BPS limit is defined by first imposing supersymmetry and then extremality. The supersymmetry is attained by imposing

$$\mathrm{e}^{4\delta} = 1 + \frac{2}{\gamma}\,. \tag{3.96}$$

The solution is now supersymmetric but not extremal, in fact it has timelike closed curves and a naked singularity. To remedy this and obtain an extremal black hole we further identify

$$m = \gamma(1+\gamma)\sqrt{2+\gamma}\,. \tag{3.97}$$

There is now only a single parameter left in the theory, namely γ. With these identifications the function Δ_r acquires a double root at

$$r^* = \gamma\sqrt{2+\gamma}\left(1+\gamma-\sqrt{\gamma(2+\gamma)}\right)\,, \tag{3.98}$$

with the other two roots becoming complex.

3.3.2 Near-horizon limit

We now want to take the near-horizon limit of the solution. It is convenient through a change of coordinates to shift the double root location in Δ_r to 0 and to rewrite the function as

$$\Delta_r = \rho^2 f(\rho)\,, \quad f(\rho) = (\rho + r^* - r^-)(\rho + r^* - r^+)\,, \tag{3.99}$$

where

$$\rho = r - r^*\,. \tag{3.100}$$

Since we will need to evaluate the function f at the horizon often, we note that

$$f(0) = 1 + \gamma\,(6 + \gamma)\,. \tag{3.101}$$

In the metric, the change of the r to ρ coordinate results only in changes in the functions (3.93), since the $\mathrm{d}r$ term is invariant. To simplify notation we will therefore shift the functions such that an argument of 0 means we evaluate at the horizon. In particular we now take

$$\tilde{r}(\rho) = \rho + r^* + 2m\sinh^2\delta\ , \tag{3.102}$$

such that $\tilde{r}(0)$ is evaluating the function $\tilde{r}$ at the horizon. Similarly $W(0,\theta)$ evaluates W at the horizon; for notational convenience we denote the functions $W(0,\theta) = W(\theta)$ and $f(0) = f_0$. Furthermore, in the BPS limit one can derive that $\tilde{r}(0) = \sqrt{\gamma}$. To take the near-horizon limit we perform the change of coordinates

$$\rho \to \epsilon\rho\,, \quad t \to \frac{t}{\epsilon}\,, \quad \phi \to \phi + \frac{\beta t}{\epsilon}\,, \tag{3.103}$$

where β is a constant that we will determine shortly an then send $\epsilon \to 0$. The near-horizon limit is now obtained by taking $\epsilon \to 0$ after making the above substitutions. The $\mathrm{d}\theta^2$ term will clearly be sent to $W(\theta)/\Delta_\theta$, and we can ignore this term for time being. We find

$$\begin{aligned}
\frac{\Delta_r}{W(r,\theta)}\left(\mathrm{d}t - \frac{\gamma\sin^2\theta}{\Xi}\mathrm{d}\phi\right)^2 &\to \frac{\rho^2 f_0}{W(\theta)}\left(1 - \frac{\beta\gamma\sin^2\theta}{\Xi}\right)^2\mathrm{d}t^2\,,\\
\frac{W(r,\theta)}{\Delta_r}\mathrm{d}r^2 &\to \frac{W(\theta)}{f_0}\frac{\mathrm{d}\rho^2}{\rho^2}\,,\\
\frac{\Delta_\theta\sin^2\theta}{W(r,\theta)}\left(\gamma\mathrm{d}t - \frac{\tilde{r}^2+\gamma^2}{\Xi}\mathrm{d}\phi\right)^2 &\to \frac{\Delta_\theta\sin^2\theta}{W(\theta)}\left[\frac{\mathrm{d}t}{\epsilon}\left(\gamma - \frac{\tilde{r}(\epsilon\rho)^2+\gamma^2}{\Xi}\beta\right) - \frac{\gamma+\gamma^2}{\Xi}\mathrm{d}\phi\right]^2\,.
\end{aligned} \tag{3.104}$$

In the last line we can expand $\tilde{r}(\epsilon\rho) \sim \sqrt{\gamma} + \epsilon\rho\tilde{r}'(0) + \mathcal{O}(\epsilon^2)$, resulting in a term which diverges as ϵ^{-1}, proportional to the constant

$$1 - \frac{1+\gamma}{\Xi}\beta\,. \tag{3.105}$$

The existence of this term is the reason we introduced the shift in the ϕ coordinate, and it can be set to zero by fixing the constant β in the shift as

$$\beta = \frac{\Xi}{1+\gamma}\,. \tag{3.106}$$

Including this factor of β we can combine the results from above and write down the final result for the near-horizon solution

$$\begin{aligned} \mathrm{d}s^2|_{\mathrm{NH}} = \frac{W(\theta)}{f_0}\Big(-\rho^2\mathrm{d}t^2 + \frac{\mathrm{d}\rho^2}{\rho^2}\Big) \\ + \frac{W(\theta)}{\Delta_\theta}\mathrm{d}\theta^2 + \frac{\sin^2\theta\,\Delta_\theta}{W(\theta)}\Big(\frac{\gamma+\gamma^2}{\Xi}\Big)^2\Big(\mathrm{d}\phi + \frac{2\sqrt{\gamma}\,\Xi}{(1+\gamma)f_0}\,\rho\,\mathrm{d}t\Big)^2\,, \end{aligned} \tag{3.107}$$

where, in order to make the AdS_2 factor manifest, we rescaled the time-coordinate

$$t \to \frac{\gamma(1+\gamma)}{f_0}t\,. \tag{3.108}$$

Consider now the gauge field. Performing the same near-horizon limit and imposing the BPS limit, we find a divergent term in the gauge field, proportional to

$$\frac{dt}{\epsilon}(\alpha_{\mathrm{gauge}} - 2)\,. \tag{3.109}$$

This term is purely gauge and we can remove it without problem by making a suitable choice for the gauge parameter. The resulting near-horizon vector field is

$$A|_{\mathrm{NH}} = \frac{2\sqrt{\gamma}\,(1+\gamma)}{W(\theta)}\Big(\frac{2\gamma - W(\theta)}{f_0}\rho\,\mathrm{d}t + \frac{\gamma\sqrt{\gamma}\sin^2\theta}{\Xi}\mathrm{d}\phi\Big)\,, \tag{3.110}$$

where of course the time coordinate has been rescaled with the same factor (3.108) as in the metric.

3.3.3 Uplift to 11d

Now that we have derived the near-horizon metric and gauge field of the AdS_4 KN solution in minimal supergravity we can consider the uplift to 11d supergravity.

The uplift of the metric and flux to eleven dimensions are given by

$$\begin{aligned} \mathrm{d}s_{11}^2 &= \mathrm{d}s_4^2 + \left(\eta + \tfrac{1}{4}A\right)^2 + \mathrm{d}s_6^2\,, \\ \mathcal{G}_4 &= \frac{3}{8}\,\mathrm{dvol}(\mathrm{AdS}_4) - \frac{1}{4}\star_4 F\wedge J\,, \end{aligned} \tag{3.111}$$

where $F = dA$ is the field strength of A, $\mathrm{d}s_4^2$ is the near-horizon metric we just derived in (3.107) and $\mathrm{d}s_6^2$ is the base of the Sasaki-Einstein manifold with $\eta = \mathrm{d}z+\sigma$ dual to the Reeb-vector ∂_z. The conventions are chosen such that $\mathrm{d}\eta = 2J$, where J is the Kähler form on $\mathrm{d}s_6^2$.

We now want to rewrite the metric and flux appearing in (3.111) in the form of our classification as presented in section 3.1.3. To recover this form, we write the metric in (3.111) such that it becomes a time-fibration over a base. It is also necessary to perform some coordinate redefinitions

$$\begin{aligned} z &\to \frac{\gamma\,(3+\gamma)}{2\,f_0}\,z\,, \\ \phi &\to \phi - \frac{\Xi}{f_0}\,z\,. \end{aligned} \tag{3.112}$$

After completing the straightforward but tedious rotations of the vielbeins and shifting the coordinates, the metric we find is of the following form

$$\mathrm{d}s_{11}^2 = \mathrm{e}^{2B}\Big[-\frac{\mathrm{e}^{2C}}{r^2}(\mathrm{d}t+a)^2 + \frac{\mathrm{d}r^2}{r^2} + \eta^2 + Y(\theta)\,\mathrm{D}\phi^2 + \frac{f_0}{\Delta_\theta}\,\mathrm{d}\theta^2 + \mathrm{e}^{-2B}\mathrm{d}s_6^2\Big]\,. \tag{3.113}$$

We will now clarify the several notational conventions used in this metric. Firstly, we have renamed the coordinate ρ to r, in order to conform with the conventions of the classification. We have also introduced the function Y, $\mathrm{D}\phi$ and redefined η as

$$\begin{aligned} Y(\theta) &= \frac{\gamma^2\,(3+\gamma)^2\,f_0\,(1-\gamma^2\cos^2\theta)\,\sin^2\theta}{\Xi^2\cos^2\theta\,(2\gamma+W(\theta))^2}\,, \\ \mathrm{D}\phi &= \mathrm{d}\phi + \frac{2\,\Xi}{\gamma\,(3+\gamma)}\,\sigma\,, \\ \eta &= \mathrm{d}z + \frac{2\,f_0}{\gamma\,(3+\gamma)}\,\sigma + \frac{f_0\,(\gamma\sin\theta)^2}{\Xi\,(2\gamma+W(\theta))}\,\mathrm{D}\phi\,. \end{aligned} \tag{3.114}$$

Note that the coordinate shift we made in (3.112) was necessary to ensure that the metric ends up with $\mathrm{d}z^2$, with its coefficient being exactly equal to one. The

scalars e^C and e^B are found to be

$$\mathrm{e}^C = \frac{\gamma(1+\gamma)\,\cos\theta\,\left(W(\theta)+2\gamma\right)}{W(\theta)\sqrt{f_0\,W(\theta)}}\,, \tag{3.115}$$

$$\mathrm{e}^B = \sqrt{\frac{W(\theta)}{4\,f_0}}\,. \tag{3.116}$$

Recall that these scalars can also be used to compute Δ in (3.20). The last remaining puzzle-piece in the metric is the fibration a, which is given by

$$a = \sqrt{\gamma}\,r\left(\frac{2\,\gamma^2\cos^2\theta-\gamma^2-1}{(1+\gamma)\,\left(W(\theta)+2\gamma\right)}\,\eta + \frac{\gamma\,(3+\gamma)\,\tan^2\theta\,(\gamma^2\,\cos^2\theta-1)f_0}{(1+\gamma)\,\Xi\,\left(W(\theta)+2\gamma\right)^2}\,\mathrm{D}\phi\right)\,. \tag{3.117}$$

The fibration is of the expected form $a = r(\alpha\,\eta + A)$, and this specification of a completes the endeavour of writing the metric in the classification form. Now we can move on to consider the flux; recall that in the classification we wrote it as

$$\begin{aligned}\mathcal{G}_4 &= -\mathrm{d}\left((\mathrm{d}t+a)\wedge\mathrm{e}^{2\phi}j\right)+\tilde{h}^{(2,2)}\,,\\ \tilde{h}^{(2,2)} &= \mathrm{d}c_3\,.\end{aligned} \tag{3.118}$$

We have already found the fibration a in (3.117) and $\mathrm{e}^{2\phi}$ is given in terms of the scalars e^B and e^C, by making use of (3.20). The ten-dimensional complex structure form j can be found from the vielbeins of the metric we found in (3.113). Our remaining tasks thus consists of finding an expression for $\tilde{h}^{(2,2)}$, which in its turn is determined by the potential c_3. The only form we have thus not yet specified is the potential c_3. After carefully rewriting the flux we obtain from (3.111), the resulting potential is given by

$$\begin{aligned}c_3 = \frac{\gamma^2\sqrt{\gamma}\,(3+\gamma)}{8\,\Xi\,\left(2\gamma+W(\theta)\right)}\Bigg(&\sin\theta\,\mathrm{d}\theta\wedge\eta\wedge\mathrm{D}\phi+\frac{(3+\gamma)(2\gamma-W(\theta))}{\gamma\,\Xi\,\cos\theta}\,\mathrm{D}\phi\wedge\mathrm{d}(\mathrm{D}\phi)\\ &+\frac{\sin^2\theta\,(2\gamma-W(\theta))}{r\,f_0\,\gamma\cos\theta}\,\mathrm{d}r\wedge\mathrm{D}\phi\wedge\eta\Bigg)\,.\end{aligned} \tag{3.119}$$

From the above expression we can immediately determine that all components of the flux in (3.29) are turned on. Having obtained the potential, and thus its field strength, we have completed our mission of embedding the AdS_4 black hole solution into the classification. We have checked that the solution satisfies all the conditions of our classification, which is a non-trivial check of the correctness of our results.

Another useful way to write the metric consists of explicitly showing the AdS_2 factor we also obtained in (3.107), which will allow us to read off the values of the

near-horizon angular velocities, denoted by k^i. These k^i are needed to define the killing vectors, over which we should integrate to find the angular momentum of the black hole. To obtain the particular form of the metric, we undo the rotation of the vielbeins (or simply do not rotate them in the first place). Instead of the time-fibration we then find a metric reminiscent of the one written in (3.162)

$$\begin{aligned} \mathrm{d}s^2 = \mathrm{e}^{2B}\left(-r^2\mathrm{d}t^2 + \frac{\mathrm{d}r^2}{r^2}\right) + \gamma_{\theta\theta}\,\mathrm{d}\theta^2 + \mathrm{d}s_6^2 \\ + \gamma_{\mu\nu}\left(\mathrm{d}\psi^\mu + M^\mu(\theta)\,\sigma + k^\mu r\mathrm{d}t\right)\left(\mathrm{d}\psi^\nu + M^\nu(\theta)\,\sigma + k^\nu r\mathrm{d}t\right), \end{aligned} \tag{3.120}$$

where the AdS$_2$ is now clearly visible. As before, $\mathrm{d}s_6$ denotes the base of the Sasaki-Einstein manifold and the one-form σ is still defined on the Kähler-Einstein space $\mathrm{d}s_6$ such that $\mathrm{d}\sigma = 2J$. Apart from these already familiar notions we established several new notational conventions; first of all we have introduced $\gamma_{\theta\theta}$ and $M^\mu(\theta)$ as

$$\gamma_{\theta\theta} = \frac{W(\theta)}{4\,\Delta_\theta}\,, \tag{3.121}$$

$$M^z = \frac{2\,f_0}{\gamma\,(3+\gamma)}\,, \tag{3.122}$$

$$M^\phi = \frac{2\,\Xi}{\gamma\,(3+\gamma)}\,. \tag{3.123}$$

Besides these coefficients we introduced indices $\mu, \nu \in \{z, \phi\}$, along with a metric $\gamma_{\mu\nu}$ we will specify below and, finally, defined $\mathrm{d}\psi$ as

$$\mathrm{d}\psi^\mu = (\mathrm{d}z,\, \mathrm{d}\phi)\,. \tag{3.124}$$

The metric (3.120) shows that only the ϕ and z coordinates are gauged over the AdS$_2$ space. We could have expected this, since the original AdS$_4$ black hole had rotation only in the ϕ direction, and in (3.111) we have gauged the Reeb-vector with respect to the four-dimensional gauge vector. The metric, $\gamma_{\mu\nu}$, we introduced for these two coordinates has the following components

$$\gamma_{zz} = \kappa^2 - \frac{\gamma^2\,(1+\gamma)\sin^2\theta}{f_0\,W(\theta)}\left(\kappa - \frac{\gamma\,(1+\gamma)\,N(\theta)}{4\,f_0\,W(\theta)}\right), \tag{3.125}$$

$$\gamma_{z\phi} = \frac{\gamma^2\,(1+\gamma)\,\sin^2\theta}{2\,\Xi\,W(\theta)}\left(\kappa - \frac{\gamma\,(1+\gamma)\,N(\theta)}{2\,f_0\,W(\theta)}\right), \tag{3.126}$$

$$\gamma_{\phi\phi} = \frac{\gamma^3\,(1+\gamma)^2\,\sin^2\theta\,N(\theta)}{4\,\Xi^2\,W(\theta)^2}\,, \tag{3.127}$$

where, to alleviate the notational clutter, we have introduced the constant κ and the function $N(\theta)$ as

$$\begin{aligned} \kappa &= \frac{\gamma\,(3+\gamma)}{2\,f_0}\,, \\ N(\theta) &= 1+\gamma-\gamma^2\cos^2\theta-\gamma^3\,\cos^4\theta\,. \end{aligned} \tag{3.128}$$

Now that we have specified the $\gamma_{\mu\nu}$ in (3.120), the description of the metric is almost complete. The last remaining unknowns are the constants k^i which specify the gauging over the AdS_2. We find

$$k^z = k^\phi = \frac{1-\gamma}{\sqrt{\gamma}\,(3+\gamma)}\,. \tag{3.129}$$

Note that the precise value of k^ϕ depends on how we scale the ϕ coordinate; the fact that both k^i are equal arises due to our conventions for the coordinates. Since the above k^i are the only non-zero ones, it follows that the AdS_4 black hole rotates only in the z and ϕ directions. We can now check the identifications (3.62) and (3.63). In order to do this we need to compute the scalars w_i and x_i appearing in (3.59) and (3.60) for our solution. For simplicity we use the basis of Killing vectors $\{z,\phi,\psi_1,\psi_2,\psi_3\}$, with the $\psi_{1,2,3}$ the Killing vectors of the 6d Kähler-Einstein base of the Sasaki–Einstein space. In the following we need only compute the scalars for z and ϕ since the solution only rotates in the z and ϕ directions. We find

$$\begin{aligned} x_\phi &= -\frac{\gamma^{5/3}(3+\gamma)(1+\gamma)^{1/3}(3+\gamma\cos^2\theta)^{1/3}}{8\Xi f_0^{2/3}}\,, & x_z &= 0\,, \\ w_\phi &= \frac{\gamma f_0\sin^2\theta}{2\Xi(3+\gamma\cos^2\theta)}\,, & w_z &= \frac{1}{2}\,. \end{aligned} \tag{3.130}$$

It is then a simple matter of substituting these and the constants k^i found in (3.129) to see that both (3.62) and (3.63) are satisfied. Moreover using the results of section 3.2.2 and appendix 3.B we can compute the entropy. With a little care in the definitions of the periods it follows that the integral (3.89) is the same as (3.95) and therefore this serves as another consistency check of our identification of the entropy and the supersymmetric action in (3.89).

3.4 Black strings in Type IIB

Having studied our 11d setup we now turn our attention to rotating black string solutions in Type IIB supergravity. We take our 11d setup and require that the

internal space admits a two-torus, T^2. The 8d balanced manifold then breaks up as a semidirect product of this torus and a 6d manifold. Wherever 8d quantities split up in components on the torus and the 6d manifold, we simply denote this with the subscripts (2) and (6). Under this assumption of a torus in the internal space we can apply dualities to arrive in Type IIB, where we find a classification of rotating black string solutions that can be interpreted as rotating D3-branes wrapped on a Riemann surface.

If we add a warp factor acting homogeneously on the torus, the balanced condition of the 8d manifold implies that the 6d manifold is conformally balanced. For simplicity we do not take into account such a warping which gives a balanced 6d manifold. As such we take the metric ansatz

$$\begin{aligned} \mathrm{d}s_{11}^2 = \mathrm{e}^{2B}\Big[&- \mathrm{e}^{2C}\Big(\frac{\mathrm{d}t}{r} + \alpha\eta + A_{(6)} + A_{(2)}\Big)^2 + \frac{\mathrm{d}r^2}{r^2} + \eta^2 \\ &+ \mathrm{e}^{-3B-C/3}\Big(\mathrm{d}s_6^2 + \frac{1}{\tau_2}(\mathrm{d}x + \tau_1 \mathrm{d}y)^2 + \tau_2 \mathrm{d}y^2\Big)\Big] , \end{aligned} \tag{3.131}$$

where τ_1 and τ_2 are scalars valued on the 6d base and the complex combination $\tau = \tau_1 + \mathrm{i}\tau_2$ is a holomorphic function ($\bar{\partial}\tau = 0$). In principle we can take the two U(1)'s of the two-torus to be fibered over AdS_2, i.e. in the language of appendix 3.B we can introduce constants k^x, k^y which are related to the angular momenta in these directions. However, introducing these parameters leads to the system becoming unreasonably complicated[14] once we arrive in Type IIB, and therefore we shall just proceed with these parameters set to zero, which in (3.131) implies that $A_{(2)} = 0$. In addition, we also assume that η has no dependence on the T^2. The final piece of the solution we need to specify is the dependence of the flux on the torus: we take $\tilde{h}^{(2,2)}$ to have no legs along the torus directions.[15] Note that this is consistent with setting the rotation of the solution along the torus directions to zero, through the condition (3.18). In addition to this, we assume that the scalars

[14] In Type IIB these extra parameters will lead to a further warping of the metric. In particular, the dilaton will not be simply the dilaton one would get from the F-theory picture, i.e. τ_2^{-1}. In addition, since we must satisfy (3.18) it is clear that turning these on will lead to turning on additional fluxes other than the self-dual five-form in Type IIB. It would be interesting to fully work out the details of this more general case, but it deserves more than this small section in this chapter and a full treatment of the most general construction.

[15] The primitive piece of this part of flux (with legs on the torus) will give rise to a transgression term like in [118, 143]. Again for our purposes such a term is an unnecessary complication, and so we set it to zero here, although it is certainly interesting to consider.

B, C are independent of the torus coordinates, and are hence defined on the 6d base.

We now reduce the 8d conditions from section 3.1.3 with this assumption of a torus in the internal space onto a set of conditions on the inherited 6d base space that has an SU(3) structure. We decompose the two-form as

$$J = J_{(6)} + J_{(2)}\,, \qquad J_{(2)} = \mathrm{d}x \wedge \mathrm{d}y\,, \tag{3.132}$$

which (using (3.34)) implies that $J_{(6)}$ is a balanced two-form: $\mathrm{d}J^2_{(6)} = 0$. Furthermore from (3.35) we find that

$$\mathrm{d}\eta \wedge \frac{J^2_{(6)}}{2!} = \mathrm{e}^{-3B-C/3}\,\frac{J^3_{(6)}}{3!}\,, \tag{3.133}$$

which implies $J_{(6)} \lrcorner\, \mathrm{d}\eta = \mathrm{e}^{-3B-C/3}$. We write the holomorphic four-form as

$$\Omega = \Omega_{(6)} \wedge \Omega_{(2)}\,, \qquad \Omega_{(2)} = \frac{1}{\sqrt{\tau_2}}\big(\mathrm{d}x + \tau \mathrm{d}y\big)\,. \tag{3.134}$$

From (3.37) it now follows that

$$\mathrm{d}\Omega_{(6)} = \mathrm{i}\big(P + \tfrac{1}{3}\mathrm{d}^c C - Q\big) \wedge \Omega_{(6)}\,, \tag{3.135}$$

where $Q = -\frac{1}{2\tau_2}\mathrm{d}\tau_1$ and we have used the holomorphicity of τ. This gives us the Ricci form on the 6d space as

$$\rho_{(6)} = \mathrm{d}\eta + \tfrac{1}{3}\mathrm{d}\mathrm{d}^c C - \mathrm{d}Q\,, \tag{3.136}$$

which is the generalization of equation (2.57) of [126] to the rotating case. The additional term changes the expression for the Chern–Ricci scalar to

$$R_{C(6)} = 2\mathrm{e}^{-3B-C/3} - \tfrac{2}{3}\Box_6 C + \frac{1}{2\tau_2^2}\,|\mathrm{d}\tau|^2\,. \tag{3.137}$$

With our ansatz the 8d Bianchi identities (3.45) for the fluxes $H^{(p,q)}$ remain the same but should be understood as 6d conditions. The expansions of these fluxes as in (3.55) require slight modifications in the numerical coefficients but are otherwise the same after the replacement $J \to J_{(6)}$. From reducing the Maxwell equations (3.48 – 3.51) we find

$$\begin{aligned}
-\mathrm{d}\star_6 \mathrm{d}\mathrm{e}^{-3B-C} + \mathrm{e}^{-2C/3}\mathrm{d}\eta \wedge \mathrm{d}\eta \wedge J_{(6)} &= 0\,,\\
\mathrm{d}\eta \wedge \mathrm{d}(\mathrm{e}^{-2C/3} J_{(6)}) &= 0\,,\\
\mathrm{d}\mathrm{d}^c(\mathrm{e}^{-2C/3} J_{(6)}) &= 0\,,\\
\mathrm{d}\star_6 \mathrm{d}\mathrm{e}^{-2C/3} &= H^{(2,2)} \wedge H^{(1,1)} + 2\mathrm{i}H^{(2,1)} \wedge H^{(1,2)}\,.
\end{aligned} \tag{3.138}$$

We can now proceed by reducing along the A-cycle $(\mathrm{d}x+\tau_1\mathrm{d}y)$ of the torus to Type IIA supergravity. Note that the Ricci form is independent of the T^2-coordinates and therefore so is the one-form η. This leads to a standard reduction of 11d supergravity to massless Type IIA. One finds that the metric in string frame is given by

$$\begin{aligned}\mathrm{d}s^2_{\mathrm{IIA}} = \mathrm{e}^{2B+2\phi_{\mathrm{IIA}}/3}\Big[&- \mathrm{e}^{2C}\Big(\frac{\mathrm{d}t}{r}+\alpha\eta+A_{(6)}\Big)^2+\frac{\mathrm{d}r^2}{r^2}+\eta^2\\ &+\mathrm{e}^{-3B-C/3}\big(\mathrm{d}s_6^2+\tau_2\mathrm{d}y^2\big)\Big]\,,\end{aligned} \tag{3.139}$$

and is supplemented by

$$\mathrm{e}^{4\phi_{\mathrm{IIA}}/3} = \frac{1}{\tau_2}\mathrm{e}^{-B-C/3}\,, \tag{3.140}$$

$$C_1^{\mathrm{IIA}} = \tau_1\mathrm{d}y\,, \tag{3.141}$$

$$C_3^{\mathrm{IIA}} = c_3-\mathrm{e}^{3B+C}\Big(\frac{\mathrm{d}t}{r}+\alpha\eta+A_{(6)}\Big)\wedge\Big(\eta\wedge\frac{\mathrm{d}r}{r}+\mathrm{e}^{-3B-C/3}J_{(6)}\Big)\,, \tag{3.142}$$

$$B_2^{\mathrm{IIA}} = \mathrm{e}^{2C/3}\Big(\frac{\mathrm{d}t}{r}+\alpha\eta+A_{(6)}\Big)\wedge\mathrm{d}y\,. \tag{3.143}$$

Recall that we can decompose the 11d gauge potential as (3.72), where c_3 is the potential corresponding to $\tilde{h}^{(2,2)}$, and $c_2=\mathrm{e}^{2\phi}j$ is fixed by supersymmetry.

By performing a T-duality along the y-direction we land in Type IIB. The metric in Einstein frame reads

$$\begin{aligned}\mathrm{d}s^2_{\mathrm{IIB}} = \mathrm{e}^{3B/2-C/6}\Big[&- \mathrm{e}^{2C}\Big(\frac{\mathrm{d}t}{r}+\alpha\eta+A_{(6)}\Big)^2+\mathrm{e}^{2C/3}\Big(\mathrm{d}y+\mathrm{e}^{2C/3}\Big(\frac{\mathrm{d}t}{r}+\alpha\eta+A_{(6)}\Big)\Big)^2\\ &+\frac{1}{r^2}\Big(\mathrm{d}r^2+r^2\big(\eta^2+\mathrm{e}^{-3B-C/3}\,\mathrm{d}s_6^2\big)\Big)\Big]\,.\end{aligned} \tag{3.144}$$

Here we have made explicit a cone in the geometry. It is useful to redefine the scalar B in the form $B=-\widetilde{B}/3+C/9$ which puts the metric in the form

$$\begin{aligned}\mathrm{d}s^2_{\mathrm{IIB}} = \mathrm{e}^{-\widetilde{B}/2}\Big[&- \mathrm{e}^{2C}\Big(\frac{\mathrm{d}t}{r}+\alpha\eta+A_{(6)}\Big)^2+\mathrm{e}^{2C/3}\Big(\mathrm{d}y+\mathrm{e}^{2C/3}\Big(\frac{\mathrm{d}t}{r}+\alpha\eta+A_{(6)}\Big)\Big)^2\\ &+\frac{\mathrm{d}r^2}{r^2}+\eta^2+\mathrm{e}^{\widetilde{B}-2C/3}\,\mathrm{d}s_6^2\Big]\,.\end{aligned} \tag{3.145}$$

If we take $C=\alpha=A_{(6)}=0$, the first line gives precisely the metric for AdS_3 written as a U(1) fibration over AdS_2. The effect of a non-trivial scalar C and connection pieces $\alpha, A_{(6)}$ is to make the black string rotate. Note that this is precisely the form of the near-horizon of the black string found in [123] uplifted to

a 10d solution of Type IIB. The fluxes consist of an axio-dilaton and five-form flux given by

$$\begin{aligned} C_0^{\rm IIB} + {\rm i}{\rm e}^{-\phi_{\rm IIB}} &= \tau_1 + {\rm i}\tau_2\,, \\ F_5^{\rm IIB} &= (1+\star_{10})\,{\rm d}\Big[c_3 \wedge \Big({\rm d}y + {\rm e}^{2C/3}\Big(\frac{{\rm d}t}{r} + \alpha\eta + A_{(6)}\Big)\Big) \\ &\quad - {\rm e}^{-\widetilde{B}+4C/3}\Big(\frac{{\rm d}t}{r} + \alpha\eta + A_{(6)}\Big) \wedge \Big(\eta \wedge \frac{{\rm d}r}{r} + {\rm e}^{\widetilde{B}-2C/3} J_{(6)}\Big) \wedge {\rm d}y\Big]\,. \end{aligned} \tag{3.146}$$

Having given the metric and fluxes we now specify the supersymmetry conditions that the geometry must satisfy. These can be derived from the 11d supergravity ones by reducing them on the torus. Note that the cone appearing in the metric in (3.144) has an SU(4) structure which is inherited from the SU(5) structure of our 11d solutions. We denote the corresponding two-form by $j_{(8)}$, and we can decompose it as

$$j_{(8)} = r\eta \wedge {\rm d}r + r^2 {\rm e}^{\widetilde{B}-2C/3}\, J_{(6)}\,, \tag{3.147}$$

where $J_{(6)}$ is the two-form that we found in the decomposition (3.132). This two-form corresponds to the balanced SU(3) structure of the 6d space. On this SU(3) structure, we previously found the conditions:

$$ {\rm d}J_{(6)}^2 = 0\,, \tag{3.148}$$

$$ {\rm d}\Omega_{(6)} = {\rm i}\big(P + \tfrac{1}{3}{\rm d}^c C - Q\big) \wedge \Omega_{(6)}\,. \tag{3.149}$$

The geometry must in addition satisfy the Bianchi identities and Maxwell equations that we discussed earlier in this section subject to the potential c_3 satisfying

$$ j_{(8)} \lrcorner\, {\rm d}c_3 = 2r^{-3}{\rm e}^{-\widetilde{B}+4C/3}{\rm d}a^{(1,1)}\,. \tag{3.150}$$

The first of the Maxwell equations (3.138) is the master equation, which can be rewritten as

$$\begin{aligned} &{\rm e}^{2C/3}\,\Box_6\big({\rm e}^{-2C/3}\big(R_{C(6)} + \tfrac{2}{3}\Box_6 C - \tfrac{1}{2\tau_2^2}\,|{\rm d}\tau|^2\big)\big) + 2\big|\rho_{(6)} - \tfrac{1}{3}{\rm d}{\rm d}^c C + {\rm d}Q\big|^2 \\ &- \tfrac{1}{2}\big(R_{C(6)} + \tfrac{2}{3}\Box_6 C - \tfrac{1}{2\tau_2^2}\,|{\rm d}\tau|^2\big)^2 \;=\; 0\,. \end{aligned} \tag{3.151}$$

Note that the master equation is independent of the fluxes here. Further, notice that the conditions reduce to those of [125] if one sets $C = \alpha = A_{(6)} = c_3 = 0$.

The solutions in this classification may be interpreted as the near-horizon geometries of rotating black strings. When one inserts a Riemann surface into the balanced 6d

base it is natural to interpret these as arising from the compactification of rotating D3-branes on the Riemann surface. Moreover, this is not the most general setup that can be considered and it would be interesting to further investigate extensions. A possible method for doing this is to reduce the 11d setup studied here on a torus which is also fibered over the AdS_2, as we alluded to at the beginning of this section. This will necessarily lead to two free constants in the Type IIB solution and also to more general fluxes. However, such solutions are far more involved than the ones presented in this section.

3.5 Conclusions and future directions

In this chapter we studied the geometry of supersymmetric solutions which may be interpreted as the near-horizon of rotating black holes and strings embedded in 11d supergravity and Type IIB respectively. This generalizes the results of [117] and [125]. Due to the generality of our ansatz the black holes covered by our classification can include both electric and magnetic flavour fluxes and angular momentum when viewed from 4d. Note that this does not translate into magnetic fluxes in 11d but rather into fibrations of the manifold.[16] Similar statements apply for the 5d black strings in Type IIB that we considered.

One natural extension of our work is to consider a more general classification of the black strings in Type IIB. In performing the duality chain we aimed for a simplified solution consisting of only five-form flux and axio-dilaton. One could in fact include a complex three-form flux in the setup. This may be achieved from 11d by allowing the flux components of $\tilde{h}^{(2,2)}$ to have legs along the torus directions. The minimal extension would be adding in a transgression term of the form discussed in [118], however we expect that one can be more general by also allowing for rotation along the T^2-directions. A preliminary analysis showed that this case is rather involved with all fluxes turned on and a non-holomorphic axio-dilaton. For the sake of presentation we have given only the simpler case.

It would be interesting to formulate an extremization principle for these geometries along the lines of [107]. This seems quite challenging though there are glimpses of hope. The entropy of the black hole and string can be seen to be given by the same

[16] The role of baryonic symmetries is slightly more mysterious but we believe that these should also be covered by our work.

formula as in the non-rotating case. In particular the actions presented in section 3.2.2 reduce to simple integrals (3.89) and (3.91) which can easily be computed in the toric case. The difficulty arises in evaluating the integrals which impose flux quantisation. One should be able to compare with the field theory results in [122, 123] for rotating black holes and black strings. We have preliminary results on this extremization problem and plan to present these in the future.

Some alternative and intriguing avenues are to attempt to perform a similar analysis for Euclidean black saddles [144], for other rotating black hole solutions and to include higher derivative corrections [145–147]. There are many results with which one could compare for black holes in other theories, for example [148–155]. It would also be desirable to understand the connection with Sen's entropy function [156–158] and whether one can perform a similar classification for near extremal black holes [159–161].

Appendices

3.A Complex Geometry

But in my opinion, all things in nature occur mathematically.

– Rene Descartes, *Correspondence with Mersenne*

In this chapter we have described the embedding of near horizons of rotating black holes into M-theory. In order to describe the geometries that arise when considering such rotating black holes, we made frequent use of complex geometry. In this section we give a lighting-review of a few tools from complex geometry that we have used. If this overview is not enough, a more elaborate review can be found in [162].

The first and foremost consideration about complex geometry is that it is complex, which in formal terms means that there exists a complex structure. The complex structure, usually denoted by J, can act upon vectors. Due to the complex coordinates, the tangent spaces (where vectors reside) are split up into holomorphic (L) and anti-holomorphic ($\bar{L}$) parts. The complex structure can locally be written in complex coordinates z^a as

$$J = i\frac{\partial}{\partial z^a} \otimes \mathrm{d}z^a - i\frac{\partial}{\partial \bar{z}^a} \otimes \mathrm{d}\bar{z}^a \ . \tag{3.152}$$

If we were to act upon vectors of the (anti) holomorphic sector with J, it would yield an eigenvalue of (-)i. Let us describe this story for the dual tangent spaces more formally: the complex structure splits the cotangent bundle of rank d into two subbundles of rank $d/2$ as

$$\Lambda^1 T^*M \otimes \mathbb{C} = \Lambda^{(1,0)} T^*M \oplus \Lambda^{(0,1)} T^*M \ , \tag{3.153}$$

where now $\theta \in \Lambda^{(1,0)} T^*M$ if and only if $\theta(X) = 0$ for all $X \in \bar{L}$.[17] The differential operator also splits, into *Dolbeault* operators

$$\mathrm{d} = \partial + \bar{\partial} \ , \tag{3.154}$$

where the operators thus work on sections of the bundles by

$$\begin{aligned} \partial &: \Gamma(\Lambda^{(p,q)} T^*M) \to \Gamma(\Lambda^{(p+1,q)} T^*M) \ , \\ \bar{\partial} &: \Gamma(\Lambda^{(p,q)} T^*M) \to \Gamma(\Lambda^{(p,q+1)} T^*M) \ . \end{aligned} \tag{3.155}$$

If we have a manifold M along with a complex structure J, we call (M, J) a complex manifold. Now let us introduce the metric, g, into the playing-field. We will require the metric to be Hermitic with respect to the complex structure which, in local coordinates, means

$$g_{\mu\nu} = J_\mu{}^\rho J_\nu{}^\sigma g_{\rho\sigma} \ . \tag{3.156}$$

Using the metric and the complex structure we can define another two-form which, by following our conventions of chapter 3, we call j:

$$j_{\mu\nu} = J_\mu{}^\rho g_{\rho\nu} \ . \tag{3.157}$$

By using the Hermiticity of the metric along with (3.152) it can be checked that j is a (1,1) form. This (1,1) form is usually called the fundamental two-form or the Kähler form, although the latter name is best reserved for the case in which our manifold is actually Kähler. When is the manifold Kähler? This depends on properties of the fundamental form; suppose we have a complex manifold of complex dimension n along with a Hermitian metric, we then call the manifold

- Kähler if $\mathrm{d}j = 0$,
- Balanced if $\mathrm{d}j^{n-1} = 0$.

[17] Similar decompositions hold for higher-rank forms, e.g. a 2-form decomposes to (2,0) + (0,2) + (1,1).

The mathematical structures we will use in chapter 3 to describe the geometries are called *G-structures*, where the G stands for a Lie group. In our scenarios we will always consider SU(5) or SU(4) structures; in this introductory section we will discuss the SU(5) structure, but the principles also hold for other groups. Following the conventions we use later on, the SU(5) structure can be described by two structure forms: a (1,1)-form denoted by j and a (5,0)-form denoted by ω.[18] The structure has a normalisation that we choose to be

$$\omega \wedge \bar{\omega} = (-2i)^5 \frac{j^5}{5!} \ , \tag{3.158}$$

where the prefactors allow us to write the structure forms in terms of a local basis of (1,0)-forms θ^a by

$$j = -\frac{i}{2} \sum_a \theta^a \wedge \bar{\theta}^a \ , \quad \omega = \theta^1 \wedge \cdots \wedge \theta^{d/2} \ . \tag{3.159}$$

The SU(5) structure can be used to investigate the geometry by considering the exterior derivatives on its structure forms. In general these exterior derivatives have the following form:

$$\mathrm{d}j = \frac{1}{8} w_1 \lrcorner \, \mathrm{Im}[\omega] + w_3 + \frac{1}{4} w_4 \wedge j \ , \tag{3.160}$$

$$\mathrm{d}\,\mathrm{Re}[\omega] = \frac{1}{3} w_1 \wedge \frac{j^2}{2!} + w_2 \wedge j - \frac{1}{8} w_5 \wedge \mathrm{Re}[\omega] \ , \tag{3.161}$$

where the w_i are called the *torsion modules*, w_1 is a real (2,0) + (0,2) form, w_2 a real primitive (3,1) + (1,3) form, w_3 a real primitive (2,1) + (1,2) form, w_4 and w_5 are real one-forms. These torsion modules prove their worth by specifying the geometry as seen in the table below. In the chapter we dealt mostly with balanced

Torsion Classes	Geometry
$w_1 = w_2 = 0$	Complex
$w_1 = w_3 = w_4 = 0$	Symplectic
$w_1 = w_2 = w_4 = 0$	Balanced
$w_1 = w_2 = w_3 = w_4 = 0$	Kähler
$w_1 = w_2 = w_3 = w_4 = w_5 = 0$	Calabi-Yau

manifolds.

[18] For an SU(n) structure, ω is a (n,0) form.

3.B Black hole near-horizons and observables

In this appendix we will study the general form of the near-horizon of a black hole. This analysis serves two purposes. Firstly it will motivate the ansatz we take in section 3.1.2 for the 11d supergravity solution, in particular the warping of the metric and the temporal fibration. Despite this, in the main text we will use a more general ansatz to the one motivated here purely for convenience of the notation. It is understood that one must impose an additional constraint on the geometry in order for it to be the near-horizon of a black hole as we will show later in this section.

The second purpose for this analysis is to determine how to evaluate the physical observables for our solution. The parametrization of the metric which is most useful for obtaining the conditions arising from supersymmetry is not the one that is most useful for defining the observables such as the entropy and angular momentum of the black hole where an explicit AdS_2 factor is used. The analysis of this section will allow us to translate between the two view-points and compute observables easily from the form of the metric obtained from supersymmetry.

3.B.1 General near-horizon metric

Following [163, 164] (see also [116] and references therein) consider a spacetime containing a smooth degenerate Killing horizon, with future directed Killing field $\tilde{K}$. Let the cross section of the Killing field be H and let the unique past-directed vector field be $\hat{U}$. The vector field $\hat{U}$ is tangent to the null geodesics orthogonal to the horizon cross section and can be normalised so that $\hat{K}\cdot\hat{U}=1$. We will consider rotating black holes which imply that the solution must admit at least one rotational U(1) symmetry, i.e. it is axisymmetric. If, in addition, the spacetime has a $\mathrm{U}(1)^m$ isometry group which acts transitively on the horizon the black hole near-horizon takes the form[19]

$$\mathrm{d}s^2=\Gamma(y)\Big[-r^2\mathrm{d}t^2+\frac{\mathrm{d}r^2}{r^2}+G_{MN}(y)\mathrm{d}y^M\mathrm{d}y^N+\gamma_{\mu\nu}(y)(\mathrm{d}\phi^\mu+k^\mu r\mathrm{d}t)(\mathrm{d}\phi^\nu+k^\nu r\mathrm{d}t)\Big]\,. \tag{3.162}$$

Here ϕ are periodic coordinates and k^μ are *constants* related to the near-horizon value of the chemical potentials of the angular momentum of the black hole. The

[19] We have made some trivial redefinitions to the form of the metric appearing in [164], in particular we have changed coordinates on AdS_2 from Gaussian Null coordinates to Poincaré coordinates and extracted an overall factor from each of the sub metrics.

functions of the metric all depend on the y coordinates and are independent of the ϕ's. We do not need to specify the ranges of the indices M and μ for the argument but let the range of $\mu \in \{1, \ldots, m\}$[20]. Note that the first two entries of the metric are precisely the metric on AdS_2 with unit radius. Moreover it is clear from this form that there is an $SO(2,1) \times U(1)^m$ isometry.[21]

The metric in this form is useful for computing the observables of the black hole however it is not as useful when trying to impose supersymmetry. Due to the gauging over AdS_2 it is finicky to try to implement SUSY preservation in this form. It is known that supersymmetry in 11d supergravity imposes that a metric admits either a timelike or null Killing vector [129, 165]. Since the form of the metric we are considering above has a timelike Killing vector we will focus on this case[22]. It is then useful to rewrite the metric so that the timelike Killing vector is manifest. This will lead to the time-direction being fibered over the remaining directions. A small rearrangement puts the metric into the form

$$\begin{aligned} \mathrm{d}s^2 =& \Gamma(y)\Bigg[-(1-\gamma_{\tau\kappa}k^\tau k^\kappa)\Big(r\mathrm{d}t - \frac{k^\mu \gamma_{\mu\nu}\mathrm{d}\phi^\nu}{1-\gamma_{\sigma\rho}k^\sigma k^\rho}\Big)^2 + \frac{\mathrm{d}r^2}{r^2} + G_{mn}(y)\mathrm{d}y^m\mathrm{d}y^n \\ &+ \Big(\gamma_{\mu\nu} + \frac{k^\sigma \gamma_{\sigma\mu} k^\rho \gamma_{\rho\nu}}{1-\gamma_{\kappa\tau}k^\tau k^\kappa}\Big)\mathrm{d}\phi^\mu \mathrm{d}\phi^\nu \Bigg] . \end{aligned} \tag{3.163}$$

The metric now exhibits the timelike Killing vector in a simple form. It is then

[20] Note that n cannot be zero otherwise the black hole is not rotating and we fall into the class of solutions given in [117].

[21] The $SO(2,1)$ algebra of the metric in these coordinates is realised by the three Killing vectors

$$H = \partial_t \,, \quad D = t\partial_t + r\partial_r \,, \quad K = (t^2 + r^{-2})\partial_t - 2tr\partial_r - 2r^{-1}k^i\partial_{\psi^i} \,,$$

where the ψ_i denote the $U(1)$ symmetries of the internal manifold. Note that the generators are twisted with respect to the $U(1)$ symmetries of the internal manifold which are gauged over the AdS_2. It is important that the twisting parameters, the k^i's are constant otherwise the $SO(2,1)$ algebra is broken. The Killing vectors satisfy the algebra

$$[H, D] = H \,, \quad [K, D] = -K \,, \quad [H, K] = 2D$$

which is precisely the algebra of the conformal group in 1d and commutes with the isometries of the internal manifold.

[22] One could also have attacked the problem using the null Killing vector of AdS_2. The benefit of using the timelike Killing vector is that it is transferable to the case of black strings in Type IIB and so we pursue this choice here.

natural to take as ansatz[23]

$$\mathrm{d}s^2 = \mathrm{e}^{2B}\Big[-\mathrm{e}^{2C}\Big(\frac{\mathrm{d}t}{r} + \hat{A}\Big)^2 + \frac{\mathrm{d}r^2}{r^2} + \mathrm{d}s_9^2\Big] \tag{3.164}$$

for the near-horizon, with $\hat{A}$ an r-independent one-form on the 9d base. In this rotated form the AdS_2 factor is obscured, however as we mentioned previously this form is far more amenable to imposing supersymmetry. However this ansatz does come with some downsides. Firstly computing observables, such as the horizon area are not nearly as clear as in the form given in the ansatz (3.162). Moreover it is not clear which solutions can be identified with the near-horizon of a rotating black hole from the form in (3.164), in particular the scalar C is arbitrary in our ansatz whilst its analogue in (3.163) is constrained. We shall study this constraint shortly however in the main text we shall refrain from imposing it for as long as possible. We will see that we can proceed unabated in the classification without needing to impose such a condition.

3.B.2 Constraints from the near-horizon

In this section we shall look at the additional constraints imposed on the metric ansatz used in the main text which follow from it being the near-horizon of a black hole. We shall compare our ansatz with the general form of the near-horizon given in the previous section, rewriting the expressions in terms of quantities adapted to the metric in the form of the classification. The classification implies that the metric takes the form

$$\mathrm{d}s^2 = \mathrm{e}^{2B}\Big[-\mathrm{e}^{2C}\Big(\frac{\mathrm{d}t}{r} + \alpha\eta + A\Big)^2 + \frac{\mathrm{d}r^2}{r^2} + G_{mn}(y)\mathrm{d}y^m\mathrm{d}y^n + g_{\mu\nu}\mathrm{d}\phi^\mu\mathrm{d}\phi^\nu\Big] \tag{3.165}$$

where we have written the metric with the same splitting as earlier. We can then identify

$$\begin{aligned} \mathrm{e}^{2B} &= \Gamma(y)\,, \\ \mathrm{e}^{2C} &= 1 - |k|_\gamma^2\,, \\ -\mathrm{e}^{-2C}k^\mu\gamma_{\mu\nu}\mathrm{d}\phi^\nu &= \alpha\eta + A\,, \\ g_{\mu\nu} &= \gamma_{\mu\nu} + \frac{k^\sigma\gamma_{\sigma\mu}k^\rho\gamma_{\rho\nu}}{1-\gamma_{\kappa\tau}k^\tau k^\kappa}\,. \end{aligned} \tag{3.166}$$

[23] We change the radial coordinate as $r \to r^{-1}$ in order to write the transverse directions to the timelike foliation as a cone in the main text.

Note that we have defined $|\cdot|_\gamma$ to be the norm with respect to the metric γ, similarly we let $|\cdot|_g$ denote the norm with respect to g. Simple manipulations of these definitions gives

$$g_{\mu\nu}k^\nu = \mathrm{e}^{-2C}\gamma_{\mu\nu}k^\nu\,, \quad |k|_g^2 = \mathrm{e}^{-2C}|k|_\gamma^2\,, \quad \mathrm{e}^{2C} = (1+|k|_g^2)^{-1}\,. \tag{3.167}$$

Note that this implies we can constrain the scalar C in terms of data of the fibration, in particular

$$\mathrm{e}^{-2C} = 1 + |\alpha\eta + A|_9^2\,. \tag{3.168}$$

Finally rewriting this in terms of the full metric of the classification we find the condition

$$\mathrm{e}^{-2C} = 1 + \alpha^2 + \mathrm{e}^{3B+C/3}|A|^2 \tag{3.169}$$

where the final norm is with respect to the metric on the balanced manifold. Let us further analyse the condition on the fibration in the time-direction. We have

$$\alpha\eta + A = -k^\mu g_{\mu\nu}\mathrm{d}\phi^\nu\,. \tag{3.170}$$

Therefore in order to specify α and A we should specify η, the metric $g_{\mu\nu}$ and a set of constants k^μ. These constants k^μ are related to the near-horizon values of the chemical potentials of the angular momentum of the black hole (when viewed from 11d). As a final step let us rewrite the metric used in the arguments above so that the R-symmetry vector is manifest. We want to identify

$$G_{mn}\mathrm{d}y^m\mathrm{d}y^n + g_{\mu\nu}\mathrm{d}\phi^\mu\mathrm{d}\phi^\nu \equiv (\mathrm{d}z+P)^2 + \mathrm{e}^D\mathrm{d}s_8^2\,. \tag{3.171}$$

Clearly the G_{mn} part fits in trivially after extracting out the required warp factor. The angular part can be written as

$$g_{\mu\nu}\mathrm{d}\phi^\mu\mathrm{d}\phi^\nu = g_{zz}\mathrm{d}z^2 + 2g_{z\hat{\mu}}\mathrm{d}z\mathrm{d}\phi^{\hat{\mu}} + g_{\hat{\mu}\hat{\nu}}\mathrm{d}z^{\hat{\mu}}\mathrm{d}z^{\hat{\nu}} \tag{3.172}$$

$$= (\mathrm{d}z + g_{z\hat{\mu}}\mathrm{d}\phi^{\hat{\mu}})^2 + (g_{\hat{\mu}\hat{\nu}} - g_{z\hat{\mu}}g_{z\hat{\nu}})\mathrm{d}\phi^{\hat{\mu}}\mathrm{d}\phi^{\hat{\nu}} \tag{3.173}$$

where we have used that $g_{zz} = 1$ and we should identify $g_{z\hat{\mu}}\mathrm{d}\phi^{\hat{\mu}} = P$. Therefore we have

$$\mathrm{d}s^2 = (\mathrm{d}z+P)^2+\mathrm{e}^D\mathrm{d}s_8^2 = (\mathrm{d}z+P)^2+G_{mn}\mathrm{d}y^m\mathrm{d}y^n+(g_{\hat{\mu}\hat{\nu}}-P_{\hat{\mu}}P_{\hat{\nu}})\mathrm{d}\phi^{\hat{\mu}}\mathrm{d}\phi^{\hat{\nu}}\,. \tag{3.174}$$

Inserting the decomposition into the connection piece of the timelike fibration we have

$$k^\mu g_{\mu\nu}\mathrm{d}\phi^\nu = k^z\mathrm{d}z + k^{\hat{\mu}}g_{\hat{\mu}z}\mathrm{d}z + k^{\hat{\mu}}g_{\hat{\mu}\hat{\nu}}\mathrm{d}\phi^{\hat{\nu}} + k^z g_{z\hat{\mu}}\mathrm{d}\phi^\mu \tag{3.175}$$

from which we find

$$-\alpha(\mathrm{d}z+P)-A=k^{\mu}g_{\mu\nu}\mathrm{d}\phi^{\nu}=(k^{z}+k^{\hat{\mu}}P_{\hat{\mu}})(\mathrm{d}z+P)+(g_{\hat{\mu}\hat{\nu}}-P_{\hat{\mu}}P_{\hat{\nu}})k^{\hat{\mu}}\mathrm{d}\phi^{\hat{\nu}}\,. \quad (3.176)$$

Therefore given a vector of constants parametrising the rotation and the internal metric one can construct $\alpha\eta+A$. In fact if one imposes that the internal manifold is toric one may write the gauge field in a simple way as we have explained in section 3.1.4.

3.B.3 Observables

Let us now use the near-horizon solution to study what observables we can compute. The three main observables are the entropy of the black hole, the angular momentum and its electric/magnetic charges, all of which can be computed in the near-horizon. One may also ask if it is possible to compute the electrostatic potential and angular velocity, however these observables require some knowledge of the UV data since they are defined as

$$\mathcal{O}_{\mathrm{BH}}=\mathcal{O}_{\mathrm{NH}}-\mathcal{O}_{\infty}\,. \quad (3.177)$$

In this section we will focus on rephrasing the computation of the entropy, electric charges and angular momentum in terms of integrals over various cycles of the internal manifold.

Entropy

First consider the entropy of the black hole. The entropy is given up to normalization by the area of the horizon of the black hole. In order to compute the horizon area one should write the metric so that a bona-fide AdS_2 factor appears in the metric and the internal manifold is fibered over this. Clearly in order to compute the entropy in this way the metric of use to us is the one given in (3.162) and not the one that naturally comes out from supersymmetry. With this rewriting the horizon is manifest and the entropy is given simply the surface area of the horizon which implies

$$S_{\mathrm{BH}}=\frac{1}{4G_2}\,, \quad (3.178)$$

where the Newton's constant is that of a 2d theory admitting the AdS_2 near-horizon as a vacuum solution. In order to compute the Newton's constant (at leading order, we will not make any comments about subleading corrections though these are

certainly very interesting) we should look at reducing the 11d Einstein-Hilbert term of 11d supergravity on the AdS_2 background in (3.162). We have[24]

$$\begin{aligned}\frac{1}{G_{11}}\int_{M_{11}} R\mathrm{dvol}_{M_{11}} &= \frac{1}{G_{11}}\int_{\mathcal{M}_2} R_2\mathrm{dvol}_2 \int_{Y_9}\Gamma(y)^{\frac{9}{2}}\sqrt{\det(G)}\sqrt{\det(\gamma)}\mathrm{d}y\wedge\mathrm{d}\phi \\ &\equiv \frac{1}{G_2}\int_{\mathcal{M}_2} R_2\mathrm{dvol}_2\,,\end{aligned} \tag{3.179}$$

from which we identify

$$\begin{aligned}\frac{1}{G_2} &= \frac{1}{G_{11}}\int_{Y_9}\Gamma(y)^{\frac{9}{2}}\sqrt{\det(G)}\sqrt{\det(\gamma)}\mathrm{d}y\wedge\mathrm{d}\phi \\ &= \frac{1}{G_{11}}\int_{Y_9}\Gamma(y)^{\frac{9}{2}}\mathrm{dvol}_9\,.\end{aligned} \tag{3.180}$$

Let us now translate this result into the notation of the metric arising from supersymmetry, namely (3.163). We expect that the difference is precisely a warping of the volume form which indeed turns out to be the case. To this end let us compute the volume of the internal manifold. We distinguish between the two volume forms by writing $\mathrm{dvol}_{\mathrm{SUSY}}$ for the volume form in the form natural from supersymmetry. We have

$$\mathrm{dvol}_{\mathrm{SUSY}} = \Gamma(y)^{\frac{9}{2}}\sqrt{\det(G)}\sqrt{\det\Big(\gamma_{\mu\nu}+\frac{k^\sigma\gamma_{\sigma\mu}k^\rho\gamma_{\rho\nu}}{1-\gamma_{\kappa\tau}k^\tau k^\kappa}\Big)}\mathrm{d}y\wedge\mathrm{d}\phi\,. \tag{3.181}$$

We can expand the determinant second determinant. Using the fact that for an invertible matrix A and vectors v, w one has

$$\det(A+vw^T) = \det(A)(1+w^TA^{-1}v)\,, \tag{3.182}$$

we have

$$\begin{aligned}\det\Big(\gamma_{\mu\nu}+\frac{k^\sigma\gamma_{\sigma\mu}k^\rho\gamma_{\rho\nu}}{1-\gamma_{\kappa\tau}k^\tau k^\kappa}\Big) &= \det(\gamma_{\mu\nu})\Big(1+\frac{1}{1-\gamma_{\kappa\tau}k^\tau k^\kappa}k^\sigma\gamma_{\sigma\mu}\gamma^{\mu\nu}k^\rho\gamma_{\rho\nu}\Big) \\ &= \frac{\det(\gamma_{\mu\nu})}{1-\gamma_{\kappa\tau}k^\tau k^\kappa}\,.\end{aligned} \tag{3.183}$$

It follows that

$$\mathrm{dvol}_{\mathrm{SUSY}} = \frac{\Gamma(y)^{\frac{9}{2}}\sqrt{\det(G)}\sqrt{\det(\gamma)}}{\sqrt{1-\gamma^\kappa\gamma^\tau\gamma_{\kappa\tau}}}\mathrm{d}y\wedge\mathrm{d}\phi\,, \tag{3.184}$$

[24]To save cluttering the notation we let $\mathrm{d}y\wedge\mathrm{d}\phi$ denote $\bigwedge\mathrm{d}y^m\wedge\bigwedge\mathrm{d}\phi^\mu$.

and therefore

$$\frac{1}{G_2} = \int_{Y_9} \Gamma(y)^{\frac{9}{2}} \sqrt{1 - \gamma_{\kappa\tau} k^\kappa k^\tau} \mathrm{dvol}_{\mathrm{SUSY}} \,. \tag{3.185}$$

Our proposal for computing the entropy is therefore

$$\begin{aligned} S_{\mathrm{BH}} =& \frac{1}{4G_{11}} \int_{Y_9} \mathrm{e}^{-3B - C/3} \eta \wedge \frac{J^4}{4!} \\ =& \frac{1}{4G_{11}} \int_{Y_9} \eta \wedge \mathrm{d}\eta \wedge \frac{J^3}{3!} \,, \end{aligned} \tag{3.186}$$

where we used (3.41) in the final equality. As discussed in section 3.2.2 this is precisely the same formula as the entropy in the non-rotating case. One should view this section as a proof that the quantity computed in section 3.2.2 really is the entropy of the black hole.

Electric charges

Next let us consider the quantization of the four-form flux which will give rise to the electric charges of the theory. In the presence of a Chern–Simons term there is more than one definition of a charge. One can consider the gauge-invariant but non-conserved charge

$$Q = \frac{1}{(2\pi\ell_p)^6} \int_{\Sigma_7} *_{11} G_4 \,, \tag{3.187}$$

where we integrate over all compact seven-cycles of the geometry. Alternatively the Page charge

$$Q = \frac{1}{(2\pi\ell_p)^6} \int_{\Sigma_7} \Big(*_{11} G_4 + \frac{1}{2} C_3 \wedge G_4 \Big) \,, \tag{3.188}$$

is conserved by application of the Maxwell equation but is not gauge invariant due to the bare potential appearing in the definition. In the following we will consider only the Page charge since it defines a conserved charge. In order to be able to write this charge we must be able to at least locally write the four-form flux in terms of a potential three-form. This is equivalent to the requirement that $\tilde{h}^{(2,2)}$ as defined in (3.14) can be written (at least locally) in terms of a potential. In fact, if we demand that it is exact, i.e. that the potential is a globally defined three-form, it follows that there is no M5-brane charge. Substituting our ansatz into the Page

charge we find

$$Q = \frac{1}{(2\pi\ell_p)^6}\int_{\Sigma_7}\eta\wedge\left[\mathrm{e}^{-2C/3}\mathrm{d}\eta\wedge\frac{J^2}{2}-\frac{1}{2}\Big(C^{(2)}\wedge H^{(2,2)}+C^{(3)}\wedge\mathrm{d}C^{(2)}\right.$$
$$\left.+\,\mathrm{e}^{2C/3}J\wedge\Big(C^{(3)}\wedge\mathrm{d}\alpha-C^{(2)}\wedge(\alpha\mathrm{d}\eta+\mathrm{d}A)\Big)\Big)\right], \quad (3.189)$$

where we have introduced the potentials

$$\begin{aligned} H^{(1,1)} &= \mathrm{d}C^{(1)}\,,\\ \mathrm{i}(H^{(2,1)}-H^{(1,2)}) &= \mathrm{d}C^{(2)}\,,\\ H^{(2,2)} &= \mathrm{d}C^{(3)} = \mathrm{d}\eta\wedge C^{(2)}\,. \end{aligned} \quad (3.190)$$

Angular momentum

We now want to find a similar formulation for computing the angular momentum of the black hole. To such an end we may use the results of [166], (see also [167] for the analogous computation for 5d black rings), which gives the formula for computing the Komar integral for the Noether current of a Killing vector, ξ in 11d supergravity. By an abuse of notation we will also call the dual one-form ξ. The angular momentum is then given by

$$J_\xi = \frac{1}{\delta_{\mathrm{SUSY}}}\int_{Y_9}\left[*_{11}\,\mathrm{d}\xi+(\xi\cdot C_3)\wedge *_{11}G_4+\frac{1}{3}(\xi\cdot C_3)\wedge C_3\wedge G_4\right] \quad (3.191)$$

where the three-form potential C_3 should be chosen so that it has vanishing Lie derivative along the given isometry. Since this formula is dependent on the choice of Killing vector we will refrain from writing this more explicitly and just include it for completeness.

Part II

Sachdev-Ye-Kitaev Models

The second part of the thesis concerns a new class of the Sachdev-Ye-Kitaev (SYK) models. We will investigate a model where instead of only fermions, we also add auxiliary bosonic fields. We investigate the various properties of the model as a function of the ratio of bosons to fermions. We will discuss the relation of this class of models to the $\mathcal{N} = 1$ supersymmetric SYK model and the original SYK model. Furthermore, we derive the effective action for the model and compute the Lyapunov exponent for the model.

Chapter 4

A new class of SYK-models

In this chapter we will discuss a generalisation of the SYK model. In the previous chapter we have focussed on specific black hole solutions in string theories; here we will take a different approach. By virtue of the AdS/CFT duality, we can learn things about gravitational objects (e.g. black holes) by studying the dual conformal field theory. The dual of SYK is though to be the two-dimensional Jackiw-Teitelboim gravity. In this chapter we will, however, focus completely on the field theory side, and we refer to e.g. [168] for an overview of the two-dimensional models.

The SYK model was introduced by Kitaev [33], based on the original Sachdev-Ye model [32, 169, 170]. We discussed this SYK model at length in section 1.3. We saw that one of the characterizing features of the model is the appearance of maximal chaos, which strongly suggests a relation to black holes, which also show this chaotic behaviour [34, 171–174]. The SYK model is a (nearly) conformal field theory (CFT) in the infrared, and as we mentioned before it is expected to have a nearly anti de sitter (AdS) dual in this regime [175, 176]. For low energies the SYK model can be described by a Schwarzian [177], which also appears on the bulk side in the AdS_2 dilaton gravity. There exist many generalisations of SYK including higher dimensions [42, 178–181], flavours [39, 43], tunable chaos [182], supersymmetry [41, 42] and many more.

In this chapter we consider a particular model closely related to the $\mathcal{N} = 1$ supersymmetric extension of SYK. Instead of having an equal number, N, of fermions and bosons we consider the case where we have M bosons and N fermions and study its behaviour as a function of the ratio M/N. In section 4.1 we will introduce the model and discuss in more detail the relation to the (supersymmetric)

SYK model. Afterwards, in section 4.2, we consider the effective action. We derive the equations of motion and consider the solutions at strong coupling. We find two families of solutions that we label by their conformal dimensions at $M = N$, which we call rational and irrational. Afterwards we elaborate on the behaviour of the conformal dimensions at different regimes, e.g. as $M/N \to \infty$ we obtain the same behaviour as in the original SYK model. In section 4.3 we compare the entropy of both solutions and perform some numerical investigations to figure out which is the dominant saddle for all M/N. In section 4.4 we compute the Lyapunov exponent and find that is independent of M/N due to a subtle cancellation.

4.1 Bosons and Fermions

The model consists out of N Majorana fermions obeying $\{\psi^i, \psi^j\} = \delta^{ij}$ and M (auxiliary) bosons. We will use indices a, b to denote the bosons and i, j, k for the fermions (no ambiguity will arise). The Lagrangian is given as follows:

$$\mathcal{L} = \frac{1}{2}\sum_{i=1}^{N} \psi^i \partial_\tau \psi^i - \frac{1}{2}\sum_{a=1}^{M} \phi^a \, \phi^a + i \sum_{a=1}^{M} \sum_{i<j=1}^{N} C_{aij} \phi^a \, \psi^i \, \psi^j \ , \tag{4.1}$$

where ψ denote the Majorana fermions and ϕ the bosons. The coupling C_{aij} is defined to be antisymmetric in the last two indices, which are contracted with the Majorana fermions. In [183] a similar term was studied as a perturbation upon the ordinary SYK model. The fermions are dimensionless, whereas the bosons ϕ and couplings C have dimension of $E^{1/2}$.

Notice that we have two parameters M and N. We are interested in taking the limits of both M and N going to infinity but keeping M/N fixed. In other words we have that $M = \alpha N$ for some fixed α. From now on we will always assume that two a indices are summed up to M whilst the other $i, j, k, ..$ are summed up to N. We let the coupling be disordered averaged by the following distribution:

$$\langle C_{aij} \rangle = 0 \ , \tag{4.2}$$

$$\langle C_{aij}^2 \rangle = \frac{2J}{N^{3/2} M^{1/2}} \ . \tag{4.3}$$

Here J has the dimension of energy and is larger than zero. We can now compute some basic one-loop diagrams for both the fermions and the bosons. We show the one-loop corrections to the two point functions in Figure 4.1, which are proportional to some power of M/N (that can easily be checked). In fact one can check that any boson loop adds a factor of $\sqrt{\frac{M}{N}}$ and each fermion loop $\sqrt{\frac{N}{M}}$.

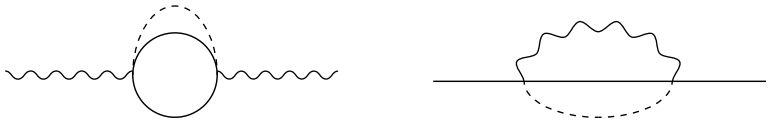

(a) *Proportional to* $\sqrt{\frac{N}{M}}$. **(b)** *Proportional to* $\sqrt{\frac{M}{N}}$.

Figure 4.1: *In this figure we show the two one-loop corrections to the two point functions. The solid lines indicate fermions, the wiggly lines the bosons and the dotted line shows the disorder average. Below the diagrams we show the power of M/N to which they are proportional.*

4.1.1 Relation to SYK

Let us first examine the relation to the original SYK model [33, 37] with Hamiltonian

$$H_{\text{SYK}} = -\frac{1}{4!} J_{ijkl}\, \psi^i\, \psi^j\, \psi^k\, \psi^l \ . \tag{4.4}$$

To check the similarity we start by plugging in the algebraic equation of motion for ϕ^a back into the Lagrangian. The equation of motion is found to be $\phi^a = \frac{i}{2} C^a_{ij}\, \psi^i\, \psi^j$. After plugging it into (4.1) we obtain the Hamiltonian:

$$H = \frac{1}{8}\, C_{aij}\, C_{akl}\, \psi^i\, \psi^j\, \psi^k\, \psi^l. \tag{4.5}$$

This is also the presentation that one can see in [183]. We can then use the antisymmetry in the last two indices of C_{aij} and the commutation relations of the Majorana fermions to rewrite this to:

$$H = \frac{1}{4!}\, \frac{1}{8}\, C_{a[ij}\, C_{|a|kl]}\, \psi^i\, \psi^j\, \psi^k\, \psi^l + E_0 \ , \tag{4.6}$$

where we defined the constant $E_0 = -\frac{1}{16} C^2_{aij}$ (recall that a is summed to M and i, j up to N). Comparing now to the standard SYK Hamiltonian, (4.4), we find:

$$J_{ijkl} = -\sum_{a=1}^{M} \frac{1}{8} C_{a[ij}\, C_{|a|kl]} \ . \tag{4.7}$$

The notation indicates that the asymmetry on the right hand side is only in i, j, k and l, which in turn of course means that J_{ijkl} is completely asymmetric. The above expression for the J coupling shows us that the model is essentially obtained by performing a Hubbard-Stratonovich (HS) transformation on SYK. Of course

apart from this HS transformation we have also chosen a different distribution (see (4.2)) compared to SYK. This means that J_{ijkl} are no longer the independent Gaussian variables and this is the cause of the differences between the models.

4.1.2 Relation to supersymmetric SYK

The $\mathcal{N} = 1$ supersymmetric SYK model was introduced in [41], the Lagrangian density is given by:

$$\mathcal{L} = \sum_{i=1}^{N} \left(\frac{1}{2}\psi^i \partial_\tau \psi^i - \frac{1}{2}\phi^i \phi^i + i \sum_{1 \leq j < k \leq N} C_{ijk} \phi^i \psi^j \psi^k \right). \tag{4.8}$$

There are two important differences compared to the model described in (4.1). The first important aspect is that there are N bosons, which is the same as the number of fermions (which has to be true for supersymmetry). Secondly the coupling C_{ijk} in the supersymmetric case has to be completely antisymmetric. Note that the equal number of bosons and fermions is also necessary for the antisymmetry in the coupling.

In other words, starting from (4.1) we can obtain the supersymmetric model by setting $M = N$ and making the coupling completely antisymmetric. It is precisely when the coupling is completely antisymmetric (and hence $M = N$) that the Lagrangian is invariant under supersymmetry transformations.

4.2 Effective action and conformal dimensions

To find the effective action we will follow the standard procedure of averaging over the disorder in C_{aij} by using the replica trick (see appendices in [39,184]). As in the usual SYK case we will assume replica diagonal matrices. To justify this we have to compare $\overline{\log Z}$ and $\log \overline{Z}$ since assuming replica diagonal matrices corresponds to evaluating the latter instead of the former. The usual argument (see [184]) is to consider diagrams that are in $\log \overline{Z}$ but not in $\overline{\log Z}$. The leading diagram belonging to the former but not the latter is shown in Figure 4.2 and as can be verified it is suppressed by $\frac{1}{N M}$. Thus in the large N limit these contributions will be subdominant. Using replica symmetry, the result of the disorder average

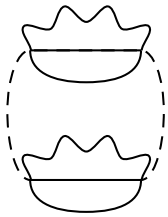

Figure 4.2: *This is the leading diagram that contributes to interactions between replicas. In the figure the top three lines would be associated with a different replica index than the other three below. One can check that this figure is proportional to* $1/N$.

becomes:

$$S_{\text{eff}} = \frac{1}{2}\int d\tau \left(\sum_{i=1}^{N} \psi^i\, \partial_\tau\, \psi^i - \sum_{a=1}^{M} \phi^a\, \phi^a\right) \tag{4.9}$$
$$- \sqrt{\frac{N}{M}}\frac{J}{2N^2}\int d\tau_1 d\tau_2 \sum_{a,(j,k)} (\phi^a(\tau_1)\phi^a(\tau_2))\, \left(\psi^j(\tau_1)\psi^j(\tau_2)\right)\, \left(\psi^k(\tau_1)\psi^k(\tau_2)\right)\ .$$

For the last term we introduced brackets below the sum to indicate that j,k sum up to N whilst a sums up to M. We now introduce bilocal fields for both the fermions and bosons as follows:

$$\begin{aligned}
&\delta\left(G_\psi(\tau_1,\tau_2) - \frac{1}{N}\sum_{i=1}^{N}\psi^i(\tau_1)\,\psi^i(\tau_2)\right) = \\
&= \int d\Sigma_\psi(\tau_1,\tau_2)\, \exp\left\{-\frac{N}{2}\,\Sigma_\psi(\tau_1,\tau_2)\left(G_\psi(\tau_1,\tau_2) - \frac{1}{N}\sum_{i=1}^{N}\psi^i(\tau_1)\,\psi^i(\tau_2)\right)\right\}, \\
&\delta\left(G_\phi(\tau_1,\tau_2) - \frac{1}{M}\sum_{a=1}^{M}\phi^a(\tau_1)\,\phi^a(\tau_2)\right) = \\
&= \int d\Sigma_\phi(\tau_1,\tau_2)\, \exp\left\{-\frac{M}{2}\,\Sigma_\phi(\tau_1,\tau_2)\left(G_\phi(\tau_1,\tau_2) - \frac{1}{M}\sum_{i=1}^{M}\phi^i(\tau_1)\,\phi^i(\tau_2)\right)\right\}.
\end{aligned} \tag{4.10}$$

We insert them into the partition function by Lagrange multipliers. Afterwards we are only left with Gaussian integrals for both the fermions and bosons. Completing

these leads to:

$$\begin{aligned}\frac{S_{\text{eff}}}{N} = &- \log \text{pf}\left(\partial_\tau - \Sigma_\psi(\tau)\right) + \frac{M}{2\,N}\log\det\left(-1-\Sigma_\phi(\tau)\right) \\ &+ \frac{1}{2}\int d\tau_1 d\tau_2 \left[\Sigma_\psi(\tau_1,\tau_2)\,G_\psi(\tau_1,\tau_2) + \frac{M}{N}\Sigma_\phi(\tau_1,\tau_2)\,G_\phi(\tau_1,\tau_2)\right. \\ &\left. - J\sqrt{\frac{M}{N}}\,G_\phi(\tau_1,\tau_2)\,G_\psi^2(\tau_1,\tau_2)\right].\end{aligned} \tag{4.11}$$

On the left hand side we divided out a factor of N, but could just as well have taken out M, since M/N is fixed. Let us now vary with respect to G_ϕ and G_ψ to obtain the self energies:

$$\Sigma_\psi = J\sqrt{\frac{M}{N}}\,G_\phi\,G_\psi\ , \tag{4.12}$$

$$\Sigma_\phi = J\sqrt{\frac{N}{M}}\,G_\psi^2\ . \tag{4.13}$$

These equations can also be obtained using the melonic structure of the Feynman diagrams at large N and M, just as in ordinary SYK. The Schwinger-Dyson equations are obtained by varying with respect to the Σ (we assume time translation symmetry and go to Fourier space):

$$G_\psi^{-1}(i\omega) = -i\omega - \Sigma_\psi(i\omega)\ , \tag{4.14}$$

$$G_\phi^{-1}(i\omega) = -1 - \Sigma_\phi(i\omega)\ . \tag{4.15}$$

4.2.1 Two saddle points

In order to solve the above equations we have to assume the strong coupling limit $\beta J \gg 1$. This implies that in (4.14) we can ignore the first terms on the right hand side. Hence we can write the equations as follows (we have Fourier transformed back to time):

$$\begin{aligned}2J\sqrt{\frac{M}{N}}\int d\tau' G_\psi(\tau,\tau')\,G_\phi(\tau',\tau'')G_\psi(\tau',\tau'') &= -\delta(\tau-\tau'')\ , \\ J\sqrt{\frac{N}{M}}\int d\tau' G_\phi(\tau,\tau')\,G_\psi^2(\tau',\tau'') &= -\delta(\tau-\tau'')\ .\end{aligned} \tag{4.16}$$

We then use the following (conformal) form for the two point functions:

$$G_\psi(\tau) = A\,\frac{\mathrm{sgn}(\tau)}{|\tau|^{2\Delta_\psi}}\ , \tag{4.17}$$

$$G_\phi(\tau) = B\,\frac{1}{|\tau|^{2\Delta_\phi}}\ . \tag{4.18}$$

To obtain conditions on the conformal dimensions we plug these into the saddle point equations above (4.16). Afterwards we Fourier transform using

$$\int d\tau e^{i\,\omega\,\tau}\,\frac{\mathrm{sgn}(\tau)}{|\tau|^{2\Delta}} = 2i\,\cos(\pi\Delta)\,\Gamma(1-2\Delta)\,\mathrm{sgn}(\omega)\,|\omega|^{2\Delta-1}, \tag{4.19}$$

$$\int d\tau e^{i\,\omega\,\tau}\,\frac{1}{|\tau|^{2\Delta}} = 2\,\sin(\pi\Delta)\,\Gamma(1-2\Delta)\,|\omega|^{2\Delta-1}. \tag{4.20}$$

Some other useful relations for Γ functions are

$$\Gamma(1-2\Delta) = \frac{2^{-2\Delta}\,\sqrt{\pi}}{\cos(\pi\Delta)}\,\frac{\Gamma(1-\Delta)}{\Gamma\left(\frac{1}{2}+\Delta\right)}\ , \tag{4.21}$$

$$\frac{\Gamma(1-\Delta)\,\Gamma(\Delta)}{\Gamma\left(\frac{1}{2}+\Delta\right)\,\Gamma\left(\frac{3}{2}-\Delta\right)} = \frac{2}{1-2\Delta}\,\frac{\cos(\pi\Delta)}{\sin(\pi\Delta)}\ . \tag{4.22}$$

After plugging this all in we obtain the following relations:

$$A^2 B\sqrt{\frac{M}{N}}\,\frac{4\,\pi\,J}{1-2\Delta_\psi}\,\frac{\cos(\pi\Delta_\psi)}{\sin(\pi\Delta_\psi)}\,|\omega|^{2(2\Delta_\psi+\Delta_\phi)-2} = 1\ , \tag{4.23}$$

$$A^2 B\sqrt{\frac{N}{M}}\,\frac{2\,\pi\,J}{1-4\Delta_\psi}\,\tan(2\pi\Delta_\psi)|\omega|^{2(2\Delta_\psi+\Delta_\phi)-2} = 1\ . \tag{4.24}$$

By comparing the frequency dependent parts we obtain the first condition on the conformal dimensions:

$$2\Delta_\psi + \Delta_\phi = 1\ . \tag{4.25}$$

As a side note, under this condition the saddle point equations have the conformal symmetry, very analogous to the original SYK model:

$$\begin{aligned} G_\psi(\tau,\tau') &= |f'(\tau)\,f'(\tau')|^{\Delta_\psi}\,G_\psi\left(f(\tau),f(\tau')\right)\ , \\ G_\phi(\tau,\tau') &= |f'(\tau)\,f'(\tau')|^{\Delta_\phi}\,G_\phi\left(f(\tau),f(\tau')\right)\ , \end{aligned} \tag{4.26}$$

where $f(\tau)$ a smooth function (in one dimension $\mathrm{Conf}(\mathbb{R}) \cong \mathrm{Diff}(\mathbb{R})$). To obtain results for finite temperature we use this symmetry with f being the exponential map for example.

Coming back to (4.23), we can obtain another constraint by taking the quotient, which yields the (transcendental) equation:

$$\frac{N}{M}\,\tan(\pi\Delta_\psi)\,\tan(2\pi\Delta_\psi) = \frac{2(1-4\,\Delta_\psi)}{1-2\Delta_\psi}\ . \tag{4.27}$$

This result, for $M = N$, is also obtained in [41]. In [183] it is also shown for $M \neq N$, albeit in a different form. The second condition, (4.27), can also be recast to an equation for Δ_ϕ using (4.25):

$$-4 + \frac{2}{\Delta_\phi} - \frac{N}{M}\,\frac{\tan(\pi\Delta_\phi)}{\tan(\frac{1}{2}\pi\Delta_\phi)} = 0\ . \tag{4.28}$$

4.2.1.1 The case $M = N$

First we solve (4.27) for M being equal to N. This case overlaps with supersymmetric SYK (as commented upon in the introduction) and we find the same solutions as in [41]. The first solution is given by:

$$\begin{aligned} \Delta_\psi &= \frac{1}{6}\ , \\ \Delta_\phi &= \frac{2}{3}\ , \\ A^2 B &= \frac{1}{6\,\pi\,J\,\sqrt{3}}\ . \end{aligned} \tag{4.29}$$

We label this solution as the 'rational' solution. In the supersymmetric model this solution is the one that preserves supersymmetry. In that case, the supersymmetric Ward identity $G_\phi = \partial_\tau G_\psi$, together with (4.17) implies $\Delta_\phi = \Delta_\psi + \frac{1}{2}$ [41], obviously obeyed by (4.29).
There is another solution with positive conformal dimensions, it is however irrational:

$$\begin{aligned} \Delta_\psi &= 0.350585...\ , \\ \Delta_\phi &= 0.29883...\ , \\ A^2 B &= \frac{0.589161...}{4\pi J}\ . \end{aligned} \tag{4.30}$$

As one can easily check this does not satisfy $\Delta_\phi = \Delta_\psi + \frac{1}{2}$ and hence would break supersymmetry. A similar situation arises in [185] where there are also two solutions, one preserving and one breaking the supersymmetry.

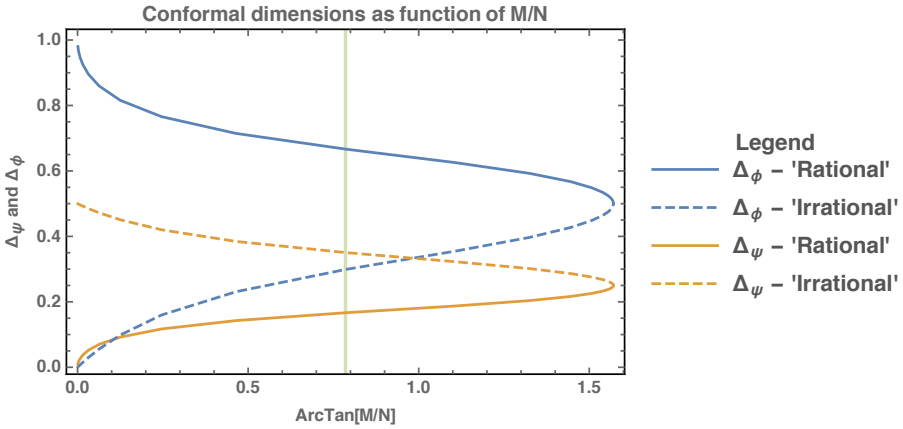

Figure 4.3: *This figure shows the conformal dimensions as a function of M/N. The two solutions are labelled by their (ir)rational behaviour at $M = N$ (which may differ for other values), see* (4.29) *and* (4.30)*. The green line represents this point where $M/N = 1$.*

4.2.1.2 Arbitrary M and N

Let us now vary the ratio M/N and find the conformal dimensions as a function of this ratio. We solve (4.27) numerically and show the results in Figure 4.3. There are two branches (or families) of solutions, labelled by their behaviour at $M = N$. The rational solution was also found in [183].

When M/N becomes large the rational and irrational flow to the same point. This can be understood by considering the defining equations (4.27) and (4.28). When one takes the limit of M/N going to infinity there is only one solution left:

$$\begin{aligned} \Delta_\psi &= \frac{1}{4} \ , \\ \Delta_\phi &= \frac{1}{2} \ . \end{aligned} \tag{4.31}$$

This is an interesting point, since we find that the conformal dimension of the fermion is exactly that which one finds in the original SYK model [37]. In particular they find that the conformal dimension for an arbitrary number of interactions q_{SYK} is given by $\frac{1}{q_{\text{SYK}}}$. Let us consider our model with q interactions as described in appendix 4.A. We derive there the relation $(q-1) = \frac{1}{2}q_{\text{SYK}}$ and furthermore

that the solution for Δ_ψ in the general q case (4.90):

$$\Delta_\psi = \frac{1}{2(q-1)} = \frac{1}{q_{\text{SYK}}} \ . \tag{4.32}$$

We find thus in the $M/N \to \infty$ limit that we obtain the same behaviour as SYK, and conclude that the two models have the same infrared fixed point.

The behaviour for small M/N can be understood by taking the small M/N limits in the defining equations. This is equivalent to considering the limit N/M going to infinity in (4.28). Consider the following two limits:

$$\lim_{\Delta_\phi \to 1} \frac{\tan(\pi\Delta_\phi)}{\tan\left(\frac{\pi}{2}\Delta_\phi\right)} = 0 \ , \qquad \lim_{\Delta_\phi \to 0} \frac{\tan(\pi\Delta_\phi)}{\tan\left(\frac{\pi}{2}\Delta_\phi\right)} = 2 \ . \tag{4.33}$$

Applying these in (4.28) shows us that for small M/N we either need to consider the case where Δ_ϕ is very small or the case where it goes to one. The latter corresponds to the rational family. For the irrational $\Delta_\phi \ll 1$ case we find from (4.28) that for small M/N it behaves as:

$$\Delta_\phi = \frac{M}{N} \ . \tag{4.34}$$

The corresponding dimensions for the fermion can be found by (4.25). Lastly let us investigate the rational Δ_ψ for small M/N. Observing Figure 4.3, we assume that Δ_ψ is small and consider (4.23) and (4.27). We can then solve as follows:

$$A^2 B = \frac{1}{4\,\pi J} \ , \qquad \Delta_\psi = \frac{1}{\pi}\sqrt{\frac{M}{N}} \ . \tag{4.35}$$

The solution corresponding with Δ_ψ going to zero might be understood from Figure 4.1, since in this limit the right diagram corresponding with the self energy corrections to the fermion vanishes. We then expect the fermion to reduce to its free propagator, i.e. with $\Delta_\psi = 0$. Such an argument can however not be made for the case where instead Δ_ϕ goes to zero.

4.3 Dominant saddle

In this section we will investigate the dominant saddle by comparing the entropies of both solutions for arbitrary M/N. For the case $M/N = 1$ in the rational branch, we can do the computation analytically. For the computation we will follow [41] and use the model for a q-interaction (meaning a vertex with one boson and $q-1$

fermions, with q odd), see appendix 4.A for an overview of the changes. The free energy becomes

$$\begin{aligned}\frac{\log(Z)}{N} &= \log \mathrm{pf}\left(\partial_\tau - \Sigma_{\psi\psi}(\tau)\right) - \frac{M}{2N}\log\det\left(-1-\Sigma_{\phi\phi}(\tau)\right) \\ &\quad - \frac{1}{2}\int d\tau_1 d\tau_2 \left[\Sigma_{\psi\psi}(\tau_1,\tau_2)\, G_{\psi\psi}(\tau_1,\tau_2) + \frac{M}{N}\Sigma_{\phi\phi}(\tau_1,\tau_2)\, G_{\phi\phi}(\tau_1,\tau_2)\right. \\ &\quad \left. -J\sqrt{\frac{M}{N}}\, G_{\phi\phi}(\tau_1,\tau_2)\, G_{\psi\psi}^{q-1}(\tau_1,\tau_2)\right].\end{aligned} \tag{4.36}$$

Now we derive with respect to q (we continue the values of q to the reals) such that we don't have to evaluate the first terms. We take the fields to be on-shell such that we only need to explicitly take the partial derivative of the last term

$$\partial_q \frac{\log(Z)}{N} = \frac{J}{2}\sqrt{\frac{M}{N}}\int d\tau\, d\tau' G_\phi(\tau-\tau')\, \log\left(G_\psi(\tau-\tau')\right)\, G_\psi^{q-1}(\tau-\tau')\ , \tag{4.37}$$

where we take the Gs to be the finite temperature versions that we obtained in (4.26):

$$G_\psi(\tau) = A\,\mathrm{sgn}(\tau)\ , \left(\frac{\pi}{\beta\,\sin\left(\frac{\pi\tau}{\beta}\right)}\right)^{2\Delta_\psi}, \qquad G_\phi(\tau) = B\left(\frac{\pi}{\beta\,\sin\left(\frac{\pi\tau}{\beta}\right)}\right)^{2\Delta_\phi}. \tag{4.38}$$

The integral can then be computed straightforwardly (using the periodicity in the τ variables):

$$\partial_q \frac{\log(Z)}{N} = \sqrt{\frac{M}{N}}\,\frac{J}{2} A^{q-1}\, B\,\pi^2\left[2\Delta_\psi + \beta\, C\right]\ , \tag{4.39}$$

where C is a constant independent of β. The constant C is a diverging quantity independent of q contributing to the ground state energy, but will not contribute to the zero temperature entropy, similar to the scenario in [41]. It is important to note that apart from the overall factor, the M/N dependence is also in $A^{q-1}B$ ((4.88)) and the conformal dimension Δ_ψ (Figure 4.3).

The zero temperature entropies S^R and S^I are labelled by their rational or irrational origin, see (4.29) and (4.30) respectively, and given by:

$$\frac{S^i}{N} = J\,\pi^2\sqrt{\frac{M}{N}}\int dq\, A^{q-1}\, B\,\Delta_\psi^i\ , \tag{4.40}$$

where then $i \in \{I, R\}$, depending on the branch we consider. We will call the integrands (including the constants) also $i(q)$ and $r(q)$. The expression for $A^{q-1}B$ is shown in (4.88) and is also dependent on the conformal dimensions. Since we don't know the analytical expressions for Δ_ψ at arbitrary M/N we will solve this problem numerically and afterwards fit these as a function of q. In particular we proceed as follows:

- Fix a value for M/N
- Solve Δ_ψ^R and Δ_ψ^I numerically
- Fit these conformal dimensions as a power series in $\frac{1}{q}$
- Find the irrational integrand $i(q)$ and the rational integrand $r(q)$

After we have the integrands we can compare both the entropies by integration. There are a couple remarks regarding the power series for the Δ_ψ. First of all, we already obtain good fits for the numerical solution when going up to order $1/q^4$. Secondly, the leading power of all the numerically computed Δ_ψ behave as $\frac{1}{2q}$. In order to illustrate the described process we will first work it out for a particular value $M/N \approx 10^{-1}$. As it turns out the other values of M/N follow qualitatively the same behaviour. Afterwards we have a short discussion for $M/N = 1$, in which case there is some more analytical control for the rational case.

4.3.1 An example: M/N ≈ 10^{-1}

We have done the above procedure for a range of values of M/N, in particular at M/N being of order 10^{-2}, 10^{-1}, 1, 10^1 and 10^2. As it turns out the behaviour is very similar at all of these values, so let us just describe one of them, 10^{-1}.

Having fixed the value of M/N and proceed with the next step, to solve the equation for Δ_ψ as a function of q (see (4.90)):

$$\frac{N}{M}\tan(\pi\Delta_\psi)\tan(\pi(q-1)\Delta_\psi) = (q-1)\frac{1-2(q-1)\Delta_\psi}{1-2\Delta_\psi} \ . \tag{4.41}$$

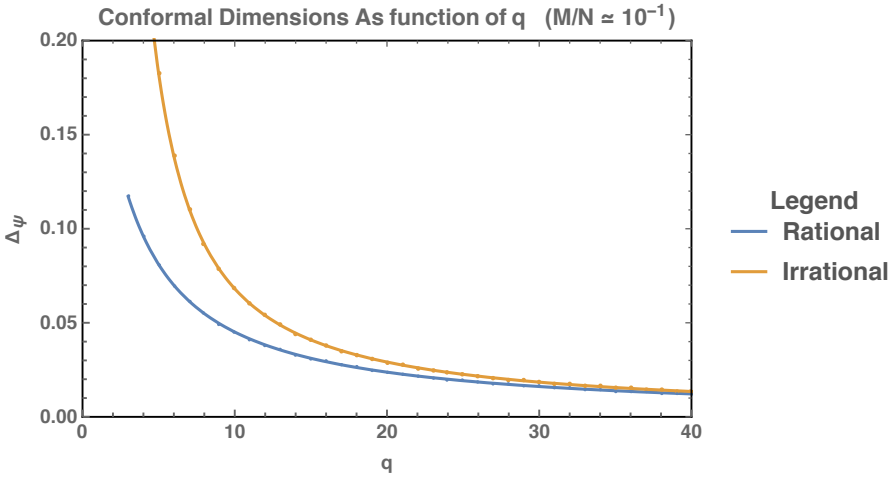

Figure 4.4: *This plot shows the conformal dimension Δ_ψ for both the irrational and the rational case as a function of q. The points indicate the numerical values, whilst the lines are the fits found in* (4.42)*. We only show a small amount of these points such that the fits can be clearly distinguished. As can be seen, the power series up to $1/q^4$ describes the results with high accuracy.*

This equation is first solved numerically for both branches. Afterwards we fitted the data with the following power series:

$$\Delta_\psi^R = \frac{0.500\ldots}{q} - \frac{0.507\ldots}{q^2} + \frac{0.127\ldots}{q^3} + \frac{0.163\ldots}{q^4} + \mathcal{O}\left(\frac{1}{q^5}\right) , \tag{4.42}$$

$$\Delta_\psi^I = \frac{0.500\ldots}{q} + \frac{1.477\ldots}{q^2} + \frac{3.723\ldots}{q^3} - \frac{3.936\ldots}{q^4} + \mathcal{O}\left(\frac{1}{q^5}\right) . \tag{4.43}$$

The results can be seen in Figure 4.4. Note that we plotted only a small region of q for clarity, we solved all the cases from $q = 3$ at least up to $q = 300$; in the plot we only show some of these data points for clarity.

As mentioned before, we can see that both the Δ_ψ have a leading order term equal (to our numerical precision) to $\frac{1}{2q}$. Motivated by this numerical result and the exact analytical result for $M/N = 1$ (which we discuss in the next section) we take the leading coefficient to be $\frac{1}{2q}$ for both the rational and irrational cases. It means that in the strict $q \to \infty$ limit the two branches coincide, and we can already expect their entropies to be the same in that limit. This might have been expected, since the large q limit in (supersymmetric) SYK is a limit in which the models become

solvable with self energies proportional to $1/q$ [41]. In the strict $q \to \infty$ limit, the model becomes a free theory in which it is exactly solvable, and there should clearly not be any difference between the branches.

Let us now compute the integrands from (4.40), which we first do numerically and then compare those with the obtained fits. We show the results in Figure 4.5. For clarity we show again only a subset of the computed q values. It becomes clear that $i(q) > r(q)$ (which also holds outside the plotted range of q), i.e. the slope of the irrational entropy is always larger than the rational one. We can then expand the integrands for large q to find also the leading behaviour of the actual entropies. This yields (we plugged in the expression for $A^{q-1}B$):

$$i(q) = \frac{\pi}{2} \frac{\left(1 - 2\,\Delta_\psi^I\right) \tan\left(\pi\,\Delta_\psi^I\right)}{q-1} \Delta_\psi^I \approx \frac{1.233\ldots}{q^3} + \frac{7.388\ldots}{q^4} + \mathcal{O}\left(\frac{1}{q^5}\right) , \quad (4.44)$$

$$r(q) = \frac{\pi}{2} \frac{\left(1 - 2\,\Delta_\psi^R\right) \tan\left(\pi\,\Delta_\psi^R\right)}{q-1} \Delta_\psi^R \approx \frac{1.233\ldots}{q^3} - \frac{2.456\ldots}{q^4} + \mathcal{O}\left(\frac{1}{q^5}\right) . \quad (4.45)$$

The fact that the first terms are the same is no coincidence, it arises from the equality of the leading order terms in (4.42). Now we can find the entropies behaviour at large q:

$$\frac{1}{N}\left(S^R - S^I\right) \overset{q\gg 1}{\approx} \frac{3.281\ldots}{q^3} + \mathcal{O}\left(\frac{1}{q^4}\right) . \quad (4.46)$$

The first thing to notice is that we find in the strict $q \to \infty$ that the entropies coincide. Apart from this we see that for $q \gg 1$ (where the above approximation is valid) the entropy of the rational branch dominates the one of the irrational branch. But we can extend this now to arbitrary q, using the behaviour of the derivatives of the entropies ($i(q)$ and $r(q)$). The numerical results shown in Figure 4.5 show that $i(q) > r(q)$. This means that the slope of the rational entropy is always smaller than the irrational one and hence we have $S^R > S^I$ for all (finite) q, indicating that the rational branch is the dominant saddle.

4.3.2 Other M/N values

The procedure outlined in the previous section we have followed also for the other values of M/N around 10^{-2}, 10^1 and 10^2. As it turns out the behaviour is always (qualitatively) similar. We indeed find that the rational branch is the dominant

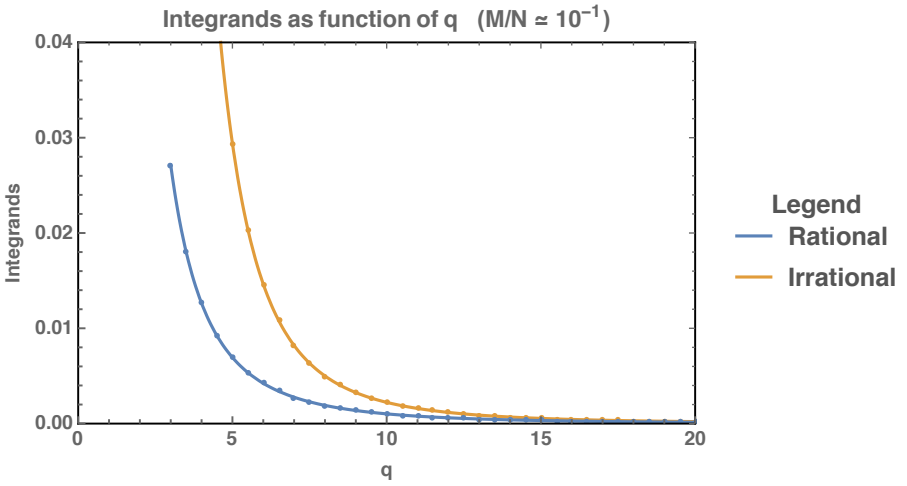

Figure 4.5: *Here we show the integrands from* (4.40) *for both branches. The dots indicate the numerical evaluation of these quantities, whilst the solid lines indicate the integrands with the fitted* Δ_ψ *behaviour of* q*. We only plot a subset of the computed* q *values for clarity.*

saddle for all the M/N values. The larger the value of M/N the smaller the difference between the entropies becomes. This can be deduced from Figure 4.3, where the branches flow to the same point as we increase M/N. Let us in this section mention the $M/N = 1$ case, where we have more analytical control for the rational branch.

Let us first consider this rational branch: in this case we can always solve the exact dependence of the conformal dimension on q (see appendix 4.A):

$$\Delta_\psi^R = \frac{1}{2q} \,, \tag{4.47}$$

which coincides with the leading order behaviour that we found for other M/N values. Plugging this expression for the conformal dimension into the integrand $r(q)$, see (4.40), yields

$$r(q) = \frac{\pi}{4q^2} \tan\left(\frac{\pi}{2q}\right) \,, \tag{4.48}$$

and hence we can compute the zero temperature entropy for the rational case:

$$\frac{S^R}{N} = \frac{1}{2} \log\left(\cos\left(\frac{\pi}{2q}\right)\right) + C \,. \tag{4.49}$$

To fix the integration constant C we will consider the limit $q \to \infty$. We can follow exactly [41], section II.C. There the results in a large q expansion are obtained:

$$G_\psi = \frac{1}{2}\,\mathrm{sgn}(\tau) + \frac{1}{2q} g_\psi(\tau) \ , \tag{4.50}$$

$$G_\phi = -\delta(\tau) + \frac{1}{2q}\, g_\phi(\tau) \ , \tag{4.51}$$

$$\frac{\log Z}{N} = \frac{1}{2}\log 2 + \frac{1}{4q^2}\left(-\frac{v^2}{4} + v\,\tan\frac{v}{2}\right) \ . \tag{4.52}$$

Note that v is an integration constant related to βJ [41]. The $q \to \infty$ limit reduces the model to free fermions. It also allows us to fix the constant C since:

$$\lim_{q\to\infty} \frac{1}{2}\log\left(\cos\left(\frac{\pi}{2q}\right)\right) = 0 \ , \tag{4.53}$$

which, in combination with (4.49), yields

$$\lim_{q\to\infty} \frac{S^R}{N} = C = \frac{1}{2}\log 2 \ , \tag{4.54}$$

where we used the above observation that it should reduce to a free fermion entropy in this limit. We will see that the irrational entropy also behaves similarly as $C_2 + f\left(\frac{1}{q}\right)$ and hence for $q \to \infty$ we find that it has the same integration constant, i.e. $C_2 = C$.

Just as in the $M/N \neq 1$ cases, we can't solve analytically the q dependence of the irrational solution. We did manage to find a good fit by $\Delta_\psi^I = -\frac{1}{2q} + \frac{1}{q-1}$, which matches the numerical results well. Note it also reduces to $\frac{1}{2q}$ for large q. In Figure 4.6 we plot the numerical results for both the rational and irrational cases. To conclude which of the entropies is bigger (i.e. which is the dominant saddle) we will investigate again the integrands as a function of q, see Figure 4.7. From this plot we can see that the irrational integrand is (as in all the M/N cases) bigger than the rational one and as q increases their difference decreases.

We now investigate the behaviour for large q. By using the approximate solution (see Figure 4.6) we can obtain an expression for $i(q)$ at large q. This is done by using the approximate solution in the integrand and expanding:

$$i(q) \overset{q\gg 1}{=} \frac{\pi(q+1)((q-2)q-1)\tan\left(\frac{\pi(q+1)}{2(q-1)q}\right)}{4(q-1)^3q^2} = \frac{\pi^2}{8q^3} + \frac{\pi^2}{2q^4} + \mathcal{O}\left(\frac{1}{q^5}\right) \ . \tag{4.55}$$

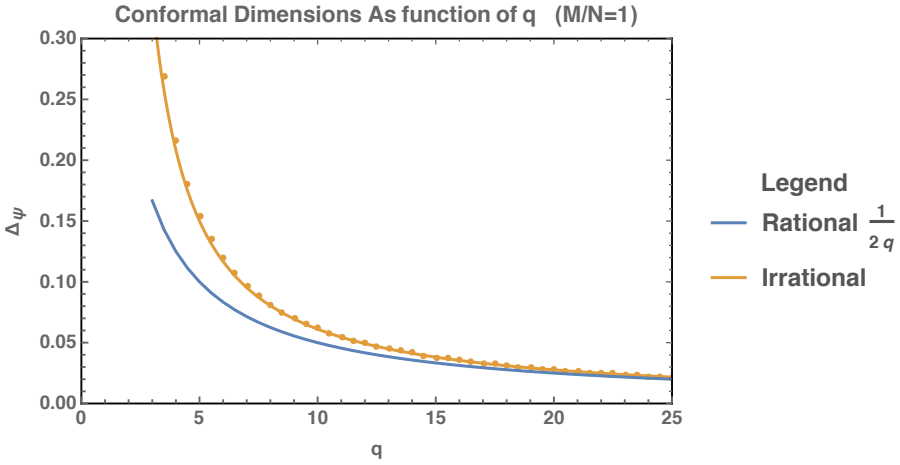

Figure 4.6: *Here we plot the dependence of the conformal dimensions on the number of interactions q. Although we do not have the exact results for the irrational case, it is well approximated by the guessed solution in green. it can be seen that for large enough q the solutions approach one another.*

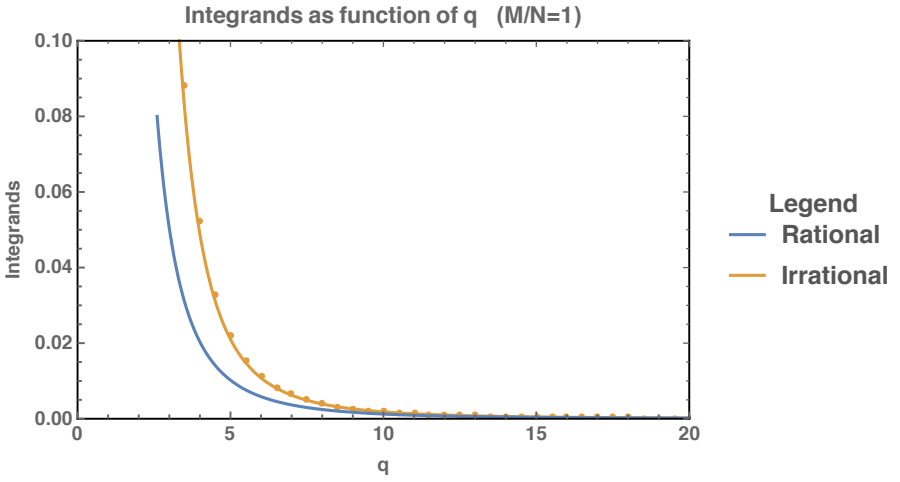

Figure 4.7 *This plot shows the dependence of the integrands at $M/N = 1$ on the number of interactions q. We can see that the irrational integrand ($i(q)$) is larger than the rational one ($r(q)$).*

From this we can find the leading order behaviour in the difference between the entropies:

$$\frac{1}{N}\left(S^R - S^I\right) \overset{q\gg 1}{\approx} \frac{\pi^2}{6q^3} + \mathcal{O}\left(\frac{1}{q^4}\right) , \tag{4.56}$$

where the integration constants cancelled each other, such that only q dependent terms remain (recall that as $q \to \infty$ we should obtain the free fermion entropy). We also used the rational entropy behaviour for large q, which can be obtained from (4.49):

$$\frac{1}{2}\log\left(\cos\left(\frac{\pi}{2q}\right)\right) = -\frac{\pi^2}{16q^2} - \frac{\pi^4}{384q^4} + \mathcal{O}\left(\frac{1}{q^5}\right) . \tag{4.57}$$

We can then conclude that for large q: $S^I < S^R$. Further more since the slope of S^R is always smaller than that of S^I (since $i(q) > r(q)$) we find that this conclusion holds for any q. So, as for the other values of M/N, we find that the rational branch is the dominant saddle.

4.4 Chaos

In this section we will investigate the chaos or Lyapunov exponent of the model as a function of the ratio M/N. We will first review shortly the basics of such a computation and then move on to our model. The main tool for quantifying quantum chaos are so called Out of Time Order Correlators (OTOC) [171, 186–189]. For a more elaborate review of chaos and calculating these correlators see chapter 8 in [42], the first section of [34] and a discussion in [184].

From a quantum mechanical point of view we can take two arbitrary Hermitian operators V and W and consider the commutator $[W(it), V(0)]$ (with real time $t \in \mathbb{R}$). The argument of the operator is imaginary since we consider it to be Euclidean time, as will be the case for our operators later on. The commutator describes the influence of small changes of V on later measurements of W (or the other way around). One particular indicator of these effects of chaos, which we will also use, puts the operators on the thermal circle [34]:

$$\langle\, [V(0), W(it)]\, [V(\beta/2), W(\beta/2 + it)]\, \rangle , \tag{4.58}$$

where the brackets $\langle\rangle$ denote the thermal trace, the precise factors of β will not be important for us. For late enough times t (to be precise, between the dissipation

and scrambling time [34]), quantum chaos dictates that this correlator will grow exponentially. By considering all the terms that arise in the above correlator one can show [34] that the exponential growth of the correlator arises due to the exponential behaviour of the related correlator:

$$F(t) = \langle\, V(0)\, W(\beta/4 + it)\, V(\beta/2)\, W(3\beta/4 + it) \,\rangle\ . \tag{4.59}$$

These out of time order correlators $F(t)$ are usually studied in the context of quantum chaos, and we will use these as well. Schematically the OTOC (4.59) behaves as [34, 42, 188]:

$$F(t) = 1 - \frac{1}{N} e^{\lambda_L t} + \dots \tag{4.60}$$

The exponent λ_L is called the Lyapunov exponent and it quantifies the chaos of the system. In the coming section our goal is to extract this Lyapunov exponent from the OTOCs. In general one can follow two approaches. The most obvious one is to compute the full four point function and continue these Euclidean correlators to real time. An easier option, however, is to consider the so called retarded kernel and its eigenfunctions [33, 37, 188]. In the context of ladder diagrams, kernels are the operators that add one more ladder to the diagram. For the OTOCs it has to be the retarded kernel due to the complex time contours specified by OTOCs similar to (4.58). For a review of this procedure including the complex time contours, ladder diagrams and the application to ordinary SYK see [42].

The key idea of this procedure is to consider an exponentially growing OTOC on which the kernel(s) are acting. Under the assumption of this exponential growth one can find that it is precisely the eigenfunctions of the kernel with eigenvalue one that govern the chaotic behaviour. More intuitively, the growth rate of OTOC is determined by the demand that adding another ladder should not change the total sum. In the rest of this section we explain this procedure in more detail.

4.4.1 Retarded kernels

Let us now turn to our model and consider the four point functions (or OTOCs) that we want to compute. We will consider the four point functions $\langle\, \psi\, \psi\, \psi\, \psi \,\rangle$, $\langle\, \psi\, \psi\, \phi\, \phi \,\rangle$, $\langle\, \phi\, \phi\, \psi\, \psi \,\rangle$ and $\langle\, \phi\, \phi\, \phi\, \phi \,\rangle$. This is because acting with kernels on these

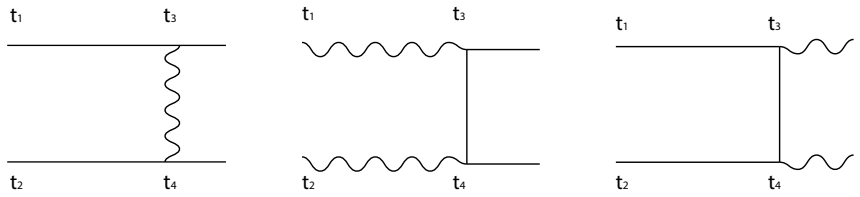

(a) K_{11} kernel **(b)** K_{21} kernel **(c)** K_{12} kernel

Figure 4.8: *Here we show the relevant kernels for the chaos computation. The subscripts of the kernels denote that they are elements of a matrix. The total matrix acts on a vector consisting of diagrams which starts with either two ψ or two ϕ lines.*

diagrams will result in mixing between them and hence we can not consider them separately. The explicit OTOCs we will consider are of the form:

$$F_{\psi\psi}(t_1, t_2) = \mathrm{Tr}\left[y\,\psi(t_1)\,y\,\psi(0)\,y\,\psi(t_2)\,y\,\psi(0)\right] \ , \tag{4.61}$$

where y is defined as $y^4 = \rho(\beta)$. Diagrammatically these OTOCs are four point functions (ladder diagrams) with an arbitrary large amount of rungs. The other combinations of ψ and ϕ listed above have similar expressions and are denoted by $F_{\psi\phi}$, $F_{\phi\psi}$ and $F_{\phi\phi}$. The two subscripts of F_{ij} denote the two incoming and two outgoing species, respectively.

Let us now consider all the (retarded) kernels necessary for our model, which we draw in Figure 4.8. Note that there is no kernel K_{22} since there is no such interaction in the Lagrangian. It then becomes clear that acting with the K_{12} and K_{21} kernels causes mixing between the four point functions. To get expressions for them we need first the necessary propagators in the diagrams. For the horizontal propagators we need the retarded ones (due to the complex time contours, see [42]):

$$\begin{aligned} G_R^{\psi}(t) &= \left(\langle\psi^i(it)\,\psi^i(0)\rangle + \langle\psi^i(0)\,\psi^i(it)\rangle\right)\theta(t) \ , \\ G_R^{\phi}(t) &= \left(\langle\phi^a(it)\,\phi^a(0)\rangle - \langle\phi^a(0)\,\phi^a(it)\rangle\right)\theta(t) \ . \end{aligned} \tag{4.62}$$

Recall that the arguments are imaginary since we consider complex Euclidean time. We can then use the finite temperature two point functions from (4.38) (at $\tau > 0$) to find:

$$G_R^{\psi}(t) = \frac{2\,A\,\cos(\pi\Delta_\psi)\,\pi^{2\Delta_\psi}}{\left(\beta\sinh\left(\frac{\pi t}{\beta}\right)\right)^{2\Delta_\psi}}\theta(t) \ . \tag{4.63}$$

And similarly for ϕ:

$$G_R^\phi(t) = -\frac{2i\,B\,\sin(\pi\Delta_\phi)\,\pi^{2\Delta_\phi}}{\left(\beta\sinh\left(\frac{\pi t}{\beta}\right)\right)^{2\Delta_\phi}}\theta(t)\ . \tag{4.64}$$

Lastly we need the ladder rung (lr) propagator,[1] which is obtained by simply continuing the Euclidean propagator $\tau \mapsto it + \frac{\beta}{2}$:

$$G_{lr}^x(t) = b_x \frac{\pi^{2\Delta_x}}{\left(\beta\cosh\left(\frac{\pi t}{\beta}\right)\right)^{2\Delta_x}}\ . \tag{4.65}$$

Here x denotes ψ or ϕ and b_x denotes A or B respectively. The form of this propagator is the same for fermions and scalars since we only need to consider $\tau > 0$ here.

We can then write down the expressions for the kernels. Note that each vertex gets a factor i from inserting it on a Lorentzian time fold in the contour and apart from this we also give K_{11} and K_{21} an additional minus sign due to the ordering of the contour (see also [44, 190]). The resulting form of the kernels is:

$$\begin{aligned}
K_{11} &= 2\sqrt{\frac{M}{N}}\,J\,G_R^\psi(t_{13})\,G_R^\psi(t_{24})\,G_{lr}^\phi(t_{34})\ ,\\
K_{12} &= -2\sqrt{\frac{M}{N}}J\,G_R^\psi(t_{13})\,G_R^\psi(t_{24})\,G_{lr}^\psi(t_{34})\ ,\\
K_{21} &= 2\sqrt{\frac{N}{M}}\,J\,G_R^\phi(t_{13})\,G_R^\phi(t_{24})\,G_{lr}^\psi(t_{34})\ .
\end{aligned} \tag{4.66}$$

The times $t_{ij} = t_i - t_j$ are shown in Figure 4.8.

4.4.2 Integral matrix equation

Now that we have obtained the retarded kernels we go back to our four out of time order correlators. All together they obey an integral matrix equation as shown in Figure 4.9, this is a generalization of the one particle version seen for example in [42]. In the figure we have put all the OTOCs in a four component vector seen on the very left (and right) side. These are exactly the OTOCs we named $F_{\psi\psi}$, $F_{\psi\phi}$, $F_{\phi\psi}$ and $F_{\phi\phi}$ before. Our (drawing) conventions are such that for the very

[1] These are also called left-right propagators since often the ladder diagrams are drawn vertically instead of horizontally, in which case the ladder rung propagates from left to right.

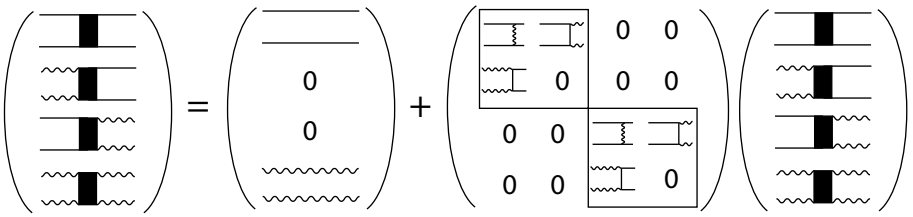

Figure 4.9: *Here we show the matrix integral equation that the OTOCs obey. The black boxes indicate the arbitrary large amount of rungs in the ladder diagrams. The very left vector consists out of all the OTOCs, the first vector on the right hand side denotes the zeroth order contributions to these and the last term is the kernel acting upon the vector of the four point functions. The matrix product also includes a convolution between the kernels and the OTOCs. Notice that the* 4×4 *kernel matrix has a* 2×2 *block diagonal structure.*

left vector the times t_1 and t_2 are on the top left and bottom left of each four point function, respectively.

The first vector on the right hand side denotes the free contributions to the four point functions. Clearly $F_{\psi\phi}$ and $F_{\phi\psi}$ don't have these since there is no such free propagator. The matrix consists out of the retarded kernels discussed above and depicted in Figure 4.8. Note that the matrix product in the last term also has an implicit convolution (which we will explicitly compute later on).

Quantum chaos implies that for late enough times these OTOCs will show exponentially growing behaviour, as discussed shortly in the introduction of this section. So let us make the following exponential growth ansatz:

$$F_{ij}(t_1, t_2) = f_{ij}(t_1 - t_2)\, e^{\frac{\lambda_L}{2}(t_1+t_2)} \ , \tag{4.67}$$

where i, j can denote ψ or ϕ and f_{ij} denote functions of the time difference. Under the assumption of exponential growth the matrix equation Figure 4.9 will simplify due to suppression of the zeroth order contributions. In fact, as one can easily check, the free diagrams will exponentially vanish compared to the exponential growth of the other terms. We are then left with the following equation:

$$\begin{pmatrix} F_{\psi\psi} \\ F_{\phi\psi} \\ F_{\psi\phi} \\ F_{\phi\phi} \end{pmatrix} = \begin{pmatrix} K_{11} & K_{12} & 0 & 0 \\ K_{21} & 0 & 0 & 0 \\ 0 & 0 & K_{11} & K_{12} \\ 0 & 0 & K_{21} & 0 \end{pmatrix} \begin{pmatrix} F_{\psi\psi} \\ F_{\phi\psi} \\ F_{\psi\phi} \\ F_{\phi\phi} \end{pmatrix} \ . \tag{4.68}$$

The Fs now obey the ansatz (4.67) and the matrix multiplication still involves the convolutions. However, we see that the problem can in fact be reduced to two identical problems because of the block diagonal structure. Hence we don't have to refer to the outgoing lines of the OTOCs (the second subscript of the F_{ij}) and consider simply:

$$\begin{pmatrix} F_\psi \\ F_\phi \end{pmatrix} = \begin{pmatrix} K_{11} & K_{12} \\ K_{21} & 0 \end{pmatrix} \begin{pmatrix} F_\psi \\ F_\phi \end{pmatrix} \ . \tag{4.69}$$

This leads to the following equations:

$$\begin{aligned} F_\psi(t_1,t_2) = \int_{-\infty}^{t_1} dt_3 \int_{-\infty}^{t_2} dt_4 [K_{11}(t_1,t_2;t_3,t_4)\, F_\psi(t_3,t_4) \\ + K_{12}(t_1,t_2;t_3,t_4)\, F_\phi(t_3,t_4)] \ , \end{aligned} \tag{4.70}$$

$$F_\phi(t_1,t_2) = \int_{-\infty}^{t_1} dt_3 \int_{-\infty}^{t_2} dt_4\, K_{21}(t_1,t_2;t_3,t_4) F_\psi(t_3,t_4) \ , \tag{4.71}$$

where we have now explicitly written out the convolutions. The two equations are mixed and can be combined to give:

$$F_\psi(t_1,t_2) = (K_{11} * F_\psi)(t_1,t_2) + (K_{12} * (K_{21} * F_\psi))(t_1,t_2) \ . \tag{4.72}$$

4.4.3 Lyapunov exponents

To actually solve the integrals we need to find the functions $f_i(t_{12})$ in (4.67) such that (4.69) is satisfied. We take the following form of the functions, similar to [37, 42, 44, 190]:

$$\begin{aligned} F_\psi(t_1,t_2) &= C_\psi \frac{e^{-\frac{\pi h}{\beta}(t_1+t_2)}}{\left(\frac{\beta}{\pi}\cosh\left(\frac{\pi t_{12}}{\beta}\right)\right)^{2\Delta_\psi - h}} \ , \\ F_\phi(t_1,t_2) &= C_\phi \frac{e^{-\frac{\pi h}{\beta}(t_1+t_2)}}{\left(\frac{\beta}{\pi}\cosh\left(\frac{\pi t_{12}}{\beta}\right)\right)^{2\Delta_\phi - h}} \ . \end{aligned} \tag{4.73}$$

Here the C_i denote non-zero real constants, and we have h as the free exponential growth parameter. The Lyapunov exponent can be found by $\lambda_L = -\frac{2\pi h}{\beta}$.

The crucial integral for the computations is as follows[2]

$$\begin{aligned}&\int_{-\infty}^{t_1} dt_3 \int_{-\infty}^{t_2} dt_4 \left(f_s(t_{13})\, f_s(t_{24})\right)^{\frac{2}{d}} f_c(t_{34})^{2-\frac{2}{d}-h}\, e^{-\frac{\pi h}{\beta}(t_3+t_4)} = \\ &= \frac{\Gamma\left(\frac{d-2}{d}\right)^2 \Gamma\left(\frac{2}{d}-h\right)}{\Gamma\left(-h-\frac{2}{d}+2\right)} f_c(t_{12})^{\frac{2}{d}-h}\, e^{-\frac{\pi h}{\beta}(t_1+t_2)} \ ,\end{aligned} \tag{4.74}$$

where d is, for now, variable and we have defined

$$f_s(t_{ij}) = \frac{\pi}{\beta \sinh\left(\frac{\pi t_{ij}}{\beta}\right)} \ , \qquad f_c(t_{ij}) = \frac{\pi}{\beta \cosh\left(\frac{\pi t_{ij}}{\beta}\right)} \ . \tag{4.75}$$

Using the above integral identity we can then calculate the following integrals, reminiscent of eigenvalue equations:

$$\begin{aligned}&\int dt_3\, dt_4\, K_{11}(t_1,t_2;t_3,t_4) F^{\psi}(t_3,t_4) = k_{11}\, F^{\psi}(t_1,t_2) \ , \\ &\int dt_3\, dt_4\, K_{12}(t_1,t_2;t_3,t_4) F^{\phi}(t_3,t_4) = \frac{C_\phi}{C_\psi}\, k_{12}\, F^{\psi}(t_1,t_2) \ , \\ &\int dt_3\, dt_4\, K_{21}(t_1,t_2;t_3,t_4) F^{\psi}(t_3,t_4) = \frac{C_\psi}{C_\phi}\, k_{21}\, F^{\phi}(t_1,t_2) \ .\end{aligned} \tag{4.76}$$

The eigenvalues k_{ij} are found to be

$$\begin{aligned}k_{11} &= 8\sqrt{\frac{M}{N}}\, J\, A^2 B\, \cos^2\left(\frac{\pi}{d}\right) \frac{\Gamma\left(\frac{d-2}{d}\right)^2 \Gamma\left(\frac{2}{d}-h\right)}{\Gamma\left(-h-\frac{2}{d}+2\right)} \ , \\ k_{12} &= -8\sqrt{\frac{M}{N}}\, J\, A^3\, \cos^2\left(\frac{\pi}{d}\right) \frac{\Gamma\left(\frac{d-2}{d}\right)^2 \Gamma\left(\frac{2}{d}-h\right)}{\Gamma\left(-h-\frac{2}{d}+2\right)} \ , \\ k_{21} &= -8\sqrt{\frac{N}{M}}\, J\, A B^2\, \sin^2\left(\pi\left(1-\frac{2}{d}\right)\right) \frac{\Gamma\left(\frac{4}{d}-1\right)^2 \Gamma\left(\frac{2\,(d-2)}{d}-h\right)}{\Gamma\left(\frac{4}{d}-h\right)} \ .\end{aligned} \tag{4.77}$$

where, importantly, d is now fixed by virtue of our expressions for F and G as

$$d = \frac{1}{\Delta_\psi} \tag{4.78}$$

We can now use the above k_{ij} along with (4.76) in the integral equation (4.72), to get:

$$F_\psi(t_1,t_2) = (k_{11} + k_{21}\, k_{12})\, F_\psi(t_1,t_2) \ . \tag{4.79}$$

[2] As a side note, one could use substitutions of the form $z = e^{i\tau}$ to simplify the integrals, making it easier to solve them. This is done in e.g. [37, 42].

Of course, one could also have used the eigenfunctions ((4.76)) first in (4.70) and afterwards solved the mixing. Either way the equation resulting from the chaos regime is:

$$k_{11} + k_{21}\, k_{12} = 1 \ . \tag{4.80}$$

We pick then some fixed M/N (which fixes Δ_ψ and A^2B) and numerically solve this equation for the Lyapunov exponent $\lambda_L = -\frac{2\,\pi\,h}{\beta}$, which yields the solution $h = -1$. As it turns out, for $h = -1$ all the M/N dependence drops out and we find in fact maximal chaos for all values of M/N:

$$\lambda_L = \frac{2\,\pi}{\beta} \ . \tag{4.81}$$

Motivated by these numerical results we analytically checked whether $k_{11} + k_{21}\, k_{12} = 1$ for $h = -1$. To do so we use the identities from (4.21) and also the following:

$$\sin(\pi z) = \frac{\pi}{\Gamma(z)\,\Gamma(1-z)} \ . \tag{4.82}$$

Using these identities and the expressions for A^2B, we obtain the following simplified expressions, valid at $h = -1$:

$$k_{11} = \frac{\Delta_\psi}{1-\Delta_\psi} \ , \tag{4.83}$$

$$k_{12}\, k_{21} = 1 - \frac{\Delta_\psi}{1-\Delta_\psi} \ . \tag{4.84}$$

Hence even though k_{11} and $k_{12}\, k_{21}$ individually depend on M/N (since Δ_ψ does), the combined result exactly cancels.

Lastly let us shortly mention another method of obtaining the chaos, outlined in [44,190]. In these articles the approach is to take the matrix of kernel eigenvalues, the k_{ij}, and diagonalize it. Afterwards one of the eigenvalues is set to one. Let us consider this matrix:

$$\begin{pmatrix} k_{11} & k_{12} \\ k_{21} & 0 \end{pmatrix} \ , \tag{4.85}$$

for which the resulting eigenvalues are $k_\pm = \frac{1}{2}\left(k_{11} \pm \sqrt{k_{11}^2 + 4\, k_{21}\, k_{12}}\right)$. The growing behaviour is found when $k_+ = 1$, which amounts to $k_{11} + k_{21} k_{12} = 1$, consistent with our method.

4.5 Discussion

In this article we have investigated new SYK-like models with M bosons and N fermions. The parameter M/N determines the behaviour of the model and for $M = N$ our model is related to the supersymmetric SYK model. We have found that there are two families of solutions in the model, distinguished by their conformal dimensions which we plotted as a function of M/N in Figure 3. For $M = N$ the rational solution coincides with the supersymmetric solution found in [41]. Another interesting regime is the $M/N \to \infty$ limit. We have shown that the solution of the fermionic conformal dimension in this limit is given by:

$$\Delta_\psi = \frac{1}{q_{\text{SYK}}} \ .$$

This shows us that in this limit our model and SYK have the same behaviour, i.e. they have the same infrared fixed point.
We have shown that the rational branch is the dominant saddle for arbitrary values of M/N (and arbitrary q) . For the generic values of M/N we have shown this by first solving the problem numerically and then fitting it (with high accuracy). When $M = N$ it can be done in a more analytical manner.

Apart from this we investigated the Lyapunov exponent and found it to be $\lambda_L = 2\pi T$, independent of M/N. This is due to some non trivial cancellations in the M/N dependences. Due to the maximal chaos the model has a holographic interpretation as a black hole. It would be interesting to understand the role of M/N in this holographic description. Concretely it would be interesting to find the Schwarzian for this model, in particular the coefficient in front of the Schwarzian action, related to the heat capacity, and its dependence on M/N.

Appendices

4.A The model for a q-point interaction

In this appendix we will shortly show how the model and some results change when we consider an interaction vertex of degree q, so an interaction with one boson and $q-1$ fermions. The integer q is supposed to be odd, but later we will continue it to arbitrary real values. The model we consider in the main text has $q = 3$. When we apply this, the coupling $\frac{i}{2}C_{aij}\phi^a\psi^i\psi^j$ goes to $\frac{i}{(q-1)!}C_{ai_1i_2\ldots i_{q-1}}\phi^a\psi^{i_1}\ldots\psi^{i_{q-1}}$.

Integrating out the bosons would lead to a Hamiltonian with a vertex containing $2(q-1)$ fermions. One can thus relate this to the interaction parameter $q_{\rm SYK}$ in [37] by $(q-1)=\frac{1}{2}q_{\rm SYK}$. The disorder average is now chosen as follows:

$$\langle C^2\rangle = \frac{(q-1)!J}{N^{-3/2+q}M^{1/2}} \ . \tag{4.86}$$

Once again we can take the conformal form (see (4.17)) for the two point functions. By following the computations done for the $q=3$ case we find that the conformal symmetry is present under the condition that (compare to (4.25)):

$$\Delta_\phi + (q-1)\Delta_\psi = 1 \ . \tag{4.87}$$

The equations for the constants in the two point functions, $A^{q-1}B$, yield (compared to (4.23)):

$$A^{q-1}B = \sqrt{\frac{N}{M}}\,\frac{(1-2\Delta_\psi)\tan(\pi\Delta_\psi)}{2\pi(q-1)J} \ , \tag{4.88}$$

$$A^{q-1}B = \sqrt{\frac{M}{N}}\,\frac{(1-2(q-1)\Delta_\psi)}{2\pi J\tan(\pi(q-1)\Delta_\psi)} \ . \tag{4.89}$$

The resulting transcendental equation for the conformal dimensions reads:

$$\frac{N}{M}\,\tan(\pi\Delta_\psi)\tan(\pi(q-1)\Delta_\psi) = (q-1)\frac{1-2(q-1)\Delta_\psi}{1-2\Delta_\psi} \ . \tag{4.90}$$

One may check that the rational value $\Delta_\psi=\frac{1}{2q}$ is a solution at $M=N$. Furthermore as we take the limit $M/N\to\infty$ we see that we find the solution:

$$\Delta_\psi = \frac{1}{2(q-1)} \ . \tag{4.91}$$

Using the above found relation $(q-1)=\frac{1}{2}q_{\rm SYK}$ we see that this is equal to $\frac{1}{q_{\rm SYK}}$.

Part III

Quark-Gluon Plasmas

The third part of the thesis concerns magnetohydrodynamics at heavy ion collisions. In particular, we discuss heavy ion collisions in the presence of strong electromagnetic fields. During the heavy ion collisions a quark-gluon plasma is formed, and we study how its expansion is affected by the electromagnetic fields by investigating flow coefficients. This is done using a combination of semi analytical and numerical methods.

Chapter 5

Magnetohydrodynamics at Heavy Ion Collisions

> *In the beginning the Universe was created. This has made many people very angry and has been widely regarded as a bad move.*
>
> – Douglas Adams, *The Restaurant at the End of the Universe*

Shortly after the big bang, up to a few microseconds afterwards to be more precise, the universe is thought to have been in a quark gluon plasma state. It is no surprise then, that such plasmas are widely studied, mostly in order to investigate the early nature of the universe.[1] In this chapter we will discuss such quark gluon plasmas, which also arise in heavy-ion collisions. In particular, we will investigate them in the presence of large electromagentic fields, which are present during the heavy-ion collisions. We will be studying very practical aspects of the quark gluon plasma (QGP) and its expansion. This also means that we will have a more vague link to black hole physics, which we have so far been discussing in the thesis. There is, however, a relation by the AdS/QCD correspondence. Similar to the SYK model of the previous chapter, it is expected that the field theory (in this case QCD) has a gravitational dual. This was also the point of study in [31], where the authors managed to compute quantities relevant for the QGP using five-dimensional black hole physics. Furthermore, there is a correspondence between fluids and gravity [191]. In essence this correspondence tells us that the holographic description of fluids can be recast to the hydrodynamic gradient expansion.

A quick overview of this chapter: we will start by a long introduction, in which we explain the different kinds of electromagnetic fields are present in non-central

[1] The quark gluon plasma might also exist in other places, such as the interior of neutron stars.

heavy-ion collisions. In the second section we discuss the numerical model setup, the computation of the electromagnetic fields and the different hydrodynamic flows we will compute. In the result section, we show the different flows and their dependence on parameters used in the model.

5.1 Introduction

In fact, large magnetic fields $\vec{B}$ are produced in all non-central heavy-ion collisions (those with nonzero impact parameter) by the moving and positively charged spectator nucleons that "miss", flying past each other rather than colliding, as well as by the nucleons that participate in the collision. Estimates obtained by applying the Biot-Savart law to collisions with an impact parameter $b = 4$ fm yield $e|\vec{B}|/m_\pi^2 \approx$ 1-3 about 0.1-0.2 fm/c after a RHIC collision with $\sqrt{s} = 200$ AGeV and $e|\vec{B}|/m_\pi^2 \approx$ 10-15 at some even earlier time after an LHC collision with $\sqrt{s} = 2.76$ ATeV [56, 192–198]. The interplay between these magnetic fields and quantum anomalies has been of much interest in recent years, as it has been predicted to lead to interesting phenomena including the chiral magnetic effect [192, 199] and the chiral magnetic wave [200, 201]. This makes it imperative to establish that the presence of an early-time magnetic field can, via Faraday's Law and the Lorentz force, have observable consequences on the motion of the final-state charged particles seen in the detectors [56]. Since the plasma produced in collisions of positively charged nuclei has a (small) net positive charge, electric effects – which is to say the Coulomb force – can also yield observable consequences to the motion of charged particles in the final state. These electric effects are distinct from the consequences of a magnetic field first studied in Ref. [56], but comparable in magnitude. Our goal in this chapter will be a qualitative, perhaps semi-quantitative, assessment of the observable effects of both magnetic and electric fields, arising just via the Maxwell equations and the Lorentz force law, so that experimental measurements can be used to constrain the strength of the fields and to establish baseline expectations against which to compare any other, possibly anomalous, experimental consequences of $\vec{B}$.

In previous work [56] three of the authors noted that the magnetic field produced in a heavy-ion collision could result in a measurable effect in the form of a charge-odd contribution to the directed flow coefficient Δv_1. This contribution has the opposite sign for positively vs. negatively charged hadrons in the final state and is odd

in rapidity. However, the authors of [56] neglected to observe that a part of this charge-odd, parity-odd effect originates from the Coulomb interaction. In particular it originates from the interaction between the positively charged spectators that have passed by the collision and the plasma produced in the collision, as will be explained in detail below.

The study in Ref. [56] was simplified in many ways, including in particular by being built upon the azimuthally symmetric solution to the equations of relativistic viscous hydrodynamics constructed by Gubser in Ref. [202]. Because this solution is analytic, various practical simplifications in the calculations of Ref. [56] followed. In reality magnetic fields do not arise in azimuthally symmetric collisions. The calculations of Ref. [56] were intended to provide an initial order of magnitude estimate of the $\vec{B}$-driven, charge-odd, rapidity-odd contribution to Δv_1 in heavy-ion collisions with a nonzero impact parameter, but the authors perturbed around an azimuthally symmetric hydrodynamic solution for simplicity. Also, the radial profile of the energy density in Gubser's solution to hydrodynamics is not realistic. Here, we shall repeat and extend the calculation of Ref. [56], this time building the perturbative calculation of the electromagnetic fields and the resulting currents upon numerical solutions to the equations of relativistic viscous hydrodynamics simulated within the `iEBE-VISHNU` framework [203] that provide a good description of azimuthally anisotropic heavy-ion collisions with a nonzero impact parameter.

The idea of Ref. [56] is to calculate the electromagnetic fields, and then the incremental contribution to the velocity fields of the positively and negatively charged components of the hydrodynamic fluid (aka the electric currents) caused by the electromagnetic forces, in a perturbative manner. A similar conclusion have been reached in [204] and [205]. One first computes the electric and magnetic fields $\vec{E}$ and $\vec{B}$ using the Maxwell equations as we describe further below. Then, at each point in the fluid, one transforms to the local fluid rest frame by boosting with the local background velocity field $\vec{v}_{\rm flow}$. Afterwards one computes the incremental drift velocity $\vec{v}_{\rm drift}$ caused by the electromagnetic forces in this frame by demanding that the electromagnetic force acting on a fluid unit cell with charge q is balanced by the drag force. One then boosts back to the lab frame to obtain the total velocity field that now includes both $\vec{v}_{\rm flow}$ and $\vec{v}_{\rm drift}$, with $\vec{v}_{\rm drift}$ taking opposite signs for the positively and negatively charged components of the fluid. The authors of Ref. [56] then use a standard Cooper-Frye freeze out analysis to show that the electromagnetic forces acting within the hydrodynamic fluid result in a contribution

to the charge-odd directed flow parameter $\Delta v_1 \equiv v_1(h^+) - v_1(h^-)$. We shall provide the (standard) definition of the directed flow v_1 in Section 5.2. The charge-odd contribution Δv_1 is small but distinctive: in addition to being anti-symmetric under the flip of charge, it is also antisymmetric under flipping the rapidity. That the contribution has opposite sign for oppositely charged hadrons is easy to understand: it results from an electric current in the plasma. The fact that it has opposite sign at positive and negative rapidity can also easily be understood, as we explain in Figure 5.1 and below.

As illustrated in Figure 5.1, there are three distinct origins for a sideways push on charged components of the fluid, resulting in a sideways current:

1. *Faraday:* as the magnetic field decreases in time (see the bottom panel of Figure 5.3 below), Faraday's law dictates the induction of an electric field and, since the plasma includes mobile charges, an electric current. We denote this electric field by $\vec{E}_F$. Since $\vec{E}_F$ curls around the (decreasing) $\vec{B}$ that points in the y-direction, the sideways component of E_F points in opposite directions at opposite rapidity, see Figure 5.1.

2. *Lorentz:* since the hydrodynamic fluid exhibits a strong longitudinal flow velocity $\vec{v}_{\rm flow}$ denoted by $\vec{u}$ in Figure 5.1, which points along the beam direction (hence perpendicular to $\vec{B}$), the Lorentz force exerts a sideways push on charged particles in opposite directions at opposite rapidity. Equivalently, upon boosting to the local fluid rest frame in which the fluid is not moving, the lab frame $\vec{B}$ yields a fluid frame $\vec{E}$ whose effects on the charged components of the fluid are equivalent to the effects of the Lorentz force in the lab frame. We denote this electric field by $\vec{E}_L$. Both $\vec{E}_F$ and $\vec{E}_L$ are of magnetic origin.

3. *Coulomb:* The positively charged spectators that have passed the collision zone exert an electric force on the charged plasma produced in the collision, which again points in opposite directions at opposite rapidity. We denote this electric field by $\vec{E}_C$. As we noted above, the authors of Ref. [56] did not identify this contribution, even though it was correctly included in their numerical results.

As is clear from their physical origins, all three of these electric fields — and the consequent electric currents — have opposite directions at positive and negative rapidity. It is also clear from Figure 5.1 that $\vec{E}_F$ and $\vec{E}_C$ have the same sign, while

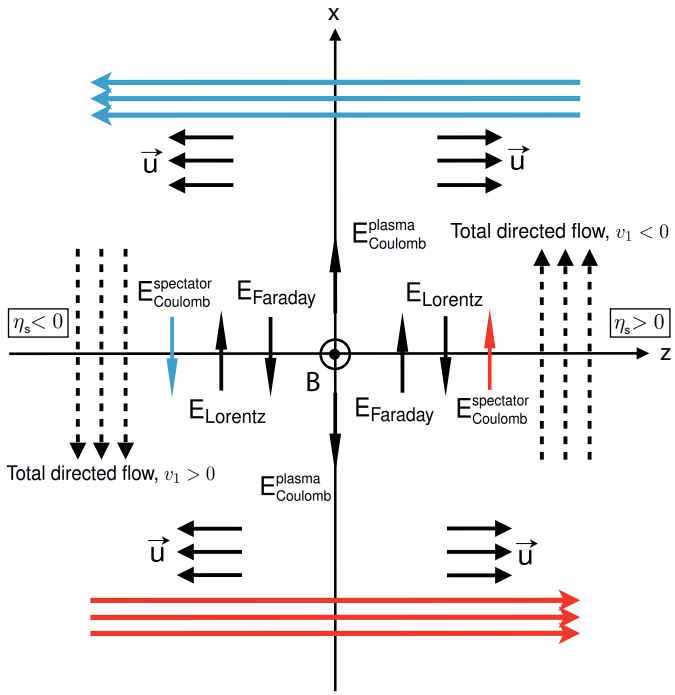

Figure 5.1: *Schematic illustration of how the magnetic field $\vec{B}$ in a heavy-ion collision results in a directed flow of electric charge, Δv_1. The collision occurs in the z-direction, meaning that the longitudinal expansion velocity $\vec{u}$ of the conducting QGP produced in the collision points in the $+z$ $(-z)$ direction at positive (negative) z. We take the impact parameter vector to point in the $+x$ direction, choosing the nucleus moving toward positive (negative) z to be located at negative (positive) x. The trajectories of the spectators that "miss" the collision because of the nonzero impact parameter are indicated by the red and blue arrows. This configuration generates a magnetic field $\vec{B}$ in the $+y$ direction, as shown. The directions of the electric fields (and hence currents) due to the Faraday, Lorentz and Coulomb effects are shown. The two different Coulomb contributions are indicated, one due to the force exerted by the spectators and the other coming from Coulomb forces within the plasma. The dashed arrows indicate the direction of the directed flow of positive charge in the case where the Faraday + spectator Coulomb effects are on balance stronger than the Lorentz effect. Hence, the total directed flow in this example corresponds to $v_1 < 0$ $(v_1 > 0)$ for positive charges at spacetime rapidity $\eta_s > 0$ $(\eta_s < 0)$, and opposite for negative charges.*

$\vec{E}_L$ opposes them. Hence, the sign of the total rapidity-odd, charge-odd, Δv_1 that results from the electric current driven by these electric fields depends on whether $\vec{E}_F + \vec{E}_C$ or $\vec{E}_L$ is dominant.

In this chapter we make three significant advances relative to the exploratory study of Ref. [56]. First, as already noted we build our calculation upon a realistic hydrodynamic description of the expansion dynamics of the droplet of matter produced in a heavy-ion collision with a nonzero impact parameter.

Second, we find that the same mechanism that produces the charge-odd Δv_1 also produces a similar charge-odd contribution to all the odd flow coefficients. The azimuthal asymmetry of the almond-shaped collision zone in a collision with nonzero impact parameter, its remaining symmetries under $x \leftrightarrow -x$ and $y \leftrightarrow -y$, and the orientation of the magnetic field $\vec{B}$ perpendicular to the beam and impact parameter directions together mean that the currents induced by the Faraday and Lorentz effects (illustrated in Figure 5.1) make a charge-odd and rapidity-odd contribution to all the odd flow harmonics, not only to Δv_1. We compute the charge-odd contribution to Δv_3 in addition to Δv_1 in this chapter.

Last but not least, we identify a new electromagnetic mechanism that generates another type of sideways current which generates a charge-odd, *rapidity-even*, contribution to the *elliptical* flow coefficient Δv_2. Although it differs in its symmetry from the three sources of sideways electric field above, it should be added to our list:

4. *Plasma:* As is apparent from the left panel of Figure 5.2 in Section 5.3 and as we show explicitly in that Section, there is a non-vanishing outward-pointing component of the electric field already in the lab frame, because the plasma (and the spectators) have a net positive charge. We denote this component of the electric field by $\vec{E}_P$, since its origin includes Coulomb forces within the plasma.

At the collision energies that we consider, $\vec{E}_P$ receives contributions both from the spectator nucleons and from the charge density deposited in the plasma by the nucleons participating in the collision. As illustrated below by the results in the left panel of Figure 5.2, the electric field will push an outward-directed current. As this field configuration is even in rapidity and odd under $x \leftrightarrow -x$ (which means that the radial component of the field is even under $x \leftrightarrow -x$), the current that it drives

will yield a *rapidity-even*, charge-odd, contribution to the *even* flow harmonics, see Figure 5.1. We shall demonstrate this by calculating the charge-dependent contribution to the radial flow, $\Delta\langle p_T\rangle$ (which can be thought of as Δv_0) and to the elliptic flow, Δv_2, that result from the electric field $\vec{E}_P$. Furthermore, we discover that these observables also receive a contribution from a component of the spectator-induced contribution to the electric field $\vec{E}_F + \vec{E}_L + \vec{E}_C$ that is odd under $x \leftrightarrow -x$ and even in rapidity.

In the next Section we set up our model. In particular, we explain the densities of the nucleons, the computation of the drift velocity, and the freezeout procedure from which we read off the charge-dependent contributions to the radial $\langle p_T\rangle$ and to the anisotropic flow parameters v_1, v_2 and v_3. In Section 5.3 we start by solving the Maxwell equations as analytically as possible. Afterward, we present numerical results for the (integrated) electromagnetic fields. Then in Section 5.4 we move on to the calculation of the flow coefficients, for collisions with both RHIC and LHC energies, for pions and for protons, for varying centralities and ranges of p_T, and for several values of the electrical conductivity σ of the plasma and the drag coefficient μm. The latter two being the properties of the plasma to which the effects that we analyse are sensitive. Finally in Section 5.5 we discuss the validity of the various approximations used in our calculations, discuss other related work, and present an outlook.

5.2 Model Setup

We simulate the dynamical evolution of the medium produced in heavy-ion collisions using the `iEBE-VISHNU` framework described in full in Ref. [203]. We take event-averaged initial conditions from a Monte-Carlo-Glauber model, obtaining the initial energy density profiles by first aligning individual bumpy events with respect to their second-order participant plane angles (the appropriate proxy for the reaction plane in a bumpy event) and then averaging over 10,000 events. The second order participant plane of the averaged initial condition, Ψ_2^{PP}, is rotated to align with the x-axis, which is to say we choose coordinates such that the averaged initial condition has $\Psi_2^{\mathrm{PP}} = 0$ and an impact parameter vector that points in the $+x$ direction. The hydrodynamic calculation that follows assumes longitudinal boost-invariance and starts at $\tau_0 = 0.4$ fm/c.[2] We then evolve the relativistic viscous

[2]Starting hydrodynamics at a different thermalization time, between 0.2 and 0.6 fm/c, only changes the hadronic observables by few percent. [206]

hydrodynamic equations for a fluid with an equation of state based upon lattice QCD calculations, choosing the s95p-v1-PCE equation of state from Ref. [207] which implements partial chemical equilibrium at $T_{\rm chem} = 150$ MeV. The kinetic freeze-out temperature is fixed to be 105 MeV to reproduce the mean p_T of the identified hadrons in the final state. Specifying the equations of relativistic viscous hydrodynamics requires specifying the temperature dependent ratio of the shear viscosity to the entropy density, $\eta/s(T)$, in addition to specifying the equation of state. Following Ref. [208], we choose

$$\frac{\eta}{s}(T) = \begin{cases} \left(\frac{\eta}{s}\right)_{\rm min} + 0.288\left(\frac{T}{T_{\rm tr}} - 1\right) + 0.0818\left(\left(\frac{T}{T_{\rm tr}}\right)^2 - 1\right) & \text{for} \quad T > T_{\rm tr} \\ \left(\frac{\eta}{s}\right)_{\rm min} + 0.0594\left(1 - \frac{T}{T_{\rm tr}}\right) + 0.544\left(1 - \left(\frac{T}{T_{\rm tr}}\right)^2\right) & \text{for} \quad T < T_{\rm tr} \end{cases} . \quad (5.1)$$

We choose $(\eta/s)_{\rm min} = 0.08$ at $T_{\rm tr} = 180$ MeV. These choices result in hydrodynamic simulations that yield reasonable agreement with the experimental measurements over all centrality and collision energies, see for example Figure 5.5 in Section 5.4 below.

The electromagnetic fields are generated by both the spectators and participant charged nucleons. The transverse distribution of the right-going (+) and left-going (−) charge density profiles $\rho^{\pm}_{\rm spectator}(\vec{x}_\perp)$ and $\rho^{\pm}_{\rm participant}(\vec{x}_\perp)$ are generated by averaging over 10,000 events using the same Monte-Carlo-Glauber model used to initialize the hydrodynamic calculation. The external charge and current sources for the electromagnetic fields are then given by

$$\rho_{\rm ext}(\vec{x}_\perp, \eta_s) = \rho^{+}_{\rm ext}(\vec{x}_\perp, \eta_s) + \rho^{-}_{\rm ext}(\vec{x}_\perp, \eta_s) \ , \vec{J}_{\rm ext}(\vec{x}_\perp, \eta_s) \quad = \vec{J}^{+}_{\rm ext}(\vec{x}_\perp, \eta_s) + \vec{J}^{-}_{\rm ext}(\vec{x}_\perp, \eta_s) \quad (5.2)$$

with

$$\rho^{\pm}_{\rm ext}(\vec{x}_\perp, \eta_s) = \rho^{\pm}_{\rm spectator}(\vec{x}_\perp)\delta(\eta_s \mp y_{\rm beam}) + \rho^{\pm}_{\rm participant}(\vec{x}_\perp) f^{\pm}(\eta_s) \quad (5.3)$$

$$\vec{J}^{\pm}_{\rm ext}(\vec{x}_\perp, \eta_s) = \vec{\beta}^{\pm}(\eta_s)\rho^{\pm}_{\rm ext}(\vec{x}_\perp, \eta_s) \quad \text{with} \quad \vec{\beta}^{\pm} = (0, 0, \pm\tanh(\eta_s)). \quad (5.4)$$

Here we are making the Bjorken approximation: the space-time rapidities η_s of the external charges are assumed equal to their rapidity. The spectators fly with the beam rapidity $y_{\rm beam}$ and the participant nucleons lose some rapidity in the collisions; their rapidity distribution in Eq. (5.3) is assumed to be [56, 192, 209]

$$f^{\pm}(y) = \frac{1}{4\sinh(y_{\rm beam}/2)} e^{\pm y/2} \quad \text{for} \quad -y_{\rm beam} < y < y_{\rm beam}. \quad (5.5)$$

The electromagnetic fields generated by the charges and currents evolve according to the Maxwell equations

$$(\nabla^2 - \partial_t^2 - \sigma\partial_t)\vec{B} = -\vec{\nabla} \times \vec{J}_{\rm ext} \tag{5.6}$$

$$(\nabla^2 - \partial_t^2 - \sigma\partial_t)\vec{E} = \frac{1}{\epsilon}\vec{\nabla}\rho_{\rm ext} + \partial_t \vec{J}_{\rm ext}\,, \tag{5.7}$$

which we will discuss in more detail in the next section. Here σ is the electrical conductivity of the QGP plasma. As in Ref. [56], we shall make the significant simplifying assumption of treating σ as if it were a constant. We make this assumption only because it permits us to use a semi-analytic form for the evolution of the electromagnetic fields rather than having to solve Eqs. (5.6) and (5.7) fully numerically. This simplification therefore significantly speeds up our calculations. In reality, σ is certainly temperature dependent: just on dimensional grounds it is expected to be proportional to the temperature of the plasma, meaning that σ should be a function of space and time as the plasma expands and flows hydrodynamically, with σ decreasing as the plasma cools. Furthermore, during the pre-equilibrium epoch σ should rapidly increase from zero to its equilibrium value. Taking all of this into consideration would require a full, numerical, magnetohydrodynamical analysis, something that we leave for the future. Throughout most of this chapter, we shall follow Ref. [56] and set the electrical conductivity to the constant value $\sigma = 0.023\ \mathrm{fm}^{-1}$ which, according to the lattice QCD calculations in Refs. [210–214], corresponds to σ in three-flavor quark-gluon plasma at $T \sim 250$ MeV.

With the evolution of the electromagnetic fields in hand, the next step is to compute the drift velocity $\vec{v}_{\rm\ drift}$ that the electromagnetic field induces at each point on the freeze-out surface. Because this drift velocity is only a small perturbation compared to the background hydrodynamic flow velocity, $|\vec{v}_{\rm drift}| \ll |\vec{v}_{\rm flow}|$, we can obtain $\vec{v}_{\rm\ drift}$ by solving the force-balance equation [56]

$$m\frac{d\vec{v}_{\rm drift}^{\rm\ lrf}}{dt} = q\vec{v}_{\rm drift}^{\rm\ lrf} \times \vec{B}^{\rm\ lrf} + q\vec{E}^{\rm\ lrf} - \mu m \vec{v}_{\rm drift}^{\rm\ lrf} = 0 \tag{5.8}$$

in its non-relativistic form in the local rest frame of the fluid cell of interest. The last term in (5.8) describes the drag force on a fluid element with mass m on which some external (in this case electromagnetic) force is being exerted, with μ the drag coefficient. The calculation of μm for quark-gluon plasma in QCD remains an open question. In the $\mathcal{N} = 4$ supersymmetric Yang-Mills (SYM) theory plasma it should be accessible via a holographic calculation. At present its value is known precisely

only for heavy quarks in $\mathcal{N} = 4$ SYM theory, in which [57–59],

$$\mu m = \frac{\pi\sqrt{\lambda}}{2}T^2 \tag{5.9}$$

with $\lambda \equiv g^2 N_c$ the 't-Hooft coupling, g being the gauge coupling and N_c the number of colors. For our purposes, throughout most of this chapter we shall follow Ref. [56] and use (5.8) with $\lambda = 6\pi$. We investigate the consequences of varying this choice in Section 5.4.2. Finally, the drift velocity $\vec{v}^{\,\rm lrf}_{\rm drift}$ in every fluid cell along the freeze-out surface is boosted by the flow velocity to bring it back to the lab frame, $V^\mu = (\Lambda_{\rm flow})^\mu{}_\nu (u^{\rm lrf}_{\rm drift})^\nu$, where $(\Lambda_{\rm flow})^\mu{}_\nu$ is the Lorentz boost matrix associated with the hydrodynamic flow velocity $u^\mu_{\rm flow}$.

With the full, charge-dependent, fluid velocity V^μ — including the sum of the flow velocity and the charge-dependent drift velocity induced by the electromagnetic fields — in hand, we now use the Cooper-Frye formula [215],

$$\frac{dN}{dy p_T dp_T d\phi} = \frac{g}{(2\pi)^3}\int_\Sigma p^\mu d\sigma_\mu \left[f_0 + f_0(1 \mp f_0)\frac{p^\mu p^\nu \pi_{\mu\nu}}{2T^2(e+P)}\right] \tag{5.10}$$

to integrate over the freezeout surface (the spacetime surface at which the matter produced in the collision cools to the freezeout temperature that we take to be 105 MeV) and obtain the momentum distribution for hadrons with different charges. Here, g is the hadron's spin degeneracy factor and the equilibrium distribution function is given by

$$f_0 = \frac{1}{\exp((p\cdot V)/T) \pm 1}. \tag{5.11}$$

With the momentum distribution for hadrons with different charge in hand, the final step in the calculation is the evaluation of the anisotropic flow coefficients as function of rapidity:

$$v_n(y) \equiv \frac{\int dp_T d\phi\, p_T \frac{dN}{dy p_T dp_T d\phi}\cos\left[n(\phi - \Psi_n)\right]}{\int dp_T d\phi\, p_T \frac{dN}{dy p_T dp_T d\phi}} \tag{5.12}$$

where $\Psi_n = 0$ is the event-plane angle in the numerical simulations. In order to define the sign of the rapidity-odd directed flow v_1, we choose the spectators at positive x to fly toward negative z, as illustrated in Figure 5.1. We can then compute the odd component of $v_1(y)$ according to

$$v_1^{\rm odd} = \frac{1}{2}(v_1(\Psi_+) - v_1(\Psi_-)), \tag{5.13}$$

Experimentally, the rapidity-odd directed flow $v_1^{\rm odd}$ is measured [216] by correlating the directed flow vector of particles of interest, $\mathbf{Q}_1^{\rm POI} = \sum_{j=1}^{M^{\rm POI}} e^{i\phi_j}$, with the flow vectors from the energy deposition of spectators in the zero-degree calorimeter (ZDC), $\mathbf{Q}_\pm^{\rm ZDC} = \sum_j E_j^\pm r_j e^{i\phi_j}$. The directed flow is defined using the scalar-product method:

$$v_1(\Psi_\pm) = \frac{1}{\langle M^{\rm POI}\rangle_{\rm ev}} \frac{\langle\ \mathbf{Q}_1^{\rm POI}\cdot(\ \mathbf{Q}_\pm^{\rm ZDC})^*\rangle_{\rm ev}}{\sqrt{\langle|\ \mathbf{Q}_+^{\rm ZDC}\cdot(\ \mathbf{Q}_-^{\rm ZDC})^*|\rangle_{\rm ev}}}\ . \tag{5.14}$$

In the definition of $\mathbf{Q}_\pm^{\rm ZDC}$, the index j runs over all the segments in the ZDC and E_j denotes the energy deposition at $\mathbf{x}_j = r_j e^{i\phi_j}$. In our notation, the flow vector angle $\Psi_+ = \pi$ in the forward ($+z$ direction) ZDC and $\Psi_- = 0$ in the backward ($-z$) direction ZDC. The odd component of $v_1(y)$ that we compute according to Eqs. (5.12) and (5.13) can be directly compared to $v_1^{\rm odd}$ defined from the experimental definition of $v_1(\Psi_\pm)$ in (5.14).

In order to isolate the small contribution to the various flow observables that was induced by the electromagnetic fields, separating it from the much larger background hydrodynamic flow, we compute the difference between the value of a given flow observable for positively and negatively charged hadrons:

$$\Delta\langle p_T\rangle \equiv \langle p_T\rangle(h^+) - \langle p_T\rangle(h^-) \tag{5.15}$$

and

$$\Delta v_n \equiv v_n(h^+) - v_n(h^-), \tag{5.16}$$

are the quantities of interest.

5.3 Electromagnetic fields

In this Section we will first investigate the Maxwell equations for our heavy-ion collision using analytical methods as much as possible. We will see that the final integrations of the electromagnetic fields have to be done numerically; we will show the results of these numerical integrations along with the time-evolution in the last part of the Section.

5.3.1 Analytical Computations

The story's starting point is the Maxwell equations for a single charge; later on we will integrate over the different particles producing such fields. First, we will

write down the Maxwell equations, including the conductivity σ, discussed in the previous section. To model the moving charge density, we use Dirac delta functions. One delta function for the $\hat{z}$ direction, in which the particle is moving, and one for the location in the transverse plane, denoted with $\vec{x}_\perp$ and $\vec{x}'_\perp$; these last two vectors denote the location where we calculate the $\vec{B}$ and the location of the particle, respectively. The electromagnetic fields are thus functions of the variables $\vec{x}_\perp$, $\vec{x}'_\perp$, z and t. Besides the charge density we incorporate the conductivity by Ohm's law $J = \sigma\vec{E}$, resulting in

$$\begin{aligned}
\vec{\nabla}\cdot\vec{B} &= 0 \ , \\
\vec{\nabla}\times\vec{E} &= -\frac{\partial\vec{B}}{\partial t} \ , \\
\vec{\nabla}\cdot\vec{E} &= e\delta(z-vt)\delta(\vec{x}_\perp - \vec{x}'_\perp) \ , \\
\vec{\nabla}\times\vec{B} &= \frac{\partial\vec{E}}{\partial t} + \sigma\vec{E} + e\,v\,\hat{z}\delta(z-vt)\delta(\vec{x}_\perp - \vec{x}'_\perp) \ .
\end{aligned} \tag{5.17}$$

We can rewrite these equations to a second order equation for the $\vec{B}$ field by taking the cross product of the last equation for $\vec{B}$ again to obtain

$$\vec{\nabla}\times(\vec{\nabla}\times\vec{B}) = \vec{\nabla}(\vec{\nabla}\cdot\vec{B}) - \vec{\nabla}^2\vec{B} \ , \tag{5.18}$$

which can be further simplified using the expressions of (5.17) to

$$\nabla^2\vec{B} - \partial_t^2\vec{B} - \sigma\partial_t\vec{B} = -e\,v\,\vec{\nabla}\times(\hat{z}\delta(z-vt)\delta(\vec{x}_\perp - \vec{x}'_\perp)) \ . \tag{5.19}$$

In a similar manner we can obtain an equation for the electric field:

$$\begin{aligned}
\nabla^2\vec{E} - \partial_t^2\vec{E} - \sigma\partial_t\vec{E} = &-e\,\vec{\nabla}(\delta(z-vt)\delta(\vec{x}_\perp - \vec{x}'_\perp)) \\
&+ ev\hat{z}\partial_t(\delta(z-vt)\delta(\vec{x}_\perp - \vec{x}'_\perp)) \ .
\end{aligned} \tag{5.20}$$

To solve such equations we can use Green's functions; here we will demonstrate the computation for the magnetic field. Using such a Green's function we get a solution for $\vec{B}$ as

$$\vec{B}(z,\vec{b},t) = \int d^4x'\, G(z-z',\vec{b}-\vec{b}',t-t')\, e\,v\,\vec{\nabla}\times\left((\hat{z}\delta(z'-vt')\delta(\vec{b}')\right) \ , \tag{5.21}$$

where our Green's function G must now satisfy our linear differential operator from Equation 5.19:

$$\vec{\nabla}^2\vec{G} - \frac{\partial^2\vec{G}}{\partial t^2} - \sigma\frac{\partial\vec{G}}{\partial t} = -\delta(z-z')\delta(\vec{b}-\vec{b}')\delta(t-t') \ . \tag{5.22}$$

This equation can be solved by Fourier transforming the coordinates such that the derivatives become less of a nuisance. The resulting solution in the Fourier transformed space reads

$$G_f(k_z, \vec{k}_\perp, \omega) = \frac{e^{-ik_z z'} e^{-i\vec{k}_\perp \cdot \vec{b}'} e^{i\omega t'}}{k_z^2 + k_\perp^2 - \omega^2 - i\sigma\omega} \ , \tag{5.23}$$

where $k_z, \vec{k}_\perp, \omega$ are the Fourier transforms of $z, \vec{b}, t$, respectively. We can then Fourier transform back to plug the result back into (5.21). This procedure results in

$$\frac{\vec{B}(z,\vec{b},t)}{2\pi e v} = \int \frac{d^2k_\perp}{(2\pi)^2} e^{i\vec{b}\cdot\vec{k}_\perp} \int \frac{dk_z}{2\pi} e^{ik_z z} \int \frac{d\omega}{2\pi} e^{-i\omega t} \frac{(i\vec{k} \times \hat{z})\delta(\omega - k_z v)}{k_z^2 + k_\perp^2 - \omega^2 - i\sigma\omega} \ . \tag{5.24}$$

From this point on, we will focus on the y-component of the $\vec{B}$ field; the other components can be calculated similarly. To get this y component, we take the inner product with $\hat{y}$:

$$(\vec{k}_\perp \times \hat{z}) \cdot \hat{y} = -k_\perp \cos(\phi) \ . \tag{5.25}$$

When we complete the integral over k_z in (5.24) we find

$$\frac{\vec{B}_y}{e} = \frac{\hat{y}}{(2\pi)^2} \int d^2k_\perp d\omega \ \frac{-ik_\perp \cos(\phi)}{(\omega/v)^2 + k_\perp^2 - \omega^2 - i\sigma\omega} \ e^{-ibk_\perp \cos(\phi)} \ e^{i\omega(\frac{z}{v} - t)} \ , \tag{5.26}$$

where $d^2k_\perp = k_\perp dk_\perp d\phi$. We can solve the ϕ integral by

$$\int_0^{2\pi} \mathrm{d}\phi - ik_\perp \cos(\phi) \mathrm{e}^{-ibk_\perp \cos(\phi)} = (2\pi)^2 k_\perp J_1(bk_\perp) \ , \tag{5.27}$$

where J_1 denotes a Bessel function; applying this to our expression for B_y yields

$$e\vec{B}_y = \frac{\alpha_{em}}{\pi} \ \hat{y} \int_0^\infty dk_\perp \ \int_{-\infty}^\infty d\omega \ \frac{J_1(bk_\perp) \ k_\perp^2}{\frac{\omega^2}{v^2} + k_\perp^2 - \omega^2 - i\sigma\omega} \ e^{i\omega(\frac{z}{v} - t)} \ , \tag{5.28}$$

where we introduced the electromagnetic coupling strength $\alpha_{em} = \frac{e^2}{4\pi}$. The next integral we will solve is the ω integral. To solve it we use a contour integral, and see that we have poles at

$$\omega_\pm = \frac{i\,\sigma\,\gamma^2\,v^2}{2} \left(1 \pm \left(1 + \frac{4\,k_\perp^2}{\sigma^2\,\gamma^2\,v^2}\right)^{\frac{1}{2}}\right) \ , \tag{5.29}$$

where $\gamma = \frac{1}{\sqrt{1-v^2}}$. We close the contour in the lower half of the complex plane, and we pick up ω_-. Using the residue theorem we complete the integral over ω and get the following expression for the integral

$$I := \int_0^\infty dk_\perp \int_{-\infty}^\infty d\omega \, \frac{J_1(bk_\perp)\, k_\perp^2}{\frac{\omega^2}{v^2} + k_\perp^2 - \omega^2 - i\sigma\omega} \, e^{i\omega(\frac{z}{v} - t)} \tag{5.30}$$

$$= 2\pi \int_0^\infty \frac{dk_\perp \, J_1(bk_\perp)\, k_\perp^2 \, e^{-|\omega_-|(t-\frac{z}{v})}}{\sigma \left(1 + \frac{4k_\perp^2}{\sigma^2 \gamma^2 v^2}\right)^{\frac{1}{2}}} \tag{5.31}$$

$$= \frac{2\pi \, (\gamma^2 \, \sigma^2 \, v^2)}{4} \, \frac{\gamma \, v}{2} \, e^{(t-\frac{z}{v}) \, \frac{\sigma \, \gamma^2 \, v^2}{2}} \sqrt{\frac{2}{\pi}} \, \beta(\alpha^2 + \beta^2)^{-\frac{3}{4}} \, K_{\frac{3}{2}}(\sqrt{\alpha^2 + \beta^2}) \, , \tag{5.32}$$

where, in the second step, we completed the contour integral, and in the last step we used an integral identity. We have defined $\alpha = (t - \frac{z}{v}) \, \frac{\sigma \, \gamma^2 \, v^2}{2}$ and $\beta = \frac{b \, \sigma \, \gamma \, v}{2}$. Furthermore, $K_{\frac{3}{2}}$ is a modified Bessel function and has an exact form:

$$K_{\frac{3}{2}}(z) = \sqrt{\frac{2}{\pi}} \, e^{-z} \, (1 + \frac{1}{z}) \, . \tag{5.33}$$

At this point we reintroduce $\vec{b} = (\vec{x}_\perp - \vec{x}'_\perp)$ and we shall also make the coordinate transformations

$$\begin{aligned} t &= \cosh(\eta_s) \, \tau \, , \\ z &= \sinh(\eta_s) \, \tau \, , \\ v &= \frac{\sinh(Y)}{\cosh(Y)} \, , \end{aligned} \tag{5.34}$$

where η_s is the pseudorapidity and Y is the rapidity. In principle we have solved the integrals for the B-field; we can however place it in a more aesthetically pleasing form. We take $x_\perp = |\vec{x}_\perp|$, which means we can express $\vec{x}_\perp = x_\perp \cos(\phi)$ with ϕ the azimuthal angle (the same applies for $\vec{x}'_\perp$). After some manipulations with the above expressions and coordinate transformations we reach the following expression for the B-field:

$$\begin{aligned} e\vec{B}_y^+(\tau, \eta, x_\perp, \phi) = \alpha_{em} \, \hat{y} \, \sinh(Y) \, (x_\perp \cos(\phi) - x'_\perp \cos(\phi')) \\ \times \frac{\left(\frac{\sigma \, |\sinh(Y)|}{2} \sqrt{\Delta} + 1\right)}{\Delta^{\frac{3}{2}}} \, e^A \, , \end{aligned} \tag{5.35}$$

where the + indicates the fact that it is a positively moving ($+\hat{z}$) particle. We have defined A and Δ as follows

$$A = \frac{\sigma}{2}\left(\sinh(Y)\,\sinh(Y-\eta) - |\sinh(Y)|\,\sqrt{\Delta}\right)\,, \tag{5.36}$$

$$\Delta = \tau^2\,\sinh^2(Y-\eta) + (x_\perp)^2 + (x'_\perp)^2 - 2\,x_\perp\,x'_\perp\,\cos(\phi-\phi')\,. \tag{5.37}$$

With this result, we conclude the computation of the single-particle magnetic field (in the y-direction). The last task that thus remains is the integration over the different particles. To get the complete contribution in either case, we need to add up the fields created by particles moving in both + and − z direction. So, the total B-field would look like $\vec{B}_{\rm tot} = \vec{B}_s^+ + \vec{B}_s^- + \vec{B}_p^+ + \vec{B}_p^-$. Here $\vec{B}_s^+$, e.g., denotes the B field due to a spectator moving in the + direction; the $\vec{B}_p$ denote the participants. Considering only the spectators for the moment, we can write down the expression for the total magnetic field in the y-direction as

$$e\,B_{y,s}(\tau,\eta,x_\perp,\phi) = -Z\int d\phi'\,dx'_\perp\,x'_\perp \times\left(\rho_+(x'_\perp)\,e\,B_y^+\,(\tau,\eta,x_\perp,\pi-\phi) + \rho_-(x'_\perp)\,e\,B_y^+\,(\tau,-\eta,x_\perp,\phi)\right)\,, \tag{5.38}$$

where Z is the charge of the nucleus; for LHC, the used nuclei are lead such that $Z = 82$. The densities $\rho_\pm$ are, in this case, the numerically modelled spectator densities that we discussed last section. When doing the computations for the participants, we replace them by the respective distributions for the participating particles.
Similar calculations can be done for the other components of the electromagnetic fields, and for the participants. As we mentioned in the previous section, for the participants we should also include a distribution for the change in rapidity due to the collisions; it is given in (5.5).

5.3.2 Numerical Integration

The integrations over the different particles in (5.38) have to be done numerically. The numerical code that we have used to compute these, and the evolution of the electromagnetic fields can be found at `https://github.com/chunshen1987/Heavy-ion_EM_fields`. In the remainder of this Section we will analyze the spatial distribution and evolution of the electromagnetic fields. Figure 5.2 presents our calculation of the magnitude and direction of the electromagnetic fields, both electric and magnetic, in the lab frame across the $z = 0$ transverse plane at a proper

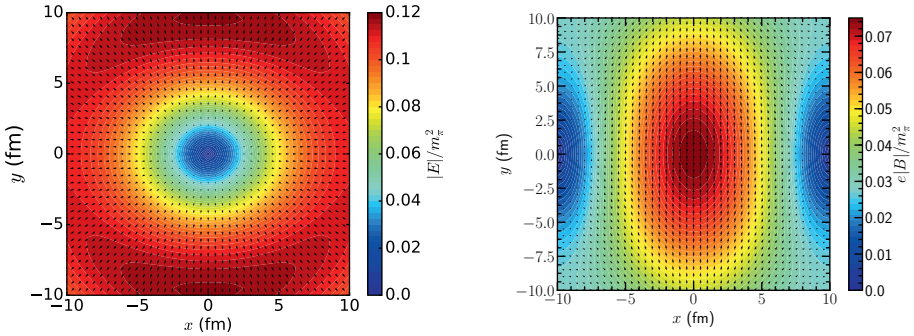

Figure 5.2: *The electric (left) and magnetic (right) fields in the transverse plane at $z = 0$ in the lab frame at a proper time $\tau = 1$ fm/c after a Pb+Pb collision with 20-30% centrality (corresponding to impact parameters in the range 6.24 fm $< b <$ 9.05 fm) and with a collision energy $\sqrt{s} = 2.76$ ATeV. The fields are produced by the spectator ions moving in the $+z$ ($-z$) direction for $x < 0$ ($x > 0$) as well as by the ions that participate in the collision. In both panels, the contribution from the spectators is larger, however. We see that the magnetic field is strongest at the center of the plasma, where it points in the $+y$ direction as anticipated in Figure 5.1. The electric field points in a generally outward direction and is strongest on the periphery of the plasma. Its magnitude is not azimuthally symmetric: the field is on average stronger where it is pointing in the $\pm y$ directions than where it is pointing in the $\pm x$ directions.*

time $\tau = 1$fm/c after a Pb+Pb collision with 20-30% centrality and a collision energy of $\sqrt{s} = 2.76$ ATeV. These electric and magnetic fields are produced by both spectator and participant ions in the two incoming nuclei. We outlined the calculation in Section 5.2; it follows Ref. [56]. The spectator nucleons give the dominant contributions to the $\vec{B}$ field. The beam directions for the ions at $x > 0$ ($x < 0$) are chosen as $-z$ ($+z$), as in Figure 5.1.

The left panel in Figure 5.2 includes three of the four different components of the electric field that we discussed in the Introduction, namely the electric field generated by Faraday's law $\vec{E}_F$, the Coulomb field sourced by the spectators $\vec{E}_C$, and the Coulomb field sourced by the net charge in the plasma $\vec{E}_P$. Their sum gives the total electric field in the lab frame, which is what is plotted. When we transform to the local rest frame of a moving fluid cell, namely the frame in which we calculate the electromagnetically induced drift velocity of positive and negative charges in that fluid cell, there is an additional component originating from the Lorentz force law, $\vec{E}_L$, as explained in the Introduction. The total electric field in the rest frame, which now also includes the E_L component, is shown below in the left panel of Figure 5.4 as a function of time.

The magnetic field in the right panel of Figure 5.2 indeed decays as a function of time as shown in the bottom panel of Figure 5.3. Via Faraday's law this induces a current in the same direction as the current pushed by the Coulomb electric field coming from the spectators, and it opposes the current caused by the Lorentz force on fluid elements moving in the longitudinal direction, as sketched in Figure 5.1 and seen in Figure 5.4.

When solving the force-balance equation, Eq. (5.8), we find that the drift velocity is mainly determined by the electric field in the local local fluid rest frame. To understand how the Coulomb, Lorentz and Faraday effects contribute to the drift velocity on the freeze-out surface it is instructive to study how the different effects contribute to the electric field in the local fluid rest frame. We do so at $\eta_s = 0$ in the top panel of Figure 5.3. At $\eta_s = 0$, only the Coulomb effect contributes. This means that when in Section 5.4 we compute the charge-odd contribution to the even flow harmonics at $\eta_s = 0$ this will provide an estimate of the magnitude of the Coulomb contribution to the flow coefficients. In Figure 5.4 we look at the different contributions to the electric field in the local fluid rest frame at $\eta_s = 1$ and $\eta_s = 3$. We see that the Coulomb + Faraday and Lorentz effects point in opposite

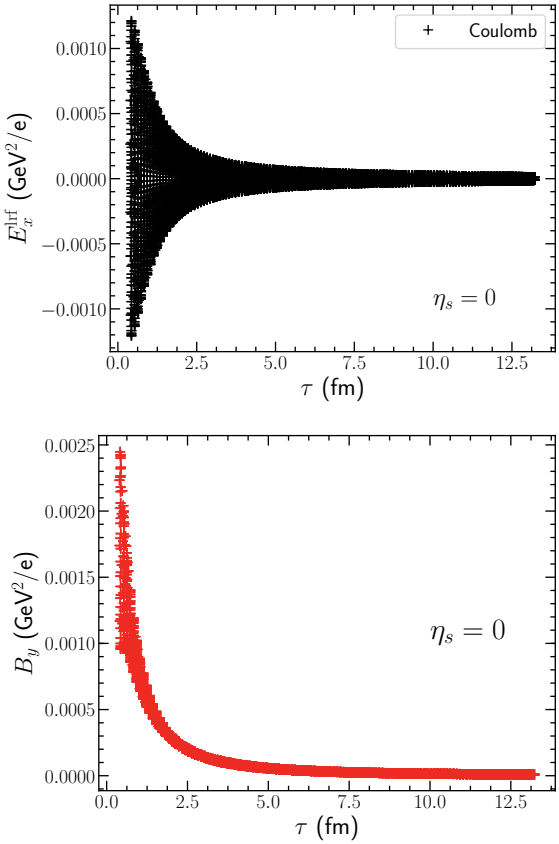

Figure 5.3: *Top: The x-component of the electric field in the local fluid rest frame at points on the freezeout surface at spacetime rapidity $\eta_s = 0$, as a function of proper time. Each cross corresponds to a single fluid cell on the freezeout surface, with the vertical line of crosses at any single τ corresponding to different points on the freezeout surface at that τ. Only the Coulomb electric field generated by the net charge in the plasma contributes at $\eta_s = 0$, and by symmetry there for every point where ${E_x}^{lrf} > 0$ there is a point where ${E_x}^{lrf} < 0$. Bottom: Time dependence of the y-component of the magnetic field in the lab frame at $\eta_s = 0$. Again, each cross corresponds to a single point on the freeze-out surface. We see that $B_y > 0$ as diagrammed in Figure 5.1 and shown in Figure 5.2, and here we can see how B_y decreases with time.*

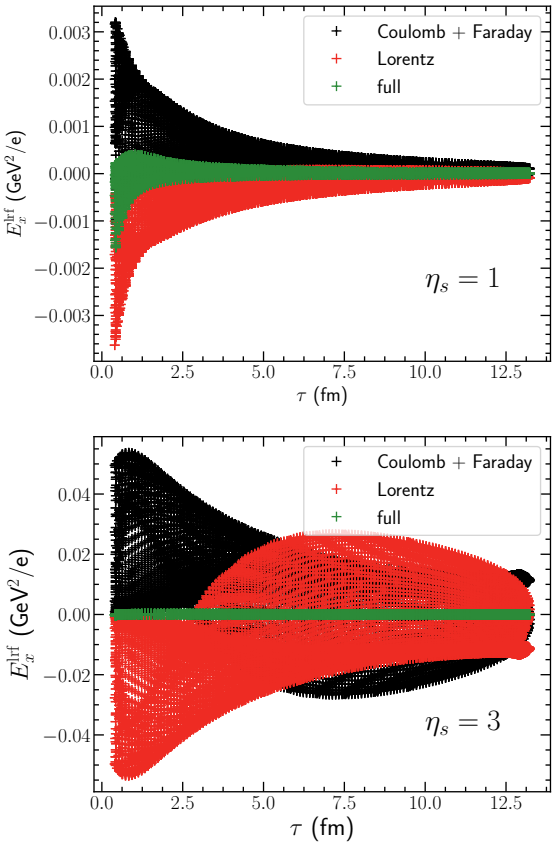

Figure 5.4: *Contributions to the electric field in the local rest frame of a unit cell in the fluid on the freezeout surface at a specified, non-vanishing, spacetime rapidity η_s: $\eta_s = 1$ in the left panel and $\eta_s = 3$ in the right panel. Each unit cell is represented in the figure by a black cross, a red cross, and a green cross. Black crosses denote the contribution to the electric field at a given fluid cell in its local rest frame coming from the Coulomb and Faraday effects. Red crosses denote the contribution from the Lorentz force. And, green crosses represent the total electric field at the fluid cell, namely the sum of a black cross and a red cross. We observe that the Coulomb+Faraday and Lorentz contributions to the electric field point in opposite directions, as sketched in Figure 5.1, and furthermore see that the two contributions almost cancel at large η_s, as we shall discuss in Section 5.4.1. We shall see there that the Coulomb+Faraday contribution is slightly larger in magnitude than the Lorentz contribution.*

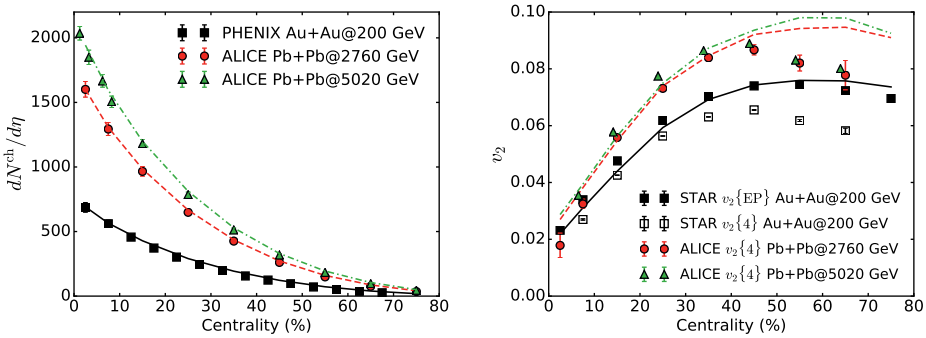

Figure 5.5: *To get a sense of how well the solution to relativistic viscous hydrodynamics upon which we build our calculation of electromagnetic fields and currents describes heavy-ion collisions, we compare our results for charged hadron multiplicities (left) and elliptic flow coefficients (right) to experimental measurements at the top RHIC and LHC energies from Refs. [217–219] and Refs. [220–222], respectively.*

directions, and almost cancel at large spacetime rapidity. We discuss the origin and consequences of this cancellation in Section 5.4.1 below.

5.4 Results

In this Section we present our results for the charge-dependent contributions to the anisotropic flow induced by the electromagnetic effects introduced in Section 5.1. As we have described in Section 5.2, to obtain the anisotropic flow coefficients we input the electromagnetic fields in the local rest frame of the fluid, calculated in Section 5.3, into the force-balance equation (5.8) which then yields the electromagnetically induced component of the velocity field of the fluid. This velocity field is then input into the Cooper-Frye freezout procedure [215] to obtain the distribution of particles in the final state and, in particular, the anisotropic flow coefficients [56].

To provide a realistic dynamical background on top of which to compute the electromagnetic fields and consequent currents, we have calibrated the solutions to relativistic viscous hydrodynamics that we use by comparing them to experimental measurements of hadronic observables. To give a sense of the agreement that we have obtained, in Figure 5.5 we show our results for the centrality dependences of

charged hadron multiplicity and elliptic flow coefficients are shown for heavy-ion collisions at three collision energies as well as data from STAR, PHENIX and ALICE Collaborations [217–222]. Since we do not have event-by-event fluctuations in our calculations, we compare our results for the elliptic flow coefficent v_2 to experimental measurements of v_2 from the 4-particle cumulant, $v_2\{4\}$ [223]. With the choice of the specific shear viscosity $\eta/s(T)$ that we have made in Eq. (5.1), our model provides a reasonable agreement with charged hadron $v_2\{4\}$ for heavy-ion collisions with centralities up to the 40-50% bin.

To isolate the effect of electromagnetic fields on charged hadron flow observables, we study the difference between the v_n of positively charged particles and the v_n of negatively charged particles as defined in Eq. (5.16). We also study the difference between the mean transverse momentum $\langle p_T \rangle$ of positively charged hadrons and that of negatively charged hadrons. This provides us with information about the modification in the hydrodynamic radial flow induced by the electromagnetic fields. The difference between the charge-dependent flow of light pions and heavy protons is also compared. Hadrons with different masses have different sensitivities to the underlying hydrodynamic flow and to the electromagnetic fields.

We should distinguish the charge-odd contributions to the odd flow moments, Δv_1, Δv_3, ..., from the charge-dependent contributions to the even ones, Δv_2, Δv_4, ..., as they have qualitatively different origins. The charge-odd contributions to the odd flow coefficients induced by electromagnetic fields, Δv_{2n-1}, are rapidity-odd: $\Delta v_{2n-1}(\eta_s) = -\Delta v_{2n-1}(-\eta_s)$. This can easily be understood by inspecting Figure 5.1, where we describe different effects that contribute to the total the electric field in the plasma. This can also be proven analytically by studying the transformation property of Δv_n under $\eta \to -\eta$. As we have seen in Section 5.1, there are three basic effects that contribute. First, there is the electric field produced directly by the positively charged spectator ions. They generate electric fields in opposite directions in the $z > 0$ and $z < 0$ regions. We call this the *Coulomb electric field* $\vec{E}_C$, as the resulting electric current in the plasma is a direct result of the Coulomb force between the spectators and charges in the plasma. Then there are the two separate magnetically induced electric fields, as discussed in Ref. [56]. The *Faraday electric field* $\vec{E}_F$ results from the rapidly decreasing magnitude of the magnetic field perpendicular to the reaction plane, see Figure 5.1, as a consequence of Faraday's law. Note that $\vec{E}_F$ and $\vec{E}_C$ point in the same directions. Finally, there is another magnetically induced electric field, the *Lorentz electric field* $\vec{E}_L$ that

can be described in the lab frame as the Lorentz force on charges that are moving because of the longitudinal expansion of the plasma and that are in a magnetic field. Upon transforming to the local fluid rest frame, the lab-frame magnetic field becomes an electric field that we denote $\vec{E}_L$.[3] As shown in Figure 5.1, $\vec{E}_L$ points in the opposite direction to $\vec{E}_F$ and $\vec{E}_C$.

On the other hand, the charge-dependent contributions to the even order anisotropic flow coefficients v_{2n} are even under $\eta_s \to -\eta_s$. Obviously this cannot arise from the rapidity-odd electric fields described above. Instead, we find that although the electromagnetic contribution to the v_{2n} receives some contribution from components of the electric fields above that are rapidity-even and that are odd under $x \to -x$, it also receives an important contribution from the Coulomb force between the net positive electric charge in the plasma. This arises as a result of the Coulomb force exerted on the charges in the plasma by each other — as opposed to the Coulomb force exerted on charges in the plasma by the spectator ions. This electric field is non-trivial even at $z = 0$ as shown in Figure 5.2 (left). We call this field the *plasma electric field* and denote it by $\vec{E}_P$. This contributes to the net Δv_2 and it is clear from the geometry that it makes no contribution to the odd flow harmonics.

In Figure 5.6, we begin the presentation of our principal results. This figure shows Δv_n, the charge-odd contribution to the anisotropic flow harmonics induced by electromagnetic fields, for pions in 20-30% Au+Au collisions at 200 GeV. It also shows the difference in the mean-p_T of particles with positive and negative charge, which shows how the electromagnetic fields modify the hydrodynamic radial flow. The radial outward pointing electric fields in Figure 5.2 increase the radial flow for positively charged hadrons while reducing the flow for negative particles. We see that the effect is even in rapidity. Figure 5.6 shows that these fields also make a charge-odd, rapidity-even contribution to v_2.

We compare the red dashed curves, arising from electromagnetic effects by spectators only, with the solid black curves that show the full calculation including the participants. Noting that the lines are significantly different it follows that the Coulomb force exerted on charges in the plasma by charges in the plasma makes a large contribution to $\Delta\langle p_T\rangle$ and Δv_2. The induced $\Delta\langle p_T\rangle$ is larger at forward and backward rapidities, because the electric fields from the spectators and from the

[3] This electric field was called the Hall electric field in Ref. [56].

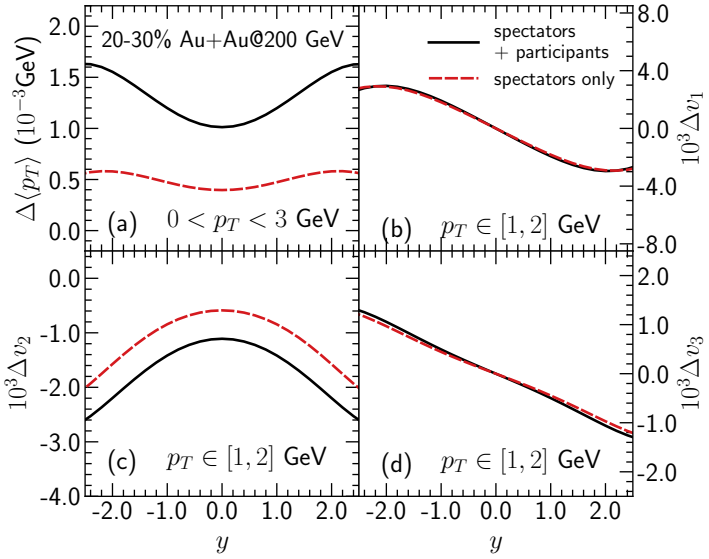

Figure 5.6: *The solid black curves display the principal results of our calculations for 20-30% centrality Au+Au collisions at 200 GeV, as at RHIC. We show the contribution to the mean-p_T of charged pions and the first three v_n coefficients induced by the electromagnetic fields that we have calculated, isolating the electromagnetically induced effects by taking the difference between the calculated value of each observable for π^+ and π^- mesons, namely the charge-odd or charge-dependent contributions that we denote $\Delta\langle p_T\rangle$ and Δv_n. We see rapidity-odd contributions Δv_1 and Δv_3 and rapidity-even contributions $\Delta\langle p_T\rangle$ and Δv_2. The red dashed curves show the results we obtain when we calculate the same observables in the presence of the electromagnetic fields produced by the spectators only. We see that the dominant contribution to the odd v_n's is generated by these spectator-induced fields, whereas the even v_n's also receive a significant contribution from the Coulomb force exerted on charges in the plasma by other charges in the plasma, originating from the participant nucleons.*

charge density in the plasma deposited according to the distribution (5.5) are both stronger there.

The electromagnetically induced elliptic flow Δv_2 originates from the Coulomb electric field in the transverse plane, depicted in Figure 5.2. We see there that the Coulomb field is stronger along the y-direction than in the x-direction. This reduces

the elliptic flow v_2 for positively charged hadrons and increases it for negatively charged hadrons. Hence, Δv_2 is negative.

Note that $\Delta\langle p_T\rangle$ and Δv_2 are much smaller than $\langle p_T\rangle$ and v_2; in the calculation of Figure 5.6, $\langle p_T\rangle \approx 0.47$ GeV and $v_2 \approx 0.048$ for both the π^+ and π^-. The differences between these observables for π^+ and π^- that we plot are much smaller, with $\Delta\langle p_T\rangle$ smaller than $\langle p_T\rangle$ by a factor of $\mathcal{O}(10^{-3})$ and Δv_2 smaller than v_2 by a factor of $\mathcal{O}(10^{-2})$ in Au+Au collisions at 200 GeV. This reflects, and is consistent with, the fact that the drift velocity induced by the electromagnetic fields is a small perturbation compared to the overall hydrodynamic flow on the freeze-out surface.

The electromagnetically induced contributions to the odd flow harmonics Δv_1 and Δv_3 are odd in rapidity. In our calculation, which neglects fluctuations, v_1 and v_3 both vanish in the absence of electromagnetic effects. We see from Figure 5.6 that the magnitudes of Δv_1 and Δv_3 are controlled by the electromagnetic fields due to the spectators, namely $\vec{E}_F$, $\vec{E}_C$ and $\vec{E}_L$. By comparing the sign of the rapidity-odd Δv_1 that we have calculated in Fig. 5.6 to the illustration in Figure 5.1, we see that the rapidity-odd electric current flows in the direction of $\vec{E}_F$ and $\vec{E}_C$, opposite to the direction of $\vec{E}_L$, meaning that $|\vec{E}_F + \vec{E}_C|$ is greater than $|\vec{E}_L|$. Our results for Δv_1 are qualitatively similar to those found in Ref. [56], although they differ quantitatively because of the differences between our realistic hydrodynamic background and the simplified hydrodynamic solution used in Ref. [56]. Here, we find a nonzero Δv_3 in addition, also odd in rapidity, and with the same sign as Δv_1 and a similar magnitude. This is natural since Δv_3 receives a contribution from the mode coupling between the electromagnetically induced Δv_1 and the background elliptic flow v_2.

In Figure 5.7 we see that the heavier protons have a larger electromagnetically induced shift in their mean p_T compared to that for the lighter pions. Because a proton has a larger mass than a pion, its velocity is slower than that of a pion with the same transverse momentum, p_T. Thus, when we compare pions and protons with the same p_T, the hydrodynamic radial flow generates a stronger blue shift effect for the less relativistic proton spectra, which is to say that the proton spectra are more sensitive to the hydrodynamic radial flow [224]. Similarly, when the electromagnetic fields that we compute induce a small difference between the radial flow velocity of positively charged particles relative to that of negatively charged particles, the

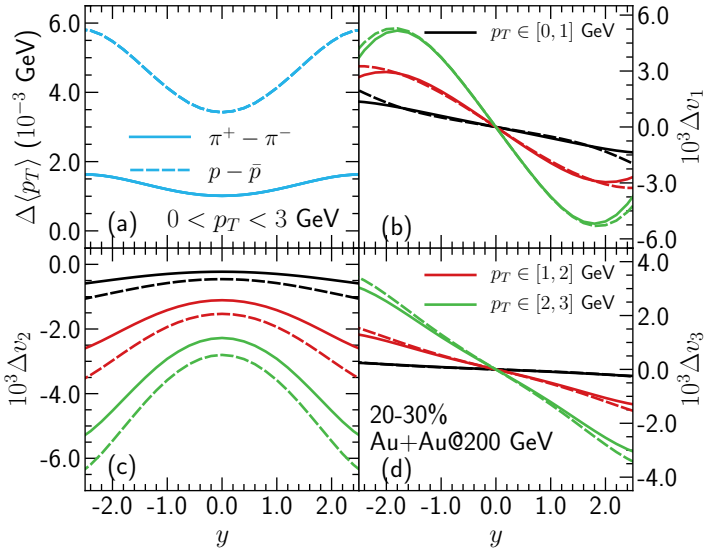

Figure 5.7: *The electromagnetically induced difference between the mean p_T and v_n coefficients of π^+ and π^- mesons (solid lines) and between protons and antiprotons (dashed lines) as a function of particle rapidity for 20-30% Au+Au collisions at 200 GeV. Three different p_T integration ranges are shown for each of the Δv_n as a function of particle rapidity.*

resulting difference between the mean p_T of protons and antiprotons is greater than the difference between the mean p_T of positive and negative pions. Turning to the Δv_n's, we see in Figure 5.7 that the difference between the electromagnetically induced Δv_n's for protons and those for pions are much smaller in magnitude. We shall also see below that these differences are modified somewhat by contributions from pions and protons produced after freezeout by the decay of resonances. For both these reasons, these differences cannot be interpreted via a simple blue shift argument. Figure 5.7 also shows the charge-odd electromagnetically induced flow coefficients Δv_n computed from charged pions and protons+antiprotons in three different p_T ranges. The Δv_1, Δv_2 and Δv_3 all increase as the p_T range increases, in much the same way that the background v_2 does. In the case of Δv_1, this agrees with what was found in Ref. [56].

In Figure 5.8 we study the centrality dependence of the electromagnetically induced

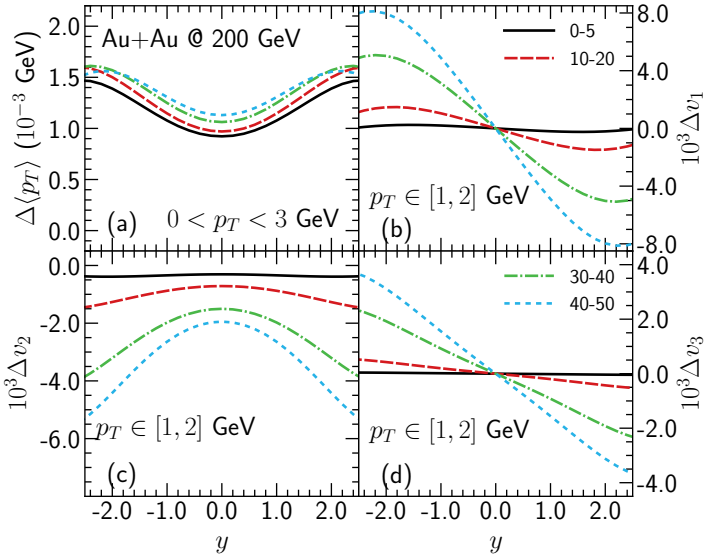

Figure 5.8: *The centrality dependence of the electromagnetically induced flow difference in π^+ vs π^- as a function of particle rapidity in Au+Au collisions at 200 GeV.*

flow in Au+Au collisions at 200 GeV. The difference between the flow of positive and negative pions, both the radial flow and the flow anisotropy coefficients, increases as one goes from central toward peripheral heavy-ion collisions. However, the increase in $\Delta\langle p_T\rangle$ and Δv_2 is smaller than the increase in the odd Δv_n's. This further confirms that the odd Δv_n's are induced by the electromagnetic fields produced by the spectator nucleons only – since the more peripheral a collision is the more spectators there are.

Compared to any of the anisotropic flow coefficients Δv_n, the $\Delta\langle p_T\rangle$ shows the least centrality dependence because, as we saw in Figure 5.6, $\Delta\langle p_T\rangle$ originates largely from the Coulomb field of the plasma, coming from the charge of the participants, with only a small contribution from the spectators. The increase of Δv_2 with centrality is intermediate in magnitude, since it originates both from the participants and from the spectators, as seen in Figure 5.6. Another origin for the increase in electromagnetically induced effects in more peripheral collisions is that the typical lifetime of the fireball in these collisions is shorter compared to that in

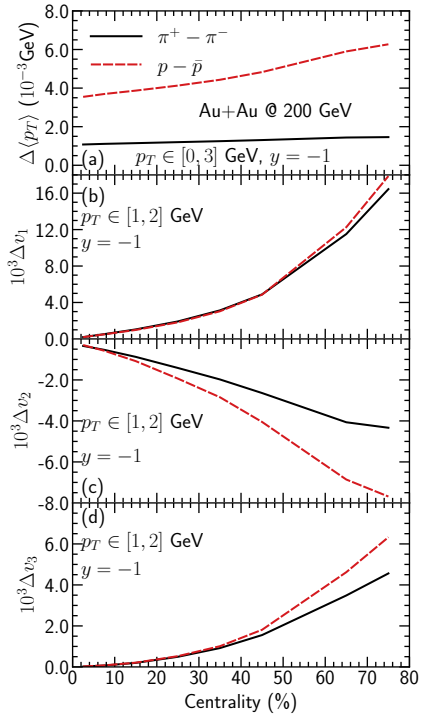

Figure 5.9: *The centrality dependence of the electromagnetically induced differences in the radial flow and anisotropic flow coefficients for positively and negatively charged hadrons, here at a fixed rapidity $y = -1$.*

central collisions. This gives less time for the electromagnetic fields to decay by the time of peak particle production in more peripheral collisions. In the case of $\Delta\langle p_T \rangle$, which is dominantly controlled by the plasma Coulomb field which is less in more peripheral collisions where there is less plasma, this effect partially cancels the effect of the reduction in the fireball lifetime, and results in $\Delta\langle p_T \rangle$ being almost centrality independent.

Figure 5.9 further shows the centrality dependence of the electromagnetically induced difference between flow observables for positive and negative particles at a fixed rapidity. We observe that $\Delta\langle p_T \rangle$ does not vanish in central collisions. This further confirms that it is largely driven by the Coulomb field created by a net positive charge density in the plasma itself, as this Coulomb field is present in

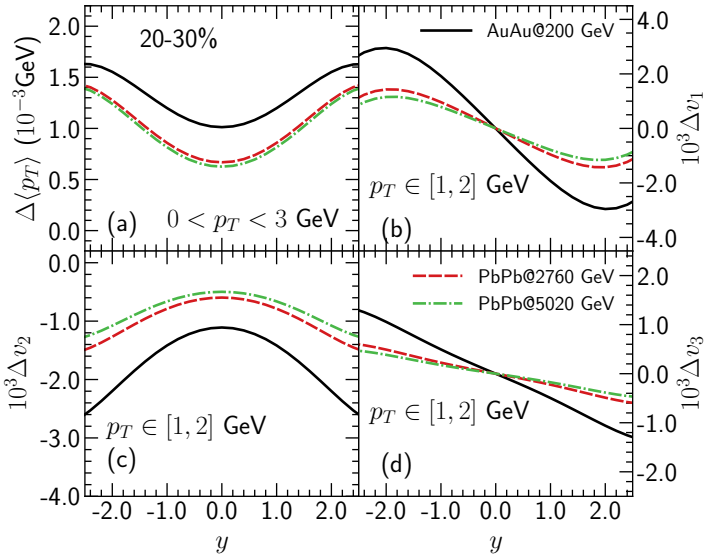

Figure 5.10: *The collision energy dependence of the electromagnetically induced charge-odd contributions to flow observables. The difference of particle mean p_T and v_n between π^+ and π^- are plotted as a function of particle rapidity for collisions at the top RHIC energy of 200 GeV and at two LHC collision energies.*

collisions with zero impact parameter whereas all spectator-induced effects vanish when there are no spectators. This charge density creates an outward electric field that generates an outward flux of positive charge in the plasma and leads to a non-vanishing charge-identified radial flow.

In Figure 5.10, we study the collision energy dependence of the effects of electromagnetic fields on charged hadron flow. The electromagnetically induced effects on the differences between flow observables for positive and negative particles are larger at the top RHIC energy than at LHC energies. This can be understood as arising from the fact that because the spectators pass by more quickly in higher energy collisions the spectator-induced electromagnetic fields decrease more rapidly with time in LHC collisions than in RHIC collisions. Furthermore, in higher energy collisions at the LHC the fireball lives longer, further reducing the magnitude of the electromagnetic fields on the freeze-out surface. The results illustrated in Fig-

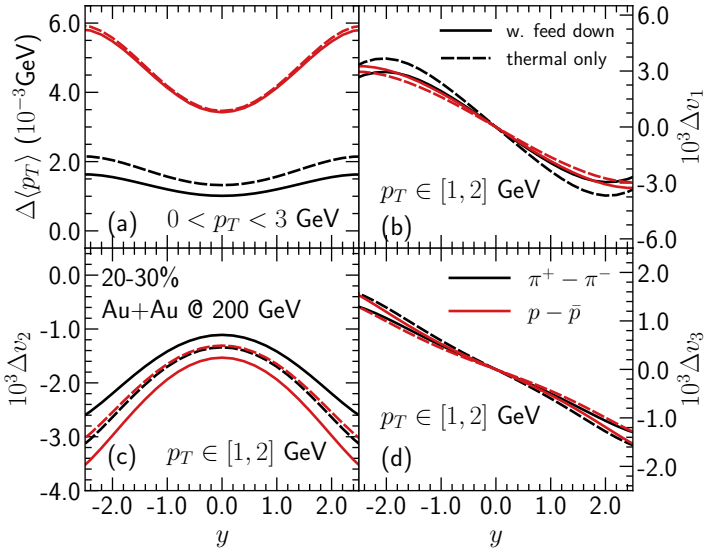

Figure 5.11: *The solid curves include the contributions to the electromagnetically induced charge-dependent flow observables of pions and protons produced after freeze-out by resonance decay, often referred to as resonance feed-down contributions. In the dashed curves, pions and protons produced from resonance feed-down are left out.*

ure 5.10 motivate repeating our analysis for the lower energy collisions being done in the RHIC Beam Energy Scan, although doing so will require more sophisticated underlying hydrodynamic calculations and we also note that in such collisions there are other physical effects that contribute significantly to $\Delta\langle p_T\rangle$ and Δv_2 [225–231], in the case of Δv_2 for protons making a contribution with opposite sign to the one that we have calculated. For both these reasons, we leave such investigations to future work.

Finally, in Figure 5.11, we investigate the contribution of resonance decays to the electromagnetically induced charge-dependent contributions to flow observables that we have computed. These contributions are included in all our calculations with the exception of those shown as the dashed lines in Figure 5.11, where we include only the hadrons produced directly at freezeout, leaving out those produced later as resonances decay. We see that the feed-down contribution from resonance

decays does not significantly dilute the effects we are interested in. To the contrary, the magnitudes of the Δv_n for protons are slightly increased by feed-down effects, in particular the significant contribution to the final proton yield coming from the decay of the Δ^{++} [232]. Because the Δ^{++} resonance carries 2 units of the charge, its electromagnetically induced drift velocity is larger than those of protons.

This concludes the presentation of our central results. In the remainder of this Section, in two subsections we shall present a qualitative argument for why Δv_1 is as small as it is, and then take a brief look at how our results depend on the value of two important material properties of the plasma, namely the drag coefficient and the electrical conductivity.

5.4.1 A qualitative argument for the smallness of Δv_1

As we have seen, the net effect on Δv_1 of the various contributions to the electric field turns out to be rather small in magnitude. This is because even though the contributions $\vec{E}_C + \vec{E}_F$ and $\vec{E}_L$ with opposite sign, shown separately in Figure 5.4, are each relatively large in magnitude they cancel each other almost precisely. This leaves only a small net contribution that generates the charge-odd contributions to the odd flow harmonics that we have computed, Δv_1 and Δv_3. We see in Figure 5.4 that this cancellation becomes more and more complete at larger η_s. In this subsection we provide a qualitative argument for this near-cancellation and explain why the cancellation becomes more complete at larger η_s.

One can find an expression for the total Faraday+Coulomb electric field $\vec{E}_{F+C} \equiv \vec{E}_F + \vec{E}_C$ by solving the Maxwell equations sourced by the spectator (and participant[4]) charges. In general this determines both the electric and the magnetic fields in terms of the sources. However, we only need to express $\vec{E}_{F+C}$ in terms of $\vec{B}$ for the argument. In particular, we are interested in the x component of this field as shown in Figure 5.1. This is given by solving Faraday's law $\nabla \times \vec{E}_{F+C} = -\partial \vec{B}/\partial t$ to obtain $E_{F+C,x} = B_y \coth(Y_0 - \eta_s)$, where Y_0 is the rapidity of the beam and η_s is the spacetime rapidity. Since for both RHIC and LHC we have $Y_0 \gg \eta_s$, one can safely ignore the η_s-dependence everywhere in the plasma, finding $E_{F+C,x} \approx B_y \coth(Y_0)$. For the same reason, as $Y_0 \gg 1$, one can further approximate $E_{F+C,x} \approx B_y$ everywhere in the plasma. The effect of this electric field on the drift velocity of the plasma charges is found by solving the null-force equation (5.8) by boosting it to the

[4]To a very good approximation, one can in fact ignore the participant contribution [56].

local fluid rest frame in a given unit cell in the plasma. This gives the contribution $E_{F+C,x}^{\text{lrf}} \approx \gamma(u) B_y$ where $\gamma(u)$ is the Lorentz gamma factor of the plasma moving with velocity u. On the other hand, the x-component of the Lorentz contribution to the force in the local fluid rest frame is to a very good approximation given by $E_{L,x}^{\text{lrf}} = -\gamma(u) u_z B_y$, where $u_z = \tanh \eta_s$ is the z-component of the background flow velocity. As is clear from Figure 5.1, the directed flow coefficient v_1 receives its largest contribution from sufficiently large η_s where $u_z \approx 1$. We now see that in the regime $2 \lesssim \eta_s \ll Y_0$ there is an almost perfect cancellation between $E_{L,x}^{\text{lrf}}$ and $E_{F+C,x}^{\text{lrf}}$, with $E_{L,x}^{\text{lrf}}$ slightly smaller on account of the fact that u_z is slightly smaller than 1. This means that the main contribution to Δv_1 should come from the mid-rapidity region where the cancellation is only partial as illustrated in Figure 5.4, meaning that Δv_1 is bound to be small in magnitude.

5.4.2 Parameter dependence of the results

Throughout this chapter, we have chosen fixed values for the two important material parameters that govern the magnitude of the electromagnetically induced contributions to flow observables, namely the drag coefficient μm defined in Eq. (5.9) and the electrical conductivity σ. Here we explore the consequences of choosing different values for these two parameters.

In Figure 5.12, we study the effect of varying the drag coefficient μm on the the magnitude of the electromagnetically induced differences between the flow of protons and antiprotons. We change the value of the drag coefficient in Eq. (5.9) by choosing different values of the 't Hooft coupling λ. (The consequences of varying μm for the differences between the flow of π^+ and π^- are similar, although the magnitude of the Δv_n's is less for pions than for protons.) We see in Figure 5.12 that all of the charge-dependent contributions to the flow that are induced by electromagnetic fields become larger when the drag coefficient μm becomes smaller, as at weaker coupling. This is because the induced drift velocity $v_{\text{drift}}^{\text{lrf}}$ in equation (5.8) is larger when the drag coefficient μm is smaller. Since throughout the chapter we have used a value of μm that is motivated by analyses of drag forces in strongly coupled plasma, meaning that we may have overestimated μm, it is possible that in so doing we have underestimated the magnitude of the charge-odd electromagnetically induced contributions to flow observables.

In Figure 5.13, we study the effect of varying the electrical conductivity σ on

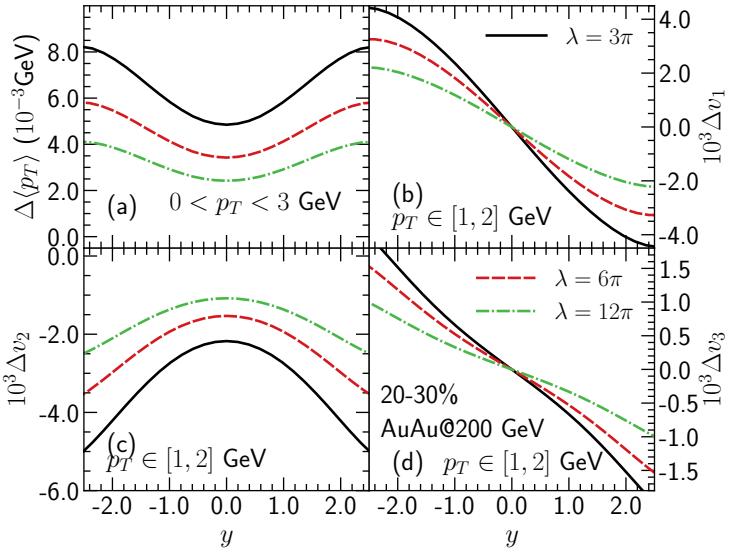

Figure 5.12: *The dependence of the electromagnetically induced differences between the flow of protons and antiprotons on the choice of the drag coefficient μm defined in Eq. (5.9). Elsewhere in this chapter, we fix μm by choosing the 't-Hooft coupling in Eq. (5.9) to be 6π. Here we explore the consequences of varying this parameter by factors of 2 and 1/2, thus varying μm by factors of $\sqrt{2}$ and $1/\sqrt{2}$.*

the magnitude of the electromagnetically induced differences between the flow of protons and antiprotons. Note that, throughout, we are treating μm and σ as constants, neglecting their temperature dependence. This is appropriate for μm, since what matters in our analysis is the value of μm at the freezeout temperature. However, σ matters throughout our analysis since it governs how fast the magnetic fields sourced initially by the spectator nucleons decay away. The value of σ that we have used throughout the rest of this chapter is reasonable for quark-gluon plasma with a temperature $T \sim 250$ MeV, as we discussed in Section 5.2. In a more complete analysis, σ should depend on the plasma temperature and hence should vary in space and time. We leave a full-fledged magnetohydrodynamic study like this to the future. Here, in order to get a sense of the sensitivity of our results to the choice that we have made for σ we explore the consequences for our results of doubling σ, and of setting $\sigma = 0$.

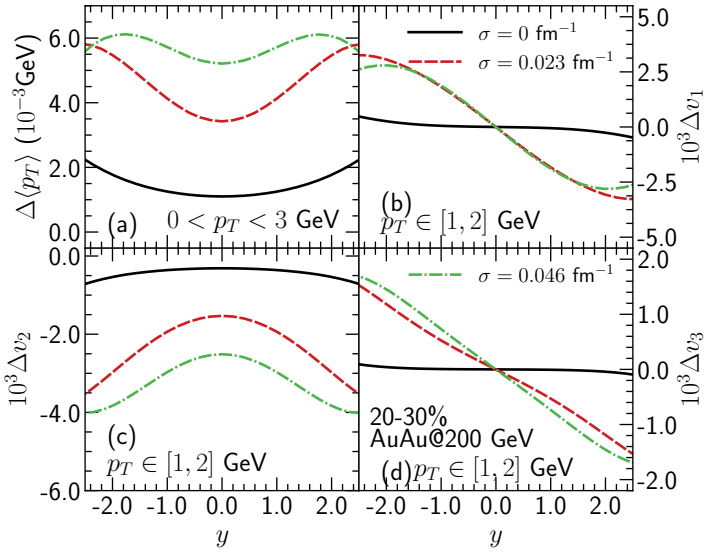

Figure 5.13: *The dependence of the electromagnetically induced differences between the flow of protons and antiprotons on the choice the electrical conductivity σ in the Maxwell equations (5.6) and (5.7).*

The electromagnetically induced charge-odd contributions to the flow observables $\Delta\langle p_T\rangle$ and Δv_2 increase in magnitude if the value of σ is increased. This is because the magnetic fields in the plasma decay more slowly when σ is large [56]. And, a larger electromagnetic field in the local fluid rest frame at the freezeout surfaces induces a larger drift velocity which drives the opposite contribution to proton and antiproton flow observables. We see, however, that the increase in the charge-odd, rapidity-odd, odd Δv_n's with increasing σ is very small, suggesting a robustness in our calculation of their magnitudes. This would need to be confirmed via a full magnetohydrodynamical calculation in future. Since $\Delta\langle p_T\rangle$ and the even Δv_n's are to a significant degree driven by Coulomb fields, it makes sense that they are closer to proportional to σ: increasing σ means that a given Coulomb field pushes a larger current, and it is the current in the plasma that leads to the charge-odd contributions to flow observables. Although not physically relevant, it is also interesting to check the consequences of setting $\sigma = 0$. What remains are small but nonzero contributions to $\Delta\langle p_T\rangle$ and the Δv_n. With $\sigma = 0$ the electric fields do not have any effects during the Maxwell evolution; the small remnant fields at freezeout

are responsible for these effects.

5.5 Discussion and Outlook

We have described the effects of electric and magnetic fields on the flow of charged hadrons in non-central heavy-ion collisions by using a realistic hydrodynamic evolution within the `iEBE-VISHNU` framework. The electromagnetic fields are generated mostly by the spectator ions. These fields induce a rapidity-odd contribution to Δv_1 and Δv_3 of charged particles, namely the difference between v_1 (and v_3) for positively and negatively charged particles. Three different effects contribute: the Coulomb field of the spectator ions, the Lorentz force due to the magnetic field sourced by the spectator ions, and the electromotive force induced by Faraday's law as that magnetic field decreases. The Δv_1 and Δv_3 in sum arise from a competition between the Faraday and Coulomb effects, which point in the same direction, and the Lorentz force, which points in the opposite direction. These effects also induce a rapidity-even contribution to $\Delta\langle p_T\rangle$ and Δv_2, as does the Coulomb field sourced by the charge within the plasma itself, deposited therein by the participant ions. We have estimated the magnitude of all of these effects for pions and protons produced in heavy-ion collisions with varying centrality at RHIC and LHC energies. Our results motivate the experimental measurement of these quantities with the goal of seeing observable consequences of the strong early time magnetic and electric fields expected in ultrarelativistic heavy-ion collisions.

In our calculations, we have treated the electrodynamics of the charged matter in the plasma in a perturbative fashion, added on top of the background flow, rather than attempting a full-fledged magnetohydrodynamical calculation. The smallness of the effects that we find supports this approach. However, we caution that we have made various important assumptions that simplify our calculations: (i) we treat the two key properties of the medium that enter our calculation, the electrical conductivity σ and the drag coefficient μm, as if they are both constants even though we know that both are temperature-dependent and hence in reality must vary in both space and time within the droplet of plasma produced in a heavy-ion collision; (ii) we neglect event-by-event fluctuations in the shape of the collision zone; (iii) rather than full-fledged magnetohydrodynamics, we follow a perturbative calculation where we neglect backreaction of various types, including the rearrangement of the net charge in response to the electromagnetic fields; (iv)

we assume that the force-balance equation (5.8) holds at any time and at any point on the plasma, meaning that we assume that the plasma equilibrates immediately by balancing the electromagnetic forces against drag. As we shall discuss in turn, relaxing these assumptions could have interesting consequences, and is worthy of future investigation. But, relaxing any of these assumptions would result in a substantially more challenging calculation.

Relaxing (i) necessitates solving the Maxwell equations on a medium with time- and space-dependent parameters, which would result in a more complicated profile for the electromagnetic fields. We expect that this would modify our results in a quantitative manner without altering main qualitative findings. We have tried to choose a value for σ corresponding roughly to a time average over the lifetime of the plasma and a value of μm corresponding roughly to its value at freezeout, which is where it is relevant to our analysis. The values of each could be revisited, of course, but our investigation in Section 5.4.2 indicates that this would not affect any qualitative results.

Relaxing (ii), which is to say adding event-by-event fluctuations in the initial conditions for the hydrodynamic evolution of the matter produced in the collision zone, as well as for the distribution of spectator charges, would have quite significant effects on the values of the charge-averaged $\langle p_T \rangle$ and v_n's, for example introducing nonzero v_1 and v_3. Solving the Maxwell equations on such a medium would of course be much more complicated. Furthermore we expect that consequences would appear in all four of the electromagnetic effects that we have analysed (the Faraday $\vec{E}_F$, the Lorentz $\vec{E}_L$, the Coulomb field of the spectators $\vec{E}_C$ and the Coulomb field of the plasma $\vec{E}_P$) resulting in each contributing at some level to each of the four observables that we have analysed ($\Delta\langle p_T \rangle$, Δv_1, Δv_2 and Δv_3). However, we expect that the electromagnetically induced contributions that we have found using a smooth hydrodynamic background without fluctuations, and whose magnitudes we have estimated, will remain the largest contributions.

Relaxing assumption (iii) may bring new effects and, as we shall explain, could potentially flip the sign of the odd flow coefficients Δv_1 and Δv_3. One particular physical effect that we neglect is the shorting, or partial shorting, of the Coulomb electric fields in the plasma, both the $\vec{E}_C$ sourced by the spectators and the $\vec{E}_P$ sourced by the plasma itself. These Coulomb fields will push charges in the plasma to rearrange in a way that reduces the electric field within the conducting plasma. We

have neglected this, and all, back reaction in our calculation. However, although it would require a fully dynamical calculation of the currents and electric and magnetic fields to estimate its extent, some degree of shorting must occur. There may, in fact, be experimental evidence of this effect: Δv_2 for pions has been measured in RHIC collisions with 30-40% centrality and collision energy $\sqrt{s} = 200$ AGeV by the STAR collaboration [233], and although it turns out to be negative as our calculations predict it is substantially smaller in magnitude than what we find. Because there are other effects (unrelated to Coulomb fields) that can contribute to Δv_2 and that are known to contribute significantly to Δv_2 in lower energy collisions [225–231], it would take substantially more analysis than we have done to use the experimentally measured results for Δv_2 to constrain the magnitude of $\vec{E}_C$ and $\vec{E}_P$ quantitatively. However, it does seem likely that, due to back reaction, they have been at least partially shorted, making them weaker in reality than in our calculation.

The likely reduction in the magnitude of $\vec{E}_C$, in turn, has implications for the odd Δv_n's. Recall that they arise from the sum of three effects, in which there is a near cancellation between $\vec{E}_F + \vec{E}_C$ and $\vec{E}_L$, which point in opposite directions. The sign of the rapidity-odd Δv_1 and Δv_3 that we have found in our calculation corresponds to $|\vec{E}_F + \vec{E}_C|$ being slightly greater than $|\vec{E}_L|$. If $|\vec{E}_C|$ is in reality smaller than in our calculation, this could easily flip the sign of Δv_1 and Δv_3. In this context, it is quite interesting that a preliminary analysis of ALICE data [216] indicates a measured value of Δv_1 for charged particles in LHC heavy-ion collisions with 5%-40% centrality and collision energy $\sqrt{s} = 5.02$ ATeV that is indeed rapidity-odd and is comparable in magnitude to the pion Δv_1 for collisions with this energy that we have found in Fig.10, but is opposite in sign.

Finally, let us consider relaxing our assumption (iv). This corresponds to considering a more general version of (5.8) with a non-vanishing acceleration on the right-hand side. The drift velocity that would be obtained in such a calculation would decay to the one that we have found by solving the force-balance equation (5.8) exponentially, with an exponent controlled by the drag coefficient μ. Thus, for very large μ we do not expect any significant deviation from our results. However, at a conceptual level relaxing assumption (iv) would change our calculation significantly, since it is only by making assumption (iv) that we are able to do a calculation in which μ enters only through the value of μm at freezeout. If we relax assumption (iv), the actual drift velocity would always be lagging behind the value obtained by solving (5.8), and determining the drift velocity at freezeout would, in principle, retain a

memory of the history of the time evolution of μ. If we use the estimate (5.9) for μ and focus only on light quarks, and hence pions and protons, as we have done we do not expect that relaxing assumption (iv) would have a qualitative effect on our results. However, μ may in reality not be as large as that in (5.9) at freezeout. And, furthermore, it is also very interesting to extend our considerations to consider heavy charm quarks, as in Ref. [234]. The charm quarks receive a substantial initial kick from the strong early time magnetic [234] and electric fields, and because they are heavy μ may not be large enough to slow them down and bring them into alignment with the small drift velocity that (5.8) predicts for heavy quarks. Hence, consideration of heavy quarks requires relaxing our assumption (iv) in a way that alters our conclusions significantly, and indeed the authors of Ref. [234] find a substantially larger Δv_1 for mesons containing charm quarks than the Δv_1 that we find for pions and protons. These considerations motivate the (challenging) experimental measurement of Δv_1 for D mesons. In [235] there is a discussion on the (mis)match between the theory and experiment.

Summary and Outlook

In this thesis, we have discussed a wide array of topics, split up into three parts. In the first part of the thesis, we focussed explicitly on black hole solutions within string theory and M-theory. In chapter 2 we focussed on black holes in string theory with duality twists. One motivation for the project was to study black holes in supersymmetry-breaking background theories. To break the supersymmetry, we made use of *Scherk-Schwarz* reductions on a circle. These reductions introduce a monodromy on the fields as they move around the circle, and the monodromies, in their turn, result in mass terms in the lower dimensional theory. When (some of) the gravitini get a mass in this manner, the supersymmetry is broken.
The chapter started by discussing the Type IIB supergravity theory in ten dimensions, subsequently reduced on T^4 to obtain a six-dimensional theory with $\mathcal{N} = (2, 2)$ supersymmetry and a Spin(5,5) duality group. Our first goal was to write this six-dimensional theory in an explicitly Spin(5,5)-covariant manner, such that we can let the monodromies act on the fields. We could then reduce on the Scherk-Schwarz circle; the monodromies were chosen to lie in the maximal torus $\mathrm{U}(1)^4$ of the R-symmetry subgroup of the total Spin(5,5) duality group. This choice meant that there are four mass parameters m_i that can be tuned to our preference; depending on which of the m_i we choose non-zero, we can end up in five-dimensions with $\mathcal{N} \in \{8, 6, 4, 2, 0\}$ supersymmetry.
The subsequent ingredients were the black holes themselves; we presented first the 10D solutions of the D1-D5-P, F1-NS5-P, and the D3-D3-P systems. Reducing these to six dimensions followed the straightforward procedure, but for the reduction on the Scherk-Schwarz circle, we had to pay close attention to the choice of monodromy. This is because each of the brane configurations is charged by different fields, and to preserve the solution, these fields must remain massless. The case where the monodromy lies within the T-duality subgroup SO(4,4) received particular attention since, in these scenarios, the theory could also be described by orbifold constructions. In particular, the case where we end up with $\mathcal{N} = 4\,(2, 0)$ supersymmetry, achieved by $m_1 = m_2$, is of interest since it lies in the T-duality subgroup and simultaneously

preserves both the F1-NS5 and D1-D5 systems.
After completing the reductions, we considered the theories as effective theories and integrated out the massive fields in the theory. This procedure generates corrections to the Chern-Simons terms of the theory, and we subsequently studied the effects the integrating has on the black hole entropy, which changes due to both the gravitational and mixed Chern-Simons terms. Lastly, we discussed the uplift of the procedure to string theory and showed that when the m_i are suitably quantized, the procedure can be embedded into string theory.

In chapter 3 we studied the geometry of supersymmetric solutions that can be interpreted as the near-horizons of rotating black holes and black strings. The near-horizon of rotating black holes is characterized by the presence of a fibration over an AdS_2 space. From the eleven-dimensional viewpoint, this means we want to consider rotating M2-branes wrapped on a Riemann surface since such geometries may give rise to near horizons of black holes. To find the geometries, we started by discussing the conditions for an 11D geometry admitting a timelike Killing vector. Preservation of supersymmetry imposes conditions on the allowed terms in the four-form flux and the SU(5) structure present on the 10D space.
The next step was to specify the ten-dimensional space conformally as a cone, under the conditions that we to recover a warped AdS_2 space along with a 9D space that is independent of the radial coordinate. The conical geometry naturally yields an R-symmetry vector, which in its turn allows us to create a holomorphic foliation of an 8D space that admits an SU(4) structure, which it inherits from the 10D SU(5) structure. We reduced the SU(5) structure to the 8D base and found that the 8D space is, in general, a balanced manifold, not necessarily Kähler. Furthermore, we reduced the fluxes to eight dimensions and derived their Bianchi identities and Maxwell equations. The first Maxwell equation is also known as the 'master equation', which we thus generalized to the rotating case.
We also give a (non-supersymmetric) Lagrangian description, from which the equations of motion can be derived. Afterward, we applied supersymmetry to the Lagrangian and showed to what extent it coincides with the non-rotating case. As an example of the classification, we embedded the asymptotically AdS_4, electrically charged, Kerr-Newman black hole in 4D $\mathcal{N} = 2$ into the classification. Lastly, assuming that the internal space admits a two-torus, we used dualities to end up in Type IIB theory and discussed the near-horizon geometries of rotating black strings similar to the black holes preceding them.

In the second part of the thesis, we switched our focus away from explicit black hole solutions and their implementations in string theory and supergravity. Instead, we focussed first on a one-dimensional conformal field theory, whose dual theory describes black holes. In this second part, we considered a generalization to the Sachdev-Ye-Kitaev model, a one-dimensional field theory. Instead of only considering N Majorana fermions, as is the case in the original SYK model, we also introduced M auxiliary bosons. We considered the model while taking both the large N and the large M limits but keeping the ratio M/N fixed. If we were to take $M = N$, we find that the model essentially reduces to the $\mathcal{N} = 1$ supersymmetric SYK model. In order to properly investigate the dynamics of the model, we derived the effective action and the corresponding equations of motion for the bilocal fields in the effective action. For general M/N, the equations of motion yield two solutions; we label them by their behavior for $M = N$ as 'rational' and 'irrational'. The rational branch has, for $M = N$, the same conformal dimensions as the supersymmetric SYK model. As we take the limit $M/N \to \infty$, we find that the branches coincide, and only one solution remains. In this limit, the conformal dimension of the fermions coincides with that of vanilla SYK, and we can consider them to have the same infrared fixed points.
To figure out which of the branches is the dominant saddle one, we performed a numerical analysis on the entropies and found that for general M/N that the rational branch dominates. Finally, we concluded the chapter by investigating the chaos in the model and found that the model is still maximally chaotic for all M/N, necessary for a possible dual interpretation as black holes.

The last part of the thesis considered heavy-ion collisions, quark-gluon plasmas, and electromagnetic fields. The relation between these three is as follows: the heavy-ion collisions, at large enough speeds (for example, at the LHC), produce the quark-gluon plasma. Not all ions collide with one another, however, and when these charged particles fly by the collision, they result in powerful electromagnetic fields. This chapter aimed to investigate the effects of the electromagnetic fields on the hydrodynamic expansion of the quark-gluon plasma. The first part of the chapter focussed on explaining the different electromagnetic fields and their origins. Firstly, the 'spectating' particles that fly by the collision cause a diminishing magnetic field in the y direction, from the plasma's point of view. Faraday's law causes an electric field E_F that curls around the decreasing magnetic field. The Lorentz force causes a second effect, also caused by the magnetic field. Lastly, there are Coulomb forces,

both from the spectators and the participants of the collision.
The setup we used consisted of a combination of numerical models. The electromagnetic fields could be solved semi-analytically by assuming that the conductivity is constant and independent of temperature. The hydrodynamic evolution was simulated using `iEBE-VISHNU` framework, where the initial conditions were determined by averaging over Monte-Carlo-Glauber events.
The effects of the electromagnetic fields were investigated using flow coefficients v_n. Specifically we considered the directed flow v_1, the elliptic flow v_2 and the triangular flow v_3. The odd flow coefficients receive an odd contribution in rapidity, while the even flow coefficients are even in rapidity. The effects of the electromagnetic fields are several orders of magnitudes smaller than the overall hydrodynamic flow of the plasma, which is consistent with the expectation that electromagnetic effects should yield a small perturbation on the expansion. In the last part of the chapter, we considered the influence of parameters on the resulting flow. We investigated the effects of centrality, the drag coefficient μm, and the conductivity σ on the resulting flow coefficients.

Outlook

Let me now discuss my broad outlook on the field and what I see as exciting and promising future directions. All of my projects were, in some way, related to black holes. Even more so than when I started my Ph.D., I believe that black holes make for a fascinating challenge in physics research; our understanding is genuinely tested under such extreme circumstances. For that reason, I think that research focussed on black holes is bound to bring us further in our knowledge. More concretely, the duality between quark-gluon plasmas and black hole physics remains one of the only ways to examine our theories experimentally. Due to the tremendous importance of experimental falsification, I sincerely hope that research will continue to blossom in this direction, both theoretically and experimentally.[1] A more in-depth study of the magnetically induced transport in the plasma can have far-reaching consequences. One of these consequences is, for example, a better understanding of the baryon asymmetry in the early universe using CP-violation. The relation between the two phenomena was made by Sakharov in 1967 [236] when he listed C- and CP-violation as one of the necessary ingredients of baryogenesis. These violations occur due

[1] Fortunately, my co-promoter has, at the time of writing, just received a Vici grant for pursuing exactly such interests.

to quantum effects in the topologically non-trivial vacuum of the standard model. Heavy-ion collisions reproduce the early universe several microseconds after the big bang; however, they cannot directly probe the topological vacuum transitions responsible for baryogenesis. Fortunately, QCD allows for a similar situation with different topological vacuum sectors when considering the chirality in heavy-ion collisions. In these chirally asymmetric situations, an imbalance between the left- and right-handed quarks exists. Since the left- and right-handed quarks are related by parity P, the vacuum transitions violate a combination of C and CP-symmetries; analogous to the baryogenesis before, we now get a 'chirogenesis' effect.

As for the string theoretical research into black holes presented, there are a few obvious and exciting follow-up directions. First, a field theory dual to the duality compactifications is bound to shed light on the microscopic details of the remaining brane systems and thus black holes. It would be fascinating to see if the black hole entropies could be reproduced in the microscopic setting. Secondly, regarding the rotating black holes: a complete understanding of the extremization for our classification would extend the current framework to a large class of rotating black holes. This extension would allow us, for example, to calculate the entropies of such black holes using only topological properties. Let me now make some more general comments about encouraging directions in the black hole physics field. Although I have not actively researched it as much as I wanted, quantum information and black holes remains, to me, a captivating subject. At the interplay between those two, we should probably learn more about both; perhaps we can even make progress in understanding the foundations of quantum mechanics. In particular, a better understanding of the information paradox seems vital for improving our understanding of black holes; the recent 'island' proposals seem to make good progress in this direction. Finally, the study of quantum information principles in string theory and holography also seems a significant field of interest. Significant steps here have already been made with, for example, holographic entanglement entropy or holographic complexity, which allow for another construction of fundamental information principles.

Samenvatting en Vooruitzicht

In dit proefschrift hebben we een breed scala aan onderwerpen besproken, opgesplitst in drie delen. In het eerste deel van het proefschrift hebben we ons expliciet gefocust op zwarte gat oplossingen binnen snaartheorie en M-theorie. In hoodstuk twee hebben we ons gericht op zwarte gaten in snaartheorie met dualiteits-draaiingen. Een motivatie voor het project was het bestuderen van zwarte gaten in supersymmetrie-brekende achtergrondtheorieën. Om de supersymmetrie te breken hebben we gebruik gemaakt van *Scherk-Schwarz* reducties op een cirkel. Deze reducties introduceren een monodromie op de velden terwijl ze rond de cirkel bewegen, en deze monodromieën resulteren in massa termen in de lager-dimensionale theorie. Wanneer (een deel van) de gravitini op deze manier een massa krijgen, wordt de supersymmetrie broken.
Het hoofdstuk begon met een bespreking van de Type IIB supergravitatie-theorie in tien dimensies, welke vervolgens gereduceerd werd op T^4 om een zes-dimensionale theorie te verkrijgen met $\mathcal{N} = (2, 2)$ supersymmetrie en een Spin(5,5) dualiteitsgroep. Ons eerste doel was om deze zes-dimensionale theorie expliciet Spin(5,5)-invariant te schrijven, zodat we de monodromieën op de velden konden laten werken. Daarna kunnen we reduceren op de Scherk-Schwarz cirkel: de mondoromieën zijn gekozen om te liggen in de maximale torus $\mathrm{U}(1)^4$ van de R-symmetrie subgroep van de totale Spin(5,5) dualiteitsgroep. Deze keuze betekende dat er vier massa parameters m_i zijn die kunnen worden afgestemd op onze voorkeur; afhankelijk van welke van de m_i we niet-nul kiezen, kunnen we eindigen in vijf dimensies met $\mathcal{N} \in \{8, 6, 4, 2, 0\}$ supersymmetrie.
De volgende ingrediënten waren de zwarte gaten zelf; we presenteerden eerst de 10D-oplossingen van de D1-D5-P, F1-NS5-P en de D3-D3-P systemen. Het terugbrengen van deze oplossingen tot zes dimensies volgde de standaard procedure, maar voor de reductie op de Scherk-Schwarz-cirkel moesten we goed letten op de keuze voor monodromie. Elk van de braan configuraties wordt geladen door verschillende velden en om de oplossing te behouden, moeten deze velden massavrij blijven. Het geval waarin de monodromie binnen de T-dualiteit subgroep SO(4,4) ligt

kreeg speciale aandacht, aangezien in deze scenario's de theorie ook door orbifold constructies beschreven kan worden. In het bijzonder het geval waarin we eindigen met $\mathcal{N} = 4\,(2,0)$ supersymmetrie, bereikt door $m_1 = m_2$, is interessant omdat het in de T-dualiteit-subgroep ligt en tegelijkertijd het zowel de F1-NS5 als de D1-D5 systemen behoudt.
Na het voltooien van de reducties beschouwden we de theorieën als effectieve theorieën en integreerden we de massieve velden uit de theorie. Deze procedure genereert correcties op de Chern-Simons-termen van de theorie, en we hebben vervolgens de effecten bestudeerd die de integratie heeft op de entropieën van de zwarte gaten, die veranderen als gevolg van zowel de zwaartekracht- als de gemengde-Chern-Simons termen. Ten slotte hebben we de ophijsing van de procedure naar de snaartheorie besproken en laten zien dat een juiste kwantisatie van de m_i ervoor zorgt dat de procedure kan worden ingebed in snaartheorie.

In het derde hoofdstuk hebben we de meetkunde van supersymmetrische oplossingen bestudeerd die kunnen worden geïnterpreteerd als de nabije horizon van roterende zwarte gaten en zwarte snaren. De nabije horizon van roterende zwarte gaten wordt gekenmerkt door de aanwezigheid van een fibratie over een AdS_2 ruimte. Vanuit het elf-dimensionale gezichtspunt betekent dit dat we roterende M2-branen willen plaatsen, gewikkeld op een Riemann-oppervlak, aangezien dergelijke geometrieën aanleiding kunnen geven tot nabije horizons van zwarte gaten. Om de geometrieën te vinden, zijn we begonnen met het bespreken van de voorwaarden voor een 11D-geometrie die een tijdachtige Killing-vector toelaat. Behoud van supersymmetrie stelt voorwaarden aan de toegestane termen in de vier-vorm flux en de SU(5)-structuur die aanwezig is op de 10D-ruimte.
De volgende stap was om de tien-dimensionale ruimte conform te specificeren als een kegel, onder de voorwaarden dat we een kromgetrokken AdS_2 ruimte willen herkennen, samen met een 9D-ruimte die onafhankelijk is van de radiale coördinaat. De conische meetkunde levert een R-symmetrievector op, die ons in staat stelt een holomorfe foliatie te creëren van een 8D-ruimte die een SU(4)-structuur toelaat, die hij erft van de 10D SU(5)-structuur. We hebben de SU(5)-structuur teruggebracht tot de 8D-basis en ontdekten dat de 8D-ruimte in het algemeen een gebalanceerde variëteit is, niet noodzakelijk Kähler. Verder hebben we de fluxen teruggebracht tot acht dimensies en hun Bianchi-identiteiten en Maxwell-vergelijkingen afgeleid. De eerste Maxwell-vergelijking staat ook bekend als de 'hoofdvergelijking', die we dus gegeneraliseerd hebben naar het roterende geval.

We geven ook een (niet-supersymmetrische) Lagrangiaanse beschrijving, waaruit de bewegingsvergelijkingen kunnen worden afgeleid. Daarna hebben we supersymmetrie toegepast op de Lagrangiaan en laten zien in hoeverre deze samenvalt met het niet-roterende geval. Als voorbeeld van de classificatie hebben we het asymptotisch AdS_4, elektrisch geladen, Kerr-Newman zwarte gat in 4D $\mathcal{N} = 2$ in de classificatie geplaatst. Ten slotte, ervan uitgaande dat de interne ruimte een twee-torus toelaat, gebruikten we dualiteiten om in Type IIB theorie terecht te komen en bespraken we de nabije horizon geometrieën van roterende zwarte snaren op een gelijkaardige manier als de zwarte gaten die eraan voorafgingen.

In het tweede deel van het proefschrift hebben we onze focus verlegd van de expliciete zwart-gatoplossingen en hun relaties tot snaartheorie en superzwaartekracht tot een één-dimensionale conforme veldentheorie. In het bijzonder hebben we een generalisatie naar het Sachdev-Ye-Kitaev-model beschouwd, een één-dimensionale veldtheorie. In plaats van alleen N Majorana-fermionen te beschouwen, zoals het geval is in het originele SYK-model, hebben we ook M hulp-bosonen geïntroduceerd. We hebben het model bekeken terwijl we zowel de grote N als de grote M limieten namen, maar de verhouding M/N vast hielden. Als we $M = N$ zouden nemen, zien we dat het model in wezen reduceert tot het $\mathcal{N} = 1$ supersymmetrische SYK-model. Om de dynamiek van het model goed te onderzoeken hebben we de effectieve actie en de bijbehorende bewegingsvergelijkingen afgeleid voor de bilocale velden in de effectieve actie. De bewegingsvergelijkingen leveren voor algemene M/N twee oplossingen op; we bestempelen ze op basis van hun gedrag voor $M = N$ als 'rationeel' en 'irrationeel'. De rationele tak heeft voor $M = N$ dezelfde conforme dimensies als het supersymmetrische SYK-model. Als we de limiet $M/N \to \infty$ nemen, zien we dat de vertakkingen samenvallen en dat er maar een enkele oplossing overblijft. In deze limiet valt de conforme dimensie van de fermionen samen met die van 'normale' SYK, en we kunnen ervan uitgaan dat ze hetzelfde infrarood vaste punt hebben.
Om erachter te komen welke van de takken het dominante zadel is, hebben we een numerieke analyse van de entropieën uitgevoerd en vastgesteld dat voor algemene M/N de rationele tak domineert. We sloten het hoofdstuk af met een onderzoek naar de chaos in het model en ontdekten dat het model nog steeds maximaal chaotisch is voor alle M/N, wat ook nodig is voor een mogelijke duale interpretatie als zwarte gaten.

Het laatste deel van het proefschrift behandelde zware ionen botsingen, quark-gluon-

plasma's en elektromagnetische velden. De relatie tussen deze drie is als volgt: de zware ionen botsingen, bij voldoende hoge snelheden (bijvoorbeeld bij de LHC), produceren het quark-gluon plasma. Niet alle ionen komen echter met elkaar in botsing, en wanneer deze geladen deeltjes door de botsing vliegen, resulteren ze in zeer sterke elektromagnetische velden. Het doel van dit hoofdstuk was om de effecten van de elektromagnetische velden op de hydrodynamische expansie van het quark-gluon plasma te onderzoeken. Het eerste deel van het hoofdstuk was gericht op het uitleggen van de verschillende elektromagnetische velden en hun oorsprong. Ten eerste veroorzaken de 'toekijkende' deeltjes die de botsing voorbij vliegen, een afnemend magnetisch veld in de y richting, vanuit het oogpunt van het plasma. Volgens de wet van Faraday veroorzaakt dit een elektrisch veld E_F dat rond het afnemende magnetische veld krult. Een tweede effect wordt veroorzaakt door de Lorentz-kracht, ook veroorzaakt door het magnetische veld. Ten slotte zijn er Coulomb-krachten, zowel van de toeschouwers als van de deelnemers aan de botsing.
De opstelling die we gebruikten, bestond uit een combinatie van numerieke modellen. De elektromagnetische velden zouden semi-analytisch kunnen worden opgelost door aan te nemen dat de geleidbaarheid constant en temperatuur onafhankelijk is. De hydrodynamische evolutie werd gesimuleerd met behulp van het `iEBE-VISHNU` -raamwerk, waarbij de initiële condities werden bepaald door middeling over Monte-Carlo-Glauber events.
De effecten van de elektromagnetische velden zijn onderzocht met behulp van stroomcoëfficiënten v_n. We hebben specifiek gekeken naar de gerichte stroom v_1, de elliptische stroom v_2 en de driehoekige stroom v_3. De oneven stroomcoëfficiënten ontvangen een bijdrage die in de rapiditeit oneven is, terwijl de even stroomcoëfficiënten ook een even contributie geven. De effecten van de elektromagnetische velden zijn enkele ordes van grootte kleiner dan de algehele hydrodynamische stroming van het plasma, wat consistent is met de verwachting dat elektromagnetische effecten een kleine verstoring van de expansie zouden opleveren. In het laatste deel van het hoofdstuk hebben we gekeken naar de invloed van parameters op de resulterende stroming. We onderzochten de effecten van centraliteit, de weerstandscoëfficiënt μm en de geleidbaarheid σ op de resulterende stromingscoëfficiënten.

Vooruitzicht

Laat me nu mijn brede kijk op het veld bespreken en mijn visie op uitdagende en veelbelovende toekomstige richtingen. Al mijn projecten waren, op de een of andere manier, gerelateerd aan zwarte gaten. Nog meer dan toen ik aan mijn doctoraat begon, geloof ik dat zwarte gaten een fascinerende uitdaging vormen voor natuurkundig onderzoek; ons begrip wordt echt op de proef gesteld onder zulke extreme omstandigheden. Om die reden denk ik dat onderzoek gericht op zwarte gaten ons zeker verder zal brengen in onze kennis. Concreet blijft de dualiteit tussen quark-gluon plasma's en de fysica van zwarte gaten één van de weinige manieren om onze theorieën experimenteel te onderzoeken. Vanwege het enorme belang van experimentele falsificatie hoop ik dat het onderzoek in deze richting zal blijven bloeien, zowel theoretisch als experimenteel.[1] Een meer diepgaande studie van het magnetisch geïnduceerde transport in het plasma kan verstrekkende gevolgen hebben. Één van deze gevolgen is, bijvoorbeeld, een beter begrip van de baryon-asymmetrie in het vroege heelal, met behulp van CP-symmetrie schending. De relatie tussen de twee fenomenen werd gelegd door Sacharov in 1967 [236] toen hij C- en CP-schending noemde als één van de noodzakelijke ingrediënten van baryogenese. Deze schendingen treden op vanwege kwantumeffecten in het topologisch niet-triviale vacuüm van het standaardmodel. Botsingen met zware ionen reproduceren het vroege heelal enkele microseconden na de oerknal; ze kunnen echter niet direct de topologische vacuümovergangen onderzoeken die verantwoordelijk zijn voor baryogenese. Gelukkig zorgt QCD voor een vergelijkbare situatie met verschillende topologische vacuümsectoren als we kijken naar de chiraliteit bij botsingen met zware ionen. In deze chiraal asymmetrische situaties bestaat er een onbalans tussen de links- en rechtshandige quarks. Aangezien de links- en rechtshandige quarks verwant zijn door pariteit P, schenden de vacuümovergangen een combinatie van C- en CP-symmetrieën; analoog aan de baryogenese voorheen, krijgen we nu een 'chirogenesis'-effect.

Wat betreft het gepresenteerde snaartheoretisch onderzoek naar zwarte gaten, zijn er een paar voor de hand liggende en uitnodigende vervolgrichtingen. Ten eerste, zal een veldtheorie die duaal is aan de dualiteits-compactificaties ongetwijfeld licht werpen op de microscopische details van de resterende braansystemen en

[1] Gelukkig heeft mijn copromotor, op het moment van schrijven, zojuist een Vici-beurs ontvangen voor precies zulke interesses.

dus zwarte gaten. Het zou fascinerend zijn om te zien of de entropieën van het zwarte gat kunnen worden gereproduceerd in de microscopische omgeving. Ten tweede, met betrekking tot de roterende zwarte gaten: een volledig begrip van de extremisering voor onze classificatie zou het huidige raamwerk uitbreiden tot een grote klasse van roterende zwarte gaten. Met deze uitbreiding zouden we bijvoorbeeld de entropie van dergelijke zwarte gaten kunnen berekenen met alleen topologische eigenschappen. Laat me nu wat meer algemene opmerkingen maken over bemoedigende richtingen op het gebied van de fysica van zwarte gaten. Hoewel ik het niet zoveel heb onderzocht als ik wilde, blijft kwantuminformatie in relatie tot zwarte gaten een erg boeiend onderwerp. Bij de wisselwerking tussen die twee zouden we waarschijnlijk meer over beide moeten leren; misschien kunnen we zelfs vooruitgang boeken in het begrijpen van de fundamenten van de kwantummechanica. Met name een beter begrip van de informatieparadox lijkt essentieel voor het verbeteren van ons begrip van zwarte gaten; de recente 'eiland'-voorstellen lijken in deze richting goede vooruitgang te boeken. Ten slotte lijkt de studie van kwantuminformatie-principes in de snaartheorie en holografie ook een belangrijk aandachtsgebied. Hier zijn al belangrijke stappen gezet met bijvoorbeeld holografische verstrengelingsentropie of holografische complexiteit, welke een andere constructie van fundamentele informatieprincipes mogelijk maken.

Acknowledgements

The last four years have marked an exhilarating, inspiring and, of course, at some points, challenging time; here I want to thank the people that have made these years such a pleasant experience. First up, I want to thank my supervisors. Stefan, bedankt voor alle vragen, inzichten, commentaren en (natuurkundige) discussies over de jaren. Het was me een waar genoegen om deze jaren met je samen te werken, en ook bedankt de vrijheid die je me hebt gegeven om vooral aan de onderwerpen te werken die me op dat moment het meest intereseerden. Umut, it has been a pleasure doing research with you over the past years. We first met in 2015, and started working on projects that retained our interest all the way into my PhD; it was always very engaging and a lot of fun to work with you.

Then on to my fellow *Tori Legend* and one of my paranymphs: Koen. We have worked together on almost all our projects in the last few years, and it has continuously been a very fruitful and enjoyable experience; *wow*. Perhaps most of all, I enjoyed our endless discussions on any topic we could find ourselves to disagree on; I hope we will continue to have them!

Damian, thanks for all the good times; you have always impressed me with your quick thinking; I'd have loved to do another five or six projects with you! Similarly, Chris, you are a very motivated, curious, and hardworking physicist. I've learned many things from you, and I feel that the physics world will be quite all right if people as determined as you continue to be its inhabitants.

I would like to thank Huibert (or Herbert) and Kilian for discussions, and also for all the fun nights out, where Herbert never missed an opportunity to shoot another embarrassing video of me. I also would like to thank Kilian for teaching me German accents. Markus, Miguel and John, thanks so much for all the (good) jokes and discussions, all of you inspired me on several fronts.

To the Amsterdam people: Antonio, Carlos, Dora and more, thanks for making the holography meetings and DRSTP schools so much more fun! Beatrix, thanks for all the company to our concerts in the past years! Greg, thanks for all the hangouts, nice pictures from Switzerland, gossip, concerts, and good friendship through the

years; I'm looking forward to our beers in NY.
Let me acknowledge Govert, Domingo, Natale and Juan for collaborations on holographic entanglement entropy and matrix quantum mechanics, which, unfortunately, we did not manage to solve in the end. Similarly, I want to thank Frits, Natale and Ronnie for collaboration on tensor models.
Joren, thank you for enlightening me on how valuable triangles can be for understanding practically anything. Also, many thanks for all the discussions on books and other things we have had throughout the years.
Thanks to my previous office mates Aron and Matti. I want to thank the people in the institute for the nice company and discussions during lunch and coffee times: Adriana, Anna, Brice, Camilo, Chongchuo, Erik, Guido, Henk, Irene, Nava, Niccolo, Pierre, Raffaele, Rembert, Ronnie, Sander & Sander, Taka, Tomislav, Tycho, Watse and many more.
Merel, thanks for being one of my paranymphs and for all the opportunities to chill, complain, drink beers and climb huge mountains. Also, many thanks for your keen sense of humor, and I hope we can make all our planned trips very soon! Similarly, thanks to Danny (or Donny) for all the forms of (digital) entertainment, humour, and friendship throughout the years. Sjors, Mark, Kelley (Kelsey), I am delighted to have you as my friends and have loved all of our evenings of gaming, our trips and holidays; I hope there will be many more! Mirte, you have been a great friend and sister-in-law; thanks for all the times where you listened to my complaining, and the many fun evenings with wine, games, and cats! Also, thanks to Pim for providing ample distractions throughout the years! Robbin, it is always a pleasure to discuss practically any topic with you; thanks for all the ideas, creativity, and fun times!
Thanks to Domingo, Danna, Natale and, since recently, Centli for all the fun board game evenings; I'm looking forward to meeting Centli real soon!
I would like to thank the people of the Oxford Karl Popper Society for introducing me to the fantastic world of epistemology and good explanations. Sam, thanks a lot for the numerous (digital) conversations. We never seem to have enough time to discuss everything we want; I look forward to visiting you in Oxford!
Baayla, thank you for all the tea sessions and the introduction to your work on Alzheimer's; I hope our collaboration on combining your work with artificial intelligence will bear its fruits soon!
Charlotte, thanks a lot for giving a very positive spin to 2020! It has been great to have you by my side during the writing of this thesis and your comments on

my intro; I will gladly return the favor! Last but certainly not least, my parents: thanks for all the support throughout the years; you have always let me follow my own path, which is part of the reason that this thesis exists in the first place.

About the author

Eric Marcus was born on the 13th of May 1994 in Meppel. In 2012 he started his bachelor's in physics at Utrecht University, which he completed cum laude in 2015. During this time, he also participated in the honors program, part of which requires an extended bachelor research project, which was supervised by Umut Gürsoy. This research concerned magnetohydrodynamics at heavy-ion collisions and was awarded several national prizes. After the bachelor program, Eric started a master's in theoretical physics, which he completed cum laude in 2017. The research subject of his master thesis was about Sachdev-Ye-Kitaev models and Jackiw-Teitelboim gravity, supervised by Stefan Vandoren.

In that same year, he started his Ph.D. under the NWO 'scanning new horizons' grant at the Institute of Theoretical Physics in Utrecht. During his Ph.D. he investigated a wide array of topics with several collaborators, concerning black holes in string theory, and follow-up projects of the research performed in his bachelor and master years. Part of this research resulted in this thesis. Apart from research, Eric also played a role in supervising students, teaching classes, and presenting the research (internationally).

More recently, Eric has also taken an interest in artificial intelligence, and in particular deep learning. He is currently engaged in an internship at the UMC Amsterdam, whereby deep learning methods are applied to Alzheimer's disease scans to determine the disease's subtypes automatically, thereby removing this time-consuming burden from the pathologists.

Bibliography

[1] C. Hull, E. Marcus, K. Stemerdink and S. Vandoren, *Black holes in string theory with duality twists*, *JHEP* **07** (2020) 86 [2003.11034].

[2] C. Couzens, E. Marcus, K. Stemerdink and D. van de Heisteeg, *The Near-Horizon Geometry of Supersymmetric Rotating AdS_4 Black Holes in M-theory*, 2011.07071.

[3] E. Marcus and S. Vandoren, *A new class of SYK-like models with maximal chaos*, *JHEP* **01** (2019) 166 [1808.01190].

[4] U. Gürsoy, D. Kharzeev, E. Marcus and K. Rajagopal, *Magnetohydrodynamics and charged flow in heavy ion collisions*, *Nucl. Phys. A* **956** (2016) 389.

[5] U. Gürsoy, D. Kharzeev, E. Marcus, K. Rajagopal and C. Shen, *Charge-dependent Flow Induced by Magnetic and Electric Fields in Heavy Ion Collisions*, *Phys. Rev. C* **98** (2018) 55201 [1806.05288].

[6] U. Gürsoy, D. E. Kharzeev, E. Marcus, K. Rajagopal and C. Shen, *Charge-dependent flow induced by electromagnetic fields in heavy ion collisions*, *Nucl. Phys. A* **1005** (2021) 121837 [2002.12818].

[7] K. Akiyama, A. Alberdi, W. Alef, K. Asada, R. Azulay, A. K. Baczko et al., *First M87 event horizon telescope results. I. The shadow of the supermassive black hole*, 2019. 10.3847/2041-8213/ab0ec7.

[8] C. Montgomery, W. Orchiston and I. Whittingham, *MICHELL, LAPLACE AND THE ORIGIN OF THE BLACK HOLE CONCEPT*, *Journal of Astronomical History and Heritage* (2009) .

[9] L. Susskind, *The black hole war*.

[10] Rantonels*Online Graphic* .

[11] S. W. Hawking, *Particle creation by black holes*, *Communications in Mathematical Physics* (1975) .

[12] A. Strominger and C. Vafa, *Microscopic origin of the Bekenstein-Hawking entropy*, *Phys. Lett.* **B379** (1996) 99 [hep-th/9601029].

[13] H. het Lam, *Black hole entropy in string theory*, Ph.D. thesis, 2020.

[14] S. Kachru, R. Kallosh, A. Linde and S. P. Trivedi, *De Sitter vacua in string theory*, *Physical Review D* (2003) [0301240].

[15] E. Palti, *The Swampland: Introduction and Review*, *Fortschritte der Physik* (2019) [1903.06239].

[16] Particle Data Group, *Supersymmetric Particle Searches*, .

[17] F. Gliozzi, J. Scherk and D. Olive, *Supersymmetry, supergravity theories and the dual spinor model*, *Nuclear Physics, Section B* (1977) .

[18] A. Sagnotti, *Open Strings and their Symmetry Groups*, (1988), 0208020, DOI.

[19] E. Witten, *String theory dynamics in various dimensions*, *Nuclear Physics, Section B* (1995) [9503124].

[20] E. Cremmer, B. Julia and J. Scherk, *Supergravity in theory in 11 dimensions*, *Physics Letters B* (1978) .

[21] K. Mayer, *On quantum corrections in string compactifications*, Ph.D. thesis, 2020.

[22] C. M. Hull and P. K. Townsend, *Unity of superstring dualities*, *Nucl. Phys.* **B438** (1995) 109 [hep-th/9410167].

[23] J. Polchinski, *Dirichlet branes and Ramond-Ramond charges*, *Physical Review Letters* (1995) [9510017].

[24] J. M. Maldacena, *Black holes in string theory*, Ph.D. thesis, Princeton U., 1996. hep-th/9607235.

[25] J. M. Maldacena, *The Large N limit of superconformal field theories and supergravity*, *Int. J. Theor. Phys.* **38** (1999) 1113 [hep-th/9711200].

[26] G. t. Hooft, *Dimensional Reduction in Quantum Gravity*, 9310026.

[27] L. Susskind, *The world as a hologram*, *Journal of Mathematical Physics* (1995) [9409089].

[28] O. Aharony, S. S. Gubser, J. Maldacena, H. Ooguri and Y. Oz, *Large N field theories, string theory and gravity*, 2000. 10.1016/S0370-1573(99)00083-6.

[29] R. Jackiw, *Lower dimensional gravity*, *Nuclear Physics, Section B* (1985) .

[30] C. Teitelboim, *Gravitation and hamiltonian structure in two spacetime dimensions*, *Physics Letters B* (1983) .

[31] P. K. Kovtun, D. T. Son and A. O. Starinets, *Viscosity in strongly interacting quantum field theories from black hole physics*, *Phys.Rev.Lett.* **94** (2005) 111601 [hep-th/0405231].

[32] S. Sachdev and J. Ye, *Gapless spin fluid ground state in a random, quantum Heisenberg magnet*, *Phys. Rev. Lett.* **70** (1993) 3339 [9212030].

[33] A. Kitaev, *A simple model of quantum holography.*, *Talks at KITP, April 7, 2015 and May 27, 2015* .

[34] J. Maldacena, S. H. Shenker and D. Stanford, *A bound on chaos*, *Journal of High Energy Physics* (2016) [1503.01409].

[35] A. Kitaev, "A simple model of quantum holography, Talks at KITP." http://online.kitp.ucsb.edu/online/entangled15/kitaev/, 2015.

[36] J. Polchinski and V. Rosenhaus, *The spectrum in the Sachdev-Ye-Kitaev model*, *Journal of High Energy Physics* (2016) [1601.06768].

[37] J. Maldacena and D. Stanford, *Remarks on the Sachdev-Ye-Kitaev model*, *Physical Review D* (2016) .

[38] D. J. Gross and V. Rosenhaus, *All point correlation functions in SYK*, *Journal of High Energy Physics* (2017) [1710.08113].

[39] D. J. Gross and V. Rosenhaus, *A generalization of Sachdev-Ye-Kitaev*, *Journal of High Energy Physics* (2017) [1610.01569].

[40] M. Mezard, G. Parisi, M. A. Virasoro and D. J. Thouless, *Spin Glass Theory and Beyond* , *Physics Today* (1988) .

[41] W. Fu, D. Gaiotto, J. Maldacena and S. Sachdev, *Supersymmetric Sachdev-Ye-Kitaev models*, *Physical Review D* (2017) .

[42] J. Murugan, D. Stanford and E. Witten, *More on supersymmetric and 2d analogs of the SYK model*, *Journal of High Energy Physics* (2017) [1706.05362].

[43] J. Yoon, *Supersymmetric SYK Model:Bi-local Collective Superfield/Supermatrix Formulation*, 2017.

[44] C. Peng, M. Spradlin and A. Volovich, *Correlators in the N= 2 supersymmetric SYK model*, *Journal of High Energy Physics* (2017) .

[45] H. D. Politzer, *Reliable perturbative results for strong interactions?*, *Physical Review Letters* (1973) .

[46] D. J. Gross and F. Wilczek, *Ultraviolet behavior of non-abelian gauge theories*, *Physical Review Letters* (1973) .

[47] S. Bethke, *Determination of the QCD coupling αs*, 2000. 10.1088/0954-3899/26/7/201.

[48] A. Aprahamian, et al., *Reaching for the horizon: The 2015 long range plan for nuclear science*, .

[49] A. D. Linde, *Phase transitions in gauge theories and cosmology*, *Reports on Progress in Physics* (1979) .

[50] J. C. Collins and M. J. Perry, *Superdense matter: Neutrons or asymptotically free quarks?*, *Physical Review Letters* (1975) .

[51] JETSCAPE, *Multi-system Bayesian constraints on the transport coefficients of QCD matter*, .

[52] G. Nijs, W. Van Der Schee, U. Gursoy and R. Snellings, *A Bayesian analysis of Heavy Ion Collisions with Trajectum*, .

[53] W. Busza, K. Rajagopal and W. Van Der Schee, *Heavy ion collisions: The big picture and the big questions*, 2018. 10.1146/annurev-nucl-101917-020852.

[54] Y.-J. Lee, A. S. Yoon and W. Busza, "http://web.mit.edu/mithig/movies/LHCanmation.mov."

[55] B. Alver, M. Baker, C. Loizides and P. Steinberg, *The PHOBOS Glauber Monte Carlo*, `0805.4411`.

[56] U. Gursoy, D. Kharzeev and K. Rajagopal, *Magnetohydrodynamics, charged currents and directed flow in heavy ion collisions*, *Phys. Rev.* **C89** (2014) 54905 [`1401.3805`].

[57] C. P. Herzog, A. Karch, P. Kovtun, C. Kozcaz and L. G. Yaffe, *Energy loss of a heavy quark moving through N=4 supersymmetric Yang-Mills plasma*, *JHEP* **07** (2006) 13 [`hep-th/0605158`].

[58] J. Casalderrey-Solana and D. Teaney, *Heavy quark diffusion in strongly coupled N=4 Yang-Mills*, *Phys. Rev.* **D74** (2006) 85012 [`hep-ph/0605199`].

[59] S. S. Gubser, *Drag force in AdS/CFT*, *Phys. Rev.* **D74** (2006) 126005 [`hep-th/0605182`].

[60] J. M. Maldacena, A. Strominger and E. Witten, *Black hole entropy in M theory*, *JHEP* **12** (1997) 2 [hep-th/9711053].

[61] C. Vafa, *Black holes and Calabi-Yau threefolds*, *Adv. Theor. Math. Phys.* **2** (1998) 207 [hep-th/9711067].

[62] B. Haghighat, S. Murthy, C. Vafa and S. Vandoren, *F-Theory, Spinning Black Holes and Multi-string Branches*, *JHEP* **01** (2016) 9 [1509.00455].

[63] A. Dabholkar and C. Hull, *Duality twists, orbifolds, and fluxes*, *JHEP* **09** (2003) 54 [hep-th/0210209].

[64] J. Scherk and J. H. Schwarz, *Spontaneous Breaking of Supersymmetry Through Dimensional Reduction*, *Phys. Lett.* **82B** (1979) 60.

[65] J. Scherk and J. H. Schwarz, *How to Get Masses from Extra Dimensions*, *Nucl. Phys.* **B153** (1979) 61.

[66] N. Gaddam, A. Gnecchi, S. Vandoren and O. Varela, *Rholography, Black Holes and Scherk-Schwarz*, *JHEP* **06** (2015) 58 [1412.7325].

[67] E. Cremmer, J. Scherk and J. H. Schwarz, *Spontaneously Broken N=8 Supergravity*, *Phys. Lett.* **84B** (1979) 83.

[68] N. Kaloper and R. C. Myers, *The Odd story of massive supergravity*, *JHEP* **05** (1999) 10 [hep-th/9901045].

[69] C. M. Hull and A. Çatal-Özer, *Compactifications with S duality twists*, *JHEP* **10** (2003) 34 [hep-th/0308133].

[70] L. Andrianopoli, S. Ferrara and M. A. Lledo, *No-scale D=5 supergravity from Scherk-Schwarz reduction of D=6 theories*, *JHEP* **06** (2004) 18 [hep-th/0406018].

[71] C. M. Hull and R. A. Reid-Edwards, *Flux compactifications of string theory on twisted tori*, *Fortsch. Phys.* **57** (2009) 862 [hep-th/0503114].

[72] C. M. Hull and R. A. Reid-Edwards, *Gauge symmetry, T-duality and doubled geometry*, *JHEP* **08** (2008) 43 [0711.4818].

[73] C. M. Hull and R. A. Reid-Edwards, *Non-geometric backgrounds, doubled geometry and generalised T-duality*, *JHEP* **09** (2009) 14 [0902.4032].

[74] C. M. Hull, D. Israël and A. Sarti, *Non-geometric Calabi-Yau Backgrounds and K3 automorphisms*, *JHEP* **11** (2017) 84 [1710.00853].

[75] Y. Gautier, C. M. Hull and D. Israël, *Heterotic/type II Duality and*

Non-Geometric Compactifications, *JHEP* **10** (2019) 214 [1906.02165].

[76] C. M. Hull, *Massive string theories from M theory and F theory*, *JHEP* **11** (1998) 27 [hep-th/9811021].

[77] C. M. Hull, *A Geometry for non-geometric string backgrounds*, *JHEP* **10** (2005) 65 [hep-th/0406102].

[78] C. M. Hull, *BPS supermultiplets in five-dimensions*, *JHEP* **06** (2000) 19 [hep-th/0004086].

[79] K. S. Narain, M. H. Sarmadi and C. Vafa, *Asymmetric Orbifolds*, *Nucl. Phys.* **B288** (1987) 551.

[80] K. S. Narain, M. H. Sarmadi and C. Vafa, *Asymmetric orbifolds: Path integral and operator formulations*, *Nucl. Phys.* **B356** (1991) 163.

[81] S. Ferrara, J. A. Harvey, A. Strominger and C. Vafa, *Second quantized mirror symmetry*, *Phys. Lett.* **B361** (1995) 59 [hep-th/9505162].

[82] F. Bonetti, T. W. Grimm and S. Hohenegger, *Exploring 6D origins of 5D supergravities with Chern-Simons terms*, *JHEP* **05** (2013) 124 [1303.2661].

[83] K. Hanaki, K. Ohashi and Y. Tachikawa, *Supersymmetric Completion of an R**2 term in Five-dimensional Supergravity*, *Prog. Theor. Phys.* **117** (2007) 533 [hep-th/0611329].

[84] A. Castro, J. L. Davis, P. Kraus and F. Larsen, *5D Black Holes and Strings with Higher Derivatives*, *JHEP* **06** (2007) 7 [hep-th/0703087].

[85] B. de Wit and S. Katmadas, *Near-Horizon Analysis of D=5 BPS Black Holes and Rings*, *JHEP* **02** (2010) 56 [0910.4907].

[86] T. W. Grimm, H. het Lam, K. Mayer and S. Vandoren, *Four-dimensional black hole entropy from F-theory*, *JHEP* **01** (2019) 37 [1808.05228].

[87] C. Couzens, H. het Lam, K. Mayer and S. Vandoren, *Black Holes and (0,4) SCFTs from Type IIB on K3*, *JHEP* **08** (2019) 43 [1904.05361].

[88] Y. Tanii, $N = 8$ *Supergravity in Six-dimensions*, *Phys. Lett.* **145B** (1984) 197.

[89] E. Bergshoeff, H. Samtleben and E. Sezgin, *The Gaugings of Maximal D=6 Supergravity*, *JHEP* **03** (2008) 68 [0712.4277].

[90] E. Cremmer, B. Julia, H. Lu and C. N. Pope, *Dualization of dualities. 1.*, *Nucl. Phys.* **B523** (1998) 73 [hep-th/9710119].

[91] A. Çatal-Özer, *Scherk-Schwarz Reductions of Effective String Theories in Even Dimensions*, Ph.D. thesis, Middle East Technical U.

[92] C. N. Pope, *Kaluza-Klein Theory*. Centre Emile Borel, Institut Henri Poincaré.

[93] E. Cremmer, *Supergravities in 5 Dimensions*, in *In *Salam, A. (ed.), Sezgin, E. (ed.): Supergravities in diverse dimensions, vol. 1* 422-437. (In *Cambridge 1980, Proceedings, Superspace and supergravity* 267-282) and Paris Ec. Norm. Sup. - LPTENS 80-17 (80,rec.Sep.) 17 p. (see Book Index)*, 1980.

[94] M. Awada and P. K. Townsend, *N=4 Maxwell-Einstein Supergravity in Five-dimensions and Its SU(2) Gauging*, *Nucl. Phys.* **B255** (1985) 617.

[95] P. K. Townsend, K. Pilch and P. van Nieuwenhuizen, *Selfduality in Odd Dimensions*, *Phys. Lett.* **136B** (1984) 38.

[96] F. Bonetti, T. W. Grimm and S. Hohenegger, *One-loop Chern-Simons terms in five dimensions*, *JHEP* **07** (2013) 43 [1302.2918].

[97] T. W. Grimm, A. Kapfer and J. Keitel, *Effective action of 6D F-Theory with U(1) factors: Rational sections make Chern-Simons terms jump*, *JHEP* **07** (2013) 115 [1305.1929].

[98] C. Hull and R. J. Szabo, *Noncommutative gauge theories on D-branes in non-geometric backgrounds*, *JHEP* **09** (2019) 51 [1903.04947].

[99] G. Villadoro and F. Zwirner, *The Minimal N=4 no-scale model from generalized dimensional reduction*, *JHEP* **07** (2004) 55 [hep-th/0406185].

[100] K. A. Intriligator and B. Wecht, *The Exact superconformal R symmetry maximizes a*, *Nucl. Phys.* **B667** (2003) 183 [hep-th/0304128].

[101] D. L. Jafferis, *The Exact Superconformal R-Symmetry Extremizes Z*, *JHEP* **05** (2012) 159 [1012.3210].

[102] F. Benini and N. Bobev, *Exact two-dimensional superconformal R-symmetry and c-extremization*, *Phys. Rev. Lett.* **110** (2013) 61601 [1211.4030].

[103] F. Benini and N. Bobev, *Two-dimensional SCFTs from wrapped branes and c-extremization*, *JHEP* **06** (2013) 5 [1302.4451].

[104] F. Benini, K. Hristov and A. Zaffaroni, *Black hole microstates in AdS_4 from supersymmetric localization*, *JHEP* **05** (2016) 54 [1511.04085].

[105] D. Martelli, J. Sparks and S.-T. Yau, *The Geometric dual of a-maximisation*

for Toric Sasaki-Einstein manifolds, *Commun. Math. Phys.* **268** (2006) 39 [hep-th/0503183].

[106] D. Martelli, J. Sparks and S.-T. Yau, *Sasaki-Einstein manifolds and volume minimisation*, *Commun. Math. Phys.* **280** (2008) 611 [hep-th/0603021].

[107] C. Couzens, J. P. Gauntlett, D. Martelli and J. Sparks, *A geometric dual of c-extremization*, *JHEP* **01** (2019) 212 [1810.11026].

[108] J. P. Gauntlett, D. Martelli and J. Sparks, *Toric geometry and the dual of c-extremization*, *JHEP* **01** (2019) 204 [1812.05597].

[109] S. M. Hosseini and A. Zaffaroni, *Proving the equivalence of c-extremization and its gravitational dual for all toric quivers*, *JHEP* **03** (2019) 108 [1901.05977].

[110] J. P. Gauntlett, D. Martelli and J. Sparks, *Toric geometry and the dual of $\mathcal{I}$-extremization*, *JHEP* **06** (2019) 140 [1904.04282].

[111] S. M. Hosseini and A. Zaffaroni, *Geometry of $\mathcal{I}$-extremization and black holes microstates*, *JHEP* **07** (2019) 174 [1904.04269].

[112] H. Kim and N. Kim, *Black holes with baryonic charge and $\mathcal{I}$-extremization*, 1904.05344.

[113] J. P. Gauntlett, D. Martelli and J. Sparks, *Fibred GK geometry and supersymmetric AdS solutions*, *JHEP* **11** (2019) 176 [1910.08078].

[114] M. van Beest, S. Cizel, S. Schafer-Nameki and J. Sparks, *$\mathcal{I}$/c-Extremization in M/F-Duality*, *SciPost Phys.* **9** (2020) 29 [2004.04020].

[115] Y. Lozano, C. Nunez, A. Ramirez and S. Speziali, *New AdS_2 backgrounds and $\mathcal{N} = 4$ Conformal Quantum Mechanics*, 2011.00005.

[116] H. K. Kunduri and J. Lucietti, *Classification of near-horizon geometries of extremal black holes*, *Living Rev. Rel.* **16** (2013) 8 [1306.2517].

[117] N. Kim and J.-D. Park, *Comments on AdS(2) solutions of D=11 supergravity*, *JHEP* **09** (2006) 41 [hep-th/0607093].

[118] A. Donos, J. P. Gauntlett and N. Kim, *AdS Solutions Through Transgression*, *JHEP* **09** (2008) 21 [0807.4375].

[119] J. Hong, N. T. Macpherson and L. A. Pando Zayas, *Aspects of AdS_2 classification in M-theory: solutions with mesonic and baryonic charges*, *JHEP* **11** (2019) 127 [1908.08518].

[120] J. Nian and L. A. Pando Zayas, *Microscopic entropy of rotating electrically charged AdS_4 black holes from field theory localization*, *JHEP* **03** (2020) 81 [1909.07943].

[121] S. Choi, C. Hwang, S. Kim and J. Nahmgoong, *Entropy Functions of BPS Black Holes in AdS_4 and AdS_6*, *J. Korean Phys. Soc.* **76** (2020) 101 [1811.02158].

[122] S. M. Hosseini, K. Hristov and A. Zaffaroni, *Gluing gravitational blocks for AdS black holes*, *JHEP* **12** (2019) 168 [1909.10550].

[123] S. M. Hosseini, K. Hristov and A. Zaffaroni, *Microstates of rotating AdS_5 strings*, *JHEP* **11** (2019) 90 [1909.08000].

[124] N. Bobev and P. M. Crichigno, *Universal spinning black holes and theories of class $\mathcal{R}$*, *JHEP* **12** (2019) 54 [1909.05873].

[125] N. Kim, *AdS_3 solutions of IIB supergravity from D3-branes*, *JHEP* **01** (2006) 94 [hep-th/0511029].

[126] C. Couzens, D. Martelli and S. Schafer-Nameki, *F-theory and AdS_3/CFT_2 (2, 0)*, *JHEP* **06** (2018) 8 [1712.07631].

[127] A. Passias and D. Prins, *On $\mathcal{N} = 1$ AdS_3 solutions of Type IIB*, 1910.06326.

[128] C. Couzens, *$\mathcal{N} = (0, 2)$ AdS_3 Solutions of Type IIB and F-theory with Generic Fluxes*, 1911.04439.

[129] J. P. Gauntlett and S. Pakis, *The Geometry of D = 11 killing spinors*, *JHEP* **04** (2003) 39 [hep-th/0212008].

[130] M. Cvetic, G. W. Gibbons, H. Lu and C. N. Pope, *Rotating black holes in gauged supergravities: Thermodynamics, supersymmetric limits, topological solitons and time machines*, 0504080.

[131] S. M. Hosseini, K. Hristov and A. Zaffaroni, *A note on the entropy of rotating BPS $AdS_7 \times S^4$ black holes*, *JHEP* **05** (2018) 121 [1803.07568].

[132] G. Kántor, C. Papageorgakis and P. Richmond, *AdS_7 black-hole entropy and 5D $\mathcal{N} = 2$ Yang-Mills*, *JHEP* **01** (2020) 17 [1907.02923].

[133] F. Benini, D. Gang and L. A. Pando Zayas, *Rotating Black Hole Entropy from M5 Branes*, *JHEP* **03** (2020) 57 [1909.11612].

[134] J. P. Gauntlett and N. Kim, *Geometries with Killing Spinors and Supersymmetric AdS Solutions*, *Commun. Math. Phys.* **284** (2008) 897 [0710.2590].

[135] B. Carter, *Global Structure of the Kerr Family of Gravitational Fields*, *Phys. Rev.* **174** (1968) 1559.

[136] V. Kostelecky and M. J. Perry, *Solitonic black holes in gauged N=2 supergravity*, *Phys. Lett. B* **371** (1996) 191 [9512222].

[137] M. M. Caldarelli and D. Klemm, *Supersymmetry of Anti-de Sitter black holes*, *Nucl. Phys.* **B545** (1999) 434 [hep-th/9808097].

[138] K. Hristov, S. Katmadas and C. Toldo, *Matter-coupled supersymmetric Kerr-Newman-AdS$_4$ black holes*, *Phys. Rev. D* **100** (2019) 66016 [1907.05192].

[139] S. M. Hosseini and A. Zaffaroni, *Universal AdS black holes in theories with sixteen supercharges and their microstates*, 2011.01249.

[140] D. D. K. Chow and G. Compère, *Dyonic AdS black holes in maximal gauged supergravity*, *Phys. Rev. D* **89** (2014) 65003 [1311.1204].

[141] K. Hristov and S. Vandoren, *Static supersymmetric black holes in AdS$_4$ with spherical symmetry*, *JHEP* **1104** (2011) 47 [1012.4314].

[142] M. M. Caldarelli, G. Cognola and D. Klemm, *Thermodynamics of Kerr-Newman-AdS black holes and conformal field theories*, *Class. Quant. Grav.* **17** (2000) 399 [9908022].

[143] C. Couzens, *to appear*, .

[144] N. Bobev, A. M. Charles and V. S. Min, *Euclidean black saddles and AdS$_4$ black holes*, *JHEP* **10** (2020) 73 [2006.01148].

[145] N. Bobev, A. M. Charles, K. Hristov and V. Reys, *The Unreasonable Effectiveness of Higher-Derivative Supergravity in AdS$_4$ Holography*, *Phys. Rev. Lett.* **125** (2020) 131601 [2006.09390].

[146] N. Bobev, A. M. Charles, D. Gang, K. Hristov and V. Reys, *Higher-Derivative Supergravity, Wrapped M5-branes, and Theories of Class $\mathcal{R}$*, 2011.05971.

[147] L. A. Pando Zayas and Y. Xin, *Universal Logarithmic Behavior in Microstate Counting and the Dual One-loop Entropy of AdS$_4$ Black Holes*, 2008.03239.

[148] A. Lanir, A. Nedelin and O. Sela, *Black hole entropy function for toric theories via Bethe Ansatz*, *JHEP* **04** (2020) 91 [1908.01737].

[149] A. Cabo-Bizet, D. Cassani, D. Martelli and S. Murthy, *Microscopic origin of the Bekenstein-Hawking entropy of supersymmetric AdS$_5$ black holes*, *JHEP*

10 (2019) 62 [1810.11442].

[150] A. Cabo-Bizet, D. Cassani, D. Martelli and S. Murthy, *The large-N limit of the 4d $\mathcal{N} = 1$ superconformal index*, 2005.10654.

[151] F. Benini, E. Colombo, S. Soltani, A. Zaffaroni and Z. Zhang, *Superconformal indices at large N and the entropy of $AdS_5 \times SE_5$ black holes*, *Class. Quant. Grav.* **37** (2020) 215021 [2005.12308].

[152] A. González Lezcano and L. A. Pando Zayas, *Microstate counting via Bethe Ansätze in the 4d $\mathcal{N} = 1$ superconformal index*, *JHEP* **03** (2020) 88 [1907.12841].

[153] D. Cassani and L. Papini, *The BPS limit of rotating AdS black hole thermodynamics*, *JHEP* **09** (2019) 79 [1906.10148].

[154] S. M. Hosseini, K. Hristov and A. Passias, *Holographic microstate counting for AdS_4 black holes in massive IIA supergravity*, *JHEP* **10** (2017) 190 [1707.06884].

[155] S. M. Hosseini, K. Hristov and A. Zaffaroni, *An extremization principle for the entropy of rotating BPS black holes in AdS_5*, *JHEP* **07** (2017) 106 [1705.05383].

[156] A. Sen, *Black hole entropy function and the attractor mechanism in higher derivative gravity*, *JHEP* **09** (2005) 38 [0506177].

[157] J. F. Morales and H. Samtleben, *Entropy function and attractors for AdS black holes*, *JHEP* **10** (2006) 74 [0608044].

[158] J. K. Ghosh and L. A. Pando Zayas, *Comments on Sen's Classical Entropy Function for Static and Rotating AdS_4 Black Holes*, 2009.11147.

[159] M. David and J. Nian, *Universal Entropy and Hawking Radiation of Near-Extremal AdS_4 Black Holes*, 2009.12370.

[160] F. Larsen and S. Paranjape, *Thermodynamics of Near BPS Black Holes in AdS_4 and AdS_7*, 2010.04359.

[161] F. Larsen, J. Nian and Y. Zeng, *AdS_5 black hole entropy near the BPS limit*, *JHEP* **06** (2020) 1 [1907.02505].

[162] P. Koerber, *Lectures on Generalized Complex Geometry for Physicists*, *Fortsch. Phys.* **59** (2011) 169 [1006.1536].

[163] H. K. Kunduri and J. Lucietti, *Uniqueness of near-horizon geometries of rotating extremal AdS(4) black holes*, *Class. Quant. Grav.* **26** (2009) 55019

[0812.1576].

[164] J. Lucietti, *Two remarks on near-horizon geometries*, *Class. Quant. Grav.* **29** (2012) 235014 [1209.4042].

[165] J. P. Gauntlett, J. B. Gutowski and S. Pakis, *The Geometry of D = 11 null Killing spinors*, *JHEP* **12** (2003) 49 [0311112].

[166] S. Katmadas and A. Tomasiello, *AdS_4 black holes from M-theory*, *JHEP* **12** (2015) 111 [1509.00474].

[167] K. Hanaki, K. Ohashi and Y. Tachikawa, *Comments on charges and near-horizon data of black rings*, *JHEP* **12** (2007) 57 [0704.1819].

[168] A. Almheiri and J. Polchinski, *Models of AdS2 backreaction and holography*, *Journal of High Energy Physics* (2015) [1402.6334].

[169] O. Parcollet and A. Georges, *Non-fermi-liquid regime of a doped mott insulator*, *Physical Review B - Condensed Matter and Materials Physics* (1999) [9806119].

[170] A. Georges, O. Parcollet and S. Sachdev, *Mean field theory of a quantum Heisenberg spin glass*, *Physical Review Letters* (2000) [9909239].

[171] S. H. Shenker and D. Stanford, *Black holes and the butterfly effect*, *Journal of High Energy Physics* (2014) [1306.0622].

[172] S. H. Shenker and D. Stanford, *Stringy effects in scrambling*, *Journal of High Energy Physics* (2015) [1412.6087].

[173] S. Sachdev, *Holographic metals and the fractionalized fermi liquid*, *Physical Review Letters* (2010) [1006.3794].

[174] S. Sachdev, *Bekenstein-hawking entropy and strange metals*, *Physical Review X* (2015) [1506.05111].

[175] J. Engelsy, T. G. Mertens and H. Verlinde, *An investigation of AdS_2 backreaction and holography*, *JHEP* **07** (2016) 139 [1606.03438].

[176] J. Maldacena, D. Stanford and Z. Yang, *Conformal symmetry and its breaking in two-dimensional nearly anti-de Sitter space*, *Progress of Theoretical and Experimental Physics* (2016) [1606.01857].

[177] K. Jensen, *Chaos in AdS2 Holography*, *Physical Review Letters* (2016) [1605.06098].

[178] M. Berkooz, P. Narayan, M. Rozali and J. Simón, *Higher dimensional*

generalizations of the SYK model, *Journal of High Energy Physics* (2017) [1610.02422].

[179] Y. Gu, X. L. Qi and D. Stanford, *Local criticality, diffusion and chaos in generalized Sachdev-Ye-Kitaev models*, *Journal of High Energy Physics* (2017) [1609.07832].

[180] S. K. Jian and H. Yao, *Solvable Sachdev-Ye-Kitaev Models in Higher Dimensions: From Diffusion to Many-Body Localization*, *Physical Review Letters* (2017) [1703.02051].

[181] G. J. Turiaci and H. Verlinde, *Towards a 2d QFT analog of the SYK model*, *Journal of High Energy Physics* (2017) [1701.00528].

[182] Y. Chen, H. Zhai and P. Zhang, *Tunable Quantum Chaos in the Sachdev-Ye-Kitaev Model Coupled to a Thermal Bath*, *JHEP* **07** (2017) 150 [1705.09818].

[183] Z. Bi, C. M. Jian, Y. Z. You, K. A. Pawlak and C. Xu, *Instability of the non-Fermi-liquid state of the Sachdev-Ye-Kitaev model*, *Physical Review B* (2017) [1701.07081].

[184] A. Kitaev and S. J. Suh, *The soft mode in the Sachdev-Ye-Kitaev model and its gravity dual*, *Journal of High Energy Physics* (2017) [1711.08467].

[185] D. Anninos, T. Anous and F. Denef, *Disordered quivers and cold horizons*, *Journal of High Energy Physics* (2016) [1603.00453].

[186] A. Larkin and Y. Ovchinnikov, *Quasiclassical Method in the Theory of Superconductivity*, *Soviet Journal of Experimental and Theoretical Physics* **28** (1969) 1200.

[187] A. Almheiri, D. Marolf, J. Polchinski, D. Stanford and J. Sully, *An apologia for firewalls*, *Journal of High Energy Physics* (2013) [1304.6483].

[188] A. Kitaev, *Hidden correlations in the Hawking radiation and thermal noise.*, *Talks at KITP, February 12, 2015* .

[189] D. A. Roberts and D. Stanford, *Two-dimensional conformal field theory and the butterfly effect*, *Phys. Rev. Lett.* **115** (2015) 131603 [1412.5123].

[190] C. Peng, M. Spradlin and A. Volovich, *Correlators in the $\mathcal{N} = 2$ Supersymmetric SYK Model*, *JHEP* **10** (2017) 202 [1706.06078].

[191] S. Bhattacharyya, S. Minwalla, V. E. Hubeny and M. Rangamani, *Nonlinear fluid dynamics from gravity*, *Journal of High Energy Physics* (2008)

[0712.2456].

[192] D. E. Kharzeev, L. D. McLerran and H. J. Warringa, *The Effects of topological charge change in heavy ion collisions: 'Event by event P and CP violation'*, *Nucl. Phys.* **A803** (2008) 227 [0711.0950].

[193] V. Skokov, A. r. Y. Illarionov and V. Toneev, *Estimate of the magnetic field strength in heavy-ion collisions*, *Int. J. Mod. Phys.* **A24** (2009) 5925 [0907.1396].

[194] K. Tuchin, *Synchrotron radiation by fast fermions in heavy-ion collisions*, *Phys. Rev.* **C82** (2010) 34904 [1006.3051].

[195] V. Voronyuk, V. D. Toneev, W. Cassing, E. L. Bratkovskaya, V. P. Konchakovski and S. A. Voloshin, *(Electro-)Magnetic field evolution in relativistic heavy-ion collisions*, *Phys. Rev.* **C83** (2011) 54911 [1103.4239].

[196] W.-T. Deng and X.-G. Huang, *Event-by-event generation of electromagnetic fields in heavy-ion collisions*, *Phys. Rev.* **C85** (2012) 44907 [1201.5108].

[197] K. Tuchin, *Particle production in strong electromagnetic fields in relativistic heavy-ion collisions*, *Adv. High Energy Phys.* **2013** (2013) 490495 [1301.0099].

[198] L. McLerran and V. Skokov, *Comments About the Electromagnetic Field in Heavy-Ion Collisions*, *Nucl. Phys.* **A929** (2014) 184 [1305.0774].

[199] K. Fukushima, D. E. Kharzeev and H. J. Warringa, *The Chiral Magnetic Effect*, *Phys. Rev.* **D78** (2008) 74033 [0808.3382].

[200] D. E. Kharzeev and H.-U. Yee, *Chiral Magnetic Wave*, *Phys. Rev.* **D83** (2011) 85007 [1012.6026].

[201] Y. Burnier, D. E. Kharzeev, J. Liao and H.-U. Yee, *Chiral magnetic wave at finite baryon density and the electric quadrupole moment of quark-gluon plasma in heavy ion collisions*, *Phys. Rev. Lett.* **107** (2011) 52303 [1103.1307].

[202] S. S. Gubser, *Symmetry constraints on generalizations of Bjorken flow*, *Phys. Rev.* **D82** (2010) 85027 [1006.0006].

[203] C. Shen, Z. Qiu, H. Song, J. Bernhard, S. Bass and U. Heinz, *The iEBE-VISHNU code package for relativistic heavy-ion collisions*, *Comput. Phys. Commun.* **199** (2016) 61 [1409.8164].

[204] V. Roy, S. Pu, L. Rezzolla and D. H. Rischke, *Effect of intense magnetic*

fields on reduced-MHD evolution in $\sqrt{s_{NN}}$ = 200 GeV Au+Au collisions, *Phys. Rev.* **C96** (2017) 54909 [1706.05326].

[205] E. Stewart and K. Tuchin, *Magnetic field in expanding quark-gluon plasma*, *Phys. Rev.* **C97** (2018) 44906 [1710.08793].

[206] C. Shen, U. Heinz, P. Huovinen and H. Song, *Systematic parameter study of hadron spectra and elliptic flow from viscous hydrodynamic simulations of Au+Au collisions at $\sqrt{s_{NN}} = 200$ GeV*, *Phys. Rev.* **C82** (2010) 54904 [1010.1856].

[207] P. Huovinen and P. Petreczky, *QCD Equation of State and Hadron Resonance Gas*, *Nucl. Phys.* **A837** (2010) 26 [0912.2541].

[208] H. Niemi, G. S. Denicol, P. Huovinen, E. Molnar and D. H. Rischke, *Influence of the shear viscosity of the quark-gluon plasma on elliptic flow in ultrarelativistic heavy-ion collisions*, *Phys. Rev. Lett.* **106** (2011) 212302 [1101.2442].

[209] D. Kharzeev, *Can gluons trace baryon number?*, *Phys. Lett.* **B378** (1996) 238 [nucl-th/9602027].

[210] H. T. Ding, A. Francis, O. Kaczmarek, F. Karsch, E. Laermann and W. Soeldner, *Thermal dilepton rate and electrical conductivity: An analysis of vector current correlation functions in quenched lattice QCD*, *Phys. Rev.* **D83** (2011) 34504 [1012.4963].

[211] A. Francis and O. Kaczmarek, *On the temperature dependence of the electrical conductivity in hot quenched lattice QCD*, *Prog. Part. Nucl. Phys.* **67** (2012) 212 [1112.4802].

[212] B. B. Brandt, A. Francis, H. B. Meyer and H. Wittig, *Thermal Correlators in the ρ channel of two-flavor QCD*, *JHEP* **03** (2013) 100 [1212.4200].

[213] A. Amato, G. Aarts, C. Allton, P. Giudice, S. Hands and J.-I. Skullerud, *Electrical conductivity of the quark-gluon plasma across the deconfinement transition*, *Phys. Rev. Lett.* **111** (2013) 172001 [1307.6763].

[214] O. Kaczmarek and M. Muller, *Temperature dependence of electrical conductivity and dilepton rates from hot quenched lattice QCD*, *PoS* **LATTICE201** (2014) 175 [1312.5609].

[215] F. Cooper and G. Frye, *Comment on the Single Particle Distribution in the Hydrodynamic and Statistical Thermodynamic Models of Multiparticle*

Production, *Phys. Rev.* **D10** (1974) 186.

[216] J. Margutti, *The search for magnetic-induced charged currents in Pb–Pb collisions with ALICE*, in *12th Workshop on Particle Correlations and Femtoscopy (WPCF 2017) Amsterdam, Netherdands, June 12-16, 2017*, 2017, http://inspirehep.net/record/1624208/files/arXiv:1709.05618.pdf [1709.05618].

[217] S. S. Adler and Others, *Systematic studies of the centrality and s(NN)**(1/2) dependence of the d E(T) / d eta and d (N(ch) / d eta in heavy ion collisions at mid-rapidity*, *Phys. Rev.* **C71** (2005) 34908 [nucl-ex/0409015].

[218] K. Aamodt and Others, *Centrality dependence of the charged-particle multiplicity density at mid-rapidity in Pb-Pb collisions at* $\sqrt{s_{NN}} = 2.76$ *TeV*, *Phys. Rev. Lett.* **106** (2011) 32301 [1012.1657].

[219] J. Adam and Others, *Centrality dependence of the charged-particle multiplicity density at midrapidity in Pb-Pb collisions at* $\sqrt{s_{NN}} = 5.02$ *TeV*, *Phys. Rev. Lett.* **116** (2016) 222302 [1512.06104].

[220] J. Adams and Others, *Azimuthal anisotropy in Au+Au collisions at s(NN)**(1/2) = 200-GeV*, *Phys. Rev.* **C72** (2005) 14904 [nucl-ex/0409033].

[221] K. Aamodt and Others, *Elliptic flow of charged particles in Pb-Pb collisions at 2.76 TeV*, *Phys. Rev. Lett.* **105** (2010) 252302 [1011.3914].

[222] J. Adam and Others, *Anisotropic flow of charged particles in Pb-Pb collisions at* $\sqrt{s_{NN}} = 5.02$ *TeV*, *Phys. Rev. Lett.* **116** (2016) 132302 [1602.01119].

[223] Z. Qiu and U. W. Heinz, *Event-by-event shape and flow fluctuations of relativistic heavy-ion collision fireballs*, *Phys. Rev.* **C84** (2011) 24911 [1104.0650].

[224] U. W. Heinz, *Concepts of heavy ion physics*, in *2002 European School of high-energy physics, Pylos, Greece, 25 Aug-7 Sep 2002: Proceedings*, pp. 165–238, 2004, http://doc.cern.ch/yellowrep/CERN-2004-001 [hep-ph/0407360].

[225] J. Xu, L.-W. Chen, C. M. Ko and Z.-W. Lin, *Effects of hadronic potentials on elliptic flows in relativistic heavy ion collisions*, *Phys. Rev.* **C85** (2012) 41901 [1201.3391].

[226] J. Steinheimer, V. Koch and M. Bleicher, *Hydrodynamics at large baryon densities: Understanding proton vs. anti-proton* v_2 *and other puzzles*, *Phys.*

Rev. **C86** (2012) 44903 [1207.2791].

[227] C. M. Ko, T. Song, F. Li, V. Greco and S. Plumari, *Partonic mean-field effects on matter and antimatter elliptic flows*, *Nucl. Phys.* **A928** (2014) 234 [1211.5511].

[228] L. Adamczyk and Others, *Observation of an Energy-Dependent Difference in Elliptic Flow between Particles and Antiparticles in Relativistic Heavy Ion Collisions*, *Phys. Rev. Lett.* **110** (2013) 142301 [1301.2347].

[229] J. Xu, T. Song, C. M. Ko and F. Li, *Elliptic flow splitting as a probe of the QCD phase structure at finite baryon chemical potential*, *Phys. Rev. Lett.* **112** (2014) 12301 [1308.1753].

[230] L. Adamczyk and Others, *Centrality dependence of identified particle elliptic flow in relativistic heavy ion collisions at* $\sqrt{s_{NN}}$*=7.7ï£¡62.4 GeV*, *Phys. Rev.* **C93** (2016) 14907 [1509.08397].

[231] J. Xu and C. M. Ko, *Collision energy dependence of elliptic flow splitting between particles and their antiparticles from an extended multiphase transport model*, *Phys. Rev.* **C94** (2016) 54909 [1610.03202].

[232] Z. Qiu, C. Shen and U. W. Heinz, *Resonance Decay Contributions to Higher-Order Anisotropic Flow Coefficients*, *Phys. Rev.* **C86** (2012) 64906 [1210.7010].

[233] L. Adamczyk and Others, *Observation of charge asymmetry dependence of pion elliptic flow and the possible chiral magnetic wave in heavy-ion collisions*, *Phys. Rev. Lett.* **114** (2015) 252302 [1504.02175].

[234] S. K. Das, S. Plumari, S. Chatterjee, J. Alam, F. Scardina and V. Greco, *Directed Flow of Charm Quarks as a Witness of the Initial Strong Magnetic Field in Ultra-Relativistic Heavy Ion Collisions*, *Phys. Lett.* **B768** (2017) 260 [1608.02231].

[235] A. Dubla, U. Gursoy and R. Snellings, *Charge-dependent flow as evidence of strong electromagnetic fields in heavy-ion collisions*, 2020. 10.1142/S0217732320503241.

[236] A. D. SAKHAROV, *VIOLATION OF CP-INVARIANCE, C-ASYMMETRY, AND BARYON ASYMMETRY OF THE UNIVERSE*, in *Sov. Phys. Usp. 34, no.5, 392-393 (1991)*, (1998), DOI.